

Evaluation of  $^{87}\text{Sr}/^{86}\text{Sr}$ ,  $\delta^{18}\text{O}$ ,  $\delta^2\text{H}$ , and Cation Contents as  
Geochemical Tracers for Provenance and  
Flow Paths of Saline Solutions in  
German Zechstein Deposits



Dissertation  
zur Erlangung des Doktorgrades  
an der Mathematisch-Naturwissenschaftlichen Fakultät  
der Georg-August-Universität zu Göttingen

vorgelegt von

**Janina Simone Klaus**

aus München

**Göttingen 2008**

**Figure front page:** Seepage site LS 1 CN 8/9 in the Lower Saxonian mine LS 1 (Photo U. Argut)

D7

Referent

Prof. Dr. B. T. Hansen

Korreferent

Dr. W. W. Beer

Tag der mündlichen Prüfung

03.11.2008

## **ACKNOWLEDGEMENTS**

Hiermit möchte ich folgenden Personen und Institutionen für die Unterstützung danken, welche ich im Laufe dieser Studie erfahren habe:

Meinen Doktorvätern Prof. Bent T. Hansen und Dr. Wolfgang W. Beer gilt mein Dank für die Übernahme des Referates sowie für die persönliche Unterstützung während aller Phasen dieser Arbeit.

Besonderer Dank sei an dieser Stelle an die K+S Gruppe gerichtet, welche das Projekt vergeben und finanziell gefördert hat. Hierbei sei vor allem die Unterstützung durch Dr. Beer und die gesamte Belegschaft der Geologie und der Werke der K+S Gruppe gewürdigt.

Herrn Prof. A. G. Herrmann danke ich für die vielen anregenden Diskussionen und Hintergrundinformationen welche wesentlich zum Gelingen der Arbeit beigetragen haben.

Danken möchte ich auch der gesamten Abteilung Isotopengeologie des GZG, vor allem Ilka Schönberg, Nicole Nolte und Brigitte Dietrich, ohne deren Hilfe ich an mancher Stelle nicht weiter gekommen wäre.

Ich danke Dr. S. Weise und Dr. K. Knöller sowie Frau G. Schäfer für die Möglichkeit, am Umweltforschungszentrum in Halle die stabilen Isotopen analysieren zu können.

Des Weiteren möchte ich Erwin Schiffcyk und Dr. Klaus Simon danken, welche mir die Analyse der Kationen am GZG ermöglicht haben.

Ein herzliches Dankeschön an meine Kollegen Christina Heller, Wencke Wegner, Silke Triebold, Stefan Möller und Andreas Kronz für die stets willkommene Zerstreuung meiner fokussierten Gedanken.

Ich danke meinen Eltern und meinem lieben Philipp für das Vertrauen in meine Fähigkeiten, und die Energie welche ich durch ihren Zuspruch bekommen habe.

## PROLOGUE

The objective of this thesis is two-fold. First of all, it is a report on how to combine several geochemical tracing methods for the identification of the provenance of saline solutions seeping into underground salt and potash mines. Secondly, it provides readers untouched by salt deposit geology with an overview of the basics to be known about the historical development of seepage tracing, the hydrochemical properties of natural saline solutions, and the overall Zechstein Basin evolution (without being exhaustive). Suggested general further readings for all discussed topics are FULDA 1935, BRAITSCH 1971, SONNENFELD 1984, CLARK & FRITZ 1997, and AGGARWAL et al. 2005.

## ABSTRACT

The assessment of flow paths of saline solutions that percolate through evaporitic deposits is an important task for a mining company to avoid loss of a mine by flooding. In this study, the provenance of such saline solutions is evaluated via the cation contents, the  $\delta^{18}\text{O}$  and  $\delta^2\text{H}$  characteristics, and the  $^{87}\text{Sr}/^{86}\text{Sr}$  ratios.

The cation patterns of evaporating brines derived from seawater show a characteristic composition for several stages of concentration in the residual brine, following the quinary phase system of seawater. Such concentration stages can be identified in the saline solutions if they were synsedimentary or postsedimentary incorporated into the evaporitic deposits (internal solutions). Most internal samples have compositions similar to that of seawater that is in equilibrium with carnallite (Q-solutions).

In contrast, samples of meteoric groundwater that percolates from its source aquifer through the deposit into a rock salt or potash mine (external solution) show a significantly different cation composition from that of the internal solutions. While highly evolved internal solutions are enriched in Mg with respect to seawater, external solutions are enriched in Na since they have not reached halite equilibrium yet. In addition, the strontium and stable isotope compositions of the external samples are similar to those of the source aquifers. This similarity of the strontium and stable isotope compositions of external solutions and the corresponding source aquifers is

shown on the basis of several solutions from Hesse and Thuringia that are already identified as being external, and therefore present an ideal test case for this question.

Similar considerations are applied on a set of internal solutions. Simultaneous evaluation of the cation concentrations and the  $^{87}\text{Sr}/^{86}\text{Sr}$  ratios of the internal solutions give evidence for water-rock interactions of solutions with the soluble and insoluble components of the salt deposits, e.g. carnallite and salt clays. Dissolution of carnallite leads to enrichment in Rb with respect to seawater (Rb excess) that causes an increase of the  $^{87}\text{Sr}/^{86}\text{Sr}$  ratio via decay of  $^{87}\text{Rb}$  to  $^{87}\text{Sr}$ . This influence is efficient because the Sr concentration of the internal solutions is very low ( $< 1.6$  ppm) and already the addition of small amounts of Rb affects the Sr budget in the solution. Furthermore, quantification of this process has shown that many of the internal solutions may be epigenetic, because the time needed to increase the  $^{87}\text{Sr}/^{86}\text{Sr}$  ratio from the Zechstein level to the modern level is less than 251 My when the Zechstein salts were deposited (given that the Rb excess was gathered upon or shortly after enclosure).

In addition to the  $^{87}\text{Sr}/^{86}\text{Sr}$  ratios, both  $\delta^{18}\text{O}$  and  $\delta^2\text{H}$  in the internal solutions are highly dependent on the concentration stage of these solutions as well. Most stable isotope compositions of external samples are in consistency with the GMWL. The samples known to be of internal origin show a shift in stable isotopes away from the Global Meteoric Water Line on a concentration hook defined by changing activities of both  $^{18}\text{O}$  and  $^2\text{H}$  with ongoing seawater concentration. However, such shift can also result from dissolution of hydrated minerals during epigenetic enclosure of the solutions.

# TABLE OF CONTENTS

## FIGURES AND TABLES

### PART I - HISTORICAL AND GEOLOGICAL BACKGROUND

|  | PAGE      |
|--|-----------|
| <b><u>1. INTRODUCTION – Seepages and Geochemical Tracers</u></b>         | <b>2</b>  |
| 1.1 Salt and its Mining History  | 3         |
| 1.2 Defining ‘Saline Solution’   | 5         |
| 1.3 State-of-the-art of Tracing the Origin of Saline Solutions           | 6         |
| 1.4 Approach for more Precise Tracing                                    | 7         |
| <b><u>2. THE ZECHSTEIN BASIN – Past, Present and Future</u></b>          | <b>9</b>  |
| 2.1 The Barred Basin Model after Ochsenius                               | 9         |
| 2.2 Past – Pangea and the Zechstein Basin                                | 10        |
| 2.2.1 Sedimentation of the Seven Zechstein Folgen                        | 14        |
| 2.3 Present – the Central European Basin                                 | 16        |
| 2.3.1 Modern Geologic Appearance in Germany                              | 17        |
| 2.3.2 Aquifers below, within, and above the Zechstein series             | 17        |
| 2.4 Future – Resources   | 18        |
| <b><u>3. SAMPLES – Encoding, Sampling, and Regional Hydrogeology</u></b> | <b>19</b> |
| 3.1 Encoding Key for Seepage Sites in German Rock Salt and Potash Mines  | 19        |
| 3.2 Sampling of Saline Solutions   | 19        |
| 3.3 Sampling Sites and Regional Hydrogeologic Features                   | 21        |
| 3.3.1 Hesse  | 21        |
| 3.3.2 Thuringia  | 26        |
| 3.3.3 Lower Saxony   | 28        |
| 3.3.4 North Rhine-Westphalia   | 30        |
| 3.3.5 Saxony-Anhalt  | 31        |

## PART II - GEOCHEMICAL BACKGROUND

|  |           |
|--|-----------|
| <b><u>4. METHODS – Sample Preparation, Analysis, Errors, and Fractionation</u></b>   | <b>33</b> |
| 4.1 Stable Isotopes  | 33        |
| 4.1.1 Preparation and Analysis of Hydrogen and Oxygen Isotopes                       | 34        |
| 4.1.2 Standards and Errors in Stable Isotope Analysis                                | 36        |
| 4.2 Strontium Isotopes   | 38        |
| 4.2.1 Preparation and Analysis of Strontium Isotopes                                 | 38        |
| 4.2.2 Standards and Errors in Strontium Isotope Analysis                             | 39        |
| 4.3 Tritium  | 41        |
| 4.3.1 Preparation and Analysis of Tritium  | 41        |
| 4.3.2 Standards and Errors in Tritium Analysis                                       | 41        |
| 4.4 Main and Trace Elements  | 42        |
| 4.5 Intensive Parameters   | 42        |
| <b><u>5. FROM WATER TO BRINE – Evaporation, Concentration, and Precipitation</u></b> | <b>44</b> |
| 5.1 The Composition of Modern and Permian Seawater                                   | 44        |
| 5.2 Marine Evaporite Minerals and their Compositions                                 | 47        |
| 5.2.1 Trace Elements   | 51        |
| 5.3 Fractionation of $^{87}\text{Sr}/^{86}\text{Sr}$ – Water-Rock Interactions       | 54        |
| 5.4 Stable Isotopes in the Water Cycle   | 55        |
| 5.4.1 The Global Meteoric Water Line (GMWL)  | 56        |
| 5.4.2 Oxygen and Hydrogen Isotope Evolution of Seawater to Brines                    | 56        |
| 5.4.3 Deuterium Excess Distribution  | 60        |
| 5.5 Strontium and Oxygen Variations in Seawater                                      | 60        |
| 5.5.1 Isotopic Variations throughout the Zechstein                                   | 61        |
| 5.6 Tritium – The Anthropogenic Time Stamp   | 63        |
| 5.7 The Composition of Saline Solutions  | 63        |

## PART III - DATA EVALUATION

|   |            |
|---|------------|
| <b>6. RESULTS – Stable Isotope, Strontium Isotope, and Cation Data</b>                              | <b>68</b>  |
| 6.1 Stable Isotope Data   | 68         |
| 6.1.1 $\delta^{18}\text{O}$ and $\delta^2\text{H}$ per Sampling Region                              | 68         |
| 6.1.2 Reproducibility of the stable isotope data over time  | 75         |
| 6.2 Strontium Data  | 77         |
| 6.2.1 $^{87}\text{Sr}/^{86}\text{Sr}$ Ratios per Sampling Region                                    | 79         |
| 6.2.2 Reproducibility of the strontium isotope data over time                                       | 86         |
| 6.3 Tritium Data  | 87         |
| 6.4 Major and Trace Cation Data   | 87         |
| 6.4.1 Sodium, Potassium, and Magnesium  | 88         |
| 6.4.2 Calcium, Rubidium, and Strontium  | 95         |
| 6.4.3 Iron, Lithium, Manganese, and Zink  | 101        |
| <b>7. DISCUSSION – Evaluating the Results with Former and New Methods</b>                           | <b>103</b> |
| 7.1. Applying and Modifying Common Evaluation Methods   | 103        |
| 7.1.1 Stable Isotope Evaluation Methods   | 103        |
| 7.1.2 Main and Trace Element Evaluation Methods   | 109        |
| 7.2. Introducing new Approaches   | 112        |
| 7.2.1 Sr Isotope Systematics and the Influence of $^{87}\text{Rb}$ decay,<br>Time, Salts, and Clays | 112        |
| 7.2.3 The Ca/Sr Ratio   | 130        |
| 7.3 Evaluation of the Seepage Sites with Ambiguous Geochemical Patterns                             | 131        |
| <b>8. CONCLUSIONS</b>   | <b>136</b> |
| <b>REFERENCES</b>   | <b>140</b> |
| <b>APPENDIX</b>   |            |
| <b>RESUME</b>   |            |



## FIGURES

- Figure 1-1: “Der Geologe” painted in 1860 by Carl Spitzweg (1808-1885; public domain).
- Figure 1-2: Working in Wieliczka mine, Poland ([www.krakow-info.com/wielicz.htm](http://www.krakow-info.com/wielicz.htm), retrieved 10/2007).
- Figure 2-1: Sketch of a barred salt depositional basin (modified after HERRMANN 1981 and BEER 1996).
- Figure 2-2: Stratigraphic chart of the Zechstein in relation to the Permian and Lower Triassic (modified after RICHTER-BERNBURG 1953b, GERMAN STRATIGRAPHIC COMMISSION 2002; KÄDING 1978).
- Figure 2-3: Plate assembly of Pangea at the Permian-Triassic boundary (251 My BP; after STAMPFLI & BOREL 2002).
- Figure 2-4: The Central European Basin (red) with the Northern (yellow) and the Southern (blue) basin part and the Ringkobing-fyn-high (grey) (modified after ZIEGLER 1990).
- Figure 3-1: The hydrogeology of northern Germany (not all formations are developed in all areas; modified after VIERHUFF et al. 1981, SCHECK & BAYER 1999, SKOWRONEK et al. 1999, GERMAN STRATIGRAPHIC COMMISSION 2002, BAYERISCHES LANDESAMT FÜR UMWELT 2007).
- Figure 3-2: Stratigraphic columns of the Zechstein facies for the mines HE 1, HE 2, LS 1, LS 5 and NW 1 (modified after BEER 1996; see Figure 2-2 for abbreviations).
- Figure 3-3: Well monitored seepage site HE 2 Loch 1/87.
- Figure 3-4: Boreholes at the internal seepage site LS1 H23 on the 470 m level (Photo U. Argut).
- Figure 3-5: The probably open seepage site LS1 CN 8/9 on the 350 m level at discovery before monitoring (Photo U. Argut).
- Figure 4-1: Distillery used to separate the H<sub>2</sub>O from dissolved solid phases of a saline solution prior to the stable isotope analysis.
- Figure 5-1: Predicted major ion secular oscillations in Phanerozoic seawater (fluxes mid ocean ridge/river water =1.25; modified after HARDIE 1996).
- Figure 5-2: Residence time of ions in seawater (modified after BROWN 1997); highlighted ions are discussed in the course of this study.
- Figure 5-3: The Global Meteoric Water Line (GMWL) after Craig (1961a).
- Figure 5-4: Evolution of oxygen and hydrogen isotopes of different water types caused by the named effects (modified after Horita 2005).
- Figure 5-5: Evaporation trajectory (red) for the stable isotope contents of fluid inclusion samples (triangles) after KNAUTH & BEEUNAS (1986).
- Figure 5-6: Comparing the trends of <sup>87</sup>Sr/<sup>86</sup>Sr and δ<sup>18</sup>O during the Upper Permian (modified after GRUSZCZYŃSKI et al. 1992).
- Figure 5-7: Quinary seawater phase system with phase transition points (Appendix V; modified after USDOWSKI & DIETZEL 1998).
- Figure 6-1: Stable isotope data of samples from boreholes (blue circles), shafts (triangles), and external (circles) and internal (squares) seepage sites per federal state; groundwater and external samples show good correlation with the GMWL (blue line); internal samples follow the concentration hook (red line; green line indicates fresh water evaporation; errors range within ±0.20 ‰ for δ<sup>18</sup>O and ±1.5 ‰ for δ<sup>2</sup>H; both δ values on concentration scale).
- Figure 6-2: Stable isotope data of selected sites per federal state; the internal samples (squares) on the left side of the GMWL may be incorporated epigenetic into the rock salt or potash deposits, or even may be of external origin.

- Figure 6-3:  $\delta^2\text{H}$  of selected sampling stations vs. sampling date, mirroring the seasonal influence of air temperature and water supply; highs (blue) are during summer, lows (white) during winter time. Differences in flow time from the surface into the mine may prohibit a complete correlation. Analytical uncertainties are within the symbol size.
- Figure 6-4: Modern groundwater, late Permian seawater and detritus (T4 Roter Salzton) end members for the external seepages; colored areas are the fields for the two-component-mixtures between one groundwater and late Permian seawater (legend shows used boreholes in parentheses; mixed water = groundwater mixed with disposal brine).
- Figure 6-5: Comparison of seepage and shaft data with aquifer end members; an excerpt with included end members is shown in Figure 6-6.
- Figure 6-6: Excerpt of Figure 6-4: Comparison of seepage and shaft data with aquifer end members; colored areas are the fields for the two-component-mixtures between one groundwater and late Permian seawater according to Figure 6-5 (su = Buntsandstein; Ca3 = Plattendolomit; pr = Rotliegend; sub+disp = boreholes influenced by subsrosion or disposal brine).
- Figure 6-7:  $^{87}\text{Sr}/^{86}\text{Sr}$  ratios of selected sampling stations vs. sampling date, showing only slight seasonal variations with lower  $^{87}\text{Sr}/^{86}\text{Sr}$  ratios around January. Analytical uncertainties are within the symbol size.
- Figure 6-8: Quinary system (simplified) showing evolutionary paths of evaporating brines up to the Q and Z solutions (Z = eutonic point, evaporation to dryness; see Chapter 5.7 for background information; modified after USDOWSKI & DIETZEL 1998).
- Figure 6-9: Distinction between the different solutions by their Na and K content; comparison with quinary evolution of seawater up to the points Q and Z helps to distinguish between groundwater and seawater sources (blue and red concentration paths adapted from BORCHERT 1940).
- Figure 6-10: Distribution of Na and K vs. Mg in samples from shafts, external and internal seepage sites; the evolutionary paths up to the points Q and Z of the quinary phase system point up the sources of the different solutions (blue and red concentration paths adapted from BORCHERT 1940).
- Figure 6-11: Density vs. Mg contents from samples from shafts, external and internal seepage sites; blue lines indicate the minimum density at the onset of the precipitation of an evaporitic mineral (precipitation stages after FONTES & MATRAY 1993).
- Figure 6-12: Ca vs. Sr distribution in samples from shafts, external and internal seepage sites; the linear trends indicate the different interdependencies in behavior of Ca and Sr for external and internal solutions. Colored lines are the median of the Ca/Sr ratio of internal (pink) and external (orange) solutions.
- Figure 6-13: Excerpt of Figure 6-12 with Ca vs. Sr distribution within the samples from shafts, external and internal seepage sites; the Ca/Sr ratio of the low concentrated external group HE 2 Loch 1/87 indicates its external origin. Note the different scale in comparison to Figure 6-12. Colored lines are the median of the Ca/Sr ratio of internal (pink) and external (orange) solutions.
- Figure 6-14: Distribution of Sr vs. Mg in samples from shafts, external and internal seepage sites compared to the Mg content. Unequivocal distinction between internal and external solution origin is possible.
- Figure 6-15: Distribution of Sr vs. Na in samples from shafts, external and internal seepage sites compared to the Na content. Internal and external solutions can be discriminated by highly differing Na concentrations.
- Figure 6-16: K vs. Rb distribution in samples from shafts, external and internal seepage sites, not showing a straight correlation to be assumed from the similar atomic structure of both elements.

- Figure 6-17: Comparison of K and Rb vs. Mg contents in internal and external solutions with phase equilibrium evolution paths up to the points Q and Z (two y-axes only for comparison purposes).
- Figure 6-18: Mn, Fe, Li, and Zn vs. Mg in samples from shafts, external and internal seepage sites.
- Figure 7-4: Comparison of spider diagrams with different y-scales; shown are 1 = Groundwater samples, 2 = Shaft samples, 3 = External solutions 4 = Internal solutions, 5 = Seawater concentration path (after FONTES & MATRAY, 1993, and references therein; groundwater and external samples were normalized on seawater, too, due to comparison purposes).
- Figure 7-1: Diagram to qualitatively evaluate saline solutions in rock salt or potash mines, showing the internal (pink) and the external/groundwater samples (orange) of the presented data set (after SCHMIEDL et al. 1982; both  $\delta$  values on concentration scale).
- Figure 7-2: Hook of the concentration path (red) caused by decreasing activity of  $\delta^2\text{H}$  and  $\delta^{18}\text{O}$  with increasing salt contents in the brine (both  $\delta$  values on concentration scale); sample symbols as in Figure 7-1.
- Figure 7-3: Sketch of the variability of the concentration hook if seawater evaporation happens under different humidities (modified after SOFER & GAT 1975); sample symbols as in Figure 7-1.
- Figure 7-5: Increase of the  $^{87}\text{Sr}/^{86}\text{Sr}$  ratio with time and Rb/Sr ratio; calculations are based on an initial  $^{87}\text{Sr}/^{86}\text{Sr}$  ratio of 0.7068 (lowest seawater ratio during Zechstein ages); timing of increase of the  $^{87}\text{Sr}/^{86}\text{Sr}$  ratio depends on the Rb/Sr ratio; at high Rb/Sr, less time is needed for the same increase as at low Rb/Sr (blue lines).
- Figure 7-6:  $^{87}\text{Sr}/^{86}\text{Sr}$  vs. Rb (log) distribution within the boreholes, the shaft waters, and the external and internal solutions; the pink field indicates an interdependency in behavior for the internal solutions with increasing Sr isotopic compositions and concentrations.
- Figure 7-7:  $^{87}\text{Sr}/^{86}\text{Sr}$  vs. Rb distribution within the boreholes, the shaft waters, and the external and internal solutions; the internal data show a trend of increasing  $^{87}\text{Sr}/^{86}\text{Sr}$  ratios with increasing Rb contents. The external solutions show no correlation.
- Figure 7-8: Increase of the  $^{87}\text{Sr}/^{86}\text{Sr}$  ratio with time and Rb/Sr ratio; calculations are based on an initial  $^{87}\text{Sr}/^{86}\text{Sr}$  ratio of 0.7068 (lowest seawater ratio during Zechstein ages).
- Figure 7-9: Rb/Sr ratios in the external and internal solutions; the high ratios of the internal solutions indicate the degree of incorporation of excess Rb.
- Figure 7-10: Variations of the Sr/Rb ratio with the  $^{87}\text{Sr}/^{86}\text{Sr}$  ratio. Most external solutions show higher variations in the Sr/Rb ratios than in the  $^{87}\text{Sr}/^{86}\text{Sr}$  ratio (yellow fields).
- Figure 7-11: Box model showing the different possible flow paths of internal and external solutions; 1a,b = Internal solutions; 2a,b = External solutions (aquifer); 3 = External solutions (meteoric); 4 = Mix if internal and external.
- Figure 7-12: Variations of Sr concentration (Sr) and isotope composition (Iso) with time of sampling for the corresponding sites LS 4 L499 900 m and LS 5 UB 784 725 m; yellow circles indicate the needed Sr concentration after passage through the T5 to model the final values via addition of other salt clays.
- Figure 7-13: Shifts in Sr concentration and isotope composition caused by salt clays upon percolation of solution LS 5 UB 784 725 m through the salt down to site LS 5 L499 900 m (percolation path from lower left through the clays over to lower right).
- Figure 7-14:  $^{87}\text{Sr}/^{86}\text{Sr}$  and Rb vs. Mg distribution within sites under question (two y-axes only for comparison purposes).

## TABLES

- Table 3-1: List of encoded site names with information on location, stratigraphy (at the emersion point within the mine openings, or at the perforated section of a borehole, respectively), and sampling.
- Table 3-2: Sampled boreholes in Hesse and Thuringia.
- Table 4-1: List of standard analyses of NBS 987 over the whole period of measurements, compared to the certified NBS 987 and the GZG mean.
- Table 5-1: Comparing modern (after \*BROWN 1997 and FONTES & MATRAY 1993) and Permian (after HORITA 1991) seawater compositions.
- Table 5-2: Major marine precipitates, their solubility and behavior for static seawater evaporation under laboratory and *natural* conditions (after HERRMANN 1981).
- Table 5-3: Distribution coefficients for traces of elements in chemical marine precipitates (modified after HOLSER 1979; USDOWSKI 1973).
- Table 5-4: Classification scheme for saline solutions in rock salt and potash mines (after HERRMANN et al. 1978).
- Table 6-1: Stable isotope data of the boreholes, the shafts, and the external and internal seepage sites at Hessian mines (errors range within  $\pm 0.20$  ‰ for  $\delta^{18}\text{O}$  and  $\pm 1.5$  ‰ for  $\delta^2\text{H}$ ).
- Table 6-2: Stable isotope data of the shafts and the external and internal seepage sites from Thuringian, North Rhine-Westphalian and Saxony-Anhaltinian mines (errors range within  $\pm 0.20$  ‰ for  $\delta^{18}\text{O}$  and  $\pm 1.5$  ‰ for  $\delta^2\text{H}$ ).
- Table 6-3: Stable isotope data of the shafts, the external and the internal seepage sites from Lower Saxonian mines (errors range within  $\pm 0.20$  ‰ for  $\delta^{18}\text{O}$  and  $\pm 1.5$  ‰ for  $\delta^2\text{H}$ ).
- Table 6-4: Strontium data of the boreholes, the shafts, the external and internal seepage sites from Hessian mines.
- Table 6-5: Strontium data of the shafts, the external and internal seepage sites from Thuringian, North Rhine-Westphalian and Saxony-Anhaltinian mines.
- Table 6-6: Strontium data of the shafts, the external and internal seepage sites from Lower Saxonian mines.
- Table 6-7: Major cation concentrations in ppm for the boreholes and meteoric water samples.
- Table 6-8: Cation concentrations in ppm for the shaft water samples.
- Table 6-9: Cation concentrations in ppm for the external seepages.
- Table 6-10: Cation concentrations in ppm for the internal seepages.
- Table 7-1: Cation contents (in ppm) during concentration of seawater until onset of bischofite precipitation (after FONTES & MATRAY 1993, and references therein).
- Table 7-2: Calculated time for ingrowth of  $^{87}\text{Sr}$  in internal solutions to increase the  $^{87}\text{Sr}/^{86}\text{Sr}$  ratio from initial (contemporaneous seawater of original strata) to the final ratio measured in the internal solutions. Different initial  $^{87}\text{Sr}/^{86}\text{Sr}$  ratios correspond to the stratigraphic position of each solution.
- Table 7-3: Clays in the flow path of LS 5 L499 900 m used for the calculations in the mixing model.

# Part I

## Historical and Geological Background

1. INTRODUCTION
2. THE ZECHSTEIN BASIN
3. SAMPLES

## 1. INTRODUCTION - Seepages and Geochemical Tracers

Since the start of historic underground salt mining within the European evaporitic *Zechstein* deposits in the 13<sup>th</sup> century in Wieliczka, Poland (JEREMIC 1994), the historic as well as the modern rock salt and potash mining has been overshadowed by several unpredictable risks induced by the mining activities (PERROW 1984). Especially explosive CO<sub>2</sub>-outbursts, cave-ins induced by karst formation, and flooding of a mine due to saline solution seepages originating from groundwater or large salt internal fluid occurrences present hazards to the companies and their workers.

Any salt body crystallized out of seawater, saline lakes, saline ground water, or hydrothermal fluids contains impurities of different dimensions. Typical anomalies within the Zechstein deposits of up to 2000 m primary thickness (ZIEGLER 1990) are voluminous CO<sub>2</sub> caverns (EHGARTNER et al. 1998) and fluid inclusions (ROEDDER 1984) as well as channels caused by e.g. karst formation (COOPER 2002) or basalt intrusions (KNIPPING 1987) that provide possible pathways for gases and fluids.

The degree of damages caused by CO<sub>2</sub>-outbursts and saline solution seepages differs on time and spatial scales. CO<sub>2</sub>-outbursts cause immediate but finite damage. In contrast, saline solution seepages into the mine openings caused by either internal fluid occurrences within the salt (syngenetic and epigenetic connate brines) or by inleakage of external water through the salt body (epigenetic brines) present a large and long-term hazard for the mine. In particular the external solutions present an indefinite source of inflowing water. With ongoing know-how and experience, these hazards have become nearly safe for the miners, but the causes cannot be eliminated. Only targeted monitoring can help to minimize the impact of such natural incidents. In the following, this study focuses on the mitigation and monitoring of saline solution seepages, whereas monitoring typically involves geochemical and hydrological tools. CO<sub>2</sub> impregnations, in contrary, can only be detected via either geophysical tools or drilling techniques that are not discussed here.

Today's risks are mainly of an economic character. The modern underground salt mining activity serves the nutrition, chemical, and fertilizing industry. The sacrifice of a mine is -besides the direct loss in reserves- an immense infrastructural loss for a mining company (e.g. GROAT 1981; GENDZWILL & MARTIN 1996; ZUBER et al. 2000).

Remedial measures need to be emplaced to mitigate the risk of water seepages. Currently, the conventional mitigation technique employs the withdrawal of inflowing water upstream of the seepage within the sediments surrounding a salt complex. However, the current prediction methods of the water's regional origin are only to a certain degree accurate (see Chapters 1.3 and 7.1). The predictions are made mainly based on the chemical characteristics of each individual liquid. Once predictions are made, they are essential information for the overall risk assessment and help to determine where resources have to be employed and further preventive measures need to be taken.

The regional origin of the seeping water can be manifold, thus resulting in different risk potentials. Syngenetic or epigenetic connate brines, in the following referred to as *internal solutions*, seeping out of a spacious inclusion will stop dripping after the inclusion is empty. Epigenetic seepages of surface water or groundwater, so-called *external solutions*, seeping through fissures into the salt can commence with a wet area on the roof, the wall or the floor of a mine opening. Such seepage can have constantly low inflow rates over decades. However, within days or weeks the flow rate of such external inflow can suddenly increase to a degree that causes the flooding of the mine (e.g. GROAT 1981, GENDZWILL & MARTIN 1996, ZUBER et al. 2000).

The investigation of a simple, but distinct chemical tool or combination of tools to distinguish between internal and external saline solutions is the aim of this work. Furthermore, the determination of the source aquifer of external groundwater seepages is the goal on the horizon.

### **1.1 Salt and its Mining History**

Due to archeological records, the first settled cultures on earth resided where salt was available. The oldest agricultural settlements in the Jordan valley about 10,000 years

before present (BP) were in close proximity to the Dead Sea and the saliferous Mt. Sodom (JEREMIC 1994). Since the emergence of trade about 6000 yrs ago rock salt has been a highly valued trade item. With its ongoing discovery in the Mediterranean area and the Middle East, salt was used as a currency ('salary') and became subject for wars all over the world.

During the early age of geology between 1790 and 1830 (Figure 1-1), the controversy between plutonism and neptunism resulted in the picture of salt domes being magmatic intrusions (HUTTON 1795), although the neptunistic explanation of a marine origin was already put forward (WERNER 1787). In the course of the 19<sup>th</sup> century, both general theories became accepted for different rock types under the support of A. v. Humboldt (1769-1859) and C. Darwin (1809-1882). Since that time, the marine origin of evaporitic deposits is undisputed.



Figure 1-1: "Der Geologe" painted in 1860 by Carl Spitzweg (1808-1885; public domain).

The first known rock salt mine in the world is located in Wieliczka, Poland, where rock salt was mined since about 3000 years BP with the first underground mine established in the 13<sup>th</sup> century as shown in Figure 1-2 (see [www.kopalnia.pl](http://www.kopalnia.pl)).

The first gallery of the first German rock salt mine in Berchtesgaden was driven into the Petersberg in 1517. In 1856, the discovery of potassium salts in Staßfurt, Germany, initiated to establish the world's first potassium mine and plant founded in 1861 (K+S GRUPPE 2006). Since then, potassium salts are in use for fertilizing purposes (see Appendix I for major evaporitic minerals). Over the decades of industrialization and development of know-how and high-tech methods for efficient mining, the potassium



salt mining industry in Germany grew to one of the five biggest in the world, besides Russia, Canada, the USA, and France.



**Figure 1-2:**

Working in Wieliczka  
mine, Poland

([www.krakow-info.com/  
wielicz.htm](http://www.krakow-info.com/wielicz.htm), retrieved  
10/2007).

## 1.2 Defining ‘Saline Solution’

A saline solution is defined to be a solution with a high salt content, expressed via the density ( $\rho$ ), the electric conductivity (EC) or the total dissolved solids (TDS).

The parameter most easily to be analyzed in mines is the density. Since fresh water normally yields a density of  $1.0 \text{ g/cm}^3$ , an elevated density of e.g.  $1.2 \text{ g/cm}^3$  signalizes a high content of dissolved salts. However, the density could normally not exceed a value of  $1.35 \text{ g/cm}^3$  since at this point the solution would reach the eutonic point and all water would evaporate (see Chapter 2.2.1; LÖWENGART 1922).

The EC is a sensitive detector for dissolved salts in water. Its unit Siemens [S] is defined as the reciprocal of the resistance ( $1 \text{ S} = 1 \text{ } \Omega^{-1}$ ). Distilled water shows an EC of  $0.0548 \text{ } \mu\text{S/cm}$  (pH 7.0 and temperature of  $25^\circ\text{C}$ ; WEAST et al. 1985). Natural tap water normally yields an EC of lower than  $500 \text{ } \mu\text{S/cm}$ . Fresh potable groundwater can yield up to  $2000 \text{ } \mu\text{S/cm}$  (BERLITZ et al. 2007). Potable mineral water should not exceed  $2500 \text{ } \mu\text{S/cm}$  (BUNDESMINISTERIUM DER JUSTIZ 2001). Seawater shows an EC of about  $50,000 \text{ } \mu\text{S/cm}$ . If the EC exceeds the groundwater value, the solution will be considered to be saline for any analytical procedure.

Additionally, the TDS [ppm], which includes everything but  $\text{H}_2\text{O}$ , describes the salinity  $S \text{ [‰]}$  ( $1000 \text{ ppm TDS} = 1 \text{ ‰ S}$ ) of a solution. Solutions containing  $10,000\text{-}100,000 \text{ ppm}$

TDS are defined to be saline, and above 100,000 ppm solutions are called brine (LLOYD & HEATHCOTE 1985). Seawater has a salinity of 35 ‰, thus containing 35,000 ppm TDS. EC and TDS are interdependent, whereas an EC of 1  $\mu\text{S}/\text{cm}$  corresponds to  $\approx 0.65$  ppm TDS (CARLSON 2005).

For the chemical characteristics of seawater solutions see Chapter 5.7.

### 1.3 State-of-the-art of Tracing the Origin of Saline Solutions

Several authors already worked on the tracing of the origin of saline ground water and solutions leaking into rock salt and potash mines. However, most of the studies focused on one method or one mine. Common in many previous studies was the approach of analyzing the major elements of the solutions, and one additional geochemical tool of the following:

- › Bromine, rubidium and lithium concentrations (Br, Rb, Li)
- › Trace metals
- › Sulfur isotopes ( $\delta^{34}\text{S}$ )
- › Carbon isotopes and dating ( $^{14}\text{C}$ )
- › Chlorine isotopes ( $\delta^{37}\text{Cl}$ )
- › Tritium contents ( $^3\text{H}$ )
- › Oxygen and hydrogen isotopes ( $\delta^{18}\text{O}$ ,  $\delta^2\text{H}$ )
- › Strontium isotopes ( $^{87}\text{Sr}/^{86}\text{Sr}$ ) and Rb/Sr dating

In this context, MÜLLER & PAPENDIECK (1975) typified deep saline waters of the Thuringian depression according to their ion contents, as did LEHMANN (1974) for the North-East German depression, with special emphasis on the Br contents. The Br/Cl ratio was used by WALTER et al. (1990) for the identification of the origin of saline fluids in the Illinois basin. NIELSEN & RAMBOW (1969) analyzed  $\delta^{34}\text{S}$  to interpret the saline origin of dissolved sulfur in Hessian mineral waters. PILOT & VOGEL (1972) discussed the dating and the designation of the origin of deep waters by using the  $^{14}\text{C}$  method (see also VEIZER et al. 1999). EGGENKAMP et al. (1995) determined the fractionation of  $\delta^{37}\text{Cl}$  in evaporites, which was important for the investigation of the origin of chloride in Permian brines in Texas by EASTOE et al. (1999). The inflow of

surface water into rock salt and potash mines determined by  $^3\text{H}$  analysis was subject of the work of HEBERT et al. (1986). Special effort was put into determining the origin of seepages in those mines that are considered for the deposition of radioactive waste, as reported by GELLERMANN et al. (1991) by using  $^3\text{H}$  and  $^{14}\text{C}$  in combination. HOLSER (1979), SCHMIEDL et al. (1982, 1983, 1986), GRABCZAK & ZUBER (1986), BOTTRELL et al. (1996) and ZUBER et al. (2000) focused on a method to determine the type of solution by using a combination of  $\delta^{18}\text{O}$  and  $\delta^2\text{H}$  and a comparison of the data with the Global Meteoric Water Line (see Chapter 5.4.1). This method is still effective for such problems, as shown by HORITA (2005) and JENSEN et al. (2006). The usefulness of the  $^{87}\text{Sr}/^{86}\text{Sr}$  ratio for seepage tracing, and the Rb/Sr dating of evaporites were discussed by KLINGENBERG (1998) for the Gorleben salt dome.

A summary of the possible tools for seepage tracing is given by HERRMANN et al. (2003).

#### **1.4 Approach for more Precise Tracing**

In this study, a combination of major and trace cations,  $^{87}\text{Sr}/^{86}\text{Sr}$  ratios and Sr concentrations as well as  $\delta^{18}\text{O}$  and  $\delta^2\text{H}$  will be tested for the identification of the origin of seepages in German rock salt and potash mines. So far, mainly the stable isotopes as well as main- and trace elements were used for this problem. Indeed, these results are insufficient for locally precise tracing. Therefore, the  $^{87}\text{Sr}/^{86}\text{Sr}$  characteristics are added as a tracer for the source aquifers as well as the rocks that get in contact with the solutions on their passage through the salt.

For evaluation and statistical purposes, fifteen seeping locations in eight German mines were sampled up to eight times over a period of two years, depending on their accessibility. The mines are chosen for their well characterized seepage sites, which have been monitored in some cases for several decades. For most of them, the internal or external origin is already determined in those long-term studies. Thus, these mines are well-defined test cases to investigate the applicability of the suggested tools. The overall number of 115 samples was analyzed for the conventional hydrogen and oxygen isotopes, as well as for strontium isotopes and cation concentrations as additional tools.

In the past two decades, the usefulness of Sr isotopes as chemical tracer for salinity changes in groundwater and seawater was demonstrated in several studies (e.g. MCNUTT et al. 1990, BANNER et al. 1994, LYONS et al. 1995, SCHMITZ et al. 1997, PIERRET et al. 2001, FLECKER et al. 2002, KLAUS et al. 2007). However, the general usefulness as tracer for flow paths of saline solutions within salt deposits is still to be investigated.

In contrast to Sr in groundwater, the overall Sr evolution in seawater is known through several studies on the Sr isotopic budget and evolution in the oceans during the Phanerozoic (BURKE et al. 1982, DENISON et al. 1994, VEIZER et al. 1999). Based on this characteristic evolution of the  $^{87}\text{Sr}/^{86}\text{Sr}$  seawater ratio through time, the Sr distribution within salts of late Permian age is assessable (see Chapter 5.5). The Sr isotopic evolution in seawater had its first major low mark in the late Permian, at the beginning of the Zechstein age, with a fast increase at the Permian-Triassic boundary (see Chapter 5.5.1). This characteristic behavior of the  $^{87}\text{Sr}/^{86}\text{Sr}$  seawater ratio during the Zechstein age is the motivation to test the usefulness of Sr isotopes in seepage-origin studies. Especially synsedimentary internal solutions might yield the Permian seawater ratio and could therefore be distinguishable from external solutions, if the system was closed for the whole time in terms of the  $^{87}\text{Sr}/^{86}\text{Sr}$  budget. The correlation of the external solutions with the groundwater of the aquifers in vicinity of the salt deposits can be difficult since in this open system the water might leach the Zechstein deposits on its passage through them. However, these processes will be investigated and quantified in the following.

## 2. THE ZECHSTEIN BASIN – Past, Present and Future

This chapter provides a brief overview of the evolution of the Zechstein Sea within the Central European Basin, and the formation of the massive Zechstein evaporites deposited within ca. 7 My up to the Permian-Triassic boundary.

Several authors focused on the evolution of salt deposits, especially within the Zechstein Basin, e.g. VAN'T HOFF (1905, 1909), JÄNECKE (1923), FULDA (1935), D'ANS & KÜHN (1940), RICHTER-BERNBURG (1953a/b), BRAITSCH (1971), HERRMANN (1981), ZHARKOV (1981, 1984), ZIEGLER (1990) and SCHOLLE et al. (1995a/b).

### 2.1 The Barred Basin Model after Ochsenius

First evidence on the evolution of salt deposits was given by J. Hutton in the controversial discussion about plutonism and neptunism (see Chapter 1.1). In one of his publications HUTTON (1795) stated:

*“The formation of salt at the bottom of the sea, without the assistance of subterranean fire, is not a thing un-supposable, as at first sight it might appear. Let us but suppose a rock placed across the gut of Gibraltar, (a case nowise unnatural), and the bottom of the Mediterranean would be certainly filled with salt, because the evaporation from the surface of that sea exceeds the measure of its supply“*

Based on this statement, C. C. OCHSENIUS (1830-1906) presented his theory on the deposition of salts in basins separated from the open sea by a threshold (natural barrier) (OCHSENIUS 1876, 1877). These epeiric -or epicontinental- basins, as shown in Figure 2-1, are suggested to provide the prerequisites for the vast deposition of salts:

A density-driven undercurrent of cold, enriched water out of the basin promotes the inflow of regular seawater which feeds the permanent deposition of evaporites triggered by high evaporation rates. Additional to the seawater inflow, groundwater is drawn through the threshold due to a high hydrostatic pressure between open and barred sea. Throughout the deposition of the evaporites, the height differential between the open sea level and the salt surface decreases due to the increase of the salt thickness. This results in a drop in hydrostatic pressure and decreasing groundwater influx, additionally decreasing the water volume and increasing the salt content within the basin (FULDA 1935).

Without constant inflow of water from the open sea, only 1.5% of the Zechstein Basin volume could be allocated to evaporites (FULDA 1935). Indeed, almost the entire basin was filled by salt deposits, up to a maximum primary thickness of ca. 2000 m (ZIEGLER 1990).

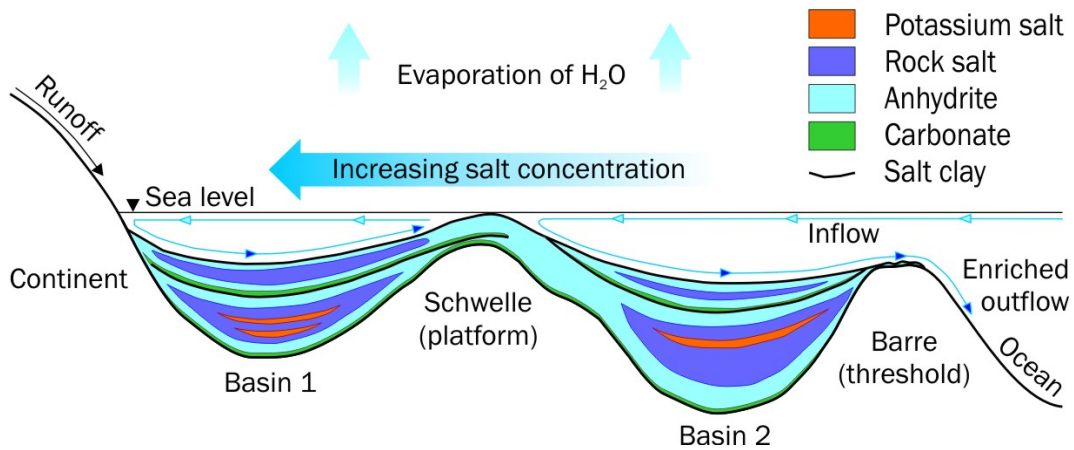


**Figure 2-1:** Sketch of a barred salt depositional basin (modified after HERRMANN 1981 and BEER 1996).

## 2.2 Past - Pangea and the Zechstein Basin

The Zechstein, as the main member of the European Upper Permian, covers a time span of ca. 7 My between 258-251 My BP as shown in Figure 2-2 (GERMAN STRATIGRAPHIC COMMISSION 2002). The age at onset of the Zechstein deposition is still under discussion due to uncertainties in the stratigraphic correlation and errors in the geochronologic dating exceeding the depositional period of 7 My.

The evolution of the Zechstein Basin within today's Europe was affected by plate movements due to the apex of the assembly of Pangea ca. 260-230 My BP. According to FULDA (1935), the initial sedimentation region of the Zechstein Basin emerged between the river Saar in Southwest Germany and Silesia in Southwest Poland throughout the Upper Carboniferous (320-296 My BP) and the Lower Permian *Rotliegend* (ca. 296-258 My BP). The development of this sedimentation region was initiated by the final opening of the Neo-Thetys in the Upper Carboniferous, propagating from Australia to the area of today's east Mediterranean until the Early Permian, as shown in Figure 2-3 (STAMPFLI & BOREL 2002).

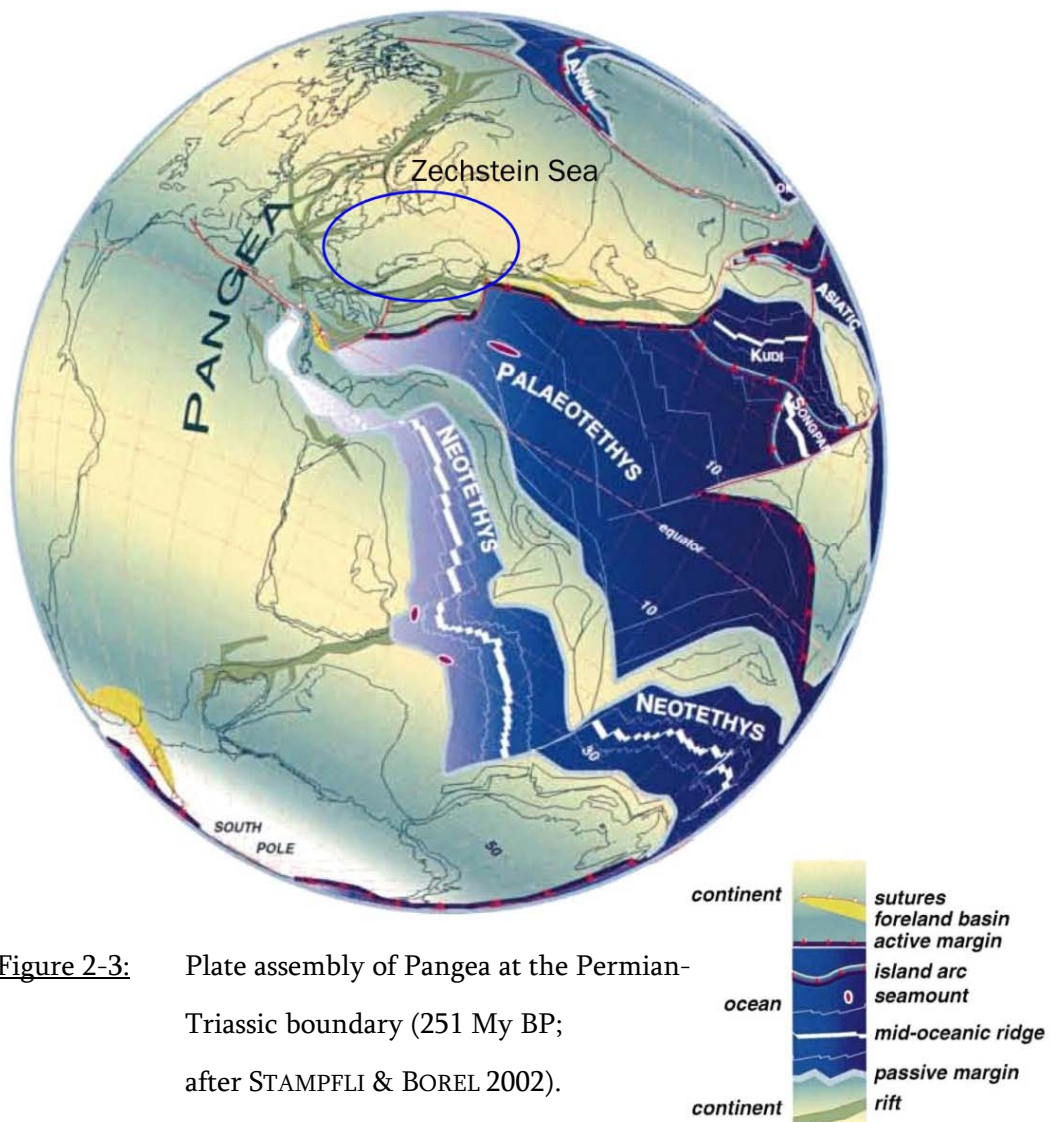
| System         | Group         | Subgroup                             | Cycle [Ma BP]   | abb. | Sequence   | Subsequence  | K+S Group  | DIN 29919   |  |  |
|----------------|---------------|--------------------------------------|-----------------|------|--|--|--|---|--|--|
| LOWER TRIASSIC | BUNTSANDSTEIN | 243 Upper <i>B. so</i>               | su              |      | Unterer Buntsandstein  |  |  | su  |  |  |
|                |               | 244.5 Middle <i>Buntsandstein sm</i> | Fulda-Folge     | z7   | Bröckelschiefer<br>Oberer Fulda-Ton<br>Oberer Fulda-Sandstein<br>Untere Fulda-Ton<br>Fulda-Sandstein   |  | z7B<br>z7Tb<br>z7Sb<br>z7Ta<br>z7Sa  | zB<br>T7r<br>S7r<br>T7<br>S7  |  |  |
|                |               | 249 Lower <i>Buntsandstein su</i>    | Friesland-Folge | z6   | Oberer Friesland-Ton<br>Friesland-Steinsalz<br>Friesland-Anhydrit<br>Friesland-Ton<br>Friesland-Sandstein  |  | z6Tb<br>z6NA<br>z6AN<br>z6Ta<br>z6Sa   | T6r<br>Na6<br>A6<br>T6<br>S6  |  |  |
|                |               |                                      | Ohre-Folge      | z5   | Oberer Ohre-Ton<br>Oberer Ohre-Sandstein<br>Grenzanhydrit<br>Ohre-Steinsalz<br>Lagenanhydrit<br>Salzbrockenton<br>Unterer Ohre-Sandstein   |  | z5Tb<br>z5Sb<br>z5ANb<br>z5NA<br>z5ANa<br>z5Ta<br>z5Sa   | T5r<br>S5r<br>A5r<br>Na5<br>A5<br>T5<br>S5  |  |  |
|                |               |                                      | Aller-Folge     | z4   | Oberer Aller-Ton<br>Oberer Aller-Anhydrit<br>Aller-Steinsalz Na4<br>Pegmatitanhydrit<br>Unterer Aller-Ton<br>Aller-Sandstein   | Grenzanhydrit<br>Tonbrockensalz<br>Mariagluck-Anhydrit<br>Rosensalz<br>Schneesalz<br>Aller-Basissalz<br>Roter Salzion  | z4Tb<br>z4ANb<br>z4NAd<br>z4AM<br>z4NAc<br>z4NAb<br>z4NAa<br>z4ANa<br>z4Ta<br>z4Sa   | T4r<br>A4r<br>Na4b<br>Na4d<br>Na4y<br>Na4b<br>Na4c<br>A4<br>T4<br>S4  |  |  |
|                |               |                                      | Leine-Folge     | z3   | Oberer Leine-Ton<br>Hauptanhydrit<br>Plattendolomit<br>Unterer Leine-Ton<br>Leine-Sandstein  | rezeßiv<br>Tonmittelsalz<br>Kaliflöz Riedel<br>Schwadensalz<br>Anhydritmittelsalz<br>Anhydritmittel<br>Kristallsalzmittel<br>Buntes Salz<br>Bändersalz<br>Kaliflöz Bergmannsseggen<br>Banksalz<br>Kaliflöz Ronnenberg<br>Orangeaugensalz<br>Liniensalz<br>Basissalz<br>Grauer Salzion/Leine-Karbonat   | z3Tb<br>z3NAr<br>z3KRi<br>z3NAh<br>z3NAg<br>z3AM (1-x)<br>z3KM<br>z3NAf<br>z3NAe<br>z3KBe<br>z3NAd<br>z3KRo<br>z3NAc<br>z3NAb<br>z3NAa<br>z3AN<br>z3CA<br>z3Ta<br>z3Sa | T3r<br>Na3tm<br>K3Ri<br>Na3b<br>Na3n<br>am<br>Na3krm<br>Na3c<br>Na3e<br>K3Be<br>Na3b<br>K3Ro<br>Na3y<br>Na3b<br>Na3c<br>A3<br>Ca3<br>T3<br>S3 |  |  |
|                |               |                                      | Staufurt-Folge  | z2   | Oberer Staufurt-Ton<br>Oberer Staufurt-Anhydrit<br>Staufurt-Steinsalz Na2<br>Unterer Staufurt-Anhydrit<br>Staufurt-Karbonat<br>Unterer Staufurt-Ton  | Gebänderter Deckanhydrit<br>Decksteinsalz<br>Kaliflöz Staufurt<br>Staufurt-Steinsalz, Kiseritzzone<br>Staufurt-Hauptsalz/Hangendsalz<br>Staufurt-Basissalz<br>Basalanhydrit<br>Hauptdolomit/Stinkschiefer<br>Untere Letten   | z2Tb<br>z2Anb<br>z2NAd<br>z2KSt<br>z2NAcK<br>z2NAb/c<br>z2NAa<br>z2AN<br>z2CA<br>z2Ta  | T2r<br>A2r<br>Na2r<br>K2<br>Na2yki<br>Na2b/y<br>Na2x<br>A2<br>Ca2<br>T2   |  |  |
|                |               |                                      | Werra-Folge     | z1   | Oberer Werra-Anhydrit β<br>Oberstes Werra-Steinsalz<br>Oberer Werra-Anhydrit α<br>Oberer Werra-Ton, Braunroter Salzion<br>Tonmittel im Na1<br>Oberes Werra-Steinsalz<br>Kaliflöz Hattorf<br>Begleitflöze<br>Kaliflöz Hessen<br>Mittleres Werra-Steinsalz<br>Kaliflöz Thüringen<br>Unteres Werra-Steinsalz<br>Unterer Werra-Anhydrit<br>Zechsteinkalk<br>Kupferschiefer<br>Zechsteinkonglomerat | Oberer Werra-Anhydrit β<br>Oberstes Werra-Steinsalz<br>Oberer Werra-Anhydrit α<br>Oberer Werra-Ton, Braunroter Salzion<br>Tonmittel im Na1<br>Oberes Werra-Steinsalz<br>Kaliflöz Hattorf<br>Kaliflöz Hessen<br>Mittleres Werra-Steinsalz<br>Kaliflöz Thüringen<br>Unteres Werra-Steinsalz<br>Unterer Werra-Anhydrit<br>Anhydritknottenschiefer | z1ANc<br>z1NAd<br>z1ANb<br>z1Tb<br>z1TM<br>z1NAc<br>z1KHa<br>z1KH<br>z1NAb<br>z1KTh<br>z1NAa<br>z1ANa<br>z1ANCA<br>z1CA<br>z1Ta<br>z1C                                 | A1r β<br>Na1r<br>A1r α<br>T1r<br>TM<br>Na1y<br>K1Ha<br>Na1yK<br>K1H<br>Na1β<br>K1Th<br>Na1α<br>A1<br>CaA1<br>Ca1<br>T1<br>Cl                  |  |  |
|                |               |                                      | Elbe Subgroup   | 258  |  |  |  |   |  |  |
|                |               |                                      | Havel Subgroup  | 262  |  |  |  |   |  |  |
| PERMIAN        | ZECHSTEIN     | 251                                  |                 |      |  |  |  |   |  |  |
|                |               | 262.5 (?)                            |                 |      |  |  |  |   |  |  |
|                |               | Nähe Subgroup                        |                 |      |  |  |  |   |  |  |
|                |               | 296                                  |                 |      |  |  |  |   |  |  |
| PERMIAN        | ROTLIEGEND    | 258                                  | pr              |      | Elbe-Subgruppe   |  |  | pr  |  |  |
|                |               | 296                                  |                 |      |  |  |  |   |  |  |

Figure 2-2: Stratigraphic chart of the Zechstein in relation to the Permian and Lower Triassic (modified after RICHTER-BERNBURG 1953b, GERMAN STRATIGRAPHIC COMMISSION 2002; KÄDING 1978).

The continental character of this broad Rotliegend denudation surface was supported by the Variscian fold belt which separated the area from the open sea and inhibited



precipitation (GLENNIE 1986). This desert climate changed to a marine environment once the Zechstein Sea flooded the area around 258 My BP in a catastrophic transgression event due to eustatic sea level rise of the open ocean and subsidence induced by rifting (STROHMENGER 1996, and references therein). The Zechstein Basin, as shown in Figure 2-4, was connected to the open boreal ocean only by the *Sinus Borealis*, a strait between today's Great Britain and Norway, or the Shetland Platform and the Fenno-Scandian High, respectively. The basin covered a bigger area than the Rotliegend Basin since the rapid flooding induced land subsidence due to the abrupt extra load of the seawater (ZIEGLER 1990).



**Figure 2-3:** Plate assembly of Pangea at the Permian-Triassic boundary (251 My BP; after STAMPFLI & BOREL 2002).

The still arid climate in this area led to an only sporadic connection with the open ocean. Therefore, a secluded marine basin was separated in which evaporation rates



frequently exceeded the runoff from the continent into the basin. At times of high evaporation rates, only some saline lakes in the deepest parts of the Zechstein Basin remained permanently wet. As a result, up to 2000 m of evaporites were deposited over seven regressive cycles within the barred basin (see Chapters 2.1 and 2.2.1).

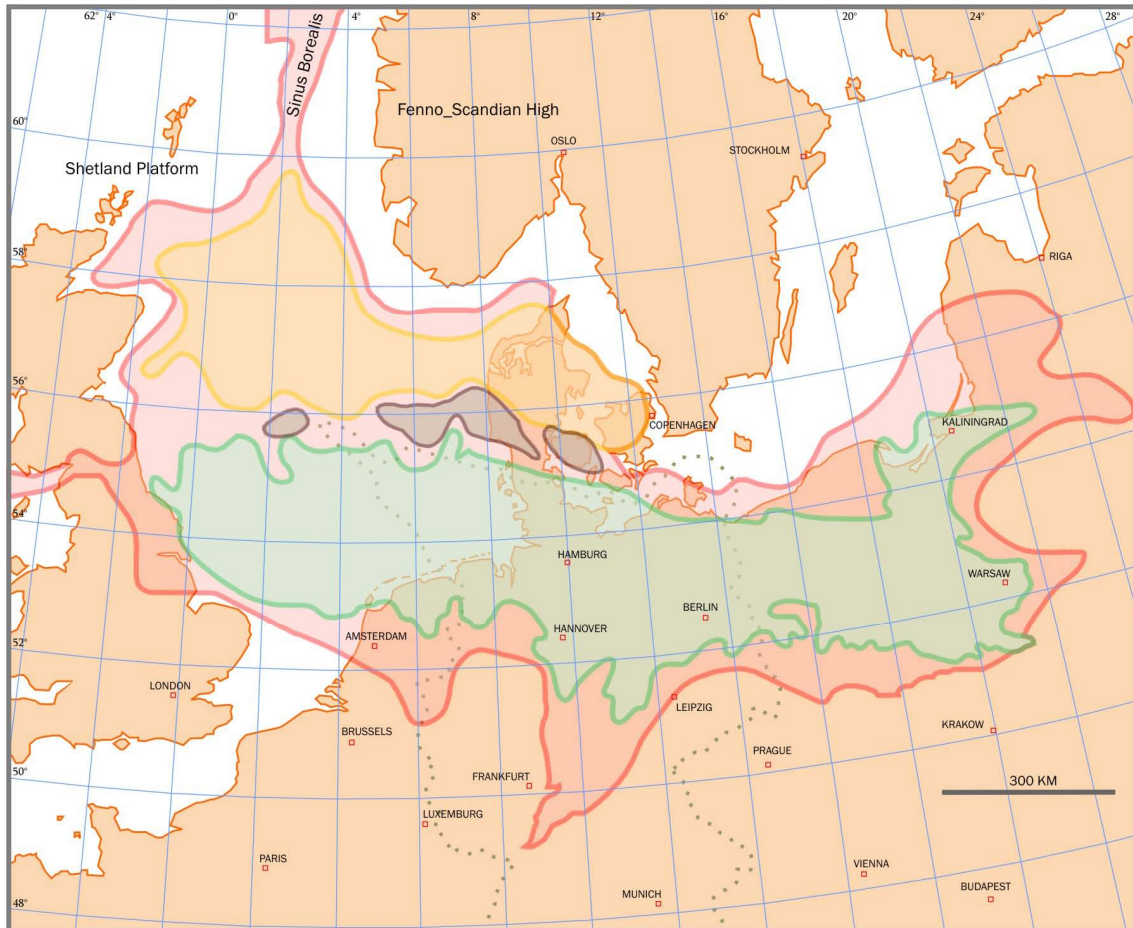


**Figure 2-4:** The Central European Basin (red) with the Northern (yellow) and the Southern (green) basin part and the Ringkøbing-fyn-high (grey) (modified after ZIEGLER 1990).

At the Permian-Triassic boundary (251 My BP) the Zechstein sedimentation was impeded by increasing clastic sedimentation due to rift activities, tectonic instabilities and thermal subsidence at the reactivated Arctic-North Atlantic rift system (ZIEGLER 1990). The Tethys sea transgraded from the South into the basin, caused by rising sea levels which originated from the deglaciation of the polar regions due to global warming probably induced -but at least coincided- by the eruption of the Siberian

Traps (RENNE & BASU 1991, KAMO et al. 2003). The sedimentation of the Lower Triassic *Buntsandstein* within the Buntsandstein Sea commenced with broad clastic deposits fed by the erosion of the Variscian Mountains (ZIEGLER 1990). The Lower Buntsandstein deposits conformably overlay the Zechstein sediments, thus indicating a continuous sedimentation (SCHOLLE et al. 1995).

### 2.2.1 Sedimentation of the Seven Zechstein Folgen

The deposition of seven evaporitic cycles was preceded by the final Rotliegend deposits, which influenced the lowermost Zechstein sediments in their chemical character. During the Upper Rotliegend, the area that would become flooded by the Zechstein Sea was lowland covered by meager vegetation. Latest Upper Rotliegend and earliest Zechstein sediments are characterized by bleached sediments. The bleaching is probably caused by rotting plants covering the lowland. Periodic precipitation facilitated the bleaching process: the water drained the dried soil and formed weathering solutions, which took up metals (in particular copper) from soil and rocks and relocated them to the earth's surface, where the water evaporated and the metals formed thin crusts, the *Rasenkupfersteine*, constituting the final deposits of the Rotliegend (FULDA 1935).

The basal Zechstein layer, the *Zechsteinkonglomerat*, is not a transgression conglomerate, but already covered the basin prior to flooding and was cemented by an initial carbonate precipitation after the flooding of the basin. In some places, the carbonate thickness exceeds the conglomerate layer. This micritic carbonate bed is called the *Mutterflöz* (FULDA 1935, STROHMENGER 1996). It was covered by the *Kupferschiefer*, which is a thin bed of marl and euxinic shales with finely distributed sulfidic ores transferred upwards from the Rasenkupfersteine (FULDA 1935).

Due to the 'basin and schwellen' topography of the basin (Figure 2-1) the Kupferschiefer shows different facies at the schwellen, varying from black and red shales to fossiliferous dolomites (PAUL 1986). Since the onset of the first 'Folge' (cycle) of the Zechstein sequence is characterized by only thin beds of the Kupferschiefer, the initial flooding of the Zechstein Sea must have been catastrophic. A smooth evolution

should have resulted in thick beds of clastic sediments. Therefore, prior to the flooding the basin bottom was probably already lower than open sea level and subsided further after the flooding due to the extra load of the water (see Chapter 2.2).

On top of the Kupferschiefer, the carbonate sedimentation formed the *Zechsteinkalk* (*CaI*), a carbonate containing up to 95% of calcite and dolomite, respectively (FULDA 1935). The basin rim was dominated by reefs and biogenic sediments. In the course of the Zechsteinkalk deposition, a regression caused the advance of the *schwellen* above sea level. Thick anhydrite layers at the *schwellen* increased the relief, which was balanced later on by vast rock salt deposition (PAUL 1986).

Seven evaporitic precipitation cycles were deposited during the Zechstein stage (Figure 2-2). All cycles represent an evaporation-driven enrichment of the seawater, with initial carbonate deposition followed by several types of evaporites according to the quinary phase system (see Chapter 5.7), driven by the increasing density of the seawater and the solubility of the salts, respectively. This change in density is directly dependent on the stage of evaporation. After LÖWENGART (1922), the following salt types precipitate with increasing water densities  $\rho$  [g/cm<sup>3</sup>]:

- › 1.00-1.155 Ca-carbonates (aragonite, calcite, diagenetic dolomite)
- › 1.155-1.22 gypsum ( $\text{CaSO}_4 \times 2 \text{H}_2\text{O}$ , later desiccated to anhydrite  $\text{CaSO}_4$ )
- › 1.22-1.28 halite ( $\text{NaCl}$ )
- › 1.28-1.32 carnallite ( $\text{KMgCl}_3 \times 6 \text{H}_2\text{O}$ )
- › 1.32-1.35 other MgCl-salts (e.g. bischofite,  $\text{MgCl}_2 \times 6\text{H}_2\text{O}$ )

The actual sequence of each precipitation cycle was driven by temporal input of very small volumes of seawater probably related to higher-order glacio-eustatic sea level variations (STROHMENGER 1996). The varying water input led to a sequence with various subcycles of alternating sodium- and potassium salts (progressive phase). This phase is usually followed by a fast and extensive transgression that induces a clastic sedimentation and a reversal of the precipitation order up to the end of each cycle (rezessive phase). Depending on the degree of dilution of the remaining seawater

solution, the deposits of this phase normally include salt clay, anhydrite and rock salt (HERRMANN 1981).

For more information on the marine minerals see Chapter 5.2 and Appendix I.

The vast evaporite sedimentation in the Zechstein Basin needed an arid, continental climate comparable to today's sub-tropical environments, such as the Persian Gulf (ALSHARHAN & KENDALL 2003, SACHSE et al. 2004). Dry and hot conditions stabilize the highly hygroscopic potassium- and magnesium salts that form the final stage in each progressive phase of a cycle. Especially MgCl-solutions hold strongly on to water, causing a very low water vapor pressure. Since MgCl-salts are also present in the Zechstein sediments, the Zechstein Sea must have been surrounded by a desert with almost no runoff. Very dry conditions are also supported by the lack of major clastic beds within the cycles. However, sporadic vegetation must have been present since some beds of salt clay and other salts contain pollen (gymnospermae, ginkgo, pteridospermae, pteridophytae), which might have been distributed by eolian transport (FULDA 1935; ECKE & LÖFFLER 1985).

### **2.3 Present - the Central European Basin**

The areal extension of the Central European Basin can be determined via the occurrence of the Zechstein strata. The Zechstein belt extends from West to East for 1600 km, with a North-South width of 300-600 km. The area exceeds 700,000 km<sup>2</sup>. The primary thickness of 600 m to 2000 m was condensed by sedimentary overburden to up to 1200 m. The total basin volume may exceed 153,000 km<sup>3</sup> with a share of the economic most important potassium salts of 1.4 % (ZHARKOV 1981, 1984).

The Zechstein deposits are developed horizontal or in diapirs, which are to be found mainly in the NW German Basin and the area below the North Sea.

Today, only the northernmost parts of the former Central European Basin are covered by water, the North Sea and the Baltic Sea. The majority of the former Central European Basin was uplifted during the orogeny of the Alps in the Tertiary (LAUBSCHER

1988). Meanwhile, a new basin was formed south of the orogen, in which the Mediterranean Sea is located today.

### 2.3.1 Modern Geologic Appearance in Germany

The area in between the Alps and the North Sea and Baltic Sea, respectively, is characterized by the glacial Northern German Lowlands, and the Middle German mountains, built up mainly by Tertiary volcanism (KNIPPING 1987). Both landforms give no visual evidence for the salt deposits to be found about 500 m below surface. Outcrops of the Zechstein facies can be found at the margins of several mountain chains, like e.g. the Harz Mountains, the Thuringian Forest and the Rhenish Slate Mountains, which were uplifted before or after the Zechstein deposition, respectively. Most of the Zechstein deposits are covered by the Buntsandstein (central Germany) with the Tertiary volcanics unconformably on top. In northern Germany the Zechstein deposits are conformably covered by the complete Mesozoic and Cenozoic sequence topped by Quaternary clastic material (northern Germany).

### 2.3.2 Aquifers below, within, and above the Zechstein series

The aquifers in the vicinity of the Zechstein deposits are the sources for most the external seepages evaluated in this study. Here, the most important aquifers in the vicinity of the Zechstein deposits are the ones below and within the Upper Rotliegend, directly within the Zechstein deposits in the carbonates of the *Ca1* and *Ca3* (Figure 2-2), as well as within and above the Buntsandstein. Additionally, several jointed, karstic, and porous water aquifers are located in the Mesozoic and Cenozoic strata of northern Germany (VIERHUFF et al. 1981).

The Rotliegend below the Zechstein deposits contains several confined joint aquifers in a matrix of sandstones, mudstones, marlstones or limestones.

The aquifers within the Zechstein strata in the carbonates of *Ca1* and *Ca3* are carstic aquifers. The matrix is mainly limestone or dolomite, respectively, and the thickness can exceed 150 m (VIERHUFF et al. 1981).

The Buntsandstein aquifers are located in the lower and middle part of this unit. Those joint aquifers within massive sandstones can reach a thickness of more than 500 m (VIERHUFF et al. 1981). Direct recharge from the surface is negligible since the upper formation of the Buntsandstein, the *Röt*, serves as an aquiclude due to its clayey character (GEYH & RAMBOW 1997).

In those aquifers described above, the groundwater can normally contain up to 200 mg/l chloride due to subsidence of the surrounding salts and immersion of disposal brine. For detailed regional information about the aquifers and the groundwater see Chapter 3.3.

#### **2.4 Future - Resources**

The Zechstein potassium salts are unique in their large proportion of sulfates. The potash seams of the Werra- and Staßfurt-Folge as well as the potash seam Bergmannsseggen of the Leine-Folge contain a share of 18% of sulfate minerals, mainly kieserite and langbeinite, and minor amounts of kainite, glaserite, leonite, and polyhalite. Only few potash sequences in the world contain such sulfate-type salts. The major amount of potash seams is typically built up by chloride-type salts, which are lacking in  $MgSO_4$  due to bacteriological or chemical processes. The uniqueness of the sulfates makes the German Zechstein deposits especially valuable as fertilizer ( $K_2SO_4$ ) and for several industries, such as chemicals producers (ZHARKOV 1981).

Most of the Zechstein deposits in Germany are still unexploited. Only minor amounts of the total workable volume are mined yet and the supply of  $K_2O$  and  $K_2SO_4$  for the world market will last for at least the next century (BEER 1996).

### 3. SAMPLES – Encoding, Sampling, and Regional Geology

Due to practical reasons, the mine localities will be given encoded in the following. This way, the reader can easily identify and distinguish between the regions where several seepage sites, shafts, and aquifers were sampled. The precise sampling location is not important for this study.

Upon request, information on the localities may be provided by the Geology Division at the K+S Aktiengesellschaft.

#### 3.1 Encoding Key for Seepage Sites in German Rock Salt and Potash Mines

The following key was used to encode the seepage sites:

- HE, TH, LS, NW, SA = Federal States Hesse, Thuringia, Lower Saxony, North-Rhine Westphalia, Saxony-Anhalt
- Numbers 1-5 = sampled mines of each federal state
- 'Qu 30/31' = actual site name used by the mining company

All samples from shafts will be endorsed with 'shaft'. Boreholes are indicated by b1 to b11. A complete list of the sampling sites can be found in the Tables 3-1 and 3-2.

#### 3.2 Sampling of Saline Solutions

Within a two year sampling period, 109 liquid samples and 6 subsamples (same day and site, different boreholes) were taken at 18 seepage sites or boreholes and seven shafts in 12 active or inactive rock salt and potash mines located mainly in the northern half of Germany. Additionally, 11 groundwater wells, two rivers, and the rainwater of Göttingen were included. At each site, sampling took place at least once and up to four times per year. At most sites only one sample was taken by the author herself. Otherwise sampling was conducted by the mine staff to reduce the interference with the mining activity.

Three different sampling methods were carried out based on the local circumstances at the seepage site (Table 3-1):

- direct sampling from the wall or from salt stalactites by using a funnel
- indirect sampling from flexible tubes, sumps, or gutters
- sampling from wellheads

Between 100 ml and 3000 ml were transferred into glass or polyethylene bottles. The bottles were filled up to the brim and closed immediately after sampling to avoid air contamination. If available, temperature and density were measured on-site electronically or by a mercury thermometer and a density spindle.

| System         | Group                 | Ma  | Hydrogeology   | Hydraulics   |
|----------------|-----------------------|-----|--|--|
| QUART.         |                       |     | Unconsolidated silicic rock (gravel, sand, silt)             | Aquitards and pore water aquifers with high permeability, partly confined              |
| TERTIARY       | Neo gene              | 1.8 | Fluvial to lacustrine clay and silt sequences                |  |
|                | Palaeo gene           |     | Unconsolidated clay, marl, sand and clastics                 | Aquicludes and pore water aquifers   |
| CRETA<br>CEOUS | Upper                 | 65  | Limestone  | Karstic aquifers   |
|                | Lower                 |     | Marlstone, sandstone   | Fissure aquifers   |
| JURASSIC       | Upper                 | 142 | Limestone, marlstone, clay                                   | Karstic aquifers   |
|                | Middle                |     | Limestone, marlstone, clay                                   | Karstic aquifers   |
|                | Lower                 |     | Limestone, marlstone, clay                                   | Karstic aquifers   |
| TRIASSIC       | Keuper                | 200 | Mudstone, marlstone, gypsum, dolostone, limestone, sandstone | Aquitards and fissure aquifers with low permeability                                   |
|                | Mu<br>schel<br>kalk   |     | Limestone, dolostone, marlstone, mudstone                    | Aquicludes, fissure and karstic aquifers with medium to low permeability,              |
|                | Bunt<br>sand<br>stein |     | Sandstone, mudstone  | Aquicludes, aquitards and fissure aquifers with changing permeability, partly confined |
| PERMIAN        | Zech<br>stein         | 251 | Ca3: lime- and dolostone                                     | Joint- and pore water aquifer with high permeability, partly confined                  |
|                | Rotlie<br>gend        | 296 | Sandstone, mudstone, marlstone, limestone                    | Joint aquifers with mostly low permeability, confined                                  |

**Figure 3-1:** The hydrogeology of northern Germany (not all formations are developed in all areas; modified after VIERHUFF et al. 1981, SCHECK & BAYER 1999, SKOWRONEK et al. 1999, GERMAN STRATIGRAPHIC COMMISSION 2002).



### 3.3 Sampling Sites and Regional Hydrogeologic Features

The following section focuses on the regional aspects of the geology and hydrogeology of each sampling site. A general overview for the Zechstein Basin is given in the Chapters 2.3.1 and 2.3.2.

The hydrogeology in the vicinity of the mines is generally characterized by a system of extensive groundwater levels with aquifers of different properties within uppermost Paleozoic (Permian), Mesozoic and -in Lower Saxony and North Rhine-Westphalia- Cenozoic deposits. The relative stratification of the aquifer system as well as the hydrogeologic and hydraulic features of each storey are shown in Figure 3-1.

Stratigraphic columns of the Zechstein facies for several regions can be found in Figure 3-2, a detailed stratigraphic chart of the Zechstein and the surrounding formations is shown in Figure 2-2.

#### 3.3.1 Hesse

Four boreholes as well as three shafts and four seepage sites in the mines HE 1 and HE 2 were sampled in North Hesse. The region belongs to the structural area of the East-Hessian 'Buntsandstein-Block' (EU water framework directive area 05201; FRITSCHÉ et al. 2003).

The northern Hessian Zechstein deposits show a horizontal stratification. The supra-Zechstein rocks at HE 1 and the Hessian boreholes are composed of up to 1100 m of mainly Triassic and sparse Cenozoic deposits. Material of all seven 'Zechstein-Folgen' (cycles) was deposited in this marginal basin, which was separated by a 'Schwelle' from the main part of the Zechstein Basin. At HE 2, the overburden does not exceed 550 m and consists of only Triassic sediments. Almost the same sequence like in the HE 1 region, but with lower rock salt thickness, was deposited in this southernmost part of the Zechstein Basin, separated from the north by the graben of Fulda-Großenlüder (KÄDING & SESSLER 1994).

The local joint aquifer system is associated with silicic rocks of the Lower (*su*) and Middle (*sm*) Buntsandstein (Figure 3-1). The permeability of these silicic rocks increases in zones of salt subsidence or at faults zones.

**Table 3-1:** List of encoded site names with information on location, stratigraphy (at the emersion point within the mine openings, or at the perforated section of a borehole, respectively), and sampling.

| Region | Site name            | Stratigraphy                             | Formation/Cycle  | Sampling   |
|--------|----------------------|--|------------------|--|
| RW 1   | RW 1 Gö              | -  | -                | sampled on roof of geology building                                    |
| RW 2   | RW 2 Ulster          | -  | -                | river  |
| RW 3   | RW 3 Werra           | -  | -                | river  |
| HE 1   | HE 1 N81             | K1H / Na1Y                               | Werra            | soda straws from ridge   |
| HE 1   | HE 1 Shaft H 546 m   | Ca3                                      | Leine            | gutter at inleakage from tubbing                                       |
| HE 1   | HE 1 Shaft R 555 m   | Ca3                                      | Leine            | gutter at inleakage (555m) from tubbing, or from container at 1. Level |
| HE 2   | HE 2 103 n. N        | K1H                                      | Werra            |  |
| HE 2   | HE 2 70.SE 141/71    | Na1                                      | Werra            |  |
| HE 2   | HE 2 Loch 1/87       | ro                                       | Rotliegend       | sampling from borehole   |
| HE 2   | HE 2 Shaft E         | su                                       | Buntsandstein    |  |
| TH 1   | TH 1 Ort 90 n. N     | Na1α/b/K1Th                              | Werra            | scooped from brine pool oozing out of level ground                     |
| TH 2   | TH 2 Qu 23 HZ 11     | Na1α, fed from ro                        | Werra/Rotliegend | tap at the feed pipe from sub-saliniferous                             |
| TH 2   | TH 2 HZ 207 E        | Na1α, fed from ro                        | Werra/Rotliegend | sampling from borehole   |
| TH 2   | TH 2 Qu 30/31        | K1H                                      | Werra            | leakage from roof, sampled from bucket below stalactites               |
| TH 2   | TH 2 Qu86 HZ 119     | Na1α, from gneiss below ro               | Werra            | Borehole chamber for SLV Qu. 86, overfall weir from borehole           |
| TH 2   | TH 2 Qu86 HZ 108     | Na1α                                     | Werra            | inflow from sub-saliniferous at Ort 19, collected by borehole 108      |
| TH 3   | TH 3 4. südl. Abt.   | Na1α/K1Th, welling up through basalt     | Werra            |  |
| TH 3   | TH 3 Shaft 1.543 m   | Ca3                                      | Leine            | pipeline through tubbing segment 14-2/3                                |
| LS 1   | LS 1 H23 470 m       | A3                                       | Leine            | on scaffold from several boreholes                                     |
| LS 1   | LS 1 H23 500 m       | A3                                       | Leine            | sampling from boreholes with standing brine                            |
| LS 1   | LS 1 CN 8/9          | T3/A3                                    | Leine            | leakage from roof, collection by funnel                                |
| LS 2   | LS 2 Shaft 2 104 m   | ju (overlying rock), Münder Mergel       | Jurassic         | gutter at inleakage from tubbing                                       |
| LS 2   | LS 2 Shaft 1 160.5 m | ju (overlying rock), grauer/roter Mergel | Jurassic         | leakage from shaft, collected via PE-tube at lower level in reservoir  |
| LS 3   | LS 3 353 m S. R.     | A3                                       | Leine            | leakage from ridge, collection by funnel on scaffold                   |
| LS 4   | LS 4 Shaft 2 140 m   | Salt surface/gypsum                      |                  | sampling from tap, collected behind tubbing                            |
| LS 5   | LS 5 UB 784          | T5r/T6                                   | Ohre-Friesland   | sampling from cased borehole   |
| LS 5   | LS 5 L499            | Na3η                                     | Leine            | sampling by tarp (5x5m2) with drain in the middle                      |
| LS 5   | LS 5 UB 810          | inflow from adjoining Röt                | Buntsandstein    | sampling from borehole   |
| NW 1   | NW 1 KA 162          | Na1α                                     | Werra            | scooped from brine pool  |
| SA 1   | SA 1 WQ17/W172       | A3                                       | Leine            | sampling from open fissure via PE tube                                 |

Below the Buntsandstein, but above the workable Zechstein deposits, one semi-confined aquifer is located within the karstified ‘*Plattendolomit*’ (*Ca3*, platy dolomite) of the ‘*Leine-Folge*’. Its groundwater takes up large amounts of dissolved solids by salt leaching and saline process water immersion. The overlying rock is partially brecciated by ongoing salt subsrosion, resulting in upwelling of mineralized water through fissures. In areas with advanced subsrosion depressions, the overlying rock forms residual breccias which can act as aquiclude (FRITSCHE et al. 2003).

**Table 3-2:** Sampled boreholes in Hesse and Thuringia.

| Region | Location             | Borehole name | Stratigraphy                             | Formation/Cycle      | Sampling       |
|--------|----------------------|---------------|--|----------------------|----------------|
| TH b1  | Sampling depth 95 m  | TH b1 130     | Ca3                                      | <i>Leine</i>         | well           |
| TH b2  | Sampling depth 70 m  | TH b2 111     | su, subsrosion water from pr             | <i>Buntsandstein</i> | well           |
| TH b3  | Sampling depth 175 m | TH b3 3       | su (lowermost)                           | <i>Buntsandstein</i> | well           |
| HE b4  | Sampling depth 135 m | HE b4 389     | su                                       | <i>Buntsandstein</i> | tap            |
| TH b5  | Sampling depth 90 m  | TH b5 45      | Ca3                                      | <i>Leine</i>         | well           |
| TH b6  | Sampling depth 210 m | TH b6 114     | Ca1                                      | <i>Werra</i>         | well           |
| TH b7  | Sampling depth 235 m | TH b7 115     | Ca3                                      | <i>Leine</i>         | well           |
| TH b8  | Sampling depth 80 m  | HE b8 346     | su (influenced by waste water disposal)  | <i>Buntsandstein</i> | well           |
| HE b9  | Sampling depth 870 m | HE b9 430     | Ca3 (influenced by waste water disposal) | <i>Leine</i>         | well           |
| HE b10 | Sampling depth 100 m | HE b10 528    | su (influenced by waste water disposal)  | <i>Buntsandstein</i> | packer in well |
| HE b11 | Sampling depth 518 m | HE b11 431    | pr                                       | <i>Rotliegend</i>    | well           |

***Boreholes (and wells)***

The aquifer system in the northern Hessian and western Thuringian salt mining area is under constant surveillance by numerous observation wells since the aquifer within the *Ca3* is used for disposal of saline waste water (SKOWRONEK 1999). The wells are drilled down into the aquifers of the Lower Buntsandstein, the *Ca3*, and the Rotliegend (*pr*, lower part of the European upper Permian *Dyas*, below the Zechstein).

During the semi-annual to annual routine sampling events, separate samples from 11 boreholes were taken twice for isotope analyses. Since some of the wells are artesian wells, the sampling is either conducted by using a special depressurizing tool or by lowering packers into the boreholes. The sampled boreholes are listed in Table 3-2 (pers. comm. Dr. S. Kluge, K+S Group, 2006).

***Mine HE 1***

Two shafts and one seepage site were sampled in the potash mine HE 1. Both shafts HE 1 Shaft H 546 m and HE 1 Shaft R

555 m show inleakages of saline groundwater from the *Ca3* aquifer, which is penetrated by both shafts at 546 m and 555 m below surface, respectively (Figure 3-2). The liquid is trapped via circular gutters and drained into containers at the levels below. Direct sampling is only possible under special security measures (pers. comm. S. Gierenz, M. Nitschke, K+S Group, 2006).

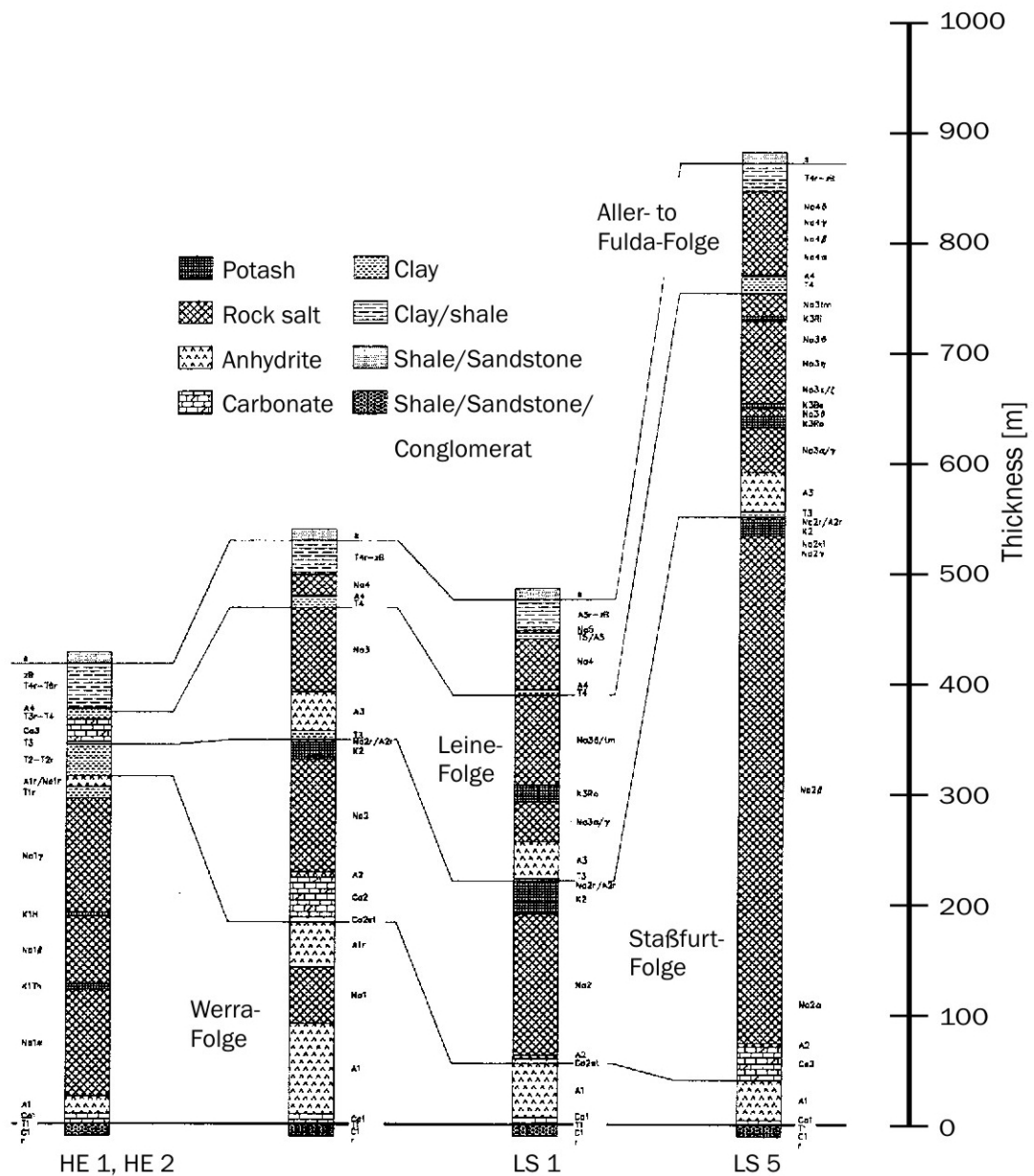


**Figure 3-2:** Stratigraphic columns of the Zechstein facies for the mines HE 1, HE 2, LS 1, LS 5 and NW 1 (modified after BEER 1996; see Figure 2-2 for abbreviations).

The internal seepage site HE 1 N81 (Revier 8, 160. Durchhieb) drains the potash seam *Hessen* and the *Upper Werra* rock salt (*K1H* and *Na1y*; Figure 2-1) of the ‘*Werra-Folge*’. The liquid leaks from the roof and leaves salt stalactites from which it is collected into a reservoir (pers. comm. U. Fischer, K.-H. Voigt, K+S Group, 2006).

### ***Mine HE 2***

In the potash mine HE 2 several small seepages are intermittent. Only one permanent seepage site has been observed. Due to their transient nature the two internal seepages HE 2 103 n. N and HE 2 70. SE 141/71 in the Werra rock salt could only be sampled once (Figure 3-2).

The shaft inleakage from the Lower Buntsandstein aquifer penetrated by shaft HE 2 Shaft E was sampled only once as well.



**Figure 3-3:** Well monitored seepage site HE 2 Loch 1/87.

The major seepage site at HE 2 Loch 1/87 has been sieved by several dozen drillings since its first occurrence. Unnecessary drillings were filled with different materials, such as Polythixon resin or Portland cement. Samples were taken directly from the borehole 1/87 shown in Figure 3-3. For this site, an external origin from the Rotliegend aquifer is proposed (pers. comm. Dr. R. Stax, O. Jungmann, K+S Group, 2006).

### 3.3.2 Thuringia

In Thuringia, three mines with five seepage occurrences and one shaft were sampled. The Thuringian depression (EU water framework directive area 05402; FRITSCHÉ et al. 2003) shows similar hydrogeologic features as the Hessian region (see Chapter 3.3.1), but additionally, the Buntsandstein is covered with the Middle Triassic *Muschelkalk* (*m*, mainly limestone). Within the Middle Muschelkalk *mm*, several aquifers can be found in karstic or fractured dolomites and limestones (Figure 3-1).

For a description of the Thuringian groundwater boreholes see Chapter 3.3.1.

#### ***Mine TH 1***

The potash mine TH 1 shows only one major internal seepage site at the second level, the TH 1 Ort 90 n. N (NE-Feld, 6. E-Abfahrt). It drains the potash seam *Thüringen* and the adjoining Lower/Middle Werra rock salt (*K1Th* and *Na1 $\alpha$ , $\beta$* , Figure 2-2). The liquid oozes out of the level bottom and has to be scooped from a pool by using a bailer (pers. comm. M. Pippig, K+S Group, 2006).

#### ***Mine TH 2***

Two of the three seepage sites at the potash mine TH 2 are controlled via several drillings (HZ = horizontal drilling), and thus sampling is from those.

At each external site two boreholes were sampled: TH 2 Qu 23 by HZ 11 and HZ 207E (Qu 23 n. W, 1. level), and TH 2 Qu 86 by HZ 108 and HZ 119 (Qu 86 n. S, Ort 18 n. S, 2. level). All of these boreholes penetrate the *Na1 $\alpha$*  and collect liquid welling up from gneiss of the bedrock below the Rotliegend, or directly from the Rotliegend, respectively.

The seepage site at TH 2 Qu 30/31 (2. level) drains the *K1Th* (Figure 2-1). Here, the saline solution drips down from the roof and leaves a curtain of stalactites from which the liquid is collected in a container. Whether it is of internal or external origin is not yet determined (pers. comm. M. Pippig, Dr. W. Beer, K+S Group, 2006).

### ***Mine TH 3***

Two samples were taken at TH 3 Shaft 1 543 m from an inleakage of the *Ca3* aquifer through the shafts tubing segment 14-2/3 at 543 m below surface.

The major seepage site TH 3 4. südl. Abt. (2. level, 4. südl. Abt. n. E) wells up through a basalt dike which intruded in the Tertiary into the *Na1 $\alpha$*  and *K1Th* layers (pers. comm. S. Gierenz, M. Nitschke, K+S Group, 2006).



Figure 3-4: Boreholes at the internal seepage site LS1 H23 on the 470 m level  
(Photo U. Argut).



### 3.3.3 Lower Saxony

The mines LS 1 to 5 in Lower Saxony are located within the North-Western German highlands and the adjacent Northern German Middle Pleistocene lowlands (EU water framework directive areas 051 and 015; ELBRACHT et al. 2007). The highlands were formed by brittle block tectonics induced mainly by salt diapirism since the Jurassic. Therefore, Cretaceous, Tertiary, and Quaternary sediments were deposited in depressions between the Jurassic ridges. The main aquifers in the highlands are situated in the Lower Buntsandstein and the Middle Buntsandstein as well as in the limestone deposits of the Muschelkalk, and in the Middle Jurassic *Cornbrash*-sandstone and Upper Jurassic limestones. The lowlands were formed during the Quaternary glaciation periods when the northern inland ice advanced to the South. In places, the glaciers eroded the highlands down to the Cretaceous, and build up to 500 m thick morains. A variety of aquifers is located within the moraine deposits of the lowlands. Towards the highlands these numerous aquifers reduce to only one developed aquifer, which shows decreasing thickness towards the end moraine (ELBRACHT et al. 2007).

#### ***Mine LS 1***

The inactive potash mine LS 1 has three seepage sites. Two of the seepage sites have the same internal origin within the ‘*Hauptanhydrit*’ anhydrite (*A3*) of the Leine-Folge (Figure 3-2). This site LS 1 H 23 shown in Figure 3-4 drains into two levels at 470 m and 500 m. Sampling via funnel is possible from several boreholes (pressures up to 40 bar).

The probably external seepage site LS 1 CN 8/9 seeps from the *A3* nearby the transition to the ‘*Unterer Leine-Ton*’ clay (*T3*). The liquid drains from the roof, leaving stalactites over an area of several square meters, as to be seen in Figure 3-5. Sampling is only possible by collecting liquid from multiple dripping stalactites with a wide funnel. Air contamination cannot be avoided since the inflow rate is very low and sampling takes several minutes (pers. comm. Dr. S. Zeibig, U. Argut, K+S Group, 2006).

#### ***Mine LS 2***

In the rock salt mine LS 2 only two shafts were sampled. Both shafts penetrate the Jurassic and its carbonatic aquifers.



LS 2 Shaft 1 160.5 m shows an inleakage at 160.5 m from the *'grauer/roter Mergel'* marl. Sampling is only possible from a reservoir at the next lower level to which the liquid is directed via a PE tube. Therefore, air contamination and influence by evaporation effects cannot be avoided.

At LS 2 Shaft 2 104 m the inleakage occurs at a depth of 104 m from the Jurassic *'Münder Mergel'* marl. Sampling is directly from the gutter at the penetrated tubing segment (pers. comm. S. Gierenz, L. Puszczak, K+S Group, 2005).



Figure 3-5: The probably open seepage site LS1 CN 8/9 on the 350 m level at discovery before monitoring (Photo U. Argut).

### ***Mine LS 3***

One internal seepage site is sampled in the potash mine LS 3 at site LS 3 353 m S. R. (353 m below surface). The liquid drips out of the *A3* from a high roof and is collected via a wide funnel in a reservoir below. The reservoir is drained frequently, also shortly before sampling, therefore

contamination by older or evaporated liquid is unlikely, but air contamination is probable (pers. comm. U. Argut, K+S Group, 2005).

#### ***Mine LS 4***

The shafts of the inactive mine LS 4 were sealed recently, thus the sampled inleakage from LS 4 Shaft 2 140 m could only be sampled once. The liquid drained from the cap rock gypsum at the salt surface and was collected from a tap at 140 m (pers. comm. Dr. S. Zeibig, K.-H. Heinemann, K+S Group, 2005).

#### ***Mine LS 5***

Special attention must be paid at the major seepage site of the potash mine LS 5 since the inflow rate at the external site LS 5 L499 from the '*Leine Steinsalz*' rock salt ( $Na_3\eta$ ) is reduced by the borehole LS 5 UB 784, drilled into the '*Oberer Ohre-Ton/Friesland-Ton*' clays ( $T5r/T6$ ) (Figure 3-2). It was targeted in the predicted direction of the inflow's origin to directly draw off the liquid upstream the seepage site into a reservoir. This way the widening of the flow path and the increase in the inflow rate at the original seepage site is minimized. Another drilling is sampled at LS 5 UB 810, which drains the '*Röt*' clay of the Lower Buntsandstein that forms the adjoining beds of the salt dome (pers. comm. Dr. R. Holländer, K+S Group, 2005).

### **3.3.4 North Rhine-Westphalia**

One mine, NW1, is located within the southern Lower Rhine depression (EU water framework directive area 02). Here, the horizontally lying Zechstein rocks deposited in a lagoon are covered by Mesozoic strata. Aquifers are developed in deposits of the Rotliegend, the Plattendolomit, and the Buntsandstein (see previous Chapters). Since the Tertiary, only unconsolidated rocks were deposited in a changing environment of continental and marine facies. The depression was formed by brittle block tectonics mainly after the Miocene. Five blocks were separated by NNW-SSE striking faults and evolved differently, leading to diverse hydrogeologic conditions. Several aquifers with unconsolidated matrix are developed that are separated by clay, silt and lignite that act

as aquitards. Some are pinching out or are divided due to changing facies of the aquitards or vertical movements of the blocks (HILDEN 1988).

#### ***Mine NW 1***

The external seepage at location NW 1 KA 162 in the rock salt mine NW 1 drains the Lower Werra rock salt ( $NaI\alpha$ ) and wells up through the bottom at approximately 900 m depth. The samples were scooped from a brine pool, and therefore air contamination and evaporation effects cannot be excluded (pers. comm. Dr. F. Becker, K+S Group, 2006).

### **3.3.5 Saxony-Anhalt**

The geology of Saxony-Anhalt (EU water framework directive area 05) is affected by extensive SE-NW block tectonics in the Upper Rotliegend, thus following the saalic movement directions of the Variscic orogeny of the Devonian/Carboniferous (ZIEGLER 1990; RADZINSKI 1995). After a settlement of the relief, the Germanic Basin subsided and was flooded by the Zechstein Sea. The lower five evaporitic sequences z1 to z5 were deposited here (Figure 2-2). During the Middle Buntsandstein the region underwent severe tectonic movements and the Thuringian-Western Brandenburg-depression was formed and covered by Mesozoic strata. In the Cenozoic, mainly unconsolidated rocks were deposited, partly of fluvial or glaciolimnic origin (RADZINSKI 1995).

#### ***Mine SA1***

The one internal seepage site SA 1 WQ17/W172 at the rock salt mine SA 1 is fed by a solution that wells up through a joint in the *A3* from which it can be collected via a PE tube (pers. comm. J. Wendzel, K+S Group, 2006).

# Part II

## Geochemical Background

4. METHODS

5. FROM WATER TO BRINE

#### 4. METHODS- Sample Preparation, Analysis, Errors, and Fractionation

The analyzing procedures for various compounds of highly saline brines need to be adjusted to the salt content of the saline solution samples to avoid composition-driven complications. Largely varying elemental concentrations in brines make the analysis of the different compounds of saline solutions challenging. High concentrations of dissolved salts contaminate the analyzing devices or suppress the water from evaporation due to a reduction in vapor pressure (SONNENFELD 1984). In addition, the activity of stable isotopes in a liquid is affected when salts are present. (see also Chapters 4.1.2 and 5.4.2).

The measurements of stable isotopes, Sr isotopes, tritium, and major and trace cations were performed at various institutions. Preparation and analysis of hydrogen and oxygen were conducted in cooperation with the Umweltforschungszentrum Halle (UFZ), division of Isotope Hydrochemistry. Tritium ( $^3\text{H}$ ) results were also generated at the UFZ. Those tritium analyses were conducted as remittance work, while preparations for the stable isotope measurements were carried out by the author. Sr isotope composition analyses were performed at the Isotope Geology department of the Geoscience Center of the University of Goettingen (GZG) by the author. Analyses of concentrations of main- and trace elements were either conducted prior to this study at the K+S Forschungsinstitut, several laboratories at the mines of the K+S Group, or during the study at the Geochemistry department of the GZG.

A list of all data is given in Appendix II.

##### 4.1 Stable Isotopes

Analyzing saline solutions for hydrogen and oxygen isotope composition involves a two-step preparation process that can be performed simultaneously for both elements. Both purification steps can result in the fractionation of hydrogen and oxygen isotopes and therefore need to be conducted following a strict procedure. The final analysis requires separation and individual measurements optimized for each element.

#### 4.1.1 Preparation and Analysis of Hydrogen and Oxygen Isotopes

In the initial preparation step a vacuum distillation procedure is employed to minimize contamination of- and fractionation within the mass spectrometer. This distillation requires a finely balanced distillery, in which both temperature and vacuum can be adjusted. Figure 4-1 shows a sketch of the distillery used at the Department of Isotope Hydrology of the UFZ. This distillery was assembled and tested to handle highly saline liquid samples. The instrument becomes necessary for samples with an electric conductivity larger than 20 mS/cm. Below that, samples can be analyzed directly.

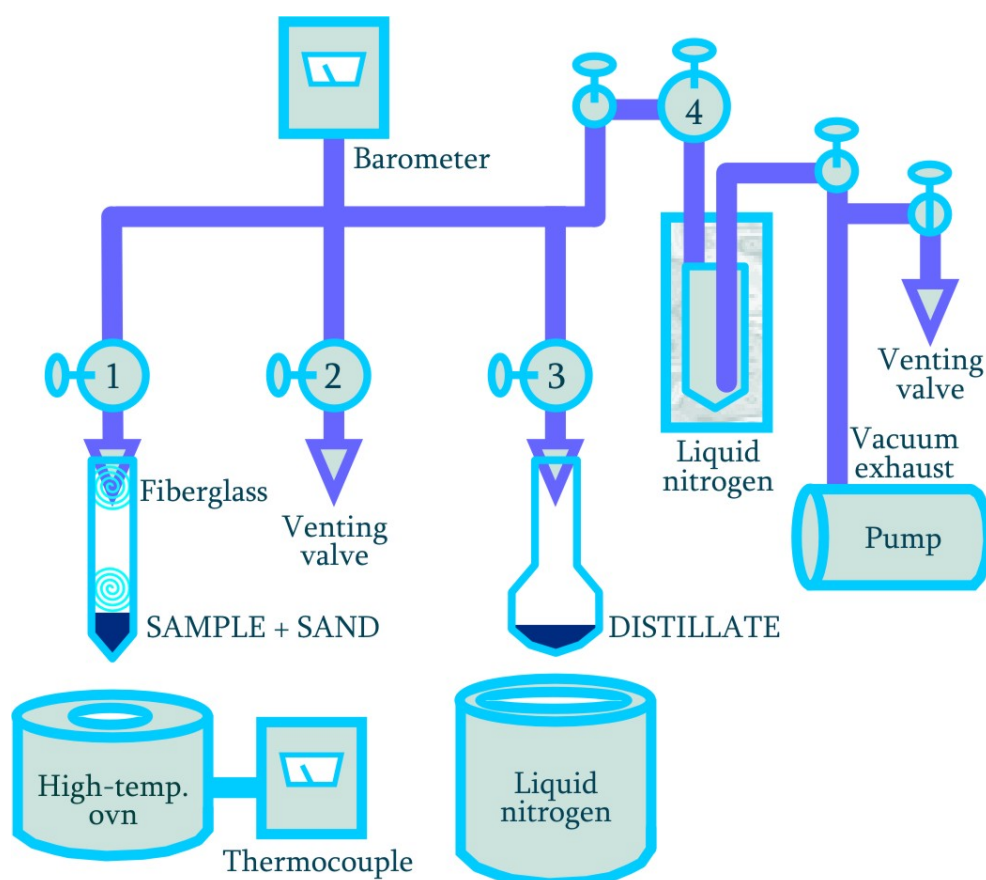


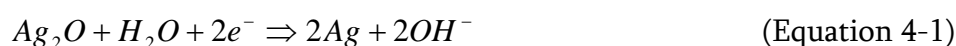
**Figure 4-1:** Distillery used to separate the H<sub>2</sub>O from dissolved solid phases of a saline solution prior to the stable isotope analysis.

For distillation, an aliquot of 1 ml of a sample is applied on a bed of quartz sand (par analysis) in a reagent vessel. Further, the vessel is attached to the distillery (Figure 4-1, port 1) and evacuated. Under ideal conditions, the vacuum reaches 1 Pa. In fact, an acceptable value of 10<sup>1</sup>-10<sup>2</sup> is reached after an appropriate time span of ca. 30 min. The

distillery is evacuated in several steps, ensuring that no sample material is lost through the withdrawn air. Potential loss of material is monitored via a cooling trap upstream of the pump. Lost vapor would freeze on the trap. This trap also serves as a protection for the pump.

After reaching the acceptable vacuum level of ca.  $10^1$  Pa, the vessel including the sample is heated to 600°C within 15 min to ensure complete evaporation of the liquid phase of the sample. The vapor is trapped in a retort cooled by liquid nitrogen (port 3). The remaining salt crystallizes within the quartz sand in the vessel. After reaching the vacuum level prior to evaporation again, and therefore indicating complete evaporation and trapping of the H<sub>2</sub>O, the frozen H<sub>2</sub>O is slowly melted and transferred into a glass vial of 1 ml volume. Pure water samples should evaporate completely, and the trapped liquid should be of the same volume as the used aliquot. For saline solutions the trapped amount of liquid is less than 1 ml due to the high amount of dissolved salts that precipitate during the distillation.

Since the distilled liquids show a pH of 6 down to 1, most of the samples need to be syntonized to a pH of at least 5. This second purification step is necessary to avoid corrosion within the mass spectrometer by the aggressive fluid. Silver oxide (Ag<sub>2</sub>O, black color) is used as neutralizing agent. The following reduction-oxidation reaction is induced by adding Ag<sub>2</sub>O:



Depending on the initial pH of the sample, portions of 50 mg up to 1500 mg are added to the sample until the precipitation of Ag is complete. This complete precipitation is indicated by no further color change (Ag<sub>2</sub>O is black; after complete reaction white to pink, pH still below 5; after incomplete reaction black, pH of  $\geq 5$  is reached). The amount of Ag<sub>2</sub>O used for the samples can be found in Appendix III.

The syntonization with Ag<sub>2</sub>O is exothermic and therefore can cause fractionation of oxygen and hydrogen through evaporation. Thus, a fast and easily closed container is used to minimize vapor loss. After the oxidation is completed and the mixture is cooled down, the container is shaken to remix the sample with its condensed portion. Finally,

the liquid is separated from the particulate Ag by using a membrane tear-through filter with a pore size of 20  $\mu\text{m}$ . The samples are stored in 1 ml glass vials with a membrane lid. These vials are mounted in the sampler of the mass spectrometer.

The analyses of hydrogen and oxygen are conducted via an Isotope Ratio Mass Spectrometer (IRMS) type ThermoQuest Finnigan Delta plus XL at the UFZ. The distilled samples are vaporized in a pyrolysis stove at 1450°C and mixed with continuously flowing helium gas. Then, one portion is directed into the IRMS to measure the hydrogen composition of the sample. The oxygen portion needs to be equilibrated with carbon dioxide ( $\text{CO}_2$ ) first. This mixture runs through a gas separation column to avoid a peak overlap with aerial nitrogen. After this step the oxygen portion enters the IRMS (pers. comm. Dr. K. Knöller, UFZ, 2005).

Both gases are measured quantitatively via scintillation counter. The results are given in delta values  $\delta^{18}\text{O}$  [‰] and  $\delta^2\text{H}$  [‰] which are expressed as

$$\delta^{18}\text{O}[\text{‰}] = \left( \frac{\left( \frac{^{18}\text{O}}{^{16}\text{O}} \right)_{\text{Sample}} - \left( \frac{^{18}\text{O}}{^{16}\text{O}} \right)_{\text{Standard}}}{\left( \frac{^{18}\text{O}}{^{16}\text{O}} \right)_{\text{Standard}}} \right) \times 10^3 \quad (\text{Equation 4-2})$$

$$\delta^2\text{H}[\text{‰}] = \left( \frac{\left( \frac{^2\text{H}}{^1\text{H}} \right)_{\text{Sample}} - \left( \frac{^2\text{H}}{^1\text{H}} \right)_{\text{Standard}}}{\left( \frac{^2\text{H}}{^1\text{H}} \right)_{\text{Standard}}} \right) \times 10^3 \quad (\text{Equation 4-3})$$

Both peaks of hydrogen and oxygen are being automatically calibrated against VSMOW (see next chapter) by using a reference gas in the course of the analysis.

#### 4.1.2 Standards and Errors in Stable Isotope Analysis

The standard commonly used in the analysis of oxygen and hydrogen was the ‘Standard Mean Ocean Water’, called SMOW (CRAIG 1961a). SMOW was a hypothetical water sample with values of  $\delta^{18}\text{O} = 0$  and  $\delta^2\text{H} = 0$ , distributed as NBS 1 by the U.S. National



Institute of Standards and Technology (NISB, former U.S. National Bureau of Standards, NBS) and as SMOW by the International Atomic Energy Agency (IAEA), unfortunately having a slightly different composition (COPLIN 1994). Due to this discrepancy, nowadays one specific mixture of seawater distillates from all over the world is in use as standard and defined as VSMOW by the IAEA in Vienna since 1968. All data collected before 1968, like the 'Global Meteoric Water Line' GMWL (CRAIG 1961b), and also many of more recent data are given in reference to SMOW. Therefore, stable isotope data should be compared with caution. The used standard should be indicated for the samples as well as for the reference data.

Given that hydrogen and oxygen are analyzed after distillation, and therefore from distilled water, the measured unit of both is their concentration (atomic) ratio, not their activity ratio or 'effective concentration'. The effective concentration refers to only those ions that actually participate in a reaction. Since in a saline solution some water molecules are 'in use' for hydration of ions, an analysis of such solution by equilibration methods reaches only those water molecules which do not participate in hydration (TAUBE 1954; SINCERO 2003). Therefore, a fractionation occurs during equilibration, and the results show the effective concentration which differs from the actual concentration by the fractionation factor  $\Gamma$  (SOFER & GAT 1975). Ideally after distillation no hydration of ions occurs and all water molecules participate in the analysis. In this case, the actual concentration is obtained (SOFER 1972). Still, some fractionation occurs during distillation, induced by hydration of ions that leads to incomplete distillation even at high temperatures over several hours (HORITA 1989).

The fractionation factor for brines, as a ratio of the activity coefficients of the heavy and light water isotope species  $R^a/R^c = \Gamma$ , is a function of the salinity. According to SOFER & GAT (1975) the difference  $\Delta\delta$  between the activity ratio  $\delta^a$  and the concentration ratio  $\delta^c$  is

$$\Delta\delta = (\delta^c - \delta^a) / (1000 + \delta^a) \times 10^3 \quad (\text{Equation 4-4})$$

Most of the literature data for oxygen in undistilled brines are on the activity scale if the measurement was conducted by equilibrating the original solution with CO<sub>2</sub>.

## 4.2 Strontium Isotopes

$^{87}\text{Sr}/^{86}\text{Sr}$  isotope analysis of saline solutions requires separation of Sr from other dissolved solids. The conventional method that has been employed here uses chromatographic columns containing pre-conditioned cation exchange resin. The exchange resin has largely varying partition coefficients for the elements dissolved in the solution. These partition coefficients are also strongly dependent on the pH and the kind of acid that is used to flush the column. The procedure described in the following chapter has shown to be efficient for different kinds of samples analyzed at the GZG.

Sr concentrations are determined by isotope dilution, in which a 'spike' solution of known isotope composition is added to the sample. Knowing the spikes isotope composition, as well as the weight of both sample and spike aliquots, allows to back-calculate the original sample Sr concentration. The amount of spike solution added depends on the expected concentration of Sr in the sample.

Highly varying compositions of samples from multiple sampling locations can cause problems during Sr analysis of saline solutions. Especially high concentrations of Rubidium ( $^{87}\text{Rb}$ ), the mother isotope of  $^{87}\text{Sr}$ , can suppress the Sr signal until all Rb is evaporated (DICKIN 2005). This may cause fractionation in the Sr isotopes due to long lasting heating prior to the measurement. One method to minimize this effect will be discussed in the following chapter.

### 4.2.1 Preparation and Analysis of Strontium Isotopes

The analysis of the  $^{87}\text{Sr}/^{86}\text{Sr}$  ratio of saline solutions is challenging for the large range of Sr concentrations (<1 ppm – 350 ppm) observed in the liquids from seepages, shafts and boreholes. Hence, the volume dilution procedure and the isotope dilution (MOORE et al. 1973) with spike Rb-Sr-17 ( $^{84}\text{Sr} = 0.0163032 \mu\text{mol/g}$ ,  $^{86}\text{Sr} = 0.0007073677 \mu\text{mol/g}$ ,  $^{87}\text{Sr} = 0.000323604 \mu\text{mol/g}$ ,  $^{88}\text{Sr} = 0.00282876 \mu\text{mol/g}$ ,  $^{85}\text{Rb} = 0.003949685 \mu\text{mol/g}$ ,  $^{87}\text{Rb} = 0.193536 \mu\text{mol/g}$ ,  $^{87}\text{Rb}/^{84}\text{Sr} = 10$ ) prior to the columnar elution (e.g. CROCK et al. 1984, DICKIN 2005) needs to be adjusted to each sample, depending on the Sr contents:

1.5 ml of a mixture of spiked sample and 2.5 N HCl in a ratio of 1:10 up to 1:150 is centrifuged and afterwards loaded on a quartz column filled with the cation exchange

resin AG 50 WX 8 mesh 200-400. During elution with 2.5 N HCl, the portion of the Sr aliquot is collected after 2 ml more washing acid than the regular 16.5 ml used at the GZG (Appendix IV). The Sr portion is reduced from normally 7 ml to 5 ml to minimize the peak overlap of the Rb and Sr released successively from the resin, in order to avoid high Rb concentrations during measurement.

The collected Sr aliquot is being evaporated at 60°C and afterwards loaded with 2.5 N HCl and a 0.2 N H<sub>3</sub>PO<sub>4</sub> 'bed' on a double Rhenium filament. The analyses are conducted on one of two Thermal Ion Mass Spectrometers (TIMS), type Finnigan TRITON and Finnigan MAT 262 at the GZG.

Samples with only a few ppb Sr were analyzed twice. In the initial analysis the aliquot of spike was too large, as indicated by an <sup>84</sup>Sr/<sup>86</sup>Sr ratio of the sample-spike mixture of higher than 2.5. In such case, the error is higher than usual, since the error on the spike calibration becomes more dominant. However, the determination of the Sr concentration is not affected. To minimize the operating expenses, a second additional run for the <sup>87</sup>Sr/<sup>86</sup>Sr ratio of such samples (<sup>84</sup>Sr/<sup>86</sup>Sr > 2.5) was accomplished without spike. Therefore, the results for the Sr concentration and the <sup>87</sup>Sr/<sup>86</sup>Sr ratio can originate from two different measurements, as indicated in Appendix II.

#### 4.2.2 Standards and Errors in Strontium Isotope Analysis

The standard solution used at the GZG for strontium isotope analysis is NBS 987 (equal to SRM 987) with the certified <sup>87</sup>Sr/<sup>86</sup>Sr ratio of 0.710240. Both instruments at the GZG, the Finnigan TRITON and MAT 262, are calibrated by using this standard solution.

In the course of the liquid analyses, a number of n = 27 standard analyses were conducted to minimize the internal error due to fluctuations within the mass spectrometers (Table 4-1). The standard serves also for verification of the comparability of the analyses conducted on two mass spectrometers. For the measuring period (2005-2007), the mean <sup>87</sup>Sr/<sup>86</sup>Sr value of the measured NBS 987 of 0.710246 ± 0.000012 is in good agreement with the overall mean of standard measurements at the GZG of 0.710258 ± 0.000087. Both values are within an acceptable range of the certified value.

**Table 4-1:** List of standard analyses of NBS 987 over the whole period of measurements, compared to the certified NBS 987 and the GZG mean.

|              | $^{87}\text{Sr}/^{86}\text{Sr}$ | $2\sigma$ error | $^{84}\text{Sr}/^{86}\text{Sr}$ | $2\sigma$ error |
|--------------|---------------------------------|-----------------|---------------------------------|-----------------|
|              | 0.710232                        | 0.000005        | 0.056514                        | 0.000002        |
|              | 0.710257                        | 0.000011        | 0.056478                        | 0.000008        |
|              | 0.710244                        | 0.000006        | 0.056494                        | 0.000004        |
|              | 0.710231                        | 0.000003        | 0.056072                        | 0.000001        |
|              | 0.710178                        | 0.000023        | 0.056385                        | 0.000014        |
|              | 0.710306                        | 0.000016        | 0.056475                        | 0.000012        |
|              | 0.710363                        | 0.000016        | 0.056614                        | 0.000010        |
|              | 0.710254                        | 0.000009        | 0.056510                        | 0.000004        |
|              | 0.710272                        | 0.000012        | 0.056542                        | 0.000007        |
| Triton       | 0.710211                        | 0.000015        | 0.056563                        | 0.000008        |
|              | 0.710204                        | 0.000015        | 0.056665                        | 0.000009        |
|              | 0.710256                        | 0.000019        | 0.056568                        | 0.000013        |
|              | 0.710231                        | 0.000008        | 0.056497                        | 0.000004        |
|              | 0.710159                        | 0.000014        | 0.056486                        | 0.000010        |
|              | 0.710244                        | 0.000007        | 0.056482                        | 0.000004        |
|              | 0.710226                        | 0.000011        | 0.056506                        | 0.000008        |
|              | 0.710295                        | 0.000009        | 0.056447                        | 0.000005        |
|              | 0.710334                        | 0.000016        | 0.056497                        | 0.000010        |
|              | 0.710224                        | 0.000014        | 0.056471                        | 0.000008        |
|              | 0.710210                        | 0.000006        | 0.056514                        | 0.000003        |
|              | 0.710301                        | 0.000012        | 0.056961                        | 0.000009        |
|              | 0.710076                        | 0.000076        | 0.057175                        | 0.000068        |
|              | 0.710237                        | 0.000048        | 0.056865                        | 0.000043        |
| MAT 262      | 0.710349                        | 0.000037        | 0.056971                        | 0.000010        |
|              | 0.710313                        | 0.000039        | 0.057395                        | 0.000024        |
|              | 0.710284                        | 0.000015        | 0.057161                        | 0.000010        |
|              | 0.710255                        | 0.000020        | 0.057184                        | 0.000015        |
| Total: 27    | 0.710246                        | 0.000012        | 0.056489                        | 0.000007        |
| Triton mean  | 0.710246                        | 0.000012        | 0.056489                        | 0.000007        |
| MAT 262 mean | 0.710259                        | 0.000035        | 0.057102                        | 0.000026        |
| Certified    | 0.710240                        |                 | 0.056490                        |                 |
| GZG mean     | 0.710258                        | 0.000087        | 0.056520                        | 0.000110        |

To minimize the error due to mass fractionation during analysis, the raw data of standards and samples were evaluated and normalized by using Rayleigh (deduced) law (HABFAST 1998) and the natural  $^{88}\text{Sr}/^{86}\text{Sr}$  ratio of 8.375209.

The internal reproducibility, expressed by the  $2\sigma$  statistical error (mean) for all successful measurements, is 0.000023, which is within the range of the mean of the standard analysis errors.

### 4.3 Tritium

The analysis of the cosmogenic nuclide tritium ( $^3\text{H}$ ) needs careful preparation due to its very short half life of 12.26 yrs (see Chapter 5.6). Its origin and presence in the atmosphere can cause contamination during the sampling process. Therefore, air contact during sampling should be minimized. The sampling containers should be filled completely to avoid further contamination. Tritium is measured in tritium units (TU), which is the equivalent to an abundance of one atom of  $^3\text{H}$  per  $10^{18}$  atoms of hydrogen (MOSER & RAUERT 1980).

#### 4.3.1 Preparation and Analysis of Tritium

The procedure of  $^3\text{H}$  analysis at the UFZ includes four preparation steps. About 10-15 ml of enriched  $^3\text{H}_2\text{O}$  is extracted during these four steps from initially at least 650 ml of the saline solution. In the first step, organic compounds, like carbohydrates, are eliminated using activated charcoal. The charcoal ensures that no organic matter contained in the solution overlaps with the organic scintillation material needed for the analysis. Secondly, the water is separated from dissolved salts in a pre-distillation step. In the following electrolysis only the light water molecules are being separated into hydrogen and oxygen. The heavy water molecules containing tritium prefer to stay in the remaining water aliquot. During this process  $^3\text{H}_2\text{O}$  is enriched by a factor of 20. In the final post-distillation step, samples are neutralized by admixture of  $\text{PbCl}_2$  and precipitation of  $\text{Pb}(\text{OH})_2$ , and mixed with an organic scintillation material. This mixture is being measured via a liquid scintillation counter (LSC) and a photo multiplier with a Perkin Elmer QUANTULUS 1220.

#### 4.3.2 Standards and Errors in Tritium Analysis

The analysis of tritium produces an absolute value, which can be evaluated directly. Calibration of the analyzing devices is conducted by using a tritium standard. The results need to be corrected to the date of sampling. Due to the short half life and the elapsed time since the main fall-out of tritium (about four half lives from the atomic

bomb testing in the 1960s up to now; see Chapter 5.6), a regular analyzing period of tree months can cause severe differences in the results, if not corrected.

#### 4.4 Main and Trace Elements

All samples were analyzed for their cation contents at the GZG by using ICP-MS (FISONS VG PQ STE with CETAC CTX-100 matrix elimination device) and ICP-OES (PERKIN ELMER Optima 3300 DV). Most samples needed to be diluted to avoid peak overlapping of the different compounds during measurement. The ICP-MS results were back-calculated to the original concentration and normalized on the internal indium standard value of 250000 counts/second (5 ppm) to eliminate dilution-driven errors.

The analysis of main and trace elements of some of the saline solutions was conducted by the K+S Forschungsinstitut and several laboratories at the mines of the K+S Group. Samples are prepared for ICP-IC analysis after testing method KAFI 0058.01, KAFI 0057.19 and VDLUFA 3.2.1, accredited by the German TÜV (For additional information, please contact the lab via [www.k-plus-s.com](http://www.k-plus-s.com)).

#### 4.5 Intensive Parameters

The intensive parameters density, temperature and especially the pH are difficult to obtain since the dissolved salts tend to manipulate the results when using standard methods.

Lead areometers and mercury thermometers were available at some mines to check density and temperature on-site. Indeed, most electronic areometers have low detection limits unsuitable for highly concentrated saline solutions.

The pH of a saline solution can vary with time due to the hydrolysis of iron (Fe). Fe(II) will be oxidized to Fe(III) upon air contact within days, and is incorporated into FeOOH precipitates. After HERRMANN et al. (2003) about 30% of Fe can be fixed into FeOOH over 7 months. Since most of the samples were taken by mine staff and needed fairly long shipping and handling time (up to several months), the original pH was no longer determinable by the author upon receipt. However, appropriate analyzing

methods for saline solutions exist (e.g. KNAUSS et al. 1990). The pH data in Appendix II were determined by the mine staff immediately after sampling, regarding DIN 21913-4.

## 5. FROM WATER TO BRINE – Evaporation, Concentration, and Precipitation

The evolution of a saline solution depends strongly on the nature of the evaporites that precipitate from it or will be dissolved and incorporated into it. In the following chapters the major phases that precipitate during evaporation of seawater will be discussed. In particular, the focus will be on the behaviour of the main elements as well as strontium, rubidium, and the isotopic evolution of oxygen and hydrogen during the precipitation of these phases. In addition, the behaviour of  $^{87}\text{Sr}/^{86}\text{Sr}$  and  $\delta^{18}\text{O}$  in the meteoric water cycle as well as their evolution in seawater throughout the Phanerozoic will be discussed.

### 5.1 The Composition of Modern and Permian Seawater

Only 11 elements make up 99.9% of the salinity of 3.5 wt.-% in modern seawater. Their concentrations are shown in Table 5-1. The sources for the ions are mainly weathering, hydrothermal convection and water-rock interactions at the ocean floor (BROWN 1997), while sedimentation is the major sink.

**Table 5-1:** Comparing modern (after \*BROWN 1997 and FONTES & MATRAY 1993) and Permian (after HORITA 1991) seawater compositions.

| Ion   | Modern seawater | Permian seawater |
|---|-----------------|------------------|
|   | ppm             | ppm              |
| Cl <sup>-</sup>                             | 19354           | 19499-25881      |
| SO <sub>4</sub> <sup>2-</sup>               | 2710            | 1921-4323        |
| HCO <sub>3</sub> <sup>-</sup>               | *140            | 9-305            |
| Br <sup>-</sup>                             | 66.5            | 70               |
| H <sub>2</sub> BO <sub>3</sub> <sup>-</sup> | *26             | -                |
| F <sup>-</sup>                              | *1              | -                |
| Na <sup>+</sup>                             | 10763           | 10575-14484      |
| Mg <sup>2+</sup>                            | 1292            | 1167-1459        |
| Ca <sup>2+</sup>                            | 411             | 200-802          |
| K <sup>+</sup>                              | 399             | 430              |
| Sr <sup>2+</sup>                            | 8               | -                |



Continental runoff of fresh water, transporting dissolved matter into the oceans, provides most of the seawater constituents, such as sodium (Na), potassium (K), calcium (Ca), magnesium (Mg), and to a lesser extent chlorine (Cl) and strontium (Sr). The other source is hydrothermal fluid convection at mid oceanic ridges (MOR). It occurs through seawater-basalt interactions providing Cl, Sr, and manganese (Mn). In addition, diagenetic pore water fluxes at the MOR cause removal of Mg and sulphates ( $\text{SO}_4$ ), but also addition of lithium (Li) and rubidium (Rb) to the seawater (BROWN 1997).

The overall seawater chemistry through time is influenced by biologic evolution and tectonic processes (HORITA et al. 2002). After FISCHER (1984) the Earth's surface processes underwent two major supercycles throughout the Phanerozoic, resulting in compositional changes in seawater chemistry. Mantle convection, plate motions and continental drift caused eustatic changes in sea level, changes in climate and biotic crises associated with long-term changes in sedimentation and seawater chemistry.

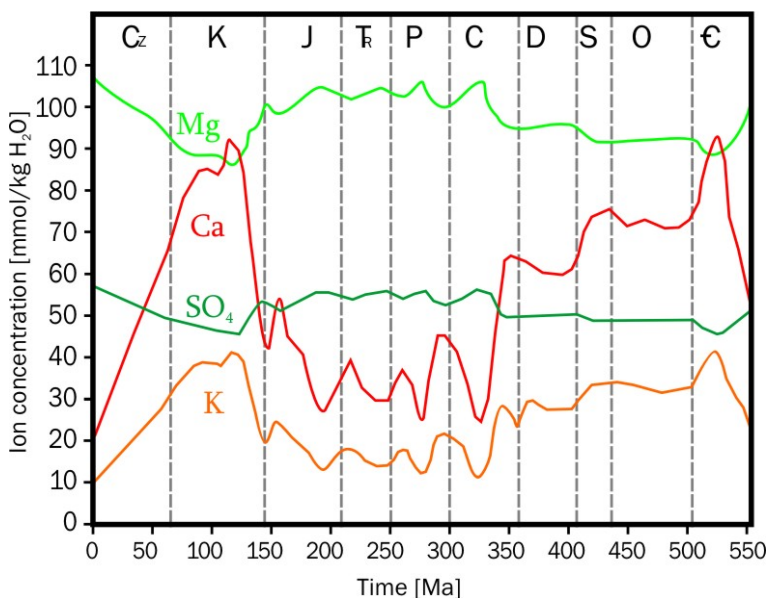


**Figure 5-1:**  
Predicted major ion  
secular oscillations in  
Phanerozoic seawater  
(fluxes mid ocean  
ridge/river water =1.25;  
modified after HARDIE  
1996).

HORITA et al. (1991) and LOWENSTEIN et al. (2005) calculated the Permian seawater concentration from fluid inclusions in Permian marine halite. According to the results shown in Table 5-1, the Permian seawater composition was very similar to the modern. Permian and Lower Triassic concentrated brines at halite saturation were of the same Na-K-Mg-Cl- $\text{SO}_4$  ( $\text{SO}_4$ -rich) chemical type as modern seawater (KOVALEVYCH et al.

2002a,b). In such a stage, the global seawater is Ca-poor ( $Mg/Ca \approx 5$ ) and therefore in a so-called 'aragonite sea' state, according to the favored precipitation of aragonite over dolomite or calcite. In contrast to an aragonite sea, cycles of a 'calcite sea' have been identified (SANDBERG 1975; HARDIE 2003), in which  $Mg/Ca$  is  $\approx 2$ . The overall seawater chemistry oscillates between both states (Figure 5-1), following a distinct pattern to be associated with the seawater chemistry supercycles of FISCHER (1984). Those cycles are recorded in a secular oscillation in potash evaporite composition. If the seawater inherits an  $Mg/Ca$  of 5, precipitation of  $MgSO_4$  is favored over  $KCl$ . Below an  $Mg/Ca$  of 2,  $KCl$  precipitates under absence of  $MgSO_4$  (SANDBERG 1975; BERNER 1975; HARDIE 1996).

In addition to these compositional changes, the residence times of ions within the ocean (dissolved mass vs. rate of supply or removal) differ widely. Some ions have shorter residence times than the overall seawater residence time of about 3900 yrs, but most conservative ions (and also those ions that are important in this study) have longer, as shown in Figure 5-2 (BROWN 1997). This is particularly important for the evaluation of seawater  $^{87}Sr/^{86}Sr$  ratios due to the long residence time of Sr of 2-5 My (see Chapters 5.2.1 and 5.5).

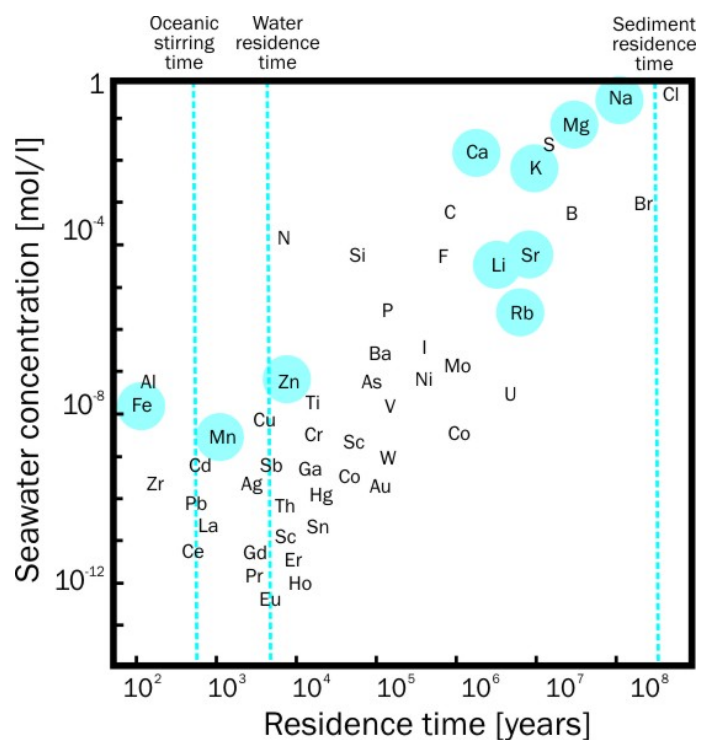


**Figure 5-2:**

Residence time of ions in seawater (modified after BROWN 1997); highlighted ions are discussed in the course of this study.

The knowledge of the Permian seawater composition contributes to the identification of syngenetic brines since internal solutions should yield a distinct pattern of major and trace elements that corresponds to the concentration of the residual brine at different stages of seawater evaporation (see Chapter 5.7). In contrast, external saline solutions should show other phase relationships depending on the evaporitic rocks through which they percolate.

## 5.2 Marine Evaporite Minerals and their Compositions

In general, the sedimentary sequences in evaporating seawater basins follow a strict depositional succession, as described in Chapter 2.2.1. Several hydrochemical factors support precipitation, such as temperature,  $P_{CO_2}$ , and the solubility of the different phases. In the following, those massive precipitates and their constituents will be discussed that may primarily influence the composition of the studied saline solutions, and thus may help to interpret and identify solutions from different origins.

**Table 5-2:** Major marine precipitates, their solubility and behavior for static seawater evaporation under laboratory and *natural* conditions (after HERRMANN 1981).

| Type                                    | Name                 | Structure   | Solubility (g/l)         |       | Temperature (°C) |      | Remaining Liquid (g) | Conc. factor |
|---|----------------------|---|--------------------------|-------|------------------|------|----------------------|--------------|
|   |                      |   | from                     | to    | from             | to   |                      |              |
| Carbonate                               | Aragonite            | CaCO <sub>3</sub>   | 0.0153                   | 0.019 | 25               | 75   | 250                  | 4            |
|   | Calcite              | CaCO <sub>3</sub>   | 0.014                    | 0.018 | 25               | 75   |                      |              |
|   | Dolomite             | Ca <sub>2</sub> Mg(CO <sub>3</sub> ) <sub>2</sub>                                   | 0.32                     |       | 18               |      |                      |              |
|   | Strontianite         | SrCO <sub>3</sub>   | 0.011                    | 0.65  | 18               | 100  |                      |              |
| Sulfate                                 | Celestite            | SrSO <sub>4</sub>   | 0.113                    | 0.114 | 0                | 30   |                      |              |
|   | Gypsum               | CaSO <sub>4</sub> ·2H <sub>2</sub> O  | 241                      | 2.22  | 0                | 100  | 322.4                | 160          |
| Chloride                                | Halite               | NaCl  | 317.8                    | 391.2 | 0                | 100  | 121.3                | 95           |
| Na-Mg-SO <sub>4</sub> salts (without K) |                      |   |                          |       |                  |      | 245                  | 41           |
| K-Mg-minerals                           | Polyhalite           | K <sub>2</sub> MgCa <sub>2</sub> (SO <sub>4</sub> ) <sub>4</sub> ·2H <sub>2</sub> O | incongruent              |       |                  |      |                      |              |
|   | Sylvite              | KCl   | 347                      | 567   | 20               | 100  |                      |              |
|   | Sakiit (Hexahydrate) | MgSO <sub>4</sub> ·6H <sub>2</sub> O  | stable between 13-31.5°C |       |                  |      |                      |              |
|   | Kieserite            | MgSO <sub>4</sub> ·H <sub>2</sub> O   | 419                      |       |                  | hot  |                      |              |
|   | Carnallite           | KMgCl <sub>3</sub> ·6H <sub>2</sub> O   | 645                      |       | 19               |      | 11.8                 | 85           |
|   | Bischofite           | MgCl <sub>2</sub> ·6H <sub>2</sub> O  | 1670                     | 3670  | cold             | hot  | 9.3                  | 108          |
|   | Tachyhydrite         | CaMg <sub>2</sub> Cl <sub>4</sub> ·12H <sub>2</sub> O                               |                          | 8000  |                  | warm |                      | 310          |

***Aragonite, Calcite ( $\text{CaCO}_3$ ) and Dolomite ( $\text{CaMg}(\text{CO}_3)_2$ )*** Aragonite is the first precipitate that forms at the onset of seawater concentration due to its low solubility (Table 5-2). Calcite only forms if the Mg content is below 243 ppm since Mg ions subdue its precipitation. This effect is negated if increased amounts of sodium chloride are present. Aragonite can incorporate much more Sr as calcite ( $D = 160$ ) due to its high distribution coefficient of  $D = 1240$  (decreases with increasing temperature; Table 5-3). If aragonite is recrystallized into calcite, some Sr will be liberated (SONNENFELD 1984). Dolomite often occurs as a product of dolomitization of aragonite by Mg-rich hypersaline brines within evaporite deposits, accompanied by dolomite enrichment in  $^{18}\text{O}$  (CLARK 1980).

The partial pressure of carbon dioxide,  $P_{\text{CO}_2}$ , determines the phase that precipitates from seawater. In the open oceans dolomite precipitation occurs permanently since  $P_{\text{CO}_2}$  in the open ocean naturally varies between  $10^{-2.9}$  and  $10^{-3.7}$ . Above  $10^{-2.9}$  dolomite decomposes. With the onset of excessive evaporation (evaporation > recharge), the  $P_{\text{CO}_2}$  drops below  $10^{-3.7}$  and gypsum starts to precipitate after the brine has passed the calcium carbonate saturation (SONNENFELD 1984).

***Strontianite ( $\text{SrCO}_3$ )*** Small amounts of strontianite can be found in geodes and veinlets in evaporite-related dolomite as a secondary product of the recrystallization of aragonite to calcite.

***Gypsum ( $\text{CaSO}_4 \cdot x \text{H}_2\text{O}$ )*** Gypsum precipitation starts at a 3.1-fold seawater concentration. Most of the Sr left after carbonate precipitation is incorporated into the gypsum ( $D = 54$ ). At seawater concentration of more than 4.5-fold, the remaining decarbonated water has a low  $P_{\text{CO}_2}$ , which further supports gypsum precipitation. Gypsum precipitation is limited to the photic zone. Algal photosynthesis keeps the oxygen supply high enough to stabilize gypsum. Gypsum is only stable if the seawater is aerated (saturated with oxygen) since in this case the activity of sulfate-reducing anaerobic bacteria is minimized (SONNENFELD 1984).

During gypsum crystallization, the ionic and isotopic composition of the brine is changed,  $^2\text{H}$  is depleted and  $^{18}\text{O}$  enriched (FONTES & GONFIANTINI 1967a,b). Fluid inclusions will be enriched in  $^{18}\text{O}$ , too (FONTES 1966; see Chapter 5.4.2).

***Halite (NaCl) and Sylvite (KCl)*** At an 8-11 fold increase in concentration of the seawater, sodium chloride precipitation commences and lowers the Na/K ratio in the brine. Initially only halite precipitation occurs at temperatures of 30-35°C (KRULL 1917, d'ANS 1947, BRAITSCH 1964, BORCHERT & MUIR 1964). Between a Na/K ratio of 2.28 and 2 (depending on the temperature; GOERGEY 1912), potassium chloride starts to co-precipitate. All water that gets in contact with halite can easily take up large amounts of NaCl to get equilibrated with it due to the dominant occurrence of halite in the Zechstein deposits and its comparably high solubility of 317.8 g/l. This is, of course, the case with the even higher soluble salts, all following a distinct phase pattern described in Chapter 5.7.

***Celestite (SrSO<sub>4</sub>)*** Celestite is a phase that precipitates during the halite precipitation stage of evaporating seawater (USDOWSKI 1973) though the solubility of celestite of 0.114 g/l at 30°C is considerably lower than that of gypsum (2.09 g/l at 30°C). Saturation with SrSO<sub>4</sub> is reached at a 4-fold seawater concentration (MÜLLER 1962). Anhydrite intercalations in halite can also contain celestite that could easily contribute to the Sr contents of a seeping solution. The solubility decreases with increasing temperature and NaCl concentration (CHOU & HAAS 1981). Equilibrium is reached at concentrations of 20-35 ppm Sr (MAY et al. 1961).

During calcium depletion of the brine, precipitation of barium and strontium forms an isomorphous series from barite via barytocelestite to celestite (SONNENFELD 1984).

***Carnallite (KMgCl<sub>3</sub> x 6H<sub>2</sub>O)*** After progressive precipitation of halite and sylvite, the brine starts to preferably precipitate carnallite due to an increase in MgCl<sub>2</sub> in the solution at a 85-fold seawater concentration. The stability of carnallite is reached at a NaCl:KCl:MgCl<sub>2</sub> ratio varying between 0.364:1:6.41 and 0.266:1:4.60

(GEORGEY 1912). In general, potassium chloride crystals can incorporate strontium or calcium up to an ionic ratio of 1:4000. Rubidium, which can decay to strontium, substitutes the potassium in carnallite in large amounts due to a distribution coefficient of up to 125 (Table 5-3).

***Bischofite ( $MgCl_2 \times 6H_2O$ ) and Tachhydrite ( $CaCl_2 \times 2MgCl_2 \times 12H_2O$ )*** Bischofite is formed only in the absence of sulfates and calcium chloride, otherwise tachhydrite precipitates. It forms in residual pools of bitterns when the seawater is concentrated 310 times. The deposition of primary tachhydrite needs high calcium chloride activities, otherwise bischofite is precipitated (SONNENFELD 1984). A Sr enrichment was produced in the Stassfurt Potash Member during formation of secondary tachhydrite by interaction of carnallite with warm calcium chloride solutions (KÜHN 1955), or by infiltrating dolomitizing solutions from above, respectively (d'ANS 1961).

***Clays*** Clastic deposits in the evaporitic basin are restricted to terrigenous sands and clays. The bottom outflowing stream (Figure 2-1) almost excludes the inflow of clay-rich seawater from the open ocean. Therefore, clastic sediments are transported into the basin only by episodic continental runoff. Siliciclastic intercalations often found in anhydrite or halite sequences imply ephemeral episodes of freshening of the whole brine column by meteoric water input. The basin wide distribution of such shale intercalations results from the fact that the particles cannot form turbidity currents. Instead, they are slowly spread out along the pycnocline (density interface due to change in salinity and temperature) by forming submarine deltas or interflows at such density interfaces. Upon direct contact with the pycnocline, the freshwater clays flocculate to semiliquid flocs of up to several centimeters in diameter. Those flocs gradually descend to the bottom of the basin. Exchange of ions between the brine and the clastics can lead to enrichment or depletion of the brine in major and trace elements, depending on the brine concentration stage (SONNENFELD 1984).

### 5.2.1 Trace Elements

Several trace elements can be incorporated into the marine minerals or are enriched in the remaining brine, according to their distribution coefficients which are tabulated in Table 5-3. Those trace elements that are important for the determination of internal and external solutions will be discussed in the following.

#### *Rubidium (Rb)*

The major source of Rb in the oceans is the diagenetic pore water flux. The low Rb concentration of 0.12 ppm in seawater (GOLDBERG 1965, BROWN 1997) is still higher than in the continental runoff. With ongoing evaporation, seawater is enriched in Rb until potash deposits start to form (SONNENFELD 1984).

Since Rb tends to replace potassium during precipitation of potassium salts with different distribution coefficients (Table 5-3), it might be useful to determine the evolutionary stage of highly evolved brines. Here, the presence of sodium chloride and the knowledge of the temperature are the key factors: with rising temperature, the distribution coefficient rises under absence of sodium chloride, but decreases when it is present (MUMINDZHANOVA & OSICHKINA 1982). For sylvite, the distribution coefficient ranges around 1.35. Carnallite incorporates Rb with an extremely high distribution coefficient of up to 125, (and a concentration of about 347 ppm; SONNENFELD 1984). At this stage, the residual brine is strongly impoverished in Rb (HOLSER 1979). With the onset of bischofite precipitation, no Rb is left in solution to be incorporated (ZHEREBTSOVA & VOLKOVA 1966). The K/Rb ratio in primary sylvite is 968 and ranges from 405 in primary to 40 in recrystallized carnallite (PETROVA 1973).

During solution metamorphism from carnallite into kieseritic hard salt the Rb contents in solution could increase because sylvite is formed from carnallite with incorporation of less Rb (HERRMANN 1981).

#### *Strontium (Sr)*

Strontium has four natural occurring stable isotopes, namely  $^{88}\text{Sr}$  (82.53 %),  $^{87}\text{Sr}$  (7.04 %),  $^{86}\text{Sr}$  (9.87 %), and  $^{84}\text{Sr}$  (0.56 %; FAURE 1986). The fraction of  $^{87}\text{Sr}$  is influenced by radioactive beta decay of  $^{87}\text{Rb}$  to  $^{87}\text{Sr}$ .

Strontium is a rather conservative element within the meteoric water cycle. Its residence time in the oceans of 2-5 My (5800-700,000 years in the upper 400 m due to sediment trap fluxes; DE VILLIERS 1999) is one of the longest for trace elements in seawater (Figure 5-2). The reported Sr concentration in modern seawater ranges between 7 (BRASS & TUREKIAN 1974) and 13 ppm (BROWN 1997). In evaporitic deposits, the most important carriers of Sr are celestite, gypsum/anhydrite and polyhalite (HERRMANN 1961). The incorporation of Sr into the different evaporites decreases with ongoing evaporation, as mirrored by decreasing distribution coefficients from 1240 in aragonite to 54 in gypsum (Table 5-3). Concurrently, the Sr concentration in the remaining solution should increase, but ongoing precipitation of Ca-Minerals in the presence of Mg causes a gradual decrease throughout the further evaporation stages.

The oceanic Sr budget is discussed separately in Chapter 5.5

### ***Bromine (Br)***

The Element Br is already in use as one important factor for the determination of saline solution origin since it accumulates in the residual brine. Modern seawater contains about 65 ppm Br (HOLSER 1979). It is not incorporated in any insoluble phase, as detritus or salt clays. During seawater evaporation, Br concentrates in the residual brine up to the eutonic point (point Z in the quinary phase system where solution evaporates at a constant composition; see Chapter 5-7; USDOWSKI & DIETZEL 1998, ZHEREBTSOVA & VOLKOVA 1966). During that, it is incorporated in the chemical precipitates and replaces Cl via solid solution, depending on its distribution coefficient in the precipitating mineral (Table 5-3). Once NaCl saturation is reached at 10.5-fold seawater concentration, the Br content has increased to 510 ppm. With the onset of halite precipitation, Br replaces Cl in halite. With its distribution coefficient of about 0.13 it will be incorporated in the first halite precipitates with  $510 \text{ ppm} \times 0.14 = 65\text{-}75 \text{ ppm}$  (HERRMANN 1972, HOLSER 1979). With ongoing evaporation, the Br contents in halite continuously increase up to 200 ppm. With the onset of potash-magnesia salts more Br is incorporated since the distribution coefficients for Br in potash-magnesia salts is 0.52-0.81.



The distribution coefficient of Br in marine evaporites never exceeds 1. Therefore, the residual brine, or equilibration solution, has always a higher Br concentration than the solid phase, respectively. The different evaporation stages show specific Br concentrations in both liquid and solid phase. Solution of a mineral by salt external water leads to distinct lower Br concentrations in the liquid phase than in a corresponding evaporated seawater at the stage of precipitation of the dissolved mineral. This characteristic can be used to distinguish between residual brine and external solution.

Table 5-3: Distribution coefficients for traces of elements in chemical marine precipitates (modified after HOLSER 1979; USDOWSKI 1973).

| Element    | Mineral    | Distribution coefficient D                   | References and remarks  |
|------------|------------|--|---|
| Br         | Halite     | 0.13±1                                       | 33-42°C, seawater; Herrmann 1972  |
|            |            | 0.14-0.07±1                                  | during addition of MgCl <sub>2</sub> ; Braitsch & Herrmann 1963                                     |
|            |            | 0.12±3                                       | Estimated for salt lakes; Valiashko & Mandrykina 1952   |
|            | Sylvite    | 0.066  | Seawater; Bloch & Schnerb 1953  |
|            |            | 0.053  | 40°C, pure NaCl solutions; Puchelt et al 1972   |
|            |            | 0.81±5                                       | Pure KCl solutions;   |
|            |            | 0.73±4                                       | Carnallite solutions; Braitsch & Herrmann 1963  |
| Carnallite | 0.66       | 40°C, pure KCl solutions; Puchelt et al 1972 |   |
|            | 0.55       | Puchelt et al 1972                           |   |
| K          | Halite     | 0.52   | Braitsch & Herrmann 1963; Kühn 1968   |
|            |            | 0.006  | Puchelt 1972  |
|            |            | <0.003                                       | Reichert 1966   |
| Na         | Aragonite  |  | Kinsman 1970  |
|            | Sylvite    | <0.005                                       | Reichert 1966   |
| Rb         | Halite     |  | Kinsman 1970  |
|            |            | 0.007±4                                      | 40°C; Schock & Puchelt 1971   |
|            | Sylvite    | 0.34±6                                       | 27°C, pure KCl solutions; McIntire 1968   |
|            |            | 0.38±6                                       | 40°C, pure KCl solutions; Reichert 1966   |
|            |            | 0.33±2                                       | 30°C, NaCl containing solutions; Kühn 1972  |
|            |            | 0.83±4                                       | 35°C, system KCl-K <sub>2</sub> SO <sub>4</sub> -MgCl <sub>2</sub> -H <sub>2</sub> O; Malikova 1967 |
|            |            | 1.35±5                                       | 30°C, + MgCl <sub>2</sub> ; Kühn (pers. comm. with Holser 1970)                                     |
|            | Carnallite | 36±1   | 30°C, NaCl solutions, increasing K/Mg; Kühn 1972a,b)  |
| 19         |            | Schock & Puchelt 1971                        |   |
| 125±5      |            | 16-20°C; Malikova 1967                       |   |
| 22±1       |            | Braitsch 1966                                |   |
| Sr         | Aragonite  | 1240   | 25°C; Usdowski 1973   |
|            | Calcite    | 160  | 25°C; Usdowski 1973   |
|            | Gypsum     | 54   | 25°C; Usdowski 1973   |
|            | Anhydrite  | 1210   | 80°C; Usdowski 1973   |

***Lithium (Li)***

The concentration of Li in modern seawater is low, with values around 0.17-0.19 ppm (HERRMANN et al. 2000). It can be leached in minor amounts from Mg rich salt clays (SONNENFELD 1984), which can have Li contents of about 47-91 ppm (OHRDORF 1968). Although Li is in the same systematic element group as Na, K, and Rb, it does not replace those elements during precipitation of salts. Indeed, it accumulates in the liquid phase with up to 17-19 ppm (at 100-fold seawater concentration), even in highly evolved brines. Therefore, if a solution yields about 19 ppm Li, it is an excellent indicator for residual brines (HOLSER 1979).

**5.3 Fractionation of  $^{87}\text{Sr}/^{86}\text{Sr}$  - Water-Rock Interactions**

The behavior of the Sr isotope distribution during water-rock interactions was evaluated in many studies to assess e.g. the flow paths of groundwater through a series of aquifers (e.g. FRAPE & FRITZ 1984; MCNUTT et al. 1984, 1990; BANNER & HANSON 1990; JOHNSON & DE PAULO 1994; WIEGAND et al. 2001; KLAUS et al. 2007).

In this study, Sr isotope systematics are evaluated for saline solutions seeping through salt deposits and leaching several evaporitic minerals as well as clay intercalations (HERRMANN 2000) on their passage through the salt deposits. In contrast to commonly evaluated water-rock interactions between aquifers and the aquifer matrix, the Sr budget in saline solutions is highly dependent on dissolution of Ca-rich rock forming minerals, like anhydrite, that can cause an enrichment of Sr in the fluid phase. On the other hand, precipitation of Ca-bearing evaporitic minerals, particularly gypsum, occurs under incorporation of Sr into the solid phase. Sr is a common substituting element for Ca, because Sr has the same ionic charge and similar atomic radius as several major elements, especially calcium. Thus, it is incorporated in significant amounts in many Ca-rich rock forming minerals. The leaching of Sr from Ca- and Sr-rich minerals is dependant on the pH and the composition of the liquid (FAURE 1986).

During Sr exchange between water and Sr-rich minerals, not only the concentration but also the isotope composition is affected. The extent of the changes depends on the isotope composition of both interacting phases and their Sr concentrations. Such two-component mixtures can be quantified based on the final Sr budget in both phases, as

will be shown in Chapter 7.2.1 for saline solutions that lose Sr through precipitation of gypsum or that scavenge Sr in contact to clays.

#### 5.4 Stable Isotopes in the Water Cycle

Oxygen and hydrogen are fairly light elements, thus the difference between their isotopes is more pronounced than for heavier elements like Sr. Isotopic fractionation for oxygen and hydrogen within the meteoric water cycle occurs continuously during evaporation, condensation, or freezing (GAT 1996). In general, the oceans contain primarily the heavier isotopes, whereas the lighter isotopes tend to stay in the gas phase, even during condensation and precipitation (UREY 1947). As one example for this kinetic fractionation, isotopically lighter water masses than the ocean water are produced by condensation and precipitation. The 'light' water is bound in the ice caps at the poles. Since the remaining gas phase is even lighter than the light water, the 'heavy' ocean water is diluted with every input from river water or groundwater, both resulting from 'light' precipitation. The resulting isotope pattern can be used e.g. for paleo-climate reconstructions (GAT 1996).

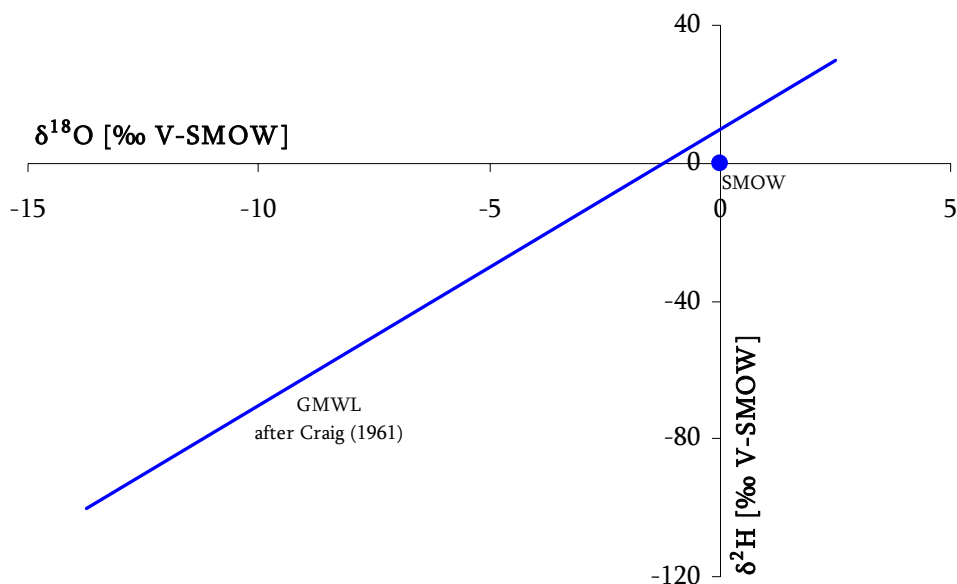


**Figure 5-3:** The Global Meteoric Water Line (GMWL) after Craig (1961a).

#### 5.4.1 The Global Meteoric Water Line (GMWL)

The different water reservoirs on Earth are interconnected via evaporation, transpiration, rainout, and runoff. With each of these steps the isotopic composition of  $^{18}\text{O}$  and  $^2\text{H}$  of the water is fractionated between the reservoirs (GAT 1996). The relationship between the isotopic contents of meteoric water reservoirs was first published by CRAIG (1961a). He stated that

*“The isotopic enrichments, relative to ocean water, display a linear correlation over the entire range for waters which have not undergone excessive evaporation”.*

His linear correlation, the Global Meteoric Water Line (GMWL) shown in Figure 5-3, is still the primary tool to interpret the stable isotopic contents of meteoric waters with its function

$$\delta^2\text{H} = x \delta^{18}\text{O} + d \quad (\text{Equation 5-1})$$

with  $x$  being the slope and  $d$  being the  $d$ -excess parameter (see Chapter 5.4.3). In general, the GMWL has a slope of 8 and a  $d$ -excess of 10. Closed basins yield a smaller slope of about 5 due to evaporitic enrichment of both heavy isotopes (HORITA 2005).

#### 5.4.2 Oxygen and Hydrogen Isotope Evolution of Seawater to Brines

In general, the isotopes of an element in aqueous solution are assumed to have indistinguishable activities and concentrations (mole fractions). The only known exceptions are the oxygen and hydrogen isotopes of saline water. Both isotopic ratios show different activities and concentrations when comparing pure water and saline solutions, especially if evaporation is involved. The dimensions of these ‘dissolved salt effects’ in saline solutions vary depending on the concentration and the temperature of the solution (HORITA 1989, 1993a,b).

The stable isotopes in connate seawater trapped in the salt deposits could have been subject to dissolved salt effects due to evaporation prior to deposition. But also the saline solutions seeping into the mine openings might undergo evaporation during and after their passage through the salt.

GONFIANTINI (1986) proposed three interdependent effects that dissolved salts could pose on the stable isotopes in evaporating water:

1. Physical properties: the thermodynamic activity and also the evaporation rate of water is decreased if dissolved salts are present;
2. Hydration of ions: different for each salt, its ions co-ordinate water molecules in the hydration sphere that show a different isotopic composition and evaporation rate than 'free' water;
3. Water of crystallization: during crystallization, each salt incorporates crystallization water with a different isotopic composition than the remaining water.

These effects vary for the different salts or ions. For example, the most common salt, sodium chloride, produces only minor hydration- and no crystallization effects.

According to HORITA (2005), several processes control the stable isotope contents of saline water at surface and in the subsurface, all contributing to the named effects. The primary processes with the highest impact besides evaporation are freezing, dissolution and precipitation of evaporite deposits and clay minerals, and subsurface membrane filtration.

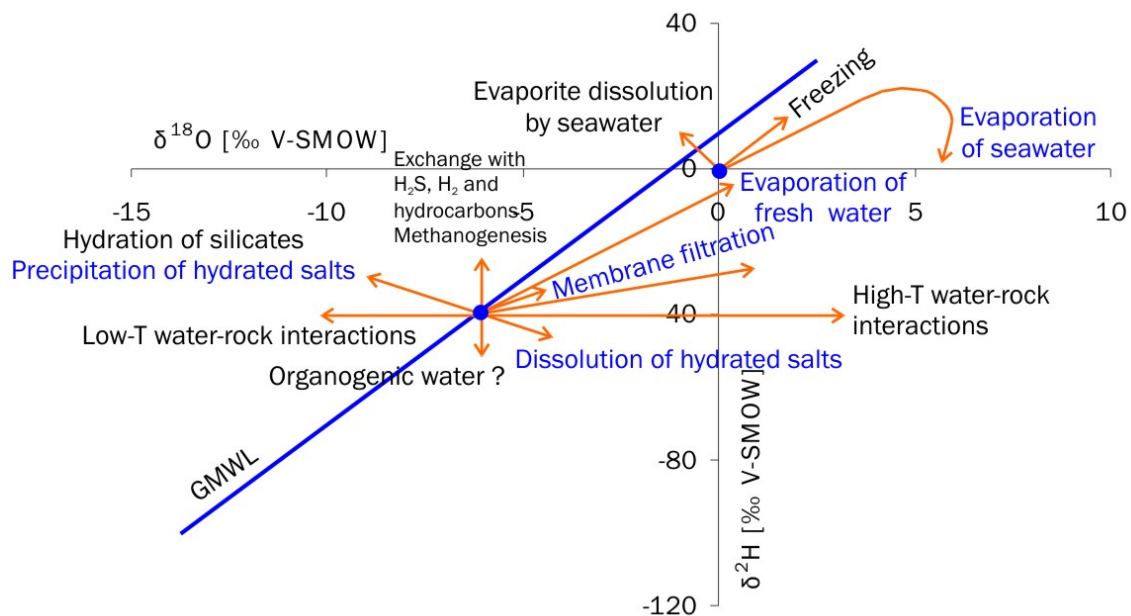


**Figure 5-4:** Evolution of oxygen and hydrogen isotopes of different water types caused by the named effects (modified after Horita 2005).

In general, evaporation produces a remaining liquid that is enriched in both  $^{18}\text{O}$  and  $^2\text{H}$  (HOLSER 1979). This initial effect is independent of the initial water composition - freshwater, seawater, brine or soil water. As shown in Figure 5-4, the slope of the trajectories is between 2-3 for soil water and 4-6 for freshwater, seawater and brines (HORITA 2005).

With ongoing evaporation, the increase in salinity in seawater causes a decrease in evaporation of light water molecules. A decrease in thermodynamic activity of the water molecules in the presence of dissolved salts leads to an activity coefficient ( $a_w$ ) of the water of  $a_w < 1$ . As a result, the relative humidity ( $h$ ) above the water becomes higher since it has to be replaced by  $h/a_w$  (ROBINSON & STOKES, 2002, tabulated the activity coefficients for most electrolytes under various conditions).

One example: during evaporation of seawater, the sodium chloride contents increase as the water activity decreases. Parallel, more and more isotopically light water molecules are evaporated and the heavy molecules are accumulated in the remaining water. At high salt concentrations the activity of  $\text{H}_2\text{O}$  is decreased strongly. Therefore, the relative rates of evaporation and condensation are affected (GONFIANTINI 1965). As a result, both  $\delta^{18}\text{O}$  and  $\delta^2\text{H}$  start to decrease at a 4-fold concentration of seawater, causing a hook in the trajectory. In addition to the decreasing activity, the water in hydration spheres of cations may interact with free water, contributing as the second salt effect to the decrease in both  $\delta^{18}\text{O}$  and  $\delta^2\text{H}$  (TAUBE 1954; this effect is already covered in Chapter 4.1.2 since it also occurs during distillation). At 10-fold concentration, the evolution of both  $\delta^{18}\text{O}$  and  $\delta^2\text{H}$  is reversed and  $\delta^2\text{H}$  becomes negative. If the sodium chloride contents reach saturation (10.5 times seawater concentration),  $a_w$  is as low as 0.75 and  $h$  is increased. At higher  $h$ , more of the heavy isotope water molecules are evaporated. Up to a 45-fold concentration (onset of precipitation of  $\text{NaMg}$ - and  $\text{Mg}$ -sulfates),  $\delta^{18}\text{O}$  as well becomes negative (Figure 5-5). Assuming this trend to be going on at least until halite precipitation ends at a 65-fold seawater concentration, the trajectory might reach the GMWL at a  $\delta^2\text{H}$  of about  $-67$  and a  $\delta^{18}\text{O}$  of about  $-10$  (LLOYD 1966; KNAUTH & BEEUNAS 1986).

Dissolution and precipitation of anhydrous and hydrous evaporites show effects opposite to each other. Dissolution of anhydrous minerals does not fractionate the isotopic compositions of the liquid. However, the isotopic activities are changed. Dissolution of hydrous minerals can affect the isotopic composition. The hydrous minerals, previously precipitated from a liquid, comprise more  $^{18}\text{O}$  but less  $^2\text{H}$  than the remaining water (CHACKO et al. 2001). Therefore, dissolution of such minerals should cause enrichment of the liquid in  $^{18}\text{O}$  and depletion in  $^2\text{H}$ .

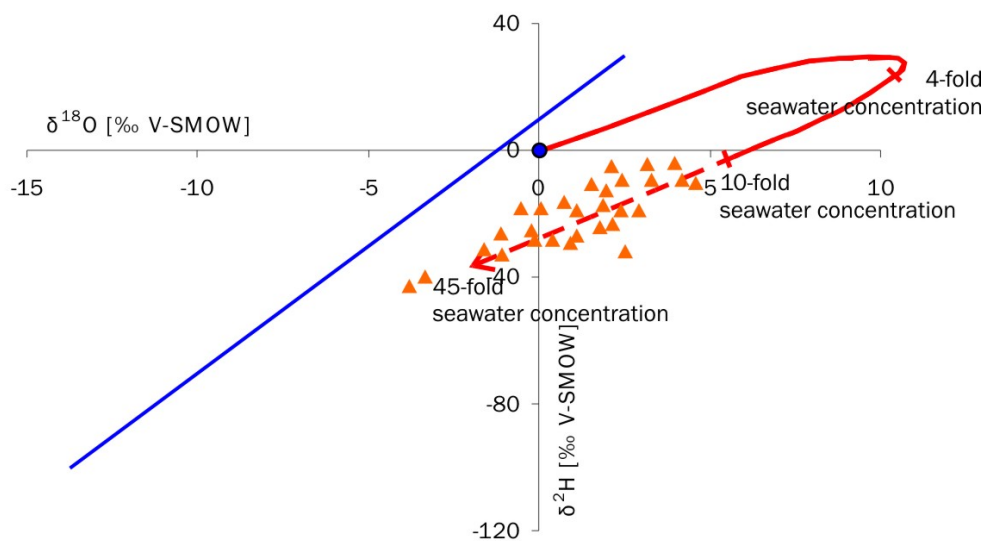


**Figure 5-5:** Evaporation trajectory (red) for the stable isotope contents of fluid inclusion samples (triangles) after KNAUTH & BEEUNAS (1986).

Subsurface membrane filtration causes an enrichment of the remaining liquid in both heavy isotopes as well as in dissolved salts. This can be addressed to a high hydration effect at the ions within the clay membrane. Especially the light water molecules are bound, and therefore the activity of the heavy isotopes increases, resulting in diffusion of both heavier isotopes away from the membrane, not through it (e.g. COPLEN & HANSHAW 1973, PHILLIPS & BENTLEY 1987).

The third main salt effect, the water of crystallization, is mainly important for the study of fluid inclusions and hydrated minerals: the water incorporated in the salt crystals has a different isotopic composition than the remaining water. This affects the fractionation factor  $f$  and also the  $\delta$ . For example, the fractionation factor between

combined and remaining water  $\alpha_c$  in gypsum is 1.0040 for  $^{18}\text{O}/^{16}\text{O}$  (GONFIANTINI & FONTES 1963) and 0.985 for  $^2\text{H}/^1\text{H}$  (FONTES & GONFIANTINI 1967a).

Secondary effects are: mixing of water masses, exchange with other liquids/gases, production and consumption of water, and water-rock interactions. Here, the temperature is one of the controlling factors: below  $100^\circ\text{C}$  such interactions lead to depletion in  $^{18}\text{O}$ , but show only small influence on  $^2\text{H}$  since hydrogen is not abundant in most rock forming minerals (HORITA 2005).

#### 5.4.3 Deuterium Excess Distribution

The d-excess parameter is the value of  $\delta^2\text{H}$  at intercept of the GMWL with the  $\delta^2\text{H}$  axis. According to equation 5-1, d-excess has a general value of 10‰ for meteoric water.

The d-excess shows regional as well as seasonal variations, depending on humidity and temperature. These characteristics make the d-excess parameter a paleoclimatic indicator (MOOK 2000). For example, d-excess is greater than 10‰ if the humidity is below the present mean value (MERLIVAT & JOUZEL 1979).

In saline solutions derived from seawater evaporation, d-excess typically is negative due to the hook of the evaporation line with a smaller slope than the GMWL. The higher the slope, the more the d-excess shifts from negative to positive values.

#### 5.5 Strontium and Oxygen Variations in Seawater

Besides the chronologic oscillations in the overall seawater chemistry, its isotopic compositions show fluctuations that are especially pronounced during Zechstein ages at the Permian-Triassic boundary (PTB).

The strontium as well as oxygen isotopic budgets in seawater are modified by the same processes as the overall seawater chemistry. Continental runoff (R) of fresh water (FC) has the largest effect on the overall Sr and O concentrations. Secondly, seawater-basalt interactions (FM) and diagenetic pore water flux (FD) have also a significant contribution to the Sr and O-budget. These three Sr-fluxes contribute to the total flux



as FC:FM:FD = 66:19:14 % (WADLEIGH et al. 1985). The fluxes total to about  $9 \times 10^{11}$  g/yr (ALBARÈDE et al. 1981, ELDERFIELD & GREAVES 1981).

The three different sources for the Sr in the ocean are characterized by different Sr isotope compositions. The juvenile material of the ocean floor produces Sr ratios as low as 0.7035 within the hydrothermal fluids. Runoff-water releases more radiogenic Sr of 0.7119 from the continents since the fresh water erodes old rocks with a long history of Rb decay and high Rb concentrations (ELDERFIELD & SCHULTZ 1996).

While the Sr isotope composition is related to the Rb concentration and the age of the altered rock, the favored explanation for the  $\delta^{18}\text{O}$  variations in the marine record is fluctuations of  $\delta^{18}\text{O}$  in seawater caused through temperature fractionation processes (JAFFRÉS et al. 2007). Low temperature continental runoff and seafloor alterations cause a decrease in  $\delta^{18}\text{O}$  in seawater, whereas high temperature hydrothermal convection and alteration extract  $^{18}\text{O}$  from the seafloor and increase  $\delta^{18}\text{O}$  in seawater (see JAFFRÉS et al., 2007, and references therein for a review of different explanations).

Overall, the presence of extensive MOR and an arid climate leads to low  $^{87}\text{Sr}/^{86}\text{Sr}$  ratios and high  $\delta^{18}\text{O}$  within the oceans, respectively (e.g. during glaciations). During intervals of less MOR and a humid climate, the  $^{87}\text{Sr}/^{86}\text{Sr}$  ratio increases and  $\delta^{18}\text{O}$  is low, respectively (e.g. during interglacial).

### 5.5.1 Isotopic Variations throughout the Zechstein

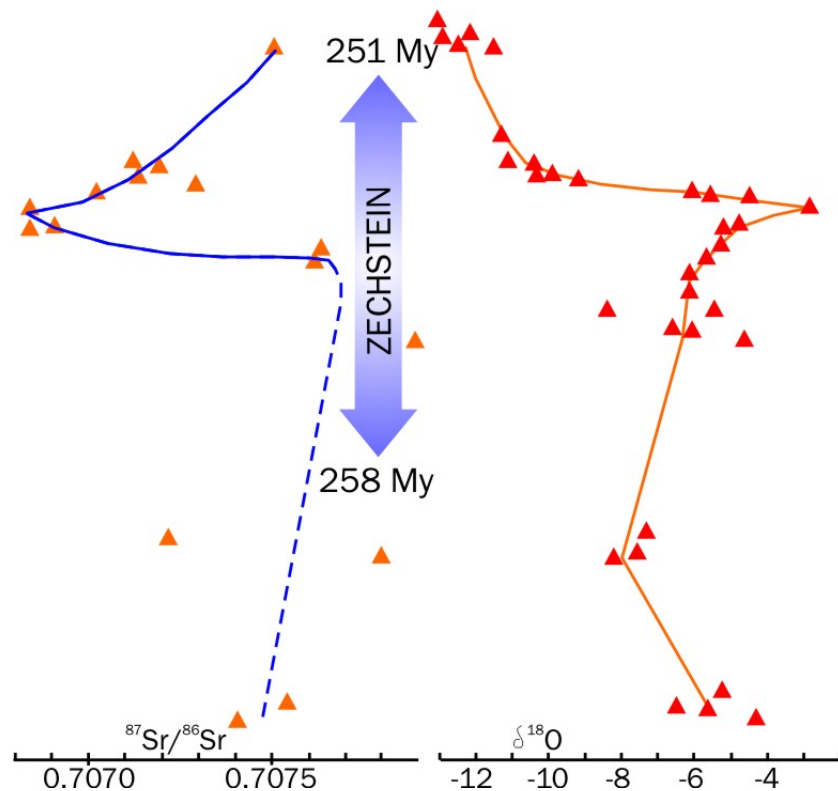
Since oxygen and strontium isotopes in seawater have the same major sources within the global water cycle both parameters show reactions on global environmental events, which are associated with changes in the water budget. Especially the Permian trends of Sr and O isotopes in seawater show a distinct pattern.

Figure 5-6 shows the evolution of the Sr and O isotopic compositions in seawater throughout the Permian. Several studies were conducted on both isotopic trends throughout the Phanerozoic, and all describe positive or negative peaks close to the Permian-Triassic boundary (PTB), respectively (e.g. BURKE et al. 1982, GRUSZCZYŃSKI et al. 1989, 1992, DENISON et al. 1994, MII et al. 1997, VEIZER et al. 1999, KORTE et al. 2003,

2004, 2006). Indeed, the peak placement varies for these studies between the middle Zechstein and the PTB.

The deep mark of the  $^{87}\text{Sr}/^{86}\text{Sr}$  seawater curve is at ca. 0.7068 and an age of ca. 254 My, which is shortly after the beginning of the Zechstein age at 258 My. Due to the assemblage of Pangea, an arid continental climate predominated our planet at that time. The vast ocean area caused the formation of many regions with seafloor spreading activities. At those mid ocean ridges, the hydrothermal activities produced a high input of juvenile Sr with low ratios around 0.704. In addition, the continental runoff which would transport more radiogenic Sr of about 0.720 to the oceans was very limited. Up to the PTB, the curve rises to its Rotliegend level of ca. 0.7076.

The  $\delta^{18}\text{O}$  seawater curve mirrors the  $^{87}\text{Sr}/^{86}\text{Sr}$  curve due to the opposite input by the different sources named in Chapter 5.5. The curve progresses from -6‰ in the upper Rotliegend to a maximum of -2.5‰ in the Zechstein, and decreases to -12.5‰ up to the PTB (Figure 5-6).



**Figure 5-6:** Comparing the trends of  $^{87}\text{Sr}/^{86}\text{Sr}$  and  $\delta^{18}\text{O}$  during the Upper Permian (modified after GRUSZCZYŃSKI et al. 1992).

The reasons for the strong and fast fluctuations in Sr and O isotopes can be manifold. GRUSZCZYŃSKI et al. (1992) saw the reason in a change between stratified and homogeneously mixed ocean water. MARTIN & MACDOUGALL (1995) took a change to an arid climate and lower erosion rates into account. According to HALLAM (1984) the fluctuations were caused by sea level changes, and KORTE et al. (2003) explained it with a lack in vegetation cover to minimize erosion. A combination of those explanations might have caused the strong fluctuations.

### 5.6 Tritium - The Anthropogenic Time Stamp

$^3\text{H}$  analysis became important after the nuclear weapon tests during the 1960s. Since this peak, the rainout into the meteoric water cycle has decreased strongly from more than 1000 TU (tritium units) to about 70 TU due to the short half life of  $4500 \pm 8$  days. The peak needs about 60 years to decay since every radioactive nuclide will almost vanish after five half lives (without further anthropogenic input). Therefore, within the upcoming twenty years the  $^3\text{H}$  level will be back down to its natural, pre-nuclear background level of about 25-70 TU (FOURRÉ et al. 2006). Groundwater that is older than 60 years should contain no  $^3\text{H}$  since all of it should be decayed by now.

### 5.7 The Composition of Saline Solutions

In general, a saline solution can be described by the charge-balanced components  $\text{CaSO}_4$ ,  $\text{NaCl}$ ,  $\text{KCl}$ ,  $\text{MgCl}_2$ ,  $\text{Na}_2\text{SO}_4$ ,  $\text{K}_2\text{SO}_4$ ,  $\text{MgSO}_4$ , and  $\text{CaCl}_2$ . According to the theoretical considerations of USDOWSKI & DIETZEL (1998), the five ions Na, K, Mg, Cl, and  $\text{SO}_4$  can form six binary, nine ternary, five quaternary, and two quinary phase systems.

The systematics of evaporite solid-solution equilibria were described in detail by e.g. JÄNECKE 1906, VAN'T HOFF (1912), D'ANS (1933), BORCHERT 1940, BRAITSCH (1971) and USDOWSKI & DIETZEL (1998). These systematics are especially important for seepage studies because every saline solution passes several concentration stages during evaporation of seawater or dissolution of evaporitic minerals on the passage through a

salt deposit. By means of these stages (phase transitions in the quinary phase system) each solution can be classified according to its maturity (Figure 5-7; Appendix V).

Under static isothermal evaporation of seawater, the evolution of the residual brine is regulated by the seawater phase system  $\text{NaCl-KCl-MgCl}_2\text{-NaSO}_4\text{-K}_2\text{SO}_4\text{-MgSO}_4\text{-H}_2\text{O}$ , which comprises all five major ions and all phase systems with five or fewer components. With every mineral that precipitates from this brine, its compositional stage moves along a univariant phase boundary in direction to the eutonic point Z (Figure 5-7). Here, the brine dries up and all remaining phases crystallize (D'ANS 1933; BORCHERT 1940).

In salt deposits, syngenetic fluid inclusions should contain a solution with a quinary composition because of their direct incorporation into the salt during seawater evaporation (HERRMANN 1997).

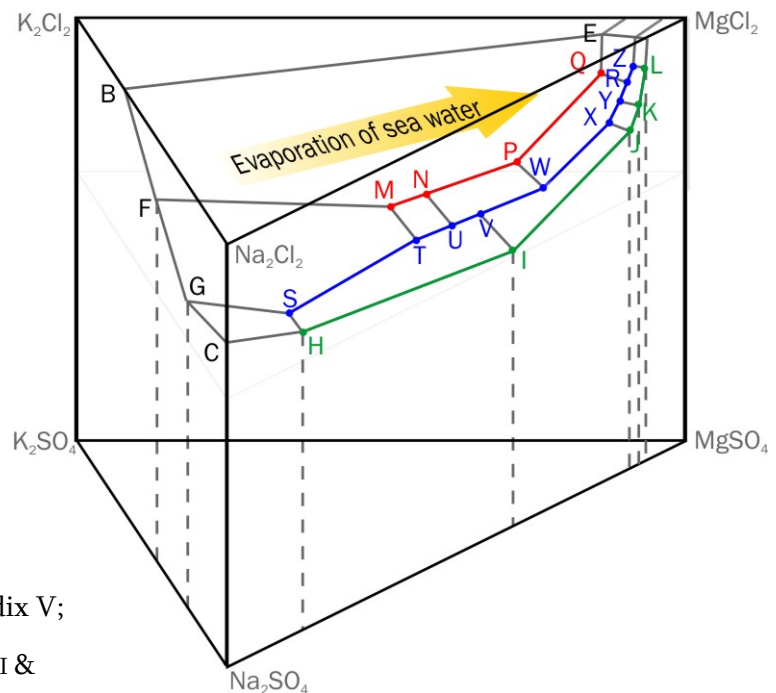


**Figure 5-7:**  
Quinary seawater  
phase system with phase  
transition points (Appendix V;  
modified after USDOWSKI &  
DIETZEL 1998).

Epigenetic internal solutions may comprise a quinary phase system because they may have percolated through the evaporation sequence before final enclosure. On their flow path, they may have dissolved different components and thereby reached a certain level of concentration, according to the quinary phase system (Figure 5-7).

Precipitation of a phase may occur if a particular phase transition is reached. Therefore, the major element composition of such epigenetic internal solutions may resemble that of the syngenetic internal solutions, although the chemical composition does not evolve by evaporation, but dissolution and precipitation (pers. comm. Dr. W. Beer, K+S Group, 2008).

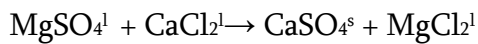
**Table 5-4:** Classification scheme for saline solutions in rock salt and potash mines (after HERRMANN et al. 1978).

| Main group | Sub-group   | Solution | mol/1000 mol H <sub>2</sub> O  | Salt content /solution          |           | Density g/cm <sup>3</sup> (20°C) |         |
|------------|-------------|----------|--------------------------------|---------------------------------|-----------|----------------------------------|---------|
|            |             |          |                                | g/100 g                         | g/1000 ml |                                  |         |
| 1          | Fresh water |          |                                | <0.1                            | <1        | <1.001                           |         |
|            |             |          |                                |                                 |           | ±0.0005                          |         |
| 2          | A           | NaCl     | NaCl>KCl and>MgCl <sub>2</sub> |                                 |           |                                  |         |
| 2          | B           | Salt     | KCl                            | KCl>NaCl and MgCl <sub>2</sub>  | >0.1 <3.5 | >1                               | >1,0005 |
| 2          | C           | water    | MgCl <sub>2</sub>              | MgCl <sub>2</sub> >NaCl and KCl |           | <35                              | <1.03   |
| 2          | D           |          | CaCl <sub>2</sub>              | CaCl <sub>2</sub> >0            |           |                                  | ±0.01   |
| 3          | A           | NaCl     | NaCl>KCl and>MgCl <sub>2</sub> |                                 |           |                                  |         |
| 3          | B           | Low      | KCl                            | KCl>NaCl and MgCl <sub>2</sub>  | >3.5      | >35                              | >1.02   |
| 3          | C           | conc.    | MgCl <sub>2</sub>              | MgCl <sub>2</sub> >NaCl and KCl | <14       | <150                             | <1.11   |
| 3          | D           | brine    | CaCl <sub>2</sub>              | CaCl <sub>2</sub> >0            |           |                                  | ±0.01   |
| 4          | A           | NaCl     | NaCl>KCl and>MgCl <sub>2</sub> |                                 |           |                                  |         |
| 4          | B           | conc.    | KCl                            | KCl>NaCl and MgCl <sub>2</sub>  | >14       | >150                             | >1.10   |
| 4          | C           | brine    | MgCl <sub>2</sub>              | MgCl <sub>2</sub> >NaCl and KCl | <27       | <350                             | <1.24   |
| 4          | D           |          | CaCl <sub>2</sub>              | CaCl <sub>2</sub> >0            |           |                                  | ±0.02   |
| 5          | A           | NaCl     | NaCl>KCl and>MgCl <sub>2</sub> |                                 |           |                                  |         |
| 5          | B           | High     | KCl                            | KCl>NaCl and MgCl <sub>2</sub>  | >27       | >350                             | >1.22   |
| 5          | C           | conc.    | MgCl <sub>2</sub>              | MgCl <sub>2</sub> >NaCl and KCl |           |                                  |         |
| 5          | D           | brine    | CaCl <sub>2</sub>              | CaCl <sub>2</sub> >0            |           |                                  |         |

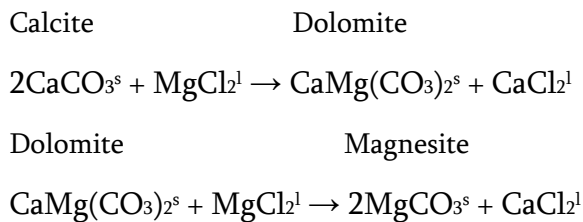
Meteoric external solutions are variable in their chemical composition and are not bound to the quinary phase system that dictates seawater solutions. However, they

depend on the composition of the evaporitic deposit through which they percolate. In general, the solution should be in disequilibrium with most or all phases since they may not fully equilibrate with the salts that they pass on their way to the seepage site. This percolation through the salt may only take days or weeks.

Saline solutions that seep into rock salt or potash mines can be classified after the scheme of HERRMANN (1978) shown in Table 5-4, based on their composition, amount of dissolved salts, and density of the solution. The CaCl<sub>2</sub>-phase shown in Table 5-4 is not a primary seawater component and can exist in solution only after all SO<sub>4</sub> is precipitated (HERRMANN et al. 1997). Therefore, precipitation of gypsum occurs in high-Mg solutions as long as MgSO<sub>4</sub> is present, and the solution will be depleted in Ca:



If no MgSO<sub>4</sub> is left, CaCl<sub>2</sub> will stay in solution. A secondary formation path of a CaCl<sub>2</sub>-solution within the evaporitic deposits could be the solution of calcite by MgCl<sub>2</sub>-rich saline solutions (HERRMANN et al. 1997, and references therein; s=solid, l=liquid):



However, this generation of CaCl<sub>2</sub>-rich solutions is questionable because e.g. ion exchange with argillaceous sediments or volcanic rocks, e.g. basalt, as well as calcite filled caverns could also cause changes in the Ca-budget of a saline solution (pers. comm. Dr. W. W. BEER 2008).

# Part III

## Data Evaluation

6. RESULTS
7. DISCUSSION
8. CONCLUSIONS

## 6. RESULTS – Stable Isotope, Strontium Isotope, and Cation Data

Results for the stable isotopes and strontium isotopes are given for each covered German federal state separately and compared to each other if needed. Cation data are presented for each cluster of ground water and shaft water as well as external and internal solution data. A list of all sampling locations can be accessed in the Tables 3.1 and 3.2. The data, as well as the analyzing method of each result (see Chapter 4), are given in Appendix II.

### 6.1 Stable Isotope Data

Stable isotope data are presented in reference to the Global Meteoric Water Line (GMWL) and the ‘concentration hook’ that is typical for evaporating seawater samples (see Chapters 5.4.1 and 5.4.2). The GMWL after CRAIG (1961a) is defined by the stable isotope composition of meteoric waters from around the globe. The divergence from this line serves as a measure of synsedimentary or postsedimentary connate water within the seepage samples. The concentration hook after LLOYD (1966) indicates the stage of evaporation of such connate samples, if derived from seawater. As presented in Chapter 5.4.2, the degree of evaporation determines the stable isotopic contents of a solution derived from seawater: both deltas become more positive until almost 4-fold seawater concentration is reached. With ongoing evaporation, and multiplied solute contents and precipitation of such, the activity of the water starts to decrease. This decrease in activity, and thus proportionally increased evaporation of the heavier isotopes, results in a drop of  $\delta^{18}\text{O}$  and, subsequently, of  $\delta^2\text{H}$ . Therefore, the evaporation path hooks back to both lower deltas as shown in Figure 6-1. In the following, the stable isotope data will be either compared to the GMWL (external origin) or the concentration hook (internal origin).

#### 6.1.1 $\delta^{18}\text{O}$ and $\delta^2\text{H}$ per Sampling Region

##### *Hessian and Thuringian Boreholes*

All stable isotope data of the groundwater samples are consistent with the GMWL (Figure 6-1a; Table 6-1). Most of



these samples (n=20) from the meteoric water cycle scatter around -10 ‰ for  $\delta^{18}\text{O}$  and -64 ‰ for  $\delta^2\text{H}$ . Only HE b8 346 (n=2) yields heavier water around -6.8 ‰ and -38 ‰ for  $\delta^{18}\text{O}$  and  $\delta^2\text{H}$ , respectively. Here, waste water disposal into the Plattendolomit *Ca3* aquifers, as conducted in this area thitherto by the K+S Group, might be a source for heavy fresh water values. However, the two boreholes actually influenced by waste water disposal, HE b9 430 and HE b10 528, do not show heavier values than the boreholes in undisturbed regions of the aquifers (Figure 6-1a; Table 6-1).

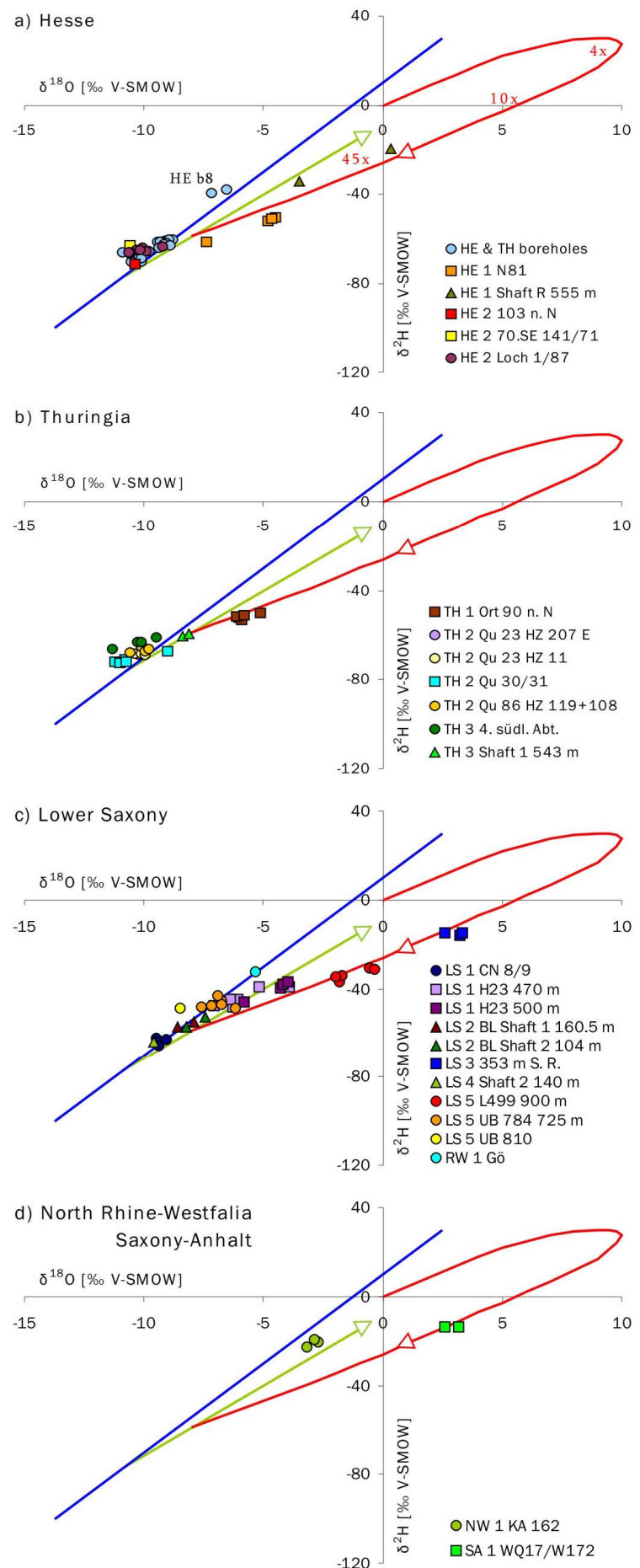
### ***Hessian Mines HE 1 and HE 2***

Two analyses of the shaft site HE 1 Shaft R 555 m yield an oxygen and hydrogen isotope composition far off the GMWL (Figure 6-1a; Table 6-1). These two analyses vary far outside of the analytical uncertainty ( $\pm 0.20$  ‰ for  $\delta^{18}\text{O}$  and  $\pm 1.5$  ‰ for  $\delta^2\text{H}$ ) by 4 and 15 units for  $\delta^{18}\text{O}$  and  $\delta^2\text{H}$ , respectively. In general, shaft water should fall on the GMWL, because it should be comprised of groundwater and rain water, respectively. In case of HE 1 Shaft R 555 m, the divergence from the GMWL probably results from long air exposure and evaporation before and during sampling from a gutter. This contamination or fractionation is not quantifiable, thus making an interpretation impossible. The second sample group of mine HE 1, taken from the internal seepage site HE 1 N81, plots on the concentration hook around -4.6 ‰ for  $\delta^{18}\text{O}$  and -51 ‰ for  $\delta^2\text{H}$  (n=3). One outlying sample shows more meteoric values of -7.40 ‰ and -61.3 ‰ for  $\delta^{18}\text{O}$  and  $\delta^2\text{H}$ . According to the seawater evaporation sequence, the stable isotope composition of all four samples of site HE 1 N81 corresponds to a concentration stage past the K-Mg-salt saturation at more than 45-fold seawater concentration.

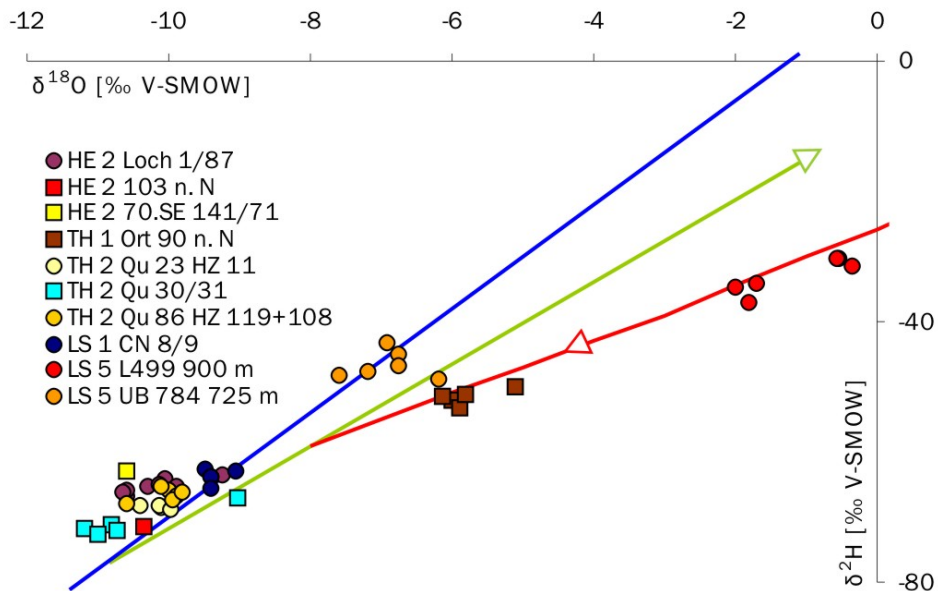
All samples (n=10) from mine HE 2 have  $\delta^{18}\text{O}$  and  $\delta^2\text{H}$  values around -10.2 ‰ and -66 ‰, respectively (Table 6-1). Thus, their stable isotope composition is similar to that of most of the groundwater samples (Figure 6-1a and 6-2). However, based on their flow rate history, two of the samples, HE 2 103 n. N and HE 2 70 SE 141/71, may be of internal origin (sites ran almost dry).

Figure 6-1:

Stable isotope data of samples from boreholes (blue circles), shafts (triangles), and external (circles) and internal (squares) seepage sites per federal state; groundwater and external samples show good correlation with the GMWL (blue line); internal samples follow the concentration hook (red line; green line indicates fresh water evaporation; errors range within  $\pm 0.20\text{‰}$  for  $\delta^{18}\text{O}$  and  $\pm 1.5\text{‰}$  for  $\delta^2\text{H}$ ; both  $\delta$  values on concentration scale).



HE 2 Loch 1/87 is an external seepage, but not yet assigned to the *su* or Rotliegend *pr* aquifer, though the regional conditions make the *pr* as source more likely. For HE 2 Shaft E the stable isotope analysis was not performed, because the sampling bottle was not completely full and air contamination was therefore very likely.



**Figure 6-2:** Stable isotope data of selected sites per federal state; the internal samples (squares) on the left side of the GMWL may be incorporated epigenetic into the rock salt or potash deposits, or even may be of external origin.

### ***Thuringian Mines TH 1 to TH 3***

The samples of the Thuringian mines TH 2 and TH 3 show similar values as the groundwater wells and the mine HE 2 (Figure 6-1b; Table 6-2). The values (n=20) range between -11.30 ‰ to -9.03 ‰ for  $\delta^{18}\text{O}$  and -72.7 ‰ to -61.4 ‰ for  $\delta^2\text{H}$ , respectively, having a little shallower slope than the GMWL. Only the internal site TH 1 Ort 90 n. N HZ 158 is displaced from the GMWL and fits the concentration hook at -5.79 ‰ for  $\delta^{18}\text{O}$  and -51.6 ‰ for  $\delta^2\text{H}$  (n=5). This indicates a concentration stage past the K-Mg salt saturation similar to that of site HE 1 N81. However, TH 1 Ort 90 n. N HZ 158 lies on a straight line with the Thuringian external and shaft samples as well as site TH 2 Qu 30/31, whose origin is still unclear. By means of its stable isotope composition that plots at the intersection of the GMWL and the hook (Figure 6-2) it cannot be associated unequivocally to either groundwater or seawater origin.

**Table 6-1:** Stable isotope data of the boreholes, the shafts, and the external and internal seepage sites at Hessian mines (errors range within  $\pm 0.20$  ‰ for  $\delta^{18}\text{O}$  and  $\pm 1.5$  ‰ for  $\delta^2\text{H}$ ).

| Boreholes |            |                                     | Sites                            |     |                    |                                     |                                  |
|-----------|------------|-------------------------------------|----------------------------------|-----|--------------------|-------------------------------------|----------------------------------|
| #         |            | $\delta^{18}\text{O}$ [‰]<br>V-SMOW | $\delta^2\text{H}$ [‰]<br>V-SMOW | #   |                    | $\delta^{18}\text{O}$ [‰]<br>V-SMOW | $\delta^2\text{H}$ [‰]<br>V-SMOW |
| 31        | TH b1 130  | -9.00                               | -62.2                            | 24  | HE 1 N81           | -4.50                               | -50.7                            |
| 95        | TH b1 130  | -8.98                               | -62.1                            | 23  | HE 1 N81           | -4.80                               | -51.9                            |
| 62        | TH b2 111  | -10.53                              | -70.1                            | 47  | HE 1 N81           | -7.40                               | -61.3                            |
| 103       | TH b2 111  | -10.12                              | -70.2                            | 69  | HE 1 N81           | -4.63                               | -50.8                            |
| 30        | TH b3 3    | -10.10                              | -66.2                            | 22  | HE 1 Shaft R 555 m | -3.50                               | -34.4                            |
| 89        | TH b3 3    | -9.80                               | -65.4                            | 55  | HE 1 Shaft R 555 m | 0.35                                | -19.9                            |
| 33        | HE b4 389  | -9.10                               | -60.8                            | 70  | HE 2 103 n. N      | -10.36                              | -71.4                            |
| 94        | HE b4 389  | -8.81                               | -60.3                            | 16  | HE 2 70.SE 141/71  | -10.60                              | -63.0                            |
| 59        | TH b5 45   | -8.96                               | -60.2                            | 38  | HE 2 Loch 1/87     | -10.30                              | -65.2                            |
| 104       | TH b5 45   | -9.08                               | -61.9                            | 44  | HE 2 Loch 1/87     | -10.60                              | -66.9                            |
| 60        | TH b6 114  | -9.42                               | -61.6                            | 71  | HE 2 Loch 1/87     | -10.04                              | -64.0                            |
| 105       | TH b6 114  | -9.20                               | -63.2                            | 87  | HE 2 Loch 1/87     | -9.24                               | -63.4                            |
| 61        | TH b7 115  | -9.28                               | -61.2                            | 86  | HE 2 Loch 1/87     | -9.90                               | -65.4                            |
| 106       | TH b7 115  | -9.31                               | -61.6                            | 99  | HE 2 Loch 1/87     | -10.59                              | -66.0                            |
| 13        | HE b8 346  | -7.20                               | -39.4                            | 100 | HE 2 Loch 1/87     | -10.65                              | -66.0                            |
| 93        | HE b8 346  | -6.52                               | -38.1                            | 101 | HE 2 Loch 1/87     | -10.15                              | -65.0                            |
| 34        | HE b9 430  | -9.40                               | -63.8                            |     |                    |                                     |                                  |
| 91        | HE b9 430  | -9.16                               | -62.3                            |     |                    |                                     |                                  |
| 11        | HE b10 528 | -10.90                              | -66.2                            |     |                    |                                     |                                  |
| 92        | HE b10 528 | -8.92                               | -62.8                            |     |                    |                                     |                                  |
| 32        | HE b11 431 | -10.20                              | -67.7                            |     |                    |                                     |                                  |
| 90        | HE b11 431 | -10.14                              | -68.7                            |     |                    |                                     |                                  |

### *Lower Saxonian Mines LS 1 to LS 5*

The external samples of LS 1 and LS 5 show meteoric values between  $-9.50$  ‰ to  $-6.20$  ‰ for  $\delta^{18}\text{O}$  and  $-65.7$  ‰ to  $-43.2$  ‰ for  $\delta^2\text{H}$  ( $n=12$ ; Figure 6-1c; Table 6-3). Only site LS 5 L499 900 m is comprised of heavier water with values of  $-1.16$  ‰ and  $-33.0$  ‰ ( $n=6$ ) for  $\delta^{18}\text{O}$  and  $\delta^2\text{H}$ , respectively. Those data plot on the concentration hook and are distinct from the GMWL. However, the meteoric origin of site LS 5 L499 900 m is confirmed by the drill hole LS 5 UB 784 725 m (see Chapter 3.3.3). Membrane filtration through clay intercalations on the groundwater's path through the evaporitic sequence (see Chapter 5.4.2) may cause this shift from LS 5 UB 784 725 on the GMWL in direction to LS 5 L499 900 m on the hook,

as would an admixture of salt internal solutions (see discussion in Chapters 7.1.1 and 7.3).

**Table 6-2:** Stable isotope data of the shafts and the external and internal seepage sites from Thuringian, North Rhine-Westphalian and Saxony-Anhaltinian mines (errors range within  $\pm 0.20$  ‰ for  $\delta^{18}\text{O}$  and  $\pm 1.5$  ‰ for  $\delta^2\text{H}$ ).

| Sites |                         | $\delta^{18}\text{O}$ [‰] | $\delta^2\text{H}$ [‰] | Sites |                    | $\delta^{18}\text{O}$ [‰] | $\delta^2\text{H}$ [‰] |
|-------|-------------------------|---------------------------|------------------------|-------|--------------------|---------------------------|------------------------|
| #     |                         | V-SMOW                    | V-SMOW                 | #     |                    | V-SMOW                    | V-SMOW                 |
| 19    | TH 1 Ort 90 n. N HZ 158 | -5.10                     | -50.0                  | 25    | TH 3 4. südl. Abt. | -9.50                     | -61.4                  |
| 26    | TH 1 Ort 90 n. N HZ 158 | -6.00                     | -52.2                  | 51    | TH 3 4. südl. Abt. | -11.30                    | -66.6                  |
| 39    | TH 1 Ort 90 n. N HZ 158 | -5.90                     | -53.3                  | 68    | TH 3 4. südl. Abt. | -10.27                    | -63.5                  |
| 67    | TH 1 Ort 90 n. N HZ 158 | -6.14                     | -51.5                  | 85    | TH 3 4. südl. Abt. | -10.10                    | -63.1                  |
| 84    | TH 1 Ort 90 n. N HZ 158 | -5.80                     | -51.1                  | 54    | TH 3 Shaft 1 543 m | -8.38                     | -60.7                  |
| 40    | TH 2 Qu 23 HZ 207 E     | -10.20                    | -68.7                  | 89    | TH 3 Shaft 1 543 m | -8.14                     | -59.4                  |
| 28    | TH 2 Qu 23 HZ 11        | -10.10                    | -68.5                  |       |                    |                           |                        |
| 42    | TH 2 Qu 23 HZ 11        | -10.40                    | -68.3                  | 53    | NW 1 KA 162        | -3.20                     | -22.8                  |
| 64    | TH 2 Qu 23 HZ 11        | -10.14                    | -68.2                  | 72    | NW 1 KA 162        | -2.72                     | -20.3                  |
| 81    | TH 2 Qu 23 HZ 11        | -9.98                     | -68.7                  | 88    | NW 1 KA 162        | -2.84                     | -19.1                  |
| 18    | TH 2 Qu 30/31           | -10.80                    | -71.0                  |       |                    |                           |                        |
| 29    | TH 2 Qu 30/31           | -11.20                    | -71.8                  | 21    | SA 1 WQ17/W172     | 2.60                      | -14.0                  |
| 41    | TH 2 Qu 30/31           | -11.00                    | -72.7                  | 108   | SA 1 WQ17/W172     | 3.18                      | -13.5                  |
| 65    | TH 2 Qu 30/31           | -10.74                    | -72.0                  |       |                    |                           |                        |
| 82    | TH 2 Qu 30/31           | -9.03                     | -67.1                  |       |                    |                           |                        |
| 30    | TH 2 Qu 86 HZ 119       | -10.00                    | -65.79                 |       |                    |                           |                        |
| 17    | TH 2 Qu 86 HZ 108       | -10.10                    | -65.31                 |       |                    |                           |                        |
| 27    | TH 2 Qu 86 HZ 108       | -9.90                     | -66.7                  |       |                    |                           |                        |
| 43    | TH 2 Qu 86 HZ 108       | -10.60                    | -68.1                  |       |                    |                           |                        |
| 66    | TH 2 Qu 86 HZ 108       | -9.95                     | -67.2                  |       |                    |                           |                        |
| 38    | TH 2 Qu 86 HZ 108       | -9.82                     | -66.1                  |       |                    |                           |                        |

The interconnected internal seepage sites LS 1 H23 470 m and LS 1 H23 500 m (see Chapter 3.3.3) show a trend apart from the GMWL in direction to the concentration hook. In comparison to the stable isotope contents of other internal sites, the stable isotope composition of LS 1 H23 is displaced to lighter oxygen or heavier hydrogen compositions, respectively, in direction to the GWWL.

**Table 6-3:** Stable isotope data of the shafts, the external and the internal seepage sites from Lower Saxonian mines (errors range within  $\pm 0.20$  ‰ for  $\delta^{18}\text{O}$  and  $\pm 1.5$  ‰ for  $\delta^2\text{H}$ ).

| Sites |                         | $\delta^{18}\text{O}$ [‰] | $\delta^2\text{H}$ [‰] | Sites |                    | $\delta^{18}\text{O}$ [‰] | $\delta^2\text{H}$ [‰] |
|-------|-------------------------|---------------------------|------------------------|-------|--------------------|---------------------------|------------------------|
| #     |                         | V-SMOW                    | V-SMOW                 | #     |                    | V-SMOW                    | V-SMOW                 |
| 15    | LS 1 CN 8/9             | -9.50                     | -62.5                  | 7     | LS 3 353 m S R.    | 3.25                      | -16.0                  |
| 50    | LS 1 CN 8/9             | -9.40                     | -63.9                  | 56    | LS 3 353 m S R.    | 3.33                      | -14.9                  |
| 57    | LS 1 CN 8/9             | -9.42                     | -63.8                  | 79    | LS 3 353 m S R.    | 2.61                      | -14.8                  |
| 80.1  | LS 1 CN 8/9             | -9.40                     | -65.7                  | 6     | LS 4 Shaft 2 140 m | -9.57                     | -64.2                  |
| 80.2  | LS 1 CN 8/9             | -9.05                     | -62.9                  | 1     | LS 5 L499 900 m    | -1.80                     | -37.0                  |
| 3     | LS 1 H23 470 m          | -3.91                     | -39.2                  | 36    | LS 5 L499 900 m    | -1.70                     | -34.2                  |
| 48.1  | LS 1 H23 470 m          | -6.30                     | -48.3                  | 52    | LS 5 L499 900 m    | -2.00                     | -34.6                  |
| 59.1  | LS 1 H23 470 m          | -6.06                     | -44.8                  | 74    | LS 5 L499 900 m    | -0.53                     | -30.4                  |
| 59.2  | LS 1 H23 470 m 19 1/1   | -6.38                     | -45.1                  | 97    | LS 5 L499 900 m    | -0.57                     | -30.4                  |
| 59.3  | LS 1 H23 470 m 21 1/0   | -5.17                     | -39.0                  | 103   | LS 5 L499 900 m    | -0.35                     | -31.5                  |
| 59.4  | LS 1 H23 470 m 21 3/3   | -7.07                     | -47.8                  | 2     | LS 5 UB 784 725 m  | -6.20                     | -48.7                  |
| 4     | LS 1 H23 500 m          | -4.26                     | -39.5                  | 37    | LS 5 UB 784 725 m  | -7.60                     | -48.3                  |
| 5     | LS 1 H23 500 m          | -5.83                     | -45.7                  | 45    | LS 5 UB 784 725 m  | -7.20                     | -47.5                  |
| 50    | LS 1 H23 500 m 16 6/2   | -4.20                     | -37.9                  | 73    | LS 5 UB 784 725 m  | -6.75                     | -45.1                  |
| 58    | LS 1 H23 500 m 16 6/2   | -3.97                     | -36.8                  | 98    | LS 5 UB 784 725 m  | -6.75                     | -46.8                  |
| 8     | LS 2 BL Shaft 1 160.5 m | -7.91                     | -54.7                  | 102   | LS 5 UB 784 725 m  | -6.92                     | -43.2                  |
| 77    | LS 2 BL Shaft 1 160.5 m | -8.58                     | -57.0                  | 46    | LS 5 UB 810        | -8.50                     | -48.8                  |
| 9     | LS 2 BL Shaft 2 104 m   | -7.46                     | -52.8                  |       |                    |                           |                        |
| 78    | LS 2 BL Shaft 2 104 m   | -8.25                     | -57.4                  | 109   | RW 1 Gö            | -5.3                      | -32.6                  |

The salt internal site LS 3 353 m S R. shows the only positive  $\delta^{18}\text{O}$  values of this Lower Saxonian suite around  $+3.06$  ‰ and  $-15.2$  ‰ for  $\delta^2\text{H}$  ( $n=3$ ), indicating an early concentration stage where halite saturation is just passed at a ca. 10.5-fold seawater concentration (see Chapter 5.2). As will be shown in Chapter 7.1.1, the solution of LS 3 353 m s. R. cannot be associated to such low concentrated seawater brine but may be incorporated into the salt at a lower humidity than the main cluster of internal samples, resulting in a different hook placement and therefore in a different positioning of this solution.

The shaft samples of LS 2 and LS 4 plot on the GMWL between the groundwater samples of HE and TH and the heavier rain water values (RW 1 Gö) of  $-5.3$  ‰ and  $-32.6$  ‰ (Figures 6-1a and 6-1c). Direct rain water infiltration near the tubings of the

shafts may cause such pattern, but in this case this process is very unlikely because very low tritium levels exclude such influence.

The two river samples RW 2 Ulster and RW 3 Werra were not analyzed for their stable isotope contents due to non-quantifiable fractionation.

***North Rhine-Westphalian Mine NW 1*** The solutions of NW 1 KA 162 (n=3; Table 6-2) shown in Figure 6-1d fall close to the GMWL at -2.9 ‰ for  $\delta^{18}\text{O}$  and -20 ‰ for  $\delta^2\text{H}$ . These comparably heavy values may result from increased evaporation of the light isotopes from the brine pool in the mine, as it occurs in the initial stages of seawater evaporation (ascending part of the hook).

***Saxony-Anhaltinian Mine SA 1*** The internal seepage site SA 1 WQ17/W172 shows positive  $\delta^{18}\text{O}$  values of +2.89 ‰. Together with the hydrogen isotope composition of -13.7 ‰ (n=2; Figure 6-1d; Table 6-2), this indicates an early concentration stage similar to solution LS 3 353 m S. R.. Both solutions originate from the Hauptanhydrit A3 of the lower Leine Folge, supporting a similar evolution for water samples from this unit during and after deposition.

### 6.1.2 Reproducibility of the stable isotope data over time

Since most of the locations were sampled irregularly, a regular time series covering all annual seasons can only be given for selected sites.

For most samples, the reproducibility of the stable isotope values is within - or only slightly exceeding - the error ranges of  $\pm 0.20$  ‰ for  $\delta^{18}\text{O}$  and  $\pm 1.5$  ‰ for  $\delta^2\text{H}$ . Mainly the shaft samples show larger variations, e.g. HE 1 Shaft R 555 m (Figure 6-1a), resulting from varying degrees of air exposure prior to sampling.

The sampling method is critical for the reproducibility of the stable isotope data, as shown by a few sites where those samples taken by the author yield different stable isotope compositions than those taken by the mine staff (e.g. HE 1 N81). Hence, a strict sampling protocol for each sampling site needs to be followed to avoid sampling-biased data variations.

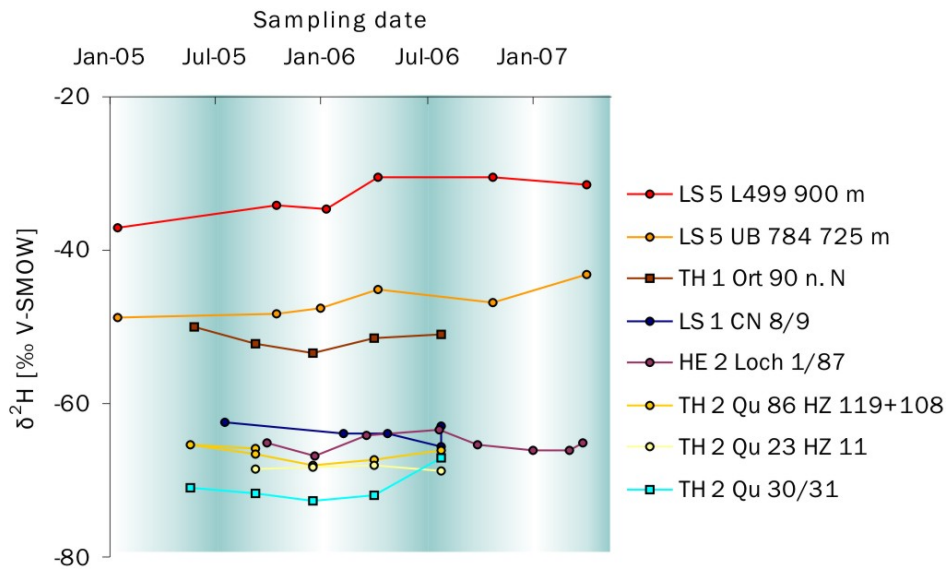


**Figure 6-3:**  $\delta^2\text{H}$  of selected sampling stations vs. sampling date, mirroring the seasonal influence of air temperature and water supply; highs (blue) are during summer, lows (white) during winter time. Differences in flow time from the surface into the mine may prohibit a complete correlation. Analytical uncertainties are within the symbol size.

Variations of the stable isotope composition within one sampling series can also be caused by seasonal fluctuations of surface temperature and water supply. During summer times the increased surface evaporation causes heavier isotope compositions for meteoric waters. Additionally, the supply of heavier rain water due to increased evaporation of  $^{16}\text{O}$  from the rain droplets is higher than during winter (GAT 1996). Some sites with a complete time series show such seasonal variations with higher stable isotope values during summer, whereas the effect is more pronounced for  $\delta^2\text{H}$  (Figure 6-3). In addition, the changes in air temperature might cause fluctuations, also at the internal sites. The air conditioning system within the mines uses surface air. Therefore the warm temperatures during summer can cause relatively higher evaporation of the lighter isotopes, causing a fractionation in direction of more positive stable isotope values (GAT 1996).



## 6.2 Strontium Isotope Data

The conventional way to evaluate  $^{87}\text{Sr}/^{86}\text{Sr}$  ratios of samples from a distinct region with similar end members is the comparison of  $^{87}\text{Sr}/^{86}\text{Sr}$  ratios with the reciprocal of the Sr contents (FAURE 1986). In this diagram a ‘two-component-mixture’ plots on a straight line between two end members. Multi-component mixtures would fall within a polygon defined by more than two end members.

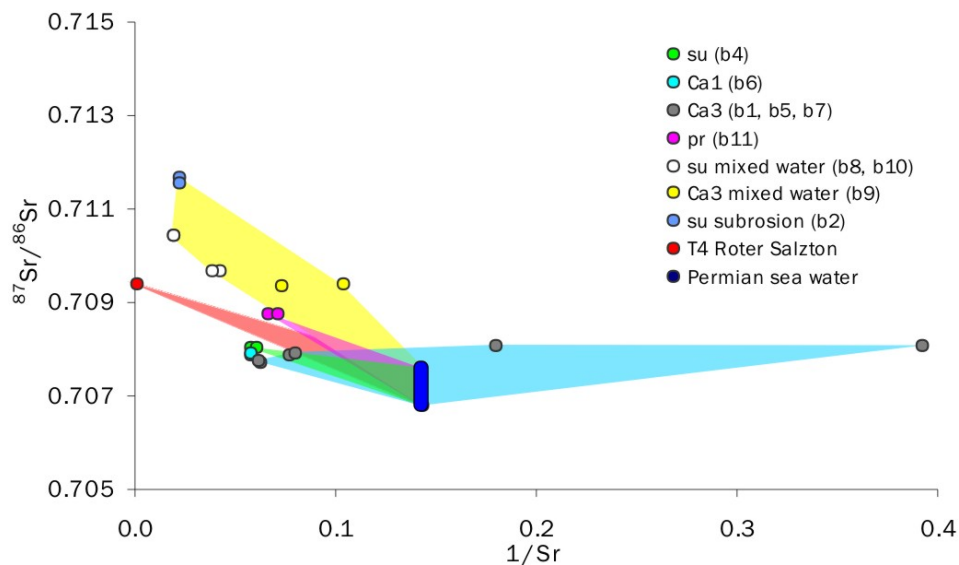


**Figure 6-4:** Modern groundwater, late Permian seawater and detritus (*T4* Roter Salzton) end members for the external seepages; colored areas are the fields for the two-component-mixtures between one groundwater and late Permian seawater (legend shows used boreholes in parentheses; mixed water = groundwater mixed with disposal brine).

The two major end members for this study are the late Permian seawater with  $^{87}\text{Sr}/^{86}\text{Sr}$  ratios between 0.7068 and 0.7076 (see Chapter 5.5.1; Figure 6-4) with an assumed Sr concentration similar to the modern value of about 8 ppm (Table 5.1), and the modern groundwater in the vicinity of the mines. Since the external seepages are fed by different aquifers, the groundwater end member can be represented by the Rotliegend *pr*, the Zechsteinkalk *Ca1*, the Plattendolomit *Ca3*, or the Lower Buntsandstein *su*. Groundwater end members will be applied only to the Hessian and Thuringian samples since aquifer data are only available from the suite of borehole data sampled in Hesse

and Thuringia. The aquifers in the vicinity of the other mines certainly yield different  $^{87}\text{Sr}/^{86}\text{Sr}$  ratios.

**Table 6-4:** Strontium data of the boreholes, the shafts, the external and internal seepage sites from Hessian mines.

| Sites | $^{87}\text{Sr}/^{86}\text{Sr}$ | $\pm 2\sigma$ | Sr       | Sites | $^{87}\text{Sr}/^{86}\text{Sr}$ | $\pm 2\sigma$      | Sr       |          |       |
|-------|---------------------------------|---------------|----------|-------|---------------------------------|--------------------|----------|----------|-------|
| #     | NBS 987                         |               | [ppm]    | #     | NBS 987                         |                    | [ppm]    |          |       |
| 31    | TH b1 130                       | 0.708069      | 0.000011 | 5.56  | 24                              | HE 1 N81           | 0.710749 | 0.000045 | 0.25  |
| 95    | TH b1 130                       | 0.708066      | 0.000009 | 2.55  | 23                              | HE 1 N81           | 0.710323 | 0.000535 | 0.25  |
| 62    | TH b2 111                       | 0.711677      | 0.000021 | 44.30 | 47                              | HE 1 N81           | 0.710557 | 0.000028 | 0.25  |
| 103   | TH b2 111                       | 0.711553      | 0.000024 | 45.09 | 69                              | HE 1 N81           | 0.710560 | 0.000022 | 0.25  |
| 30    | TH b3 3                         | 0.708027      | 0.000005 | 17.46 | 22                              | HE 1 Shaft H 546 m | 0.707930 | 0.000004 | 39.31 |
| 89    | TH b3 3                         | 0.708022      | 0.000011 | 16.57 | 55                              | HE 1 Shaft R 555 m | 0.708230 | 0.000016 | 28.85 |
| 33    | HE b4 389                       | 0.707591      | 0.000030 | 0.08  | 70                              | HE 1 Shaft R 555 m | 0.708236 | 0.000018 | 42.80 |
| 94    | HE b4 389                       | 0.711306      | 0.000010 | 0.08  | 16                              | HE 2 Loch 1/87     | 0.709049 | 0.000012 | 0.64  |
| 59    | TH b5 45                        | 0.707884      | 0.000013 | 13.02 | 38                              | HE 2 Loch 1/87     | 0.708984 | 0.000006 | 2.16  |
| 104   | TH b5 45                        | 0.707910      | 0.000018 | 12.47 | 44                              | HE 2 Loch 1/87     | 0.709038 | 0.000012 | 1.44  |
| 60    | TH b6 114                       | 0.707879      | 0.000015 | 17.43 | 71                              | HE 2 Loch 1/87     | 0.709015 | 0.000018 | 2.15  |
| 105   | TH b6 114                       | 0.707935      | 0.000019 | 17.45 | 87                              | HE 2 Loch 1/87     | 0.709049 | 0.000016 | 8.22  |
| 61    | TH b7 115                       | 0.707738      | 0.000017 | 16.08 | 86                              | HE 2 Loch 1/87     | 0.708996 | 0.000009 | 1.77  |
| 106   | TH b7 115                       | 0.707761      | 0.000012 | 16.15 | 99                              | HE 2 Loch 1/87     | 0.708998 | 0.000014 | 4.09  |
| 13    | HE b8 346                       | 0.710452      | 0.000014 | 51.32 | 100                             | HE 2 Loch 1/87     | 0.709018 | 0.000020 | 4.75  |
| 93    | HE b8 346                       | 0.710449      | 0.000009 | 50.89 | 101                             | HE 2 Shaft E       | 0.709450 | 0.000005 | 8.15  |
| 34    | HE b9 430                       | 0.709396      | 0.000014 | 9.67  |                                 |                    |          |          |       |
| 91    | HE b9 430                       | 0.709376      | 0.000016 | 13.63 | 76                              | RW 2 Ulster        | 0.708069 | 0.000007 | 0.36  |
| 11    | HE b10 528                      | 0.709697      | 0.000005 | 23.39 | 75                              | RW 3 Werra         | 0.708183 | 0.000012 | 0.68  |
| 92    | HE b10 528                      | 0.709676      | 0.000006 | 25.71 |                                 |                    |          |          |       |
| 32    | HE b11 431                      | 0.708778      | 0.000046 | 14.98 |                                 |                    |          |          |       |
| 90    | HE b11 431                      | 0.708764      | 0.000012 | 14.06 |                                 |                    |          |          |       |

The *Ca3* and *su* aquifers in Hesse and Thuringia are also influenced by waste water disposal, which has been monitored in three boreholes in this study. The disposal brine contributes to the Sr budget in the vicinity of those boreholes used for injection (Table 3.2).

For each sampling site the  $^{87}\text{Sr}/^{86}\text{Sr}$  ratios as well as the number of analyses (n) are given in the course of the following section. Outliers are discussed separately but are included in the mean value, if not indicated otherwise. Sr concentration will only be discussed where it is necessary to distinguish between different samples. The entire element chemistry is presented in Chapter 6.4.

### 6.2.1 $^{87}\text{Sr}/^{86}\text{Sr}$ Ratios per Sampling Region

#### ***Hessian and Thuringian Boreholes***

Borehole samples from *Ca3*, *Ca1*, and *su* have a very similar Sr isotope composition ranging from 0.70759 to 0.70803 (n=9; one outlier with  $0.71131 \pm 1$  not included; Table 6-4; Figure 6-4). The Rotliegend borehole HE b11 431 shows elevated  $^{87}\text{Sr}/^{86}\text{Sr}$  ratios of about 0.70877 (n=2). Any higher values for the Sr isotope composition are restricted to samples that are subject to waste water disposal or subsidence. At these contaminated sites HE b8 346, HE b9 430 and HE b10 528 the  $^{87}\text{Sr}/^{86}\text{Sr}$  ratios range between 0.70938 and 0.71168 (n=8) due to higher  $^{87}\text{Sr}/^{86}\text{Sr}$  ratios in the disposal brine caused by dissolution of large amounts of salts containing much Rb. The radioactive  $^{87}\text{Rb}$  decays over time, causing higher  $^{87}\text{Sr}/^{86}\text{Sr}$  ratios in the salts (see Chapter 7.2.1).

Most groundwater samples have higher  $^{87}\text{Sr}/^{86}\text{Sr}$  ratios and higher Sr concentrations than is estimated for the Permian seawater and therefore both are distinguishable from each other (if the original seawater ratio is retained in a seawater solution). Only HE b4 389 yields one similar ratio of 0.70759. However, the two measured ratios of  $0.70759 \pm 3$  and  $0.71133 \pm 1$  vary highly. Therefore, this borehole will be discarded for the following discussion.

Due to the very similar strontium isotope compositions of the three upper aquifers around 0.70789, a distinction between the *Ca1*, the *Ca3*, and the *su* aquifer is impossible based on the  $^{87}\text{Sr}/^{86}\text{Sr}$  ratios alone.

#### ***Hessian Mines HE 1 and HE 2***

Sr isotope compositions in the solutions from mine HE 1 show large variations between 0.70793 and 0.71075. The internal seepage site HE 1 N81 shows varying  $^{87}\text{Sr}/^{86}\text{Sr}$  ratios between 0.71032 and 0.71075 (n=4; Table 6-4; Figure 6-5a). The Sr contents of this site are very low with 0.25 ppm and facilitate contamination by high Sr content fluids or rocks.

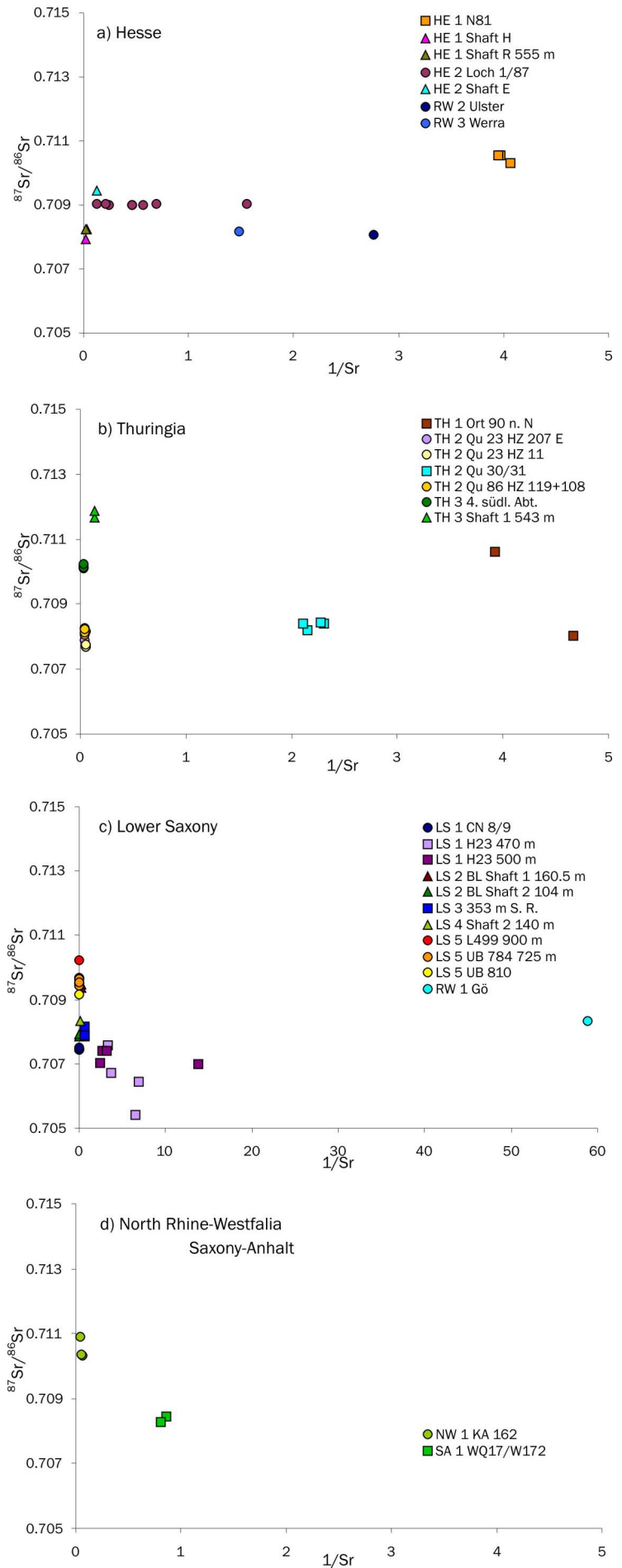


**Figure 6-5:**

Comparison of seepage and shaft data with aquifer end members; an excerpt with included end members is shown in Figure 6-6.

In contrast to HE 1 N81, the two shafts HE 1 Shaft H 546 m and HE 1 Shaft R 555 m have much lower  $^{87}\text{Sr}/^{86}\text{Sr}$  ratios of  $0.70793\pm 1$  and  $0.70823\pm 03$  ( $n=2$ ), respectively, which are in agreement with the ratios from the pierced *Ca3* aquifer (Figure 6-6a).

Three seepage sites were sampled in mine HE 2 (Table 6-4). The two sites HE 2 103 n. N and HE 2 70. SE 141/71 yield such low Sr concentrations that the  $^{87}\text{Sr}/^{86}\text{Sr}$  ratios are not determinable via the regular procedure. The sample amount needed for the columnar elution would yield high salt concentrations that would precipitate prior or during the columnar elution. Therefore, those samples have not been analyzed for  $^{87}\text{Sr}/^{86}\text{Sr}$  ratios. The variations of the Sr isotope composition at site HE 1 N 81 may be addressable to similar problems. At this site, the low Sr contents of 0.25 ppm could be the reason for varying results. However, this is unavoidable without elaborated preparation procedures, like elimination of the major cations by repeated columnar elution prior to the Sr separation.

Seepage site HE 2 Loch 1/87 shows constant values with a mean of 0.70902 ( $n=8$ ) over the whole sampling period. However, its Sr contents vary strongly between 0.64 and 8.22 ppm. With respect to the  $^{87}\text{Sr}/^{86}\text{Sr}$  ratio of HE 2 Loch 1/87, this value is in fairly good agreement with the Rotliegend aquifer value of  $0.70877\pm 1$ . The large variations in Sr contents could result from ongoing gypsum precipitation and dissolution in the contact zone of the water and the Portland cement used to fill several unused boreholes in this area.

Shaft HE 2 Shaft E was only sampled once and yields an  $^{87}\text{Sr}/^{86}\text{Sr}$  ratio of  $0.70945\pm 1$  that is not in agreement with the distinct lower value of the penetrated Lower Buntsandstein.

### ***Thuringian Mines TH 1 to TH 3***

The seepages from Thuringian mines yield highly varying  $^{87}\text{Sr}/^{86}\text{Sr}$  ratios (Table 6-5; Figures 6-5b and 6-6b) that require different origins and different modes of contamination, respectively. The seepage site TH 1 Ort 90 n. N HZ 158 ( $n=3$ ) at mine TH 1 shows very variable  $^{87}\text{Sr}/^{86}\text{Sr}$  ratios between  $0.70803\pm 2$  to  $0.71155\pm 7$ . Two samples were not analyzable due to very low Sr concentrations of about 0.1 ppm (see comment for samples from mine HE 2).

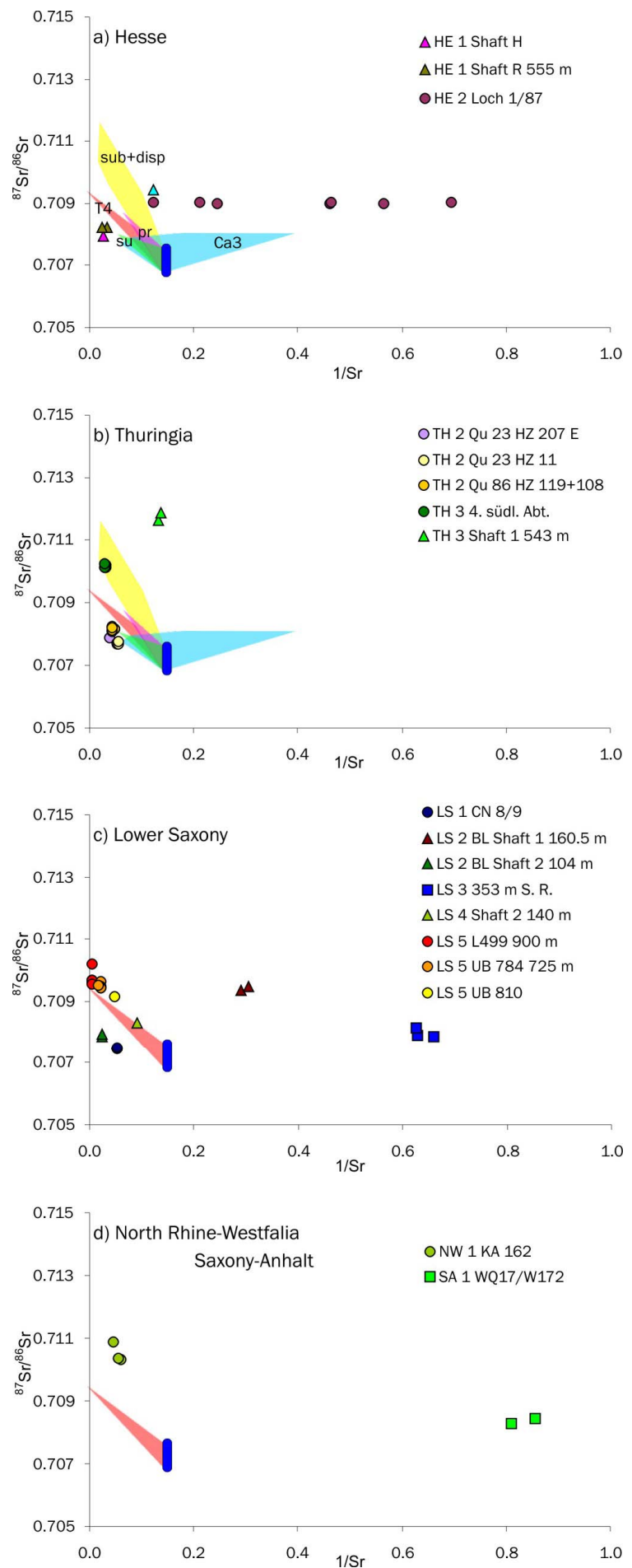


**Figure 6-6:**

Excerpt of Figure 6-5:

Comparison of seepage and shaft data with aquifer end members; colored areas are the fields for the two-component-mixtures between one groundwater and late Permian seawater according to Figure 6-5 (su = Buntsandstein; Ca3 = Plattendolomit; pr = Rotliegend; sub+disp = boreholes influenced by subsrosion or disposal brine).

All samples from mine TH 2 have a Sr isotope composition between 0.70768 and 0.70840 (n=16) similar to that of the three sampled aquifers. Even the Sr concentrations are similar with 13.5 ppm versus 11.7 ppm for the aquifers (Figure 6-6b).

**Table 6-5:** Strontium data of the shafts, the external and internal seepage sites from Thuringian, North Rhine-Westphalian and Saxony-Anhaltinian mines.

| Sites |                         |                                 |               | Sites |     |                                 |               |          |       |
|-------|-------------------------|---------------------------------|---------------|-------|-----|---------------------------------|---------------|----------|-------|
| #     |                         | $^{87}\text{Sr}/^{86}\text{Sr}$ | $\pm 2\sigma$ | Sr    | #   | $^{87}\text{Sr}/^{86}\text{Sr}$ | $\pm 2\sigma$ | Sr       |       |
|       |                         | NBS 987                         |               | [ppm] |     | NBS 987                         |               | [ppm]    |       |
| 19    | TH 1 Ort 90 n. N HZ 158 | 0.708027                        | 0.000015      | 0.21  | 25  | TH 3 4. südl. Abt.              | 0.710181      | 0.000007 | 31.02 |
| 26    | TH 1 Ort 90 n. N HZ 158 | 0.711552                        | 0.000066      |       | 51  | TH 3 4. südl. Abt.              | 0.710102      | 0.000021 | 32.11 |
| 39    | TH 1 Ort 90 n. N HZ 158 | 0.710606                        | 0.000040      | 0.25  | 68  | TH 3 4. südl. Abt.              | 0.710138      | 0.000037 | 34.14 |
| 67    | TH 1 Ort 90 n. N HZ 158 |                                 |               |       | 84  | TH 3 4. südl. Abt.              | 0.710249      | 0.000032 | 35.64 |
| 84    | TH 1 Ort 90 n. N HZ 158 |                                 |               |       | 54  | TH 3 Shaft 1 543 m              | 0.711655      | 0.000007 | 7.59  |
| 40    | TH 2 HZ 207 E           | 0.707899                        | 0.000012      | 26.79 | 89  | TH 3 Shaft 1 543 m              | 0.711880      | 0.000020 | 7.36  |
| 28    | TH 2 Qu 23 HZ 11        | 0.707707                        | 0.000005      | 19.08 |     |                                 |               |          |       |
| 42    | TH 2 Qu 23 HZ 11        | 0.707680                        | 0.000022      | 18.88 | 53  | NW 1 KA 162                     | 0.710326      | 0.000009 | 16.87 |
| 64    | TH 2 Qu 23 HZ 11        | 0.707696                        | 0.000015      | 18.40 | 72  | NW 1 KA 162                     | 0.710367      | 0.000008 | 18.15 |
| 81    | TH 2 Qu 23 HZ 11        | 0.707745                        | 0.000013      | 18.49 | 88  | NW 1 KA 162                     | 0.710895      | 0.000015 | 21.44 |
| 18    | TH 2 Qu 30/31           | 0.708398                        | 0.000012      | 0.43  |     |                                 |               |          |       |
| 29    | TH 2 Qu 30/31           | 0.708188                        | 0.000024      | 0.47  | 21  | SA 1 WQ17/W172                  | 0.708445      | 0.000016 | 1.17  |
| 41    | TH 2 Qu 30/31           | 0.708396                        | 0.000010      |       | 108 | SA 1 WQ17/W172                  | 0.708281      | 0.000017 | 1.23  |
| 65    | TH 2 Qu 30/31           | 0.708427                        | 0.000009      | 0.44  |     |                                 |               |          |       |
| 82    | TH 2 Qu 30/31           | 0.708406                        | 0.000009      | 0.47  |     |                                 |               |          |       |
| 30    | TH 2 Qu 86 HZ 119       | 0.708073                        | 0.000013      | 23.01 |     |                                 |               |          |       |
| 17    | TH 2 Qu 86 HZ 108       | 0.708155                        | 0.000007      | 20.36 |     |                                 |               |          |       |
| 27    | TH 2 Qu 86 HZ 108       | 0.708165                        | 0.000006      | 20.48 |     |                                 |               |          |       |
| 43    | TH 2 Qu 86 HZ 108       | 0.708123                        | 0.000023      | 23.71 |     |                                 |               |          |       |
| 66    | TH 2 Qu 86 HZ 108       | 0.708249                        | 0.000025      | 22.83 |     |                                 |               |          |       |
| 38    | TH 2 Qu 86 HZ 108       | 0.708217                        | 0.000014      | 23.70 |     |                                 |               |          |       |

In contrast to the very constant and low  $^{87}\text{Sr}/^{86}\text{Sr}$  ratios of 0.70810 for solutions from mine TH 2, site TH 3 4. südl. Abt. shows high  $^{87}\text{Sr}/^{86}\text{Sr}$  ratios around 0.71017 (n=4). A contamination may result from the basalt dike through which the solution percolates up into the mine. TH 3 Shaft 1 543 m shows even higher  $^{87}\text{Sr}/^{86}\text{Sr}$  ratios of  $0.71177 \pm 11$  (n=2), the highest  $^{87}\text{Sr}/^{86}\text{Sr}$  ratio of the whole data set. The similar high  $^{87}\text{Sr}/^{86}\text{Sr}$  ratios of those groundwater samples influenced by disposal brine suggest a contamination of the pierced *Ca3* aquifer with such disposal brines in this area.

**Lower Saxonian Mines LS 1 to LS 5**

Based on the  $^{87}\text{Sr}/^{86}\text{Sr}$  vs.  $1/\text{Sr}$  plot each mine in Lower Saxony shows a distinct behavior (Table 6-6; Figure 6-5c and 6-6c). At LS 1, the two sites LS 1 H23 470 m and LS 1 H23 500 m of one corresponding internal seepage site show unexpected different  $^{87}\text{Sr}/^{86}\text{Sr}$  ratios of 0.70768 (n=2) and 0.70722 (n=4), respectively. The external seepage site LS 1 CN 8/9 yields a value of 0.70746 (n=5) which is in the same range as the other samples from LS 1.

The two sampled shafts at LS 2, LS 2 BL Shaft 1 160.5 m and LS 2 BL Shaft 2 104 m show different  $^{87}\text{Sr}/^{86}\text{Sr}$  ratios of 0.70949 (n=2) and 0.70789 (n=2), respectively. They also vary strongly in Sr concentrations with around 3 ppm at Shaft 1 and 40 ppm at shaft 2. Both seepages are on the level of Jurassic strata that is comprised by marls. Since the samples of shaft 1 were taken from an open reservoir, those values should be interpreted with caution due to possible contamination by mixing of other saline water into the reservoir.

Sr isotope compositions at the internal seepage site LS 3 353 m S R. vary around 0.70797 (n=3). This value is in fairly good agreement with those of LS 1 H23, potentially due to the origin from the same host rock. All those internal sites drain the A3. However, LS 3 353 m S R. shows slightly higher Sr concentrations than the samples from LS 1 with 1.6 ppm versus 0.2 ppm.

The inleakage at LS 4 Shaft 2 140 m yields an  $^{87}\text{Sr}/^{86}\text{Sr}$  ratio of  $0.70832 \pm 1$  which is in good agreement with the value of the rainwater of Göttingen (Table 6-6), suggesting that this inleakage is fed by modern rain water. However, its stable isotope composition located on the GMWL, but with distinct lighter values than the rain water, makes groundwater seepage more likely.

The related sites LS 5 L499 900 m and LS 5 UB 784 725 m (see Chapter 3.3.3) show similar  $^{87}\text{Sr}/^{86}\text{Sr}$  ratios of 0.70973 (n=6) and 0.70951 (n=6), though the Sr concentrations differ highly (Table 6-6; see Chapter 6.4.2). Site LS 5 UB 810 yields a lower value of  $0.70917 \pm 1$ . Although all those sites are proofed to be fed by the *su*, their  $^{87}\text{Sr}/^{86}\text{Sr}$  ratios do not correspond to the Thuringian *su* ratio of 0.70802. This shows that certainly the Sr isotope composition of groundwater varies regionally. Therefore, seepages sites from



federal states other than Hesse and Thuringia should not be compared with groundwater data from this region.

**Table 6-6:** Strontium data of the shafts, the external and internal seepage sites from Lower Saxonian mines.

| Strontium data of the shafts |                                 |               |       | Strontium data of the external and internal seepage sites |                                 |               |        |
|------------------------------|---------------------------------|---------------|-------|---|---------------------------------|---------------|--------|
| Sites                        | $^{87}\text{Sr}/^{86}\text{Sr}$ | $\pm 2\sigma$ | Sr    | Sites   | $^{87}\text{Sr}/^{86}\text{Sr}$ | $\pm 2\sigma$ | Sr     |
| #                            | NBS 987                         |               | [ppm] | #   | NBS 987                         |               | [ppm]  |
| 15 LS 1 CN 8/9               | 0.707444                        | 0.000006      | 18.81 | 6 LS 4 Shaft 2 140 m                                      | 0.708320                        | 0.000010      | 10.99  |
| 50 LS 1 CN 8/9               | 0.707453                        | 0.000007      | 19.06 | 1 LS 5 L499 900 m   | 0.709675                        | 0.000003      | 169.00 |
| 57 LS 1 CN 8/9               | 0.707478                        | 0.000015      | 18.71 | 36 LS 5 L499 900 m  | 0.709668                        | 0.000045      | 200.81 |
| 80.1 LS 1 CN 8/9             | 0.707448                        | 0.000026      | 18.74 | 52 LS 5 L499 900 m  | 0.709598                        | 0.000020      | 213.57 |
| 80.2 LS 1 CN 8/9             | 0.707496                        | 0.000015      | 19.19 | 74 LS 5 L499 900 m  | 0.709688                        | 0.000029      | 225.19 |
| 3 LS 1 H23 470 m             | 0.707561                        | 0.000015      | 0.30  | 97 LS 5 L499 900 m  | 0.709548                        | 0.000012      | 237.56 |
| 48.1 LS 1 H23 470 m          | 0.706705                        | 0.000083      | 0.27  | 103 LS 5 L499 900 m                                       | 0.710212                        | 0.000006      | 248.56 |
| 48.3 LS 1 H23 470 m          | 0.706442                        | 0.000200      | 0.14  | 2 LS 5 UB 784 725 m                                       | 0.709641                        | 0.000003      | 45.81  |
| 48.4 LS 1 H23 470 m          | 0.705425                        | 0.003722      | 0.15  | 37 LS 5 UB 784 725 m                                      | 0.709494                        | 0.000011      | 46.46  |
| 4 LS 1 H23 500 m             | 0.707043                        | 0.000160      | 0.42  | 45 LS 5 UB 784 725 m                                      | 0.709450                        | 0.000030      | 45.70  |
| 5 LS 1 H23 500 m             | 0.707010                        | 0.000297      | 0.07  | 73 LS 5 UB 784 725 m                                      | 0.709490                        | 0.000015      | 45.40  |
| 49 LS 1 H23 500 m 16 6/2     | 0.707414                        | 0.000018      | 0.37  | 98 LS 5 UB 784 725 m                                      | 0.709440                        | 0.000011      | 44.70  |
| 58 LS 1 H23 500 m 16 6/2     | 0.707393                        | 0.000014      | 0.31  | 102 LS 5 UB 784 725 m                                     | 0.709533                        | 0.000010      | 56.83  |
| 8 LS 2 BL Shaft 1 160.5 m    | 0.709364                        | 0.000005      | 3.45  | 46 LS 5 UB 810  | 0.709166                        | 0.000007      | 20.87  |
| 77 LS 2 BL Shaft 1 160.5 m   | 0.709466                        | 0.000018      | 3.29  |   |                                 |               |        |
| 9 LS 2 BL Shaft 2 104 m      | 0.707852                        | 0.000005      | 41.64 | 109 RW 1 Gö   | 0.708323                        | 0.000036      | 0.02   |
| 78 LS 2 BL Shaft 2 104 m     | 0.707928                        | 0.000017      | 40.35 |   |                                 |               |        |
| 7 LS 3 353 m S R.            | 0.707859                        | 0.000016      | 1.52  |   |                                 |               |        |
| 56 LS 3 353 m S R.           | 0.707899                        | 0.000013      | 1.59  |   |                                 |               |        |
| 79 LS 3 353 m S R.           | 0.708155                        | 0.000046      | 1.60  |   |                                 |               |        |

### ***North Rhine-Westphalian Mine NW 1***

The one seepage site NW 1 KA 162 shows varying  $^{87}\text{Sr}/^{86}\text{Sr}$  ratios around 0.71053 (n=3; Table 6-5; Figure 6-6d). The Sr concentrations are constant with values around 18.8 ppm. This most likely excludes an internal origin since all undoubted internal seepages yield Sr concentrations not exceeding 1.6 ppm. The similarity with the contaminated groundwater is not noteworthy since in that area no waste water disposal is conducted.

### ***Saxony-Anhaltinian Mine SA 1***

The  $^{87}\text{Sr}/^{86}\text{Sr}$  ratios of site SA 1 WQ 17/W172 around 0.70836 (n=2; Table 6-5; Figure 6-6d) slightly exceed those of LS 1 H

23 and LS 3 353 m S R., though all drain the *A3*. The Sr concentration of 1.2 ppm is in the same dimension.

### ***Rain water and River Water***

The rainwater of Göttingen, RW 1 Gö, shows an  $^{87}\text{Sr}/^{86}\text{Sr}$  ratio of  $0.70832 \pm 4$  (Table 6-6; Figure 6-5c).

Both rivers RW 2 Ulster and RW 3 Werra show similar  $^{87}\text{Sr}/^{86}\text{Sr}$  ratios of  $0.70807 \pm 1$  and  $0.70818 \pm 1$  (Table 6-4; Figure 6-5a), which are in fairly good agreement with the rainwater value, respectively.

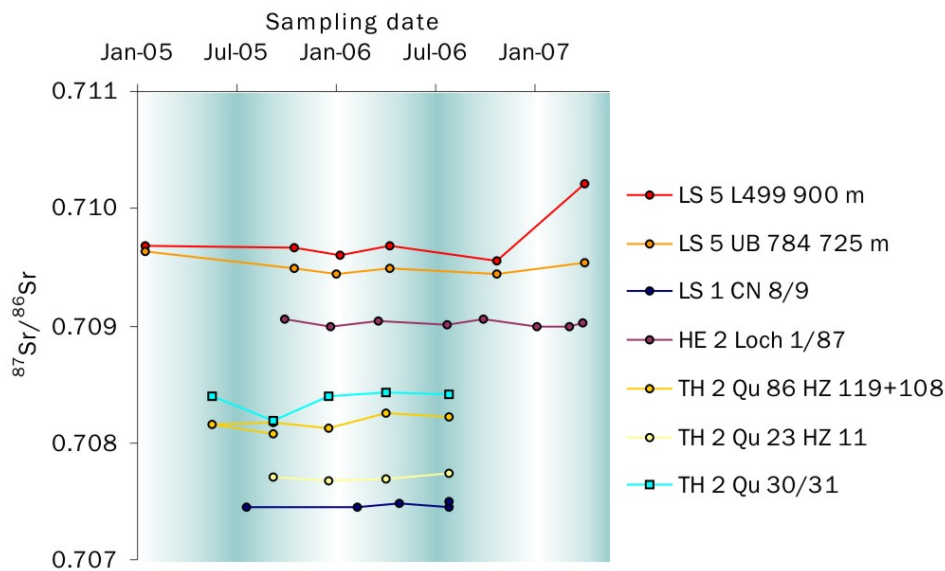


**Figure 6-7:**  $^{87}\text{Sr}/^{86}\text{Sr}$  ratios of selected sampling stations vs. sampling date, showing only slight seasonal variations with lower  $^{87}\text{Sr}/^{86}\text{Sr}$  ratios around January. Analytical uncertainties are within the symbol size.

### **6.2.2 Reproducibility of the strontium isotope data over time**

A time series covering all annual seasons can only be given for selected sites due to irregular sampling. Figure 6-7 shows  $^{87}\text{Sr}/^{86}\text{Sr}$  ratios of such sites, corresponding to Figure 6-2 that shows the time series of  $\delta^2\text{H}$ . For the  $^{87}\text{Sr}/^{86}\text{Sr}$  ratio, a regular seasonal variation with lower values around January is only suggestively pronounced. For the external sites, this trend could be influenced by rain water that dilutes the seeping water in spring, causing a mixture with a lower  $^{87}\text{Sr}/^{86}\text{Sr}$  ratio than the original water.

The measurement stability of the saline solutions is very strong, though the  $^{87}\text{Sr}/^{86}\text{Sr}$  ratios vary more or less pronounced at each sampling site. Only three  $^{87}\text{Sr}/^{86}\text{Sr}$  ratios were measured with errors higher than the GZG mean of  $\pm 0.000083$  ( $2\sigma$ ; see Chapter 4.2.2). Therefore, the variations in  $^{87}\text{Sr}/^{86}\text{Sr}$  ratio cannot be addressed to measurement errors.

### 6.3 Tritium Data

18 analyses of  $^3\text{H}$  for selected samples (mainly groundwater and shaft water) were commissioned to the UFZ. 11 results were below the detection limit, thus indicating no connection between surface water and the analyzed sample. Four data were below 1.3 TU (Tritium units; see Chapter 4.3). Those results could represent artifacts of the sampling and contamination by air. The three higher results were obtained from the groundwater samples HE b9 430, HE b10 528 and shaft HE 1 shaft R 555 m. The groundwater values of 4.4 and 9.3 TU, respectively, might be associated with the waste water disposal by which both groundwater boreholes are influenced. The shaft water value of 5.8 TU could be addressed to the sampling from a reservoir fed by the shaft water via a gutter since in this setting contamination by disposal brine is likely.

### 6.4 Major and Trace Cation Data

The concentrations of major cations give first evidence for the origin and saturation history of a saline solution encountered in a rock salt or potash mine. In the following, each group of the significant cation data is evaluated separately. Samples are divided into groundwater-, shaft-, external-, and internal liquid samples. Outliers and samples with disputed origin will be given particular attention. The major cation results provide a basis for integrating the different geochemical tools to determine the solution origin. A synthesis and detailed interpretation of the data set is performed in Chapter 7. The whole cation data set can be accessed in Appendix II.

**Table 6-7:** Major cation concentrations in ppm for the boreholes and meteoric water samples.

| NAME                              | Na       | K       | Ca      | Mg      | Rb    | Sr    | Fe    | Li    | Mn   | Zn   |
|-----------------------------------|----------|---------|---------|---------|-------|-------|-------|-------|------|------|
| <b># Boreholes &amp; Meteoric</b> |          |         |         |         |       |       |       |       |      |      |
| 31 TH b1 130                      | 18061.44 | 134.84  | 285.67  | 265.52  | 0.32  | 5.63  | 0.00  | 0.84  | 1.58 | 0.00 |
| 95 TH b1 130                      | 18571.12 | 138.81  | 141.99  | 269.15  | 0.42  | 5.03  | 0.00  | 1.26  | 0.11 | 0.00 |
| 62 TH b2 111                      | 23660.76 | 239.39  | 1607.34 | 372.03  | 0.96  | 56.24 | 0.00  | 5.80  | 5.80 | 0.00 |
| 103 TH b2 111                     | 21547.49 | 209.73  | 1447.85 | 333.31  | 1.09  | 61.60 | 0.05  | 6.63  | 6.68 | 0.00 |
| 30 TH b3 3                        | 43808.79 | 342.17  | 1193.37 | 289.23  | 0.34  | 20.49 | 0.16  | 0.83  | 3.74 | 0.00 |
| 89 TH b3 3                        | 44159.02 | 363.35  | 1136.56 | 310.94  | 0.41  | 23.24 | 11.99 | 1.06  | 5.12 | 0.00 |
| 33 HE b4 389                      | 19.92    | 1.94    | 35.62   | 18.65   | 0.00  | 0.11  | 0.00  | 0.03  | 0.01 | 0.04 |
| 94 HE b4 389                      | 17.55    | 2.58    | 30.49   | 18.52   | 0.00  | 0.14  | 0.00  | 0.04  | 0.01 | 0.00 |
| 59 TH b5 45                       | 12511.78 | 182.72  | 1088.43 | 137.34  | 0.54  | 17.34 | 0.04  | 0.48  | 0.01 | 0.00 |
| 104 TH b5 45                      | 12078.59 | 182.67  | 1078.13 | 134.49  | 0.54  | 16.54 | 0.00  | 0.46  | 0.01 | 0.00 |
| 60 TH b6 114                      | 16097.25 | 147.22  | 1534.19 | 163.45  | 0.23  | 22.57 | 13.83 | 0.52  | 3.09 | 0.00 |
| 105 TH b6 114                     | 16508.17 | 153.84  | 1533.18 | 168.73  | 0.24  | 23.26 | 0.03  | 0.54  | 3.23 | 0.00 |
| 61 TH b7 115                      | 9802.27  | 86.59   | 1370.35 | 149.15  | 0.12  | 20.69 | 0.20  | 0.28  | 0.14 | 0.00 |
| 106 TH b7 115                     | 9712.34  | 88.94   | 1347.81 | 146.62  | 0.12  | 21.18 | 0.00  | 0.28  | 0.17 | 0.00 |
| 13 HE b8 346                      | 45126.30 | 816.04  | 2387.25 | 1721.03 | 1.23  | 53.95 | 0.00  | 11.06 | 3.88 | 0.00 |
| 93 HE b8 346                      | 44817.28 | 750.49  | 2328.43 | 1692.16 | 1.53  | 67.56 | 0.06  | 15.04 | 5.31 | 0.00 |
| 34 HE b9 430                      | 46950.42 | 6062.84 | 786.19  | 8412.31 | 21.87 | 15.33 | 0.00  | 4.24  | 2.76 | 0.00 |
| 91 HE b9 430                      | 43535.57 | 5708.87 | 735.63  | 8142.15 | 25.29 | 18.44 | 0.42  | 5.09  | 3.59 | 0.00 |
| 11 HE b10 528                     | 55789.13 | 2852.18 | 1262.83 | 6689.83 | 4.46  | 24.86 | 0.00  | 0.65  | 1.41 | 0.00 |
| 92 HE b10 528                     | 52161.55 | 2589.58 | 1172.27 | 6089.62 | 5.59  | 31.67 | 4.47  | 0.97  | 1.57 | 0.00 |
| 32 HE b11 431                     | 5972.88  | 68.19   | 743.35  | 202.92  | 0.11  | 17.89 | 0.00  | 0.40  | 2.66 | 0.20 |
| 90 HE b11 431                     | 5860.63  | 66.43   | 742.06  | 200.43  | 0.00  | 0.00  | 0.00  | 0.00  | 0.00 | 0.00 |
| 108 RW 1 Gö                       | 2.17     | 1.09    | 0.78    | 0.12    | 0.00  | 0.00  | 0.00  | 0.00  | 0.00 | 0.12 |
| 75 RW 2 Ulster                    | 9.65     | 2.32    | 54.49   | 15.22   | 0.00  | 0.69  | 0.00  | 0.00  | 0.00 | 0.02 |
| 74 RW 3 Werra                     | 36.80    | 3.86    | 37.67   | 10.74   | 0.01  | 0.57  | 0.00  | 0.01  | 0.00 | 0.00 |

#### 6.4.1 Sodium, Potassium, and Magnesium

The relationships of Na, K, and Mg concentrations in a brine derived by evaporation from seawater decide about its evolutionary stage between purely halite and bischofite precipitation. As shown in Figure 6-8, the quinary seawater phase system provides mainly two paths of phase equilibria until the eutonic point Z is reached where all water is evaporated (Z can also be reached from a Q solution via the transition line to R; see Chapter 5.7 for background information). The comparison of the Na, K, and Mg contents of the samples with those two paths gives evidence whether a saline solution emanates from seawater or groundwater since the ratios between Na, K, and Mg behave differently (concentration paths for all figures are adapted from BORCHERT

1940). Upon percolation of fluids through salt deposits, processes of dissolution and (re)crystallization caused by changes in the equilibrium conditions can alter the original phase equilibria. Such processes can also produce solutions that comprise fewer phases than the comprehensive quinary phase system. For instance, if groundwater percolates through pure rock salt deposits, the phase system will be a binary NaCl-H<sub>2</sub>O system. But also the quinary phase system can be reached via dissolution of various salt minerals. This fact makes the distinction between syngenetic and epigenetic internal solutions challenging.

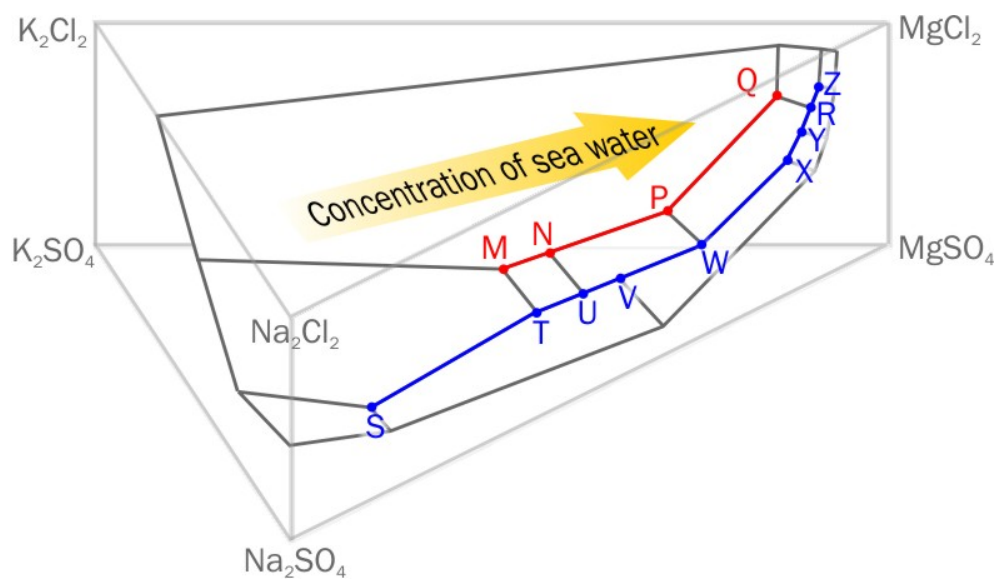


**Figure 6-8:** Quinary system (simplified) showing evolutionary paths of evaporating brines up to the Q and Z solutions (Z = eutonic point, evaporation to dryness; see Chapter 5.7 for background information; modified after USDOWSKI & DIETZEL 1998).

Figure 6-9 shows a distinction between the different solutions with respect to their Na and K contents. The groundwater samples (light blue) can be subdivided into one group that yields less than ca. 24000 ppm Na and less than ca. 183 ppm K, and a second cluster with more than ca. 43000 ppm Na and up to ca. 6000 ppm K (Table 6-7). The latter are affected by the contamination with disposal brine in the aquifers. Only the two samples of TH b2 111 are known to be uncontaminated, but plot in the second

cluster. The groundwater at this borehole is highly mineralized (Table 6-7) probably due to its vicinity to the salt deposits.

The shaft samples (green) show high variations in both Na and K concentrations. The values partly exceed those of the contaminated groundwater samples (Figure 6-9; Table 6-8) but do not reach as high Na concentrations as the external solutions (orange).

**Table 6-8:** Cation concentrations in ppm for the shaft water samples.

| NAME                       | Na       | K        | Ca      | Mg       | Rb    | Sr    | Fe   | Li    | Mn   | Zn    |
|----------------------------|----------|----------|---------|----------|-------|-------|------|-------|------|-------|
| <b># Shafts</b>            |          |          |         |          |       |       |      |       |      |       |
| 20 HE 1 Shaft H 546 m      | 70246.75 | 1643.39  | 1177.90 | 2849.63  | 3.69  | 46.03 | 0.00 | 18.86 | 0.51 | 0.00  |
| 22 HE 1 Shaft R 555 m      | 48907.62 | 1750.60  | 1276.61 | 2346.32  | 3.54  | 32.89 | 0.00 | 8.40  | 0.28 | 1.69  |
| 55 HE 1 Shaft R 555 m      | 81022.26 | 2161.01  | 917.87  | 3084.46  | 4.94  | 48.29 | 0.20 | 18.81 | 0.40 | 0.00  |
| 11 HE 2 Shaft E            | 29.54    | 19.72    | 621.49  | 120.58   | 0.03  | 9.14  | 0.00 | 0.14  | 0.00 | 0.09  |
| 8 LS 2 BL Shaft 1 160.5 m  | 4824.23  | 69.90    | 112.96  | 43.76    | 0.08  | 3.84  | 0.00 | 0.69  | 0.00 | 0.00  |
| 77 LS 2 BL Shaft 1 160.5 m | 8276.97  | 119.63   | 149.35  | 74.32    | 0.18  | 8.27  | 0.00 | 1.68  | 0.00 | 0.00  |
| 9 LS 2 BL Shaft 2 104 m    | 829.67   | 24.49    | 865.69  | 210.70   | 0.01  | 22.51 | 0.39 | 0.18  | 0.00 | 0.10  |
| 78 LS 2 BL Shaft 2 104 m   | 850.55   | 25.36    | 874.65  | 214.40   | 0.01  | 26.80 | 0.00 | 0.23  | 0.00 | 0.00  |
| 6 LS 4 Shaft 2 140 m       | 87733.38 | 36522.35 | 1072.56 | 3344.32  | 10.40 | 13.71 | 0.00 | 0.62  | 3.69 | 0.43  |
| 54 TH 3 Shaft 1 543 m      | 80045.79 | 9028.66  | 515.16  | 12105.67 | 29.98 | 13.85 | 0.32 | 0.79  | 2.83 | 0.00  |
| 89 TH 3 Shaft 1 543 m      | 73567.33 | 8381.18  | 468.91  | 10716.87 | 29.27 | 13.48 | 0.00 | 0.81  | 5.45 | 17.56 |

The external solutions (and also the shaft waters) should be considered with caution since they do not necessarily yield a quinary solution. The samples show the highest Na concentrations of the whole data set around 100000 ppm. Most of the external solutions plot in a distinct area with high Na and low K contents (Figures 6-9, 6-10; Table 6-9) and hence a high Na/K ratio of 12-152, which is on the same order as the seawater ratio of 28. In such solutions only little precipitation of early evaporitic minerals like gypsum occurs. The density evolution shown in Figure 6-11 supports this since the density range of the external solutions is very narrow and shows only insignificant changes with increasing Mg content. This behavior is in contrast to all other samples, even the groundwater samples, which also increase in density with rising Mg contents.

In comparison to the majority of the internal samples (pink) with not more than 12000 ppm Na, the shaft and external solutions did not reach a high level of concentration. In those solutions, the extent of precipitation is limited by the low concentrations of the other components, like K and Mg, since the solution does not yield a quinary phase system.

Only after a certain level of concentration of Mg and K is reached, like in most of the internal solutions between point X (or Q) and Z (Figures 6-9 and 6-10), the halite precipitation occurs in such amounts that the Na (and K) contents decrease to almost 0 (point Z). At that point Mg dominates the solution (BORCHERT 1940, STEWART 1963). Indeed, Figure 6-10 shows such a trend for Na vs. Mg and K vs. Mg, respectively.

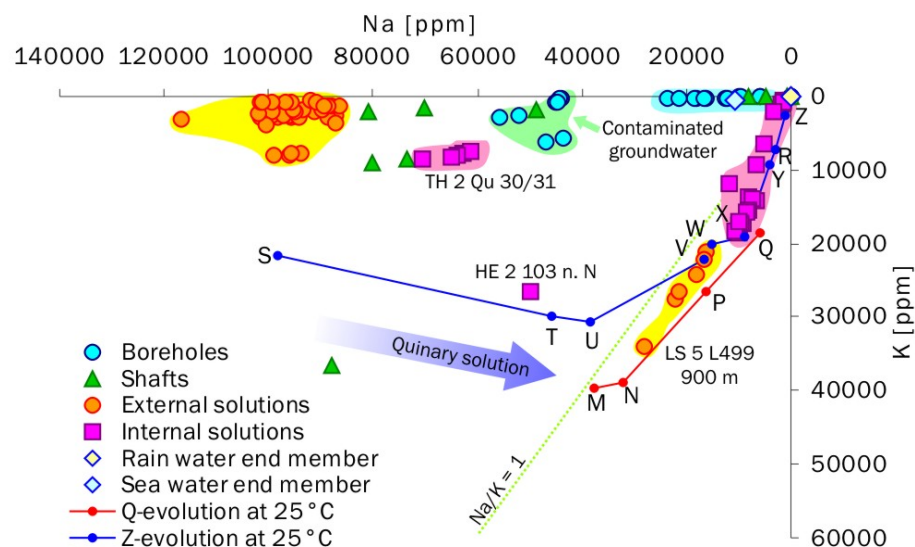


**Figure 6-9:** Distinction between the different solutions by their Na and K contents; comparison with quinary evolution of seawater up to the points Q and Z helps to distinguish between groundwater and seawater sources (blue and red concentration paths adapted from BORCHERT 1940).

Most internal solutions yield distinct Na, K, and Mg contents (Table 6-10) with lower (Na) and higher (K, Mg) than seawater that separates this group from the other groups and point out their seawater origin. Especially in Figure 6-10 the K contents spread the internal samples along the evolutionary path from about X (or Q) stage to a Z solution, respectively. The increase in density with increasing Mg contents, as seen in Figure 6-

11, backs up the advanced stage in evaporation of the original seawater. This further confirms results from stable isotope data (see Chapter 6.1.1).

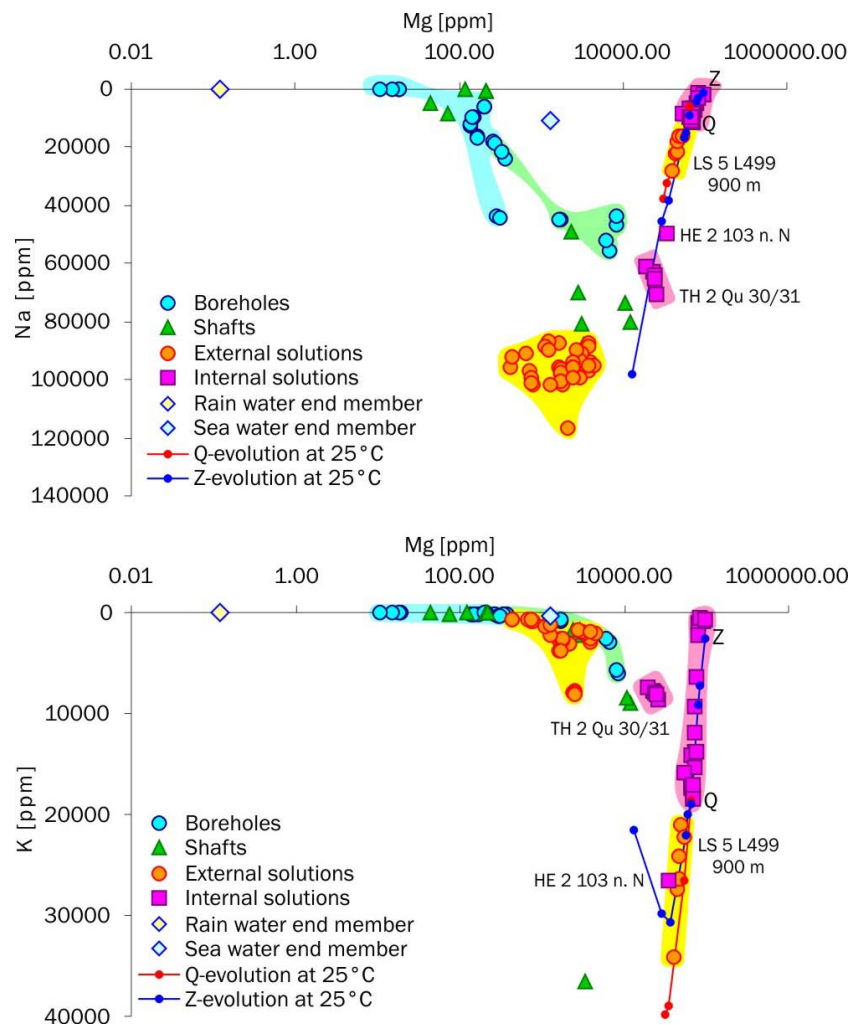


**Figure 6-10:** Distribution of Na and K vs. Mg in samples from shafts, external and internal seepage sites; the evolutionary paths up to the points Q and Z of the quinary phase system point up the sources of the different solutions (blue and red concentration paths adapted from BORCHERT 1940).

The solutions of site LS 5 L499 900 m show an atypical behavior to their external origin when comparing their Na, K, and Mg contents (Figures 6-9 and 6-10). The Na/K ratio is around 1 (Figure 6-9), which is in the range of concentrated seawater solutions from that K-Mg minerals precipitate ( $\text{Na/K} \ll 4.6$ ). Additionally, the density range (Figure 6-11) does support such an advanced stage close to the onset of carnallite precipitation (Q solution), possibly reached through excessive dissolution of various salt minerals.



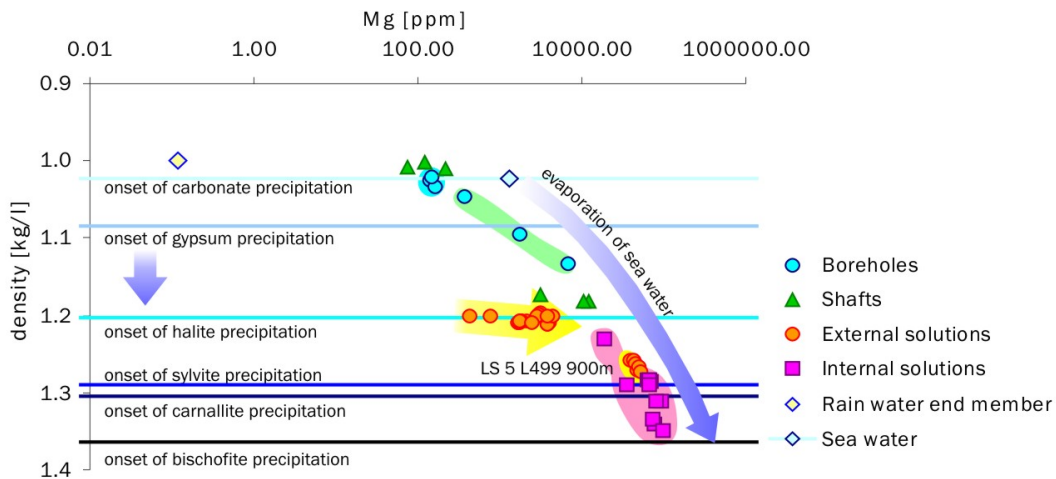


**Figure 6-11:** Density vs. Mg contents from samples from shafts, external and internal seepage sites; blue lines indicate the minimum density at the onset of the precipitation of an evaporitic mineral (precipitation stages after FONTES & MATRAY 1993).

Two of the questionable internal solution groups, the sites HE 2 103 n. N and TH 2 Qu 30/31, do not fit into the pattern of other internal solutions, though their density is higher than in the external samples and the composition is more advanced (Figures 6-10 and 6-11). The Na concentrations are about six times higher than in seawater, whereas all other internal samples yield significantly less Na. This may indicate an epigenetic (or even external) origin of both solutions, and an early concentration stage before or within halite precipitation. Final evaluation will be done separately in Chapter 7.3.

To conclude, the distinction between regular internal and external solutions is possible by comparison of Na, K, and Mg. Only epigenetic internal solutions, or those that seem to be a mixture of internal and external solutions, cannot be identified unequivocally. In such cases, additional tools are needed to be included in the considerations.

Table 6-9: Cation concentrations in ppm for the external seepages.

| NAME                  | Na        | K        | Ca      | Mg       | Rb     | Sr     | Fe      | Li    | Mn     | Zn                 |
|-----------------------|-----------|----------|---------|----------|--------|--------|---------|-------|--------|--------------------|
| # External seepages   |           |          |         |          |        |        |         |       |        | *calibration error |
| 38 HE 2 Loch 1/87     | 95850.20  | 2727.85  | 18.38   | 1630.60  | 2.59   | 0.09   | 0.66    | 4.35  | 0.03   | 0.00               |
| 44 HE 2 Loch 1/87     | 95532.60  | 2668.76  | 8.19    | 1693.64  | 2.97   | 0.00   | 0.00    | 5.52  | 0.00   | 0.00               |
| 71 HE 2 Loch 1/87     | 98346.61  | 2732.19  | 24.08   | 1770.25  | 3.00   | 0.62   | 0.00    | 6.47  | 0.02   | 0.00               |
| 87 HE 2 Loch 1/87     | 101695.69 | 2717.14  | 12.62   | 1865.73  | 3.38   | 0.02   | 0.00    | 6.87  | 0.13   | 0.00               |
| 86 HE 2 Loch 1/87     | 96072.30  | 2503.76  | 10.83   | 1747.26  | 3.24   | 0.00   | 0.00    | 6.51  | 0.12   | 0.00               |
| 99 HE 2 Loch 1/87     | 116759.39 | 3170.66  | 22.39   | 2122.33  | 3.78   | 0.68   | 0.06    | 6.93  | 1.77   | 0.00               |
| 100 HE 2 Loch 1/87    | 99442.35  | 2701.97  | 25.29   | 1789.80  | 3.24   | 0.84   | 0.00    | 6.15  | 1.59   | 3.19               |
| 101 HE 2 Loch 1/87    | 97287.33  | 2560.77  | 20.94   | 1734.22  | 2.98   | 0.24   | 0.00    | 5.65  | 1.32   | 0.10               |
| 15 LS 1 CN 8/9        | 87110.40  | 2664.78  | 429.82  | 3871.01  | 2.26   | 23.61  | 1.63    | 0.37  | 3.99   | 0.00               |
| 50 LS 1 CN 8/9        | 88673.48  | 2797.17  | 413.71  | 3793.54  | 2.30   | 25.58  | 0.03    | 0.40  | 4.31   | 0.00               |
| 57 LS 1 CN 8/9        | 94098.62  | 2937.49  | 441.10  | 3917.45  | 2.24   | 24.24  | 0.00    | 0.39  | 4.26   | 0.00               |
| 80.1 LS 1 CN 8/9      | 97217.42  | 2664.95  | 480.10  | 3849.77  | 1.93   | 21.93  | 0.37    | 0.31  | 3.50   | 0.00               |
| 1 LS 5 L499 900 m     | 28122.62  | 34107.61 | 5316.31 | 39240.50 | 106.73 | 189.03 | 4182.63 | 19.57 | 265.98 | 34.13              |
| 36 LS 5 L499 900 m    | 22288.53  | 27428.86 | 5623.10 | 43223.33 | 120.41 | 220.45 | 2946.47 | 24.17 | 318.72 | 40.11              |
| 52 LS 5 L499 900 m    | 21315.04  | 26399.35 | 6236.86 | 45945.70 | 145.03 | 278.52 | 3385.76 | 30.64 | 383.96 | 51.53              |
| 74 LS 5 L499 900 m    | 18187.56  | 24105.47 | 6384.61 | 46728.48 | 148.66 | 291.56 | 3496.75 | 31.83 | 394.22 | 52.56              |
| 97 LS 5 L499 900 m    | 16146.25  | 21117.51 | 6714.11 | 49046.46 | 157.51 | 322.18 | 3550.96 | 34.86 | 406.97 | 55.96              |
| 103 LS 5 L499 900 m   | 16443.30  | 22188.23 | 7502.54 | 52675.19 | 162.77 | 355.37 | 4592.03 | 37.51 | 414.60 | 60.11              |
| 2 LS 5 UB 784 725 m   | 91161.90  | 1998.76  | 1897.11 | 3129.20  | 4.63   | 40.16  | 2.73    | 2.13  | 2.75   | 0.00               |
| 37 LS 5 UB 784 725 m  | 94745.84  | 1877.94  | 1961.77 | 3021.00  | 6.03   | 57.14  | 0.42    | 3.62  | 3.89   | 0.00               |
| 45 LS 5 UB 784 725 m  | 93494.11  | 1855.40  | 1961.23 | 2922.61  | 5.96   | 57.81  | 1.73    | 4.00  | 3.82   | 0.00               |
| 73 LS 5 UB 784 725 m  | 99525.15  | 1941.31  | 2037.36 | 2983.88  | 6.19   | 62.25  | 0.00    | 4.47  | 3.68   | 0.00               |
| 98 LS 5 UB 784 725 m  | 89609.24  | 1732.00  | 1923.35 | 2771.43  | 6.20   | 61.99  | 0.37    | 4.04  | 3.81   | 0.00               |
| 102 LS 5 UB 784 725 m | 95114.96  | 2088.80  | 2374.56 | 4453.61  | 5.80   | 68.79  | 2.06    | 5.68  | 4.86   | 0.00               |
| 46 LS 5 UB 810        | 95123.97  | 1840.69  | 847.48  | 3795.26  | 3.69   | 26.14  | 0.00    | 5.91  | 8.88   | 142.15             |
| 53 NW 1 KA 162        | 87125.43  | 3715.59  | 572.44  | 1637.15  | 2.41   | 20.13  | 0.05    | 6.40  | 0.33   | 0.00               |
| 72 NW 1 KA 162        | 100503.28 | 3801.83  | 748.76  | 1704.76  | 2.54   | 25.41  | 0.00    | 8.46  | 0.06   | 0.00               |
| 88 NW 1 KA 162        | 101776.97 | 2322.91  | 1042.22 | 1275.92  | 3.00   | 29.34  | 0.00    | 10.19 | 0.00   | 0.00               |
| 40 TH 2 HZ 207 E      | 95713.47  | 731.61   | 1162.93 | 423.51   | 1.87   | 25.77  | 0.00    | 1.75  | 1.48   | 0.00               |
| 28 TH 2 Qu 23 HZ 11   | 93642.86  | 7824.71  | 307.30  | 2458.47  | 4.83   | 20.26  | 0.79    | 2.16  | 2.34   | 0.49               |
| 42 TH 2 Qu 23 HZ 11   | 95860.32  | 7872.20  | 325.99  | 2423.64  | 4.10   | 18.60  | 0.00    | 1.87  | 2.06   | 0.00               |
| 64 TH 2 Qu 23 HZ 11   | 95513.21  | 7846.30  | 339.62  | 2463.59  | 5.03   | 24.73  | 0.14    | 2.30  | 2.60   | 0.00               |
| 81 TH 2 Qu 23 HZ 11   | 99031.42  | 8056.87  | 381.48  | 2500.34  | 5.31   | 25.53  | 0.00    | 2.65  | 2.39   | 0.00               |
| 30 TH 2 Qu 86 HZ 119  | 91966.44  | 606.94   | 1078.18 | 436.93   | 2.39   | 27.97  | 0.00    | 1.95  | 2.39   | 0.00               |
| 17 TH 2 Qu 86 HZ 108  | 96779.63  | 792.43   | 964.71  | 734.13   | 4.53   | 21.09  | 0.00    | 2.35  | 3.21   | 0.00               |
| 27 TH 2 Qu 86 HZ 108  | 90735.86  | 768.91   | 891.75  | 668.29   | *0.00  | *0.00  | *0.00   | *0.00 | *0.00  | *0.00              |
| 43 TH 2 Qu 86 HZ 108  | 99212.14  | 849.08   | 1018.71 | 758.32   | 4.95   | 26.14  | 0.00    | 2.85  | 3.05   | 0.00               |
| 66 TH 2 Qu 86 HZ 108  | 101484.78 | 785.65   | 1060.23 | 790.22   | 5.29   | 27.75  | 0.03    | 3.25  | 4.06   | 0.00               |
| 83 TH 2 Qu 86 HZ 108  | 101290.62 | 764.46   | 1014.72 | 746.37   | 5.52   | 29.47  | 6.81    | 3.49  | 3.86   | 0.00               |
| 25 TH 3 4. südl. Abt. | 87886.18  | 1214.16  | 1384.93 | 1171.11  | 4.00   | 33.24  | 0.37    | 15.54 | 1.69   | 0.32               |
| 51 TH 3 4. südl. Abt. | 86597.61  | 1265.29  | 1378.59 | 1242.57  | 4.85   | 40.62  | 0.21    | 21.17 | 2.13   | 0.36               |
| 68 TH 3 4. südl. Abt. | 88530.50  | 1330.78  | 1322.72 | 1110.70  | 4.45   | 37.05  | 0.06    | 19.31 | 1.94   | 0.28               |
| 85 TH 3 4. südl. Abt. | 89559.00  | 1289.16  | 1455.88 | 1235.79  | 5.30   | 44.66  | 2.49    | 22.86 | 1.78   | 0.00               |

Table 6-10: Cation concentrations in ppm for the internal seepages.

|                            | NAME                    | Na       | K        | Ca     | Mg       | Rb     | Sr   | Fe     | Li     | Mn      | Zn     |
|----------------------------|-------------------------|----------|----------|--------|----------|--------|------|--------|--------|---------|--------|
| <b># Internal seepages</b> |                         |          |          |        |          |        |      |        |        |         |        |
| 24                         | HE 1 N81                | 9345.94  | 17279.53 | 18.50  | 65560.48 | 93.53  | 0.00 | 0.00   | 1.84   | 2.07    | 0.00   |
| 23                         | HE 1 N81                | 9953.43  | 18180.74 | 24.70  | 69191.09 | 96.37  | 0.00 | 0.00   | 1.80   | 2.26    | 0.00   |
| 47                         | HE 1 N81                | 9394.55  | 17346.23 | 21.74  | 64539.43 | 92.53  | 0.00 | 0.00   | 1.77   | 2.10    | 0.00   |
| 69                         | HE 1 N81                | 9797.58  | 17619.15 | 21.63  | 67714.26 | 95.38  | 0.00 | 0.00   | 1.84   | 2.02    | 0.00   |
| 70                         | HE 2 103 n. N           | 49699.82 | 26526.75 | 12.88  | 34766.53 | 13.97  | 0.00 | 0.00   | 2.35   | 3.61    | 0.00   |
| 16                         | HE 2 70.SE 141/71       | 8300.84  | 13738.62 | 17.10  | 70583.24 | 275.13 | 0.00 | 0.00   | 1.33   | 1.35    | 0.00   |
| 3                          | LS 1 H23 470 m          | 1918.06  | 933.62   | 13.62  | 93755.28 | 0.14   | 0.00 | 695.10 | 16.19  | 45.39   | 10.32  |
| 48.1                       | LS 1 H23 470 m          | 5003.37  | 6332.13  | 27.04  | 77337.06 | 32.60  | 0.00 | 416.52 | 9.70   | 52.68   | 51.89  |
| 59.1                       | LS 1 H23 470 m 19 1/1   | 6729.22  | 9303.10  | 26.34  | 73051.96 | 36.20  | 0.00 | 572.74 | 5.99   | 51.02   | 13.40  |
| 4                          | LS 1 H23 500 m          | 1899.62  | 1102.27  | 13.04  | 80958.53 | 0.23   | 0.00 | 531.49 | 13.31  | 37.87   | 8.33   |
| 5                          | LS 1 H23 500 m          | 11660.50 | 11959.47 | 26.90  | 72617.04 | 21.05  | 0.00 | 95.59  | 3.11   | 35.69   | 5.95   |
| 49                         | LS 1 H23 500 m 16 6/2   | 1314.55  | 543.32   | 7.86   | 84552.61 | 0.16   | 0.00 | 619.01 | 34.21  | 55.06   | 16.48  |
| 58                         | LS 1 H23 500 m 16 6/2   | 1563.53  | 663.79   | 10.07  | 96533.89 | 0.12   | 0.00 | 925.60 | 29.90  | 48.74   | 12.86  |
| 7                          | LS 3 353 m S R.         | 6821.49  | 14151.88 | 158.53 | 64058.69 | 13.10  | 1.05 | 0.37   | 73.07  | 1090.63 | 299.60 |
| 56                         | LS 3 353 m S R.         | 7215.54  | 13830.15 | 173.68 | 74237.14 | 18.99  | 2.17 | 1.37   | 129.85 | 1654.24 | 428.88 |
| 79                         | LS 3 353 m S R.         | 8300.22  | 15401.17 | 181.76 | 70777.24 | 21.21  | 2.18 | 2.13   | 118.45 | 1574.72 | 402.18 |
| 108                        | SA 1 WQ17/W172          | 3224.90  | 2169.99  | 37.03  | 81011.67 | 1.98   | 1.52 | 212.25 | 120.74 | 65.37   | 7.66   |
| 19                         | TH 1 Ort 90 n. N HZ 158 | 10145.68 | 18461.88 | 29.87  | 66942.51 | 176.91 | 0.00 | 0.04   | 6.69   | 3.09    | 0.00   |
| 26                         | TH 1 Ort 90 n. N HZ 158 | 8412.29  | 15833.48 | 25.00  | 54354.04 | 163.66 | 0.00 | 0.16   | 6.20   | 2.40    | 0.00   |
| 39                         | TH 1 Ort 90 n. N HZ 158 | 9627.77  | 17314.36 | 21.47  | 66004.52 | 84.59  | 0.00 | 0.00   | 1.43   | 1.85    | 0.00   |
| 67                         | TH 1 Ort 90 n. N HZ 158 | 10647.96 | 18391.63 | 15.51  | 66930.83 | 182.48 | 0.00 | 0.00   | 7.61   | 3.51    | 2.09   |
| 84                         | TH 1 Ort 90 n. N HZ 158 | 9868.07  | 17055.54 | 11.01  | 68510.89 | 198.28 | 0.00 | 0.63   | 7.96   | 2.80    | 11.55  |
| 18                         | TH 2 Qu 30/31           | 70628.24 | 8563.20  | 190.29 | 25311.97 | 26.14  | 0.00 | 0.00   | 6.50   | 0.54    | 0.00   |
| 29                         | TH 2 Qu 30/31           | 62938.65 | 7812.19  | 173.33 | 22826.21 | 28.57  | 0.00 | 0.00   | 7.10   | 0.61    | 0.00   |
| 41                         | TH 2 Qu 30/31           | 61265.09 | 7365.60  | 141.31 | 19086.37 | 22.04  | 0.00 | 0.00   | 5.21   | 0.53    | 0.00   |
| 65                         | TH 2 Qu 30/31           | 64032.97 | 8005.61  | 179.83 | 23854.02 | 28.84  | 0.00 | 0.00   | 7.61   | 0.80    | 0.00   |
| 82                         | TH 2 Qu 30/31           | 65100.30 | 8175.31  | 181.92 | 24371.42 | 31.83  | 0.00 | 0.62   | 8.75   | 0.72    | 0.00   |

#### 6.4.2 Calcium, Strontium, and Rubidium

Ca and Sr behave chemically similar during precipitation of an evaporitic sequence due to their same ionic charge (+2) and similar atomic radius ( $\text{Ca}^{2+} = 0.99 \text{ \AA}$ ,  $\text{Sr}^{2+} = 1.12 \text{ \AA}$ , six-fold coordination; WEAST 1984). In aqueous solutions both elements also occur as +2 ions. Therefore, one can assume that Ca and Sr behave similarly in the saline solutions. As shown in Figure 6-12, the similarity in behavior becomes visible via the straight trend in the external solutions between Ca (307-7502 ppm) and Sr (17-286 ppm; Tables 6-7 to 6-10) with a fairly constant Ca/Sr ratio of 17 to 57 (median = 38; excluding one outlier = 153). Even group HE 2 Loch 1/87, which yields very little Ca

and Sr similar to the contents of the internal solutions, shows Ca/Sr ratios within this range, with the exception of the one mentioned outlier. The internal solutions yield very little of both Ca (< 190 ppm) and Sr (< 1.7 ppm) with varying Ca/Sr ratios of 34 to 2906 (median = 245). Site LS 5 L499 900 m, which has an external origin, is clearly distinct from all other solutions including other external solutions. It is highly enriched in Ca and Sr with comparison to other external solutions and shows some of the lowest measured Ca/Sr ratios in the data set.

Low Ca and Sr concentrations can be used to identify internal seepages. While the external outliers of group HE 2 Loch 1/87 plot in the same concentration range as the internal solutions, their slope of Ca/Sr is distinct and indicates their affiliation with the external group (Figure 6-13).

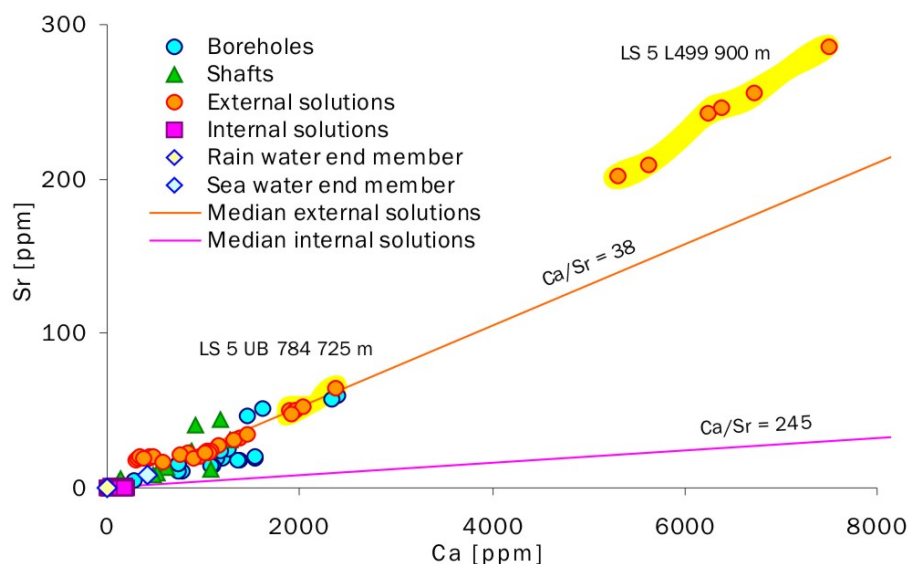


**Figure 6-12:** Ca vs. Sr distribution in samples from shafts, external and internal seepage sites; the linear trends indicate the different interdependencies in behavior of Ca and Sr for external and internal solutions. Colored lines are the median of the Ca/Sr ratio of internal (pink) and external (orange) solutions.

In addition to one external outlier, Figure 6-13 highlights three outliers for the data set of internal solutions. These three sites have Ca/Sr ratios that range around the median for internal solutions, but show either elevated Sr or Ca concentrations. Sample SA 1 WQ 17/W172 as well as the group LS 3 353 m s. R. originate from the *A3* (Figure 2-2).

Upon percolation through the anhydrite deposits on the way into the mine openings, the liquid could take up Ca and Sr from the anhydrite that exceeds the presumed levels for internal solutions originating from evaporated seawater. This demonstrates the importance for considering the composition of the host rock in the determination of the origin of a seeping solution. However, the internal solutions of site LS 1 H23 plot in the main cluster of internal solutions, although they seep from the *A3* as well.

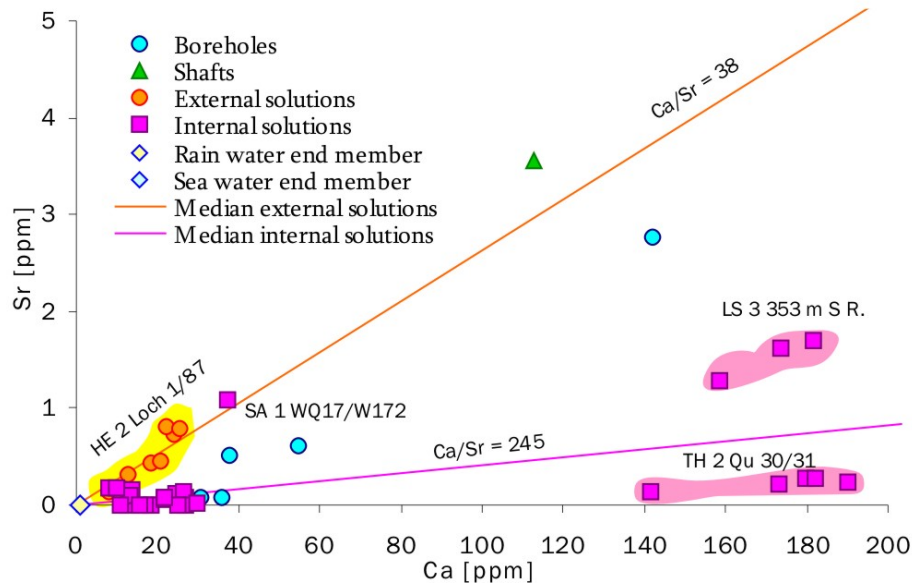


**Figure 6-13:** Excerpt of Figure 6-12 with Ca vs. Sr distribution within the samples from shafts, external and internal seepage sites; the Ca/Sr ratio of the low concentrated external group HE 2 Loch 1/87 indicates its external origin. Note the different scale in comparison to Figure 6-12. Colored lines are the median of the Ca/Sr ratio of internal (pink) and external (orange) solutions.

While HE 2 Loch 1/87, SA 1 WQ 17/W172 and LS 3 353 m s. R. only diverge in Sr (and Ca) concentrations from the general pattern of external and internal solutions, LS 5 L499 900 m and TH 2 Qu 30/31 are also distinct in Mg and Na concentrations in addition to the elevated Ca (both) and elevated Sr concentrations (LS 5 L499 900m only; Figures 6-12 and 6-13). Figure 6-14 highlights LS 5 L499 900 m and TH 2 Qu 30/31 in a Sr-Mg diagram and shows their distinction from other internal and external groups. LS 5 L499 900 m yields high Sr (and Ca) and high Mg contents, while other external solutions have low Mg concentrations. For internal solutions, TH 2 Qu 30/31

has the lowest Mg concentrations, though its distinct composition is not as pronounced. The separation of TH 2 Qu 30/31 from other internal solutions is more distinct when comparing Sr with Na (Figure 6-15). Here, TH 2 Qu 30/31 shows a mixed pattern with Na values around 60000 ppm that almost reach the external range around 90000 ppm, but the same low Sr concentrations as the internal solutions. For site LS 5 L499 900 m both Figures 6-11 and 6-12 make obvious that an assumption about LS 5 L499 900 m to be a mixture from internal and external solution does not suffice to explain its cation composition, especially the high Sr concentrations. Therefore, another parameter must be predominant that alters the Sr (and Ca) contents (see Chapter 7.3). In contrast to the uncertainty about LS 5 L499 900 m, the evolution of group Th 2 Qu 30/31 becomes apparent in Figures 6-14 and 6-15. All patterns forebode an epigenetic enclosure into the salt after a low halite concentration level is reached.

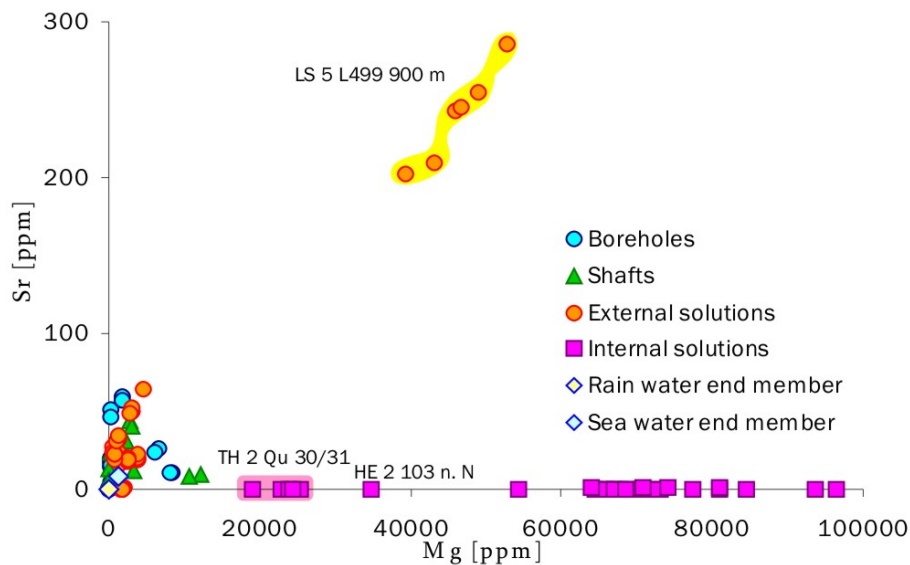


**Figure 6-14:** Distribution of Sr vs. Mg in samples from shafts, external and internal seepage sites compared to the Mg contents. Unequivocal distinction between internal and external solution origin is possible.

Analogous to Ca and Sr, K and Rb behave also similar and should precipitate simultaneously in the evaporitic sequence. The distribution coefficients for Rb in K-Mg salts are shown in Table 5-3. However, even though K and Rb precipitate simultaneously they do not show a strong correlation like Ca and Sr (Figure 6-13). One

possible mechanism that may alter such a correlation is the decay of  $^{87}\text{Rb}$  to  $^{87}\text{Sr}$  (see Chapter 7.2.1), but also the temperature dependency of the distribution coefficient of Rb e.g. in sylvite (Table 5-3) may already cause different K/Rb ratios upon (re)crystallization of K-Mg salts.

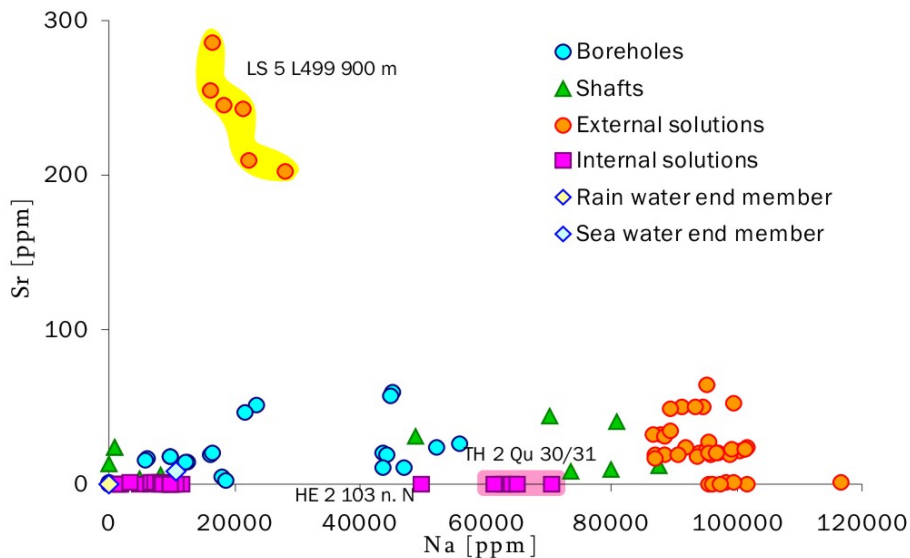


**Figure 6-15:** Distribution of Sr vs. Na in samples from shafts, external and internal seepage sites compared to the Na contents. Internal and external solutions can be discriminated by highly differing Na concentrations.

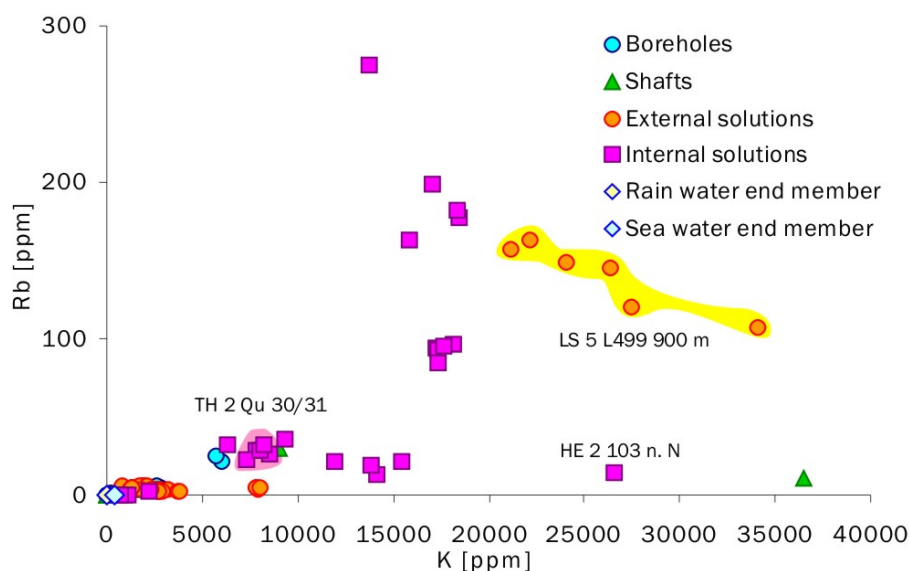


**Figure 6-16:** K vs. Rb distribution in samples from shafts, external and internal seepage sites, not showing a straight correlation to be assumed from the similar atomic structure of both elements.

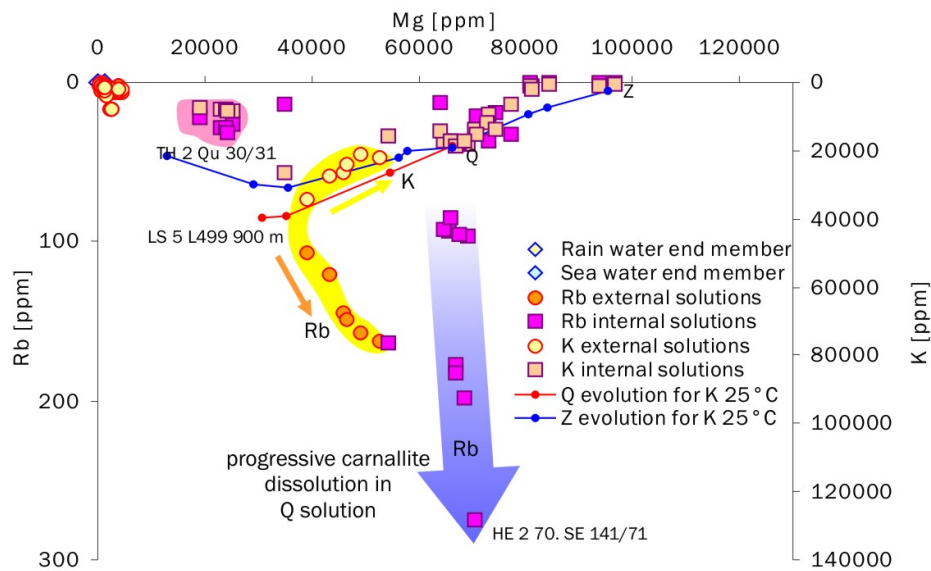


**Figure 6-17:** Comparison of K and Rb vs. Mg contents in internal and external solutions with phase equilibrium evolution paths up to the points Q and Z (two y-axes only for comparison purposes).

Especially the dissolution of K-Mg salts may have a great influence on the composition of a percolating solution, but in this case both K and Rb concentrations in the solution should increase proportionally. Indeed, Figure 6-16 mirrors this trend only partly. Here, many of the internal and most of the external solutions show very similar chemical behavior in K and Rb, but internal samples with Rb contents higher than about 80 ppm do not show a simultaneous increase in K contents (see arrow in Figure 6-17). All of those solutions seep from one of the potash seams of the Werra series. As stated by PETROVA (1973), the initial K/Rb ratio of 405 in carnallite drops down to 40 during the process of repeated recrystallization (CLAUER & CHAUDHURI 1992, OSICHKINA 2006). This causes enrichment of Rb in the carnallite if compared to the K contents. Therefore, the K/Rb ratio is not the same in every carnallite and dissolution of such could cause an 'excess' Rb in the solution. The magnitude in excess Rb becomes visible in Figure 6-17 where the blue arrow indicates the proceeding carnallite dissolution. Such solutions need to be enclosed in the system for a certain period of time to allow extensive carnallite dissolution. This process may be quantifiable in the course of the quantification of the influence of excess Rb on the  $^{87}\text{Sr}/^{86}\text{Sr}$  ratio (see Chapter 7.2.1).



Site LS 5 L499 900m shows decreasing K and increasing Rb with time of sampling (Figure 6-17).

#### 6.4.3 Iron, Lithium, Manganese, and Zink

According to HERRMANN et al. (2000, 2003) trace cations, like Fe, Li, Mn, and Zn, are important for the considerations on the origin of saline solutions and fluid inclusions. There is no evidence so far that elevated concentrations of trace elements can originate from external waters. Figure 6-18 shows the Fe, Li, Mn, and Zn contents of the samples from shafts, external and internal seepage sites versus the Mg contents (Tables 6-7 to 6-10). It is striking that again group LS 5 L499 900 m behaves different to the other external groups, the ground water samples and the shaft samples. The original orange color and low pH of 1.6 of the solution already gave evidence for oxidizing iron ( $\text{Fe}^{2+} \rightarrow \text{Fe}^{3+}$ ). One source for those trace metals could be the source strata of the solution, the detritic salt clays (Figure 2-2), which could contribute to the trace metal contents as well as to the elevated Li contents (HERRMANN et al. 2000, 2003).

The internal solution LS 3 353 m S. R. shows highly elevated Mn, Li, and Zn concentrations in comparison to the other internal solutions. Following the same argument as for LS 5 L499 900 m, the solution must have been in contact with a salt clay for a certain period of time, although the Fe contents of LS 3 353 m S. R. is not elevated. The Li contents of e.g. the Roter Salzton (*T4*) can be 47-91 ppm (OHRDORF 1968), which would be enough to increase the original Li contents of such solutions to more than 100 ppm, provided that the time of percolation and leaching was sufficient (HERRMANN 2000).

The influence of detritic material seems to be of major importance for the composition of mainly the internal solutions. Since it cannot be ruled out that the  $^{87}\text{Sr}/^{86}\text{Sr}$  ratio is influenced by the detritus as well, this possibility will be discussed in Chapter 7.2.1.

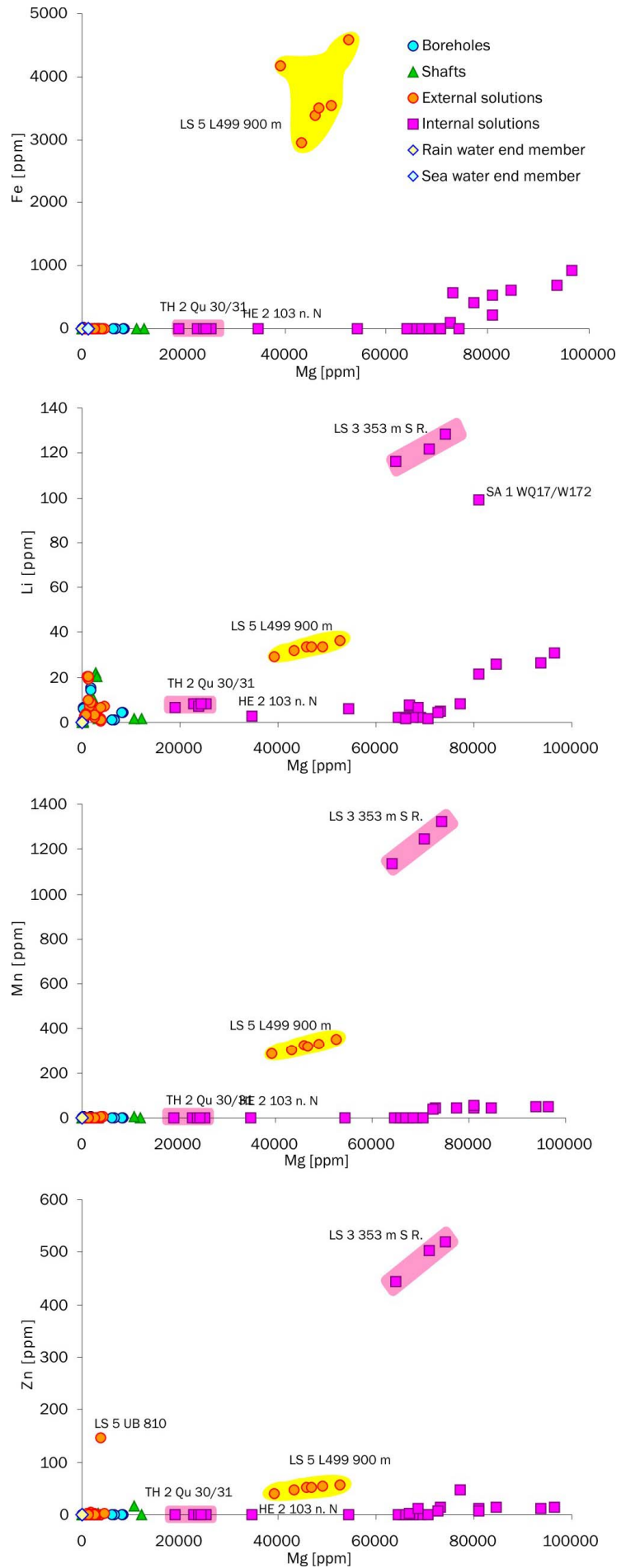


**Figure 6-18:**

Mn, Fe, Li, and Zn vs. Mg in samples from shafts, external and internal seepage sites.

## 7. DISCUSSION – Evaluating the Results with Former and New Methods

The evaluation of the data set described in the former chapter will be presented by using traditional methods as well as own concepts. Thereby, the usefulness of each method for the determination between external and internal origin of a solution is tested. For the external solutions, an identification of the source aquifer is aspired and will be tested by using the Sr isotope composition.

The general origin of most of the sampled solutions has already been determined by the mining company and mine geology staffs, respectively, via long-term observations of major and trace element behavior, inflow rate, and density as well as earlier stable isotope and tritium data. Therefore, the sampling sites provide an ideal test case to identify the most effective tools and combinations of those.

### 7.1 Applying and Modifying Common Evaluation Methods

In this section, common evaluation methods for the determination of the origin of a seeping solution will be evaluated and compared. There are other methods, like the Br distribution between external and internal solutions (e.g. Herrmann et al. 2003; see Chapter 1.3), which have not been evaluated in the scope of this project due to the focus on stable and strontium isotope data as well as the cation contents.

#### 7.1.1 Stable Isotope Evaluation Methods

For the evaluation of the stable isotope contents of saline solutions that seep into rock salt or potash mines one graphical method after SCHMIEDL et al. (1982) is in use that was tested to be suitable. In this method, SCHMIEDL et al. (1982) summarized their own and previous evaluation trials for the origin of saline solutions from rock salt or potash mines. When comparing their samples with this diagram as shown in Figure 7-1, their solutions were qualitatively classified into meteoric infiltration water (external solutions; red field), solutions with increased element concentrations (dashed field), and connate saline solutions (internal solutions; green field).

For the data shown by SCHMIEDL et al. (1982) the discriminating fields in the stable isotope diagram (Figure 7-1) were in good agreement because all solutions previously proved to be connate (internal) plotted in the corresponding field for connate saline solutions. The external solutions investigated by SCHMIEDL et al. (1982) showed restricted values that were consistent with the discriminating fields of Figure 7-1.

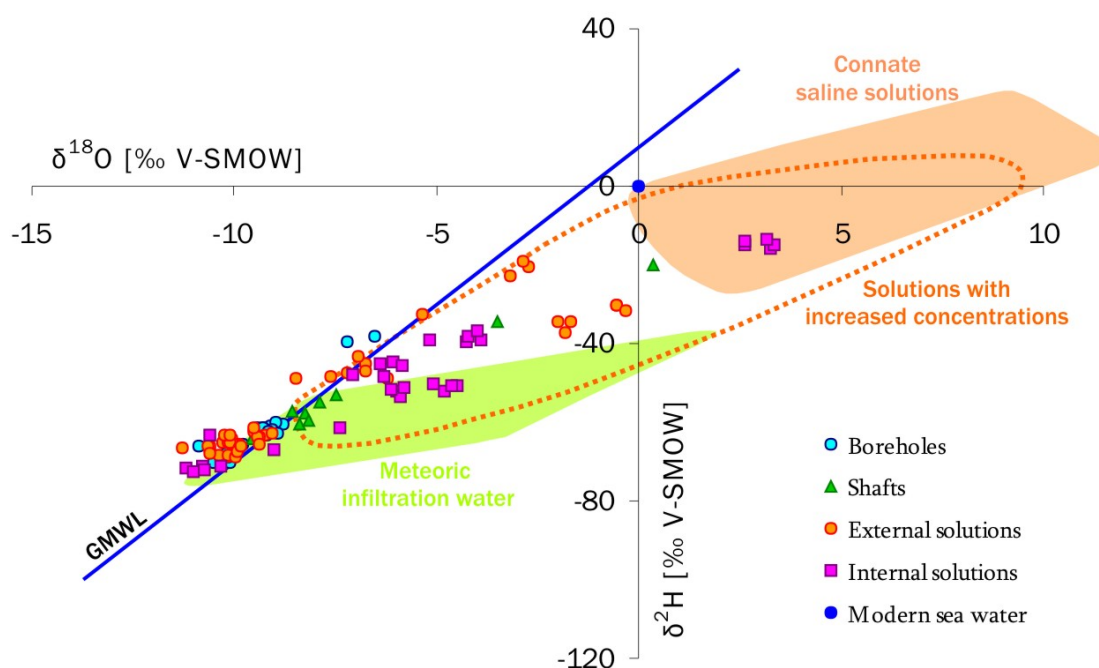


**Figure 7-1:** Diagram to qualitatively evaluate saline solutions in rock salt or potash mines, showing the internal (pink) and the external/groundwater samples (orange) of the presented data set (after SCHMIEDL et al. 1982; both  $\delta$  values on concentration scale).

The data from the northern German rock salt and potash mines in this study contradict the conventional diagram by SCHMIEDL et al. (1982). Most internal solutions plot outside the connate field. Some of the internal solutions fall within the mixing field or even in the field of meteoric infiltration water, though the bulk plots more to the right of the GMWL than the external solutions (Figure 7-1). Overall, especially the internal data in this study cannot be evaluated in detail by using this conventional evaluation method.

A more promising approach to distinguish between internal and external solutions is the comparison of the stable isotope contents of each solution with the stable isotope contents of the remaining liquid during seawater concentration (Figure 7-2). With ongoing seawater evaporation, the stable isotope composition of these concentrated seawater brines follow a path that first increases to positive values. Shortly prior the onset of gypsum precipitation the stable isotope composition of the seawater brine decreases with a shallower slope than the GMWL. This concentration hook is caused by several dissolved salt effects that cause a decrease in the activity of both  $\delta^2\text{H}$  and  $\delta^{18}\text{O}$  in the remaining liquid upon ongoing seawater evaporation (see Chapter 5.4.2).

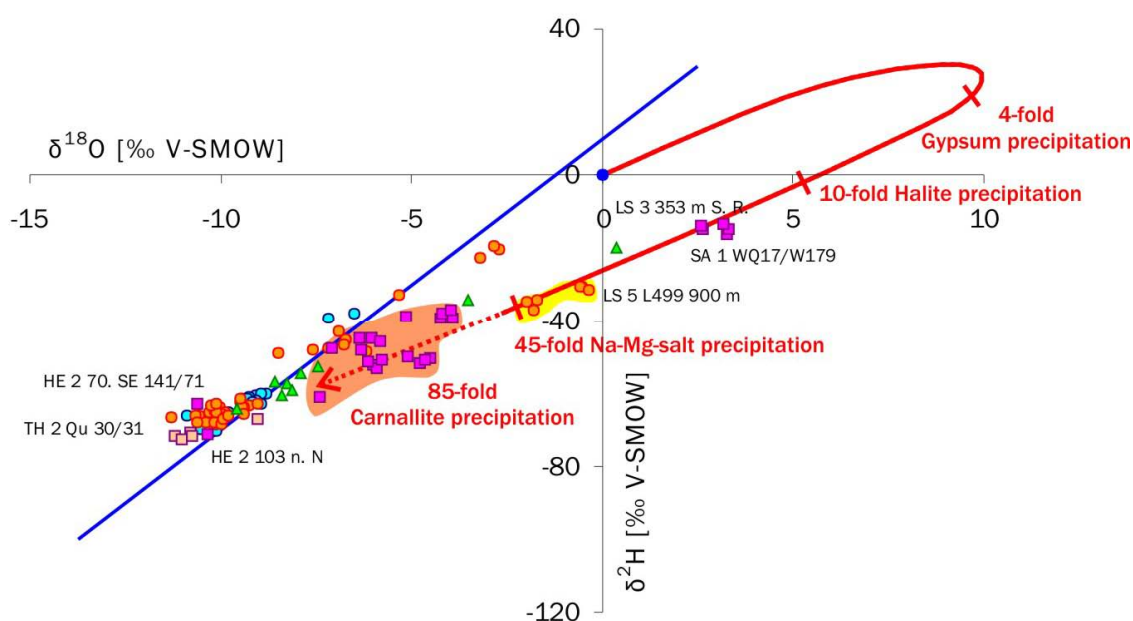


**Figure 7-2:** Hook of the concentration path (red) caused by decreasing activity of  $\delta^2\text{H}$  and  $\delta^{18}\text{O}$  with increasing salt contents in the brine (both  $\delta$  values on concentration scale); sample symbols as in Figure 7-1.

Several authors described the general characteristics of this concentration hook derived from seawater evaporation (LLOYD 1966; SOFER & GAT 1975; HOLSER 1979; HEINZINGER 1980; GONFIANTINI 1965, 1986; CLARK & FRITZ 1997; HORITA 2005). However, a transfer from laboratory experiments to real samples was performed only for small-scale fluid inclusions by e.g. ROEDDER (1984) and KNAUTH & BEEUNAS (1985). KNAUTH & BEEUNAS (1985) even gave information on the stage of concentration (dashes on solid red line in

Figure 7-2). These concentration stages are in fairly good agreement with the saline solutions of large volumes analyzed in this study if the cation contents of each stage is compared to that of the samples.

In fact, neither ROEDDER 1984, nor KNAUTH & BEEUNAS 1985 or LLOYD 1966 gave evidence for a continuation of the hook beyond a 45-fold seawater concentration. However, the data from this study show that such a continuation of the hook in direction of higher concentrated brines undergoing carnallite precipitation is very likely (dashed red line in Figure 7-2).

The grading of the hook into degrees of concentration and therefore ranges of precipitation of different salts may be used to classify the internal solutions in more detail. Considering the cation composition of the internal solutions (see Chapter 7.1.2 and Figure 7-4), the samples comprising Q (or R) solutions (onset of carnallite precipitation) are located in the red field in Figure 7-2. Therefore, this range on the hook should correspond to an 85-fold seawater concentration at which carnallite starts to precipitate.

This classification of the data into concentration stages is another advantage over the first evaluation method in Figure 7-1, in which no classification was possible. However, in some cases evaluating the data with respect to the concentration hook preclude the distinction between highly concentrated internal solutions and external solutions. Those highly concentrated internal solutions may plot around the point where the hook intersects the GMWL and coincides with common external solutions (Figure 7-2). While the concentration hook explains most internal solutions very accurately, a few samples cannot be interpreted with this simple concentration scheme. The samples of HE 2 103 n. N and TH 2 Qu 30/31 across the hook (Figure 7-2) give evidence for a limitation of this evaluation method. By considering the cation contents of these samples, it becomes clear that they are concentrated only up to the halite precipitation stage. Since they do not yield stable isotope compositions that would be attributed to this concentration stage, the similarity to the external and groundwater samples might give evidence for an epigenetic or even external origin of those solutions. In addition to this misfit, the two sites LS 3 353 m S. R. and SA 1 WQ17/W172, which both yield

positive  $\delta^{18}\text{O}$  values (Figure 7-2), should be positioned in the carnallite precipitation range, but plot in the range of halite precipitation. This misplacement of some samples may be attributed to different paths that the concentration hook can describe under time-dependent variations in humidity during seawater evaporation (SOFER & GAT 1975).

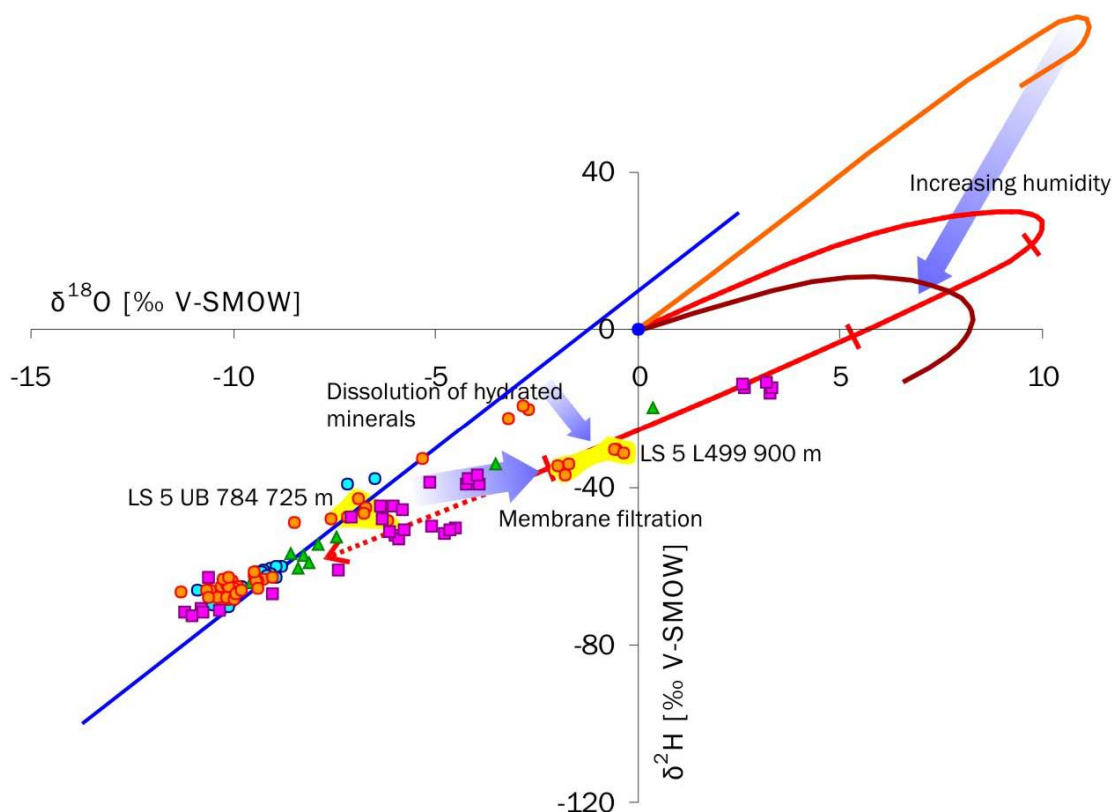


**Figure 7-3:** Sketch of the variability of the concentration hook if seawater evaporation happens under different humidity (modified after SOFER & GAT 1975); sample symbols as in Figure 7-1.

The dependency of the concentration hook on the humidity is controlled by a stronger decrease of the activity of both deltas with increasing humidity, further supporting the general decrease in activity due to dissolve salt effects (see Chapter 5.4.2). But only the initial slope of the hook is affected and shows shallower slopes at higher humidity. The final slope after the curvature of the hook is not affected (SOFER & GAT 1975). Overall, with decreasing humidity the curvature of the hook moves from the position used for

data evaluation (red line in Figures 7-1 and 7-2) to higher delta values. Figure 7-3 shows a sketch of the variability of the hook with the humidity.

Taking this variable hook placement into account, the misplaced samples could be incorporated into the salt at times of humidity different than for the main cluster of samples. However, for a precise interpretation the humidity must be known to adjust the hook accordingly.

Another possibility to shift the stable isotope compositions of some solutions, like LS 5 L499 900 m, might be membrane filtration through clay beds, which results in both higher  $\delta^2\text{H}$  and  $\delta^{18}\text{O}$  in the solution (Figure 7-3). In addition, dissolution of hydrous minerals, like gypsum or carnallite, would lead to enrichment of  $^{18}\text{O}$  and depletion of  $^2\text{H}$  in the solution, which would shift the stable isotope contents away from the GMWL in direction of the hook (see Chapter 5.4.2; Figure 7-3).

For the extrapolated continuation of the hook throughout carnallite precipitation stage, and for the possibility of varying hook placements under different humidity, the behavior of  $\delta^2\text{H}$  and  $\delta^{18}\text{O}$  during seawater evaporation should be determined experimentally under varying humidity in a future work. Such experiments would highly support the usefulness of this evaluation method for similar problems.

The correlation of the stable isotope composition of salt minerals with the corresponding seawater curve (see Chapter 5.5.1) may be one option to test whether the salts yield the isotope values of the open sea during Zechstein ages. For this study, correlation of the data known to be of external origin with the oxygen seawater curve (see Chapter 5.5.1) does not produce meaningful results since the external solutions are not comprised of seawater and therefore may have a completely different oxygen isotope composition. The comparison of the data with known internal origin to the oxygen seawater curve is not possible due to the decreasing activity of  $\delta^{18}\text{O}$  with ongoing seawater evaporation, and changes caused by dissolution of hydrous minerals.



### 7.1.2 Major and Trace Element Evaluation Methods

The evaluation of the element contents is the first action that is taken by the geology staff of a mining company if they encounter a new seepage site during the mining activities. The general characteristics of external and internal solutions are easily distinguishable since especially the Na and Mg contents vary highly between those two types of solutions. However, a mixture of internal and external solutions cannot be identified unequivocally.

Figure 7-4 shows three different sets of discrimination diagrams for the cation contents of the solutions. All three types have the same elements on the x-axis. Those elements are arranged according to their chemical association. Here, K, Rb, and Na of the halide group are followed by Mg, Ca, and Sr of the sulfate-carbonate group (MÖLLER et al. 2006). Anions should be inserted accordingly, if data are available. In contrast to the detailed evaluation of the solution compositions done in Chapter 6.4, these diagrams summarize the most important elements for a fast and concise data evaluation.

The y-axis of the three sets of diagrams changes in complexity from left to right. While the left column simply shows the element concentrations, the middle column uses a logarithmic scale. The right column is the most complex with the logarithm of the cations normalized on modern seawater.

The lowermost diagrams of the three sets show the changes in constituents in seawater with ongoing evaporation. As shown in Chapter 5.1, the Permian seawater had a composition similar to the modern seawater. Therefore, the modern concentration series data is used as an analogue for Permian seawater evaporation and the saline solutions can be compared with these data. The lowermost diagram of each column serves the purpose of such comparison for determination of the evolutionary stage of each solution.

The first set of diagrams has a regular y-axis showing the concentration in ppm. Especially for the external and internal solutions the comparison with the seawater concentration pattern (lowermost diagram) helps to identify discrepancies between the main cluster of data and samples that do not fulfill the requirements for a classification into external and internal solutions.

According to the results shown in Chapter 6.4.2, the concentrations of Ca and Sr are crucial for a final classification of outlying samples. The data show that Ca and Sr in internal samples are depleted in comparison to seawater. This can be attributed to ongoing precipitation of Ca-minerals in the presence of Mg (see Chapter 5.7). Unfortunately, the concentrations of Ca and Sr are too low to be unambiguous in this simplest evaluation method of the elements.

In contrast to the simple concentration diagrams in the left column, the second set of diagrams uses a logarithmic scale that enhances the varying concentrations of Ca and Sr. However, while low concentrated elements are enhanced in this discrimination, elements with high concentrations cannot be distinguished anymore. Overall, the distinction between high Na and Mg contents is not as clear as in the first method.

With respect to high Na and Mg and low Ca and Sr contents, the third set of diagrams shows the most differentiated picture. Here, the samples are normalized with the same modern seawater values that are used for the concentration series in the lowermost diagram (MÖLLER et al. 2007). In addition, the logarithm of these normalized data is shown to further highlight the deviation of each element from the original seawater composition. In contrast to the first and the second set of diagrams, the Ca and Sr distributions are widely spread and the distinction between high Na and Mg contents is pronounced since for internal solutions Na is similar or depleted and Mg is enriched with respect to the original seawater composition. Even the Rb excess (see Chapter 6.x) can be easily recognized when comparing the bulk of internal data with the seawater concentration pattern. Based on the third evaluation method, especially those solutions can be evaluated in detail that deviate from the main cluster of external or internal data, respectively. A final evaluation of such samples will be done in Chapter 7.3 under consideration of all parameters determined in this study.

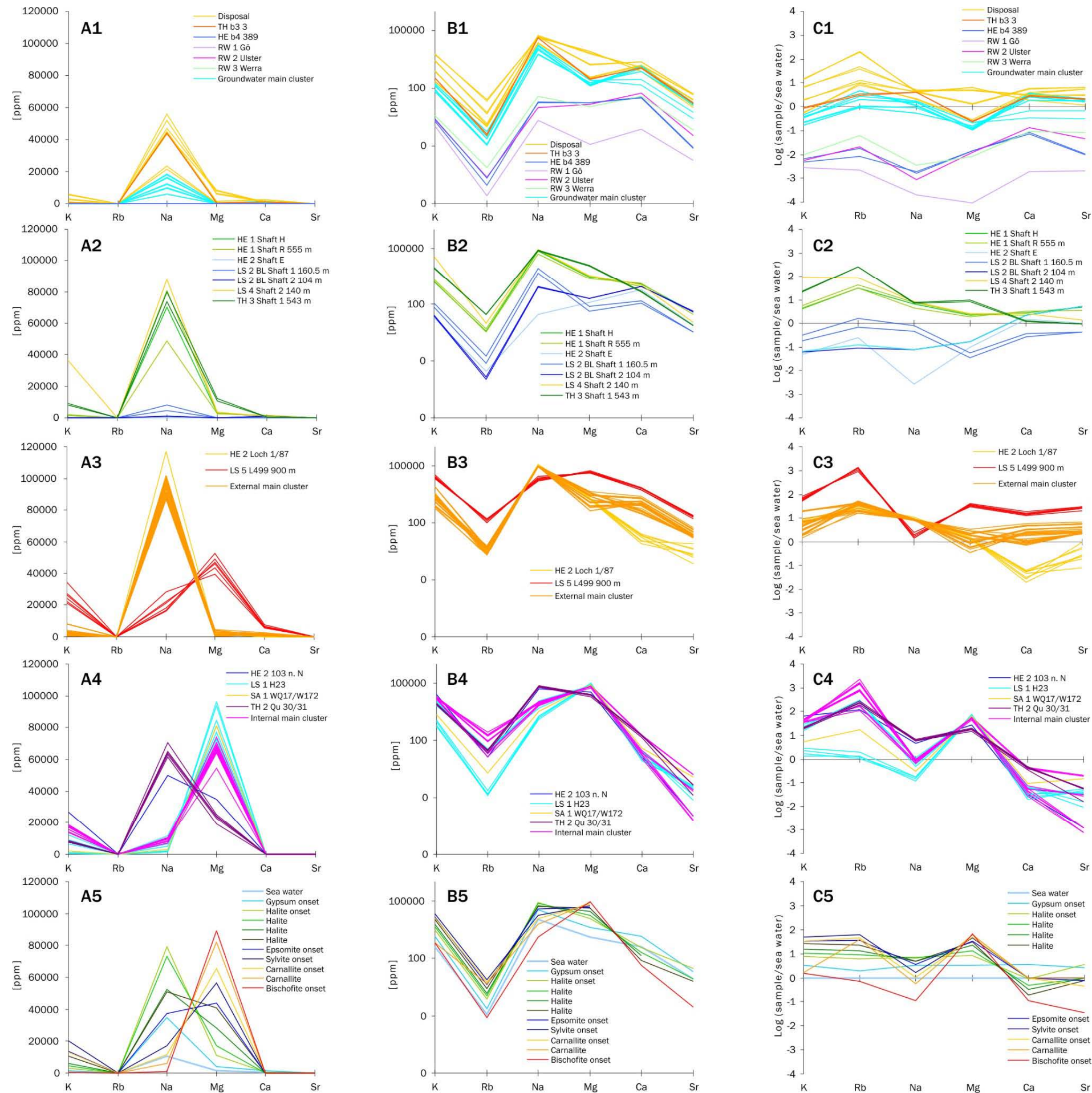


Figure 7-4: Comparison of spider diagrams with

different y-scales; shown are

1 = Groundwater samples

2 = Shaft samples

3 = External solutions

4 = Internal solutions

5 = Sea water evaporation path

(after FONTES & MATRAY, 1993, and references therein).

## 7.2 Introducing new Approaches

In this section, new approaches for the determination between external, and syngenetic or epigenetic internal solutions will be presented. The major ambition is the classification and the correlation of the data with the end members groundwater, seawater and old groundwater that was incorporated after deposition of the salts.

### 7.2.1 Sr Isotope Systematics and the Influence of $^{87}\text{Rb}$ Decay, Time, Salts, and Clays

The Sr isotopic composition of saline solutions that percolate through salt deposits may be subject to several processes that can alter the  $^{87}\text{Sr}/^{86}\text{Sr}$  ratio in direction towards higher values.

The admixture of a high  $^{87}\text{Sr}/^{86}\text{Sr}$  ratio material to the saline solution is the simplest process that can alter the  $^{87}\text{Sr}/^{86}\text{Sr}$  ratio in a saline solution. In the Zechstein sequence, mainly two components are present that can yield  $^{87}\text{Sr}/^{86}\text{Sr}$  ratios different from the main bulk of salts:

- salt clays, intercalated in most Zechstein Folgen
- carnallite (or sylvite) within the potash seams.

The salt clays yield high  $^{87}\text{Sr}/^{86}\text{Sr}$  ratios of up to 0.71481 (red salt clay *T4*) due to detritic input of highly radiogenic material from the continent via runoff into the Zechstein basin. High  $^{87}\text{Sr}/^{86}\text{Sr}$  ratios of carnallite result from the decay of  $^{87}\text{Rb}$  to  $^{87}\text{Sr}$  over 258-251 My from its deposition to present time. Sylvite should show less elevated  $^{87}\text{Sr}/^{86}\text{Sr}$  ratios since it incorporates less Rb than carnallite and therefore experiences less ingrowth. However, both minerals have only small Sr concentrations, and therefore cannot influence the Sr budget of a solution on a larger scale.

For the calculation of  $^{87}\text{Sr}/^{86}\text{Sr}$  mixtures between two end members, like a solution and a clay or carnallite, the  $^{87}\text{Sr}/^{86}\text{Sr}$  ratio and Sr concentration of each contributing end member must be known. The calculations are based on the mixing hyperbola of two end members A and B in an  $^{87}\text{Sr}/^{86}\text{Sr}$  vs. Sr [ppm] diagram. Following FAURE (1986) this mixing hyperbola is based on the mass balance equation

$$x_M = f \times (x_A - x_B) + x_B \quad (\text{Equation 7-1})$$

with the mixing parameter  $f$  being

$$f = (x_M - x_B)/(x_A + x_B) \quad (\text{Equation 7-2})$$

and  $x_A$  and  $x_B$  are the concentrations of the element  $x$  in component (end member) A and B, respectively. The general equation for a two-component mixing system is

$$R_M = R_A f \times \frac{x_A}{x_M} + R_B (1-f) \times \frac{x_B}{x_M} \quad (\text{Equation 7-3})$$

with  $R_M$ ,  $R_A$  and  $R_B$  being the isotope ratios of the mixture M and the components (end member) A and B, respectively.

If the mixing parameter  $f$  is incorporated into the mixing equation 7-3, the resulting  $^{87}\text{Sr}/^{86}\text{Sr}$  ratio of the mixture M is defined as (e.g. STOSCH 2002):

$$\left(\frac{^{87}\text{Sr}}{^{86}\text{Sr}}\right)_M = \frac{1}{Sr_M} \times \frac{Sr_A Sr_B \left[ \left(\frac{^{87}\text{Sr}}{^{86}\text{Sr}}\right)_B - \left(\frac{^{87}\text{Sr}}{^{86}\text{Sr}}\right)_A \right]}{(Sr_A - Sr_B)} + \frac{Sr_A \left(\frac{^{87}\text{Sr}}{^{86}\text{Sr}}\right)_A - Sr_B \left(\frac{^{87}\text{Sr}}{^{86}\text{Sr}}\right)_B}{Sr_A - Sr_B} \quad (\text{Eq. 7-4})$$

The resulting  $^{87}\text{Sr}/^{86}\text{Sr}$  ratio and Sr concentration of the mixture vary in an ( $^{87}\text{Sr}/^{86}\text{Sr}$  vs.  $1/\text{Sr conc.}$ ) diagram on a straight line between the two end members, depending on the fraction and the Sr isotopic composition of each end member in the mixture (e.g. Figure 6-4).

**Table 7-1:** Cation contents (in ppm) during concentration of seawater until onset of bischofite precipitation (after FONTES & MATRAY 1993, and references therein).

| Precipitation stage | Na    | Mg    | K     | Rb   | Ca   | Sr    |
|---------------------|-------|-------|-------|------|------|-------|
| Seawater            | 10763 | 1292  | 399   | 0.12 | 411  | 8.00  |
| Gypsum onset        | 34871 | 4179  | 1356  | 0.22 | 1421 | 20.48 |
| Halite onset        | 78987 | 11130 | 2990  | 0.72 | 374  | 29.65 |
| Halite              | 72951 | 17131 | 4344  | 1.09 | 194  | 7.93  |
| Halite              | 52606 | 28468 | 6199  | 1.50 | 136  | 0.00  |
| Halite              | 50889 | 40792 | 10420 | 2.57 | 78   | 5.95  |
| Epsomite onset      | 37481 | 43639 | 13748 | 4.29 | 0    | 6.33  |
| Sylvite onset       | 17132 | 56512 | 20078 | 7.30 | 0    | 0.00  |
| Carnallite onset    | 11494 | 65670 | 13027 | 5.36 | 0    | 3.60  |
| Carnallite          | 6151  | 82113 | 649   | 4.53 | 0    | 0.00  |
| Bischofite onset    | 1232  | 89443 | 630   | 0.08 | 44   | 0.29  |

Besides the admixture of high  $^{87}\text{Sr}/^{86}\text{Sr}$  phases another process with a high impact on the  $^{87}\text{Sr}/^{86}\text{Sr}$  ratio is the decay of  $^{87}\text{Rb}$  in the solution to  $^{87}\text{Sr}$  with ongoing time. The effect is strongest for high Rb/Sr ratios in the solution. However, since Rb is incorporated into potassium bearing minerals due to its similar chemical behavior to K, highly evolved brines that have already undergone K-mineral precipitation do not contain high Rb concentrations (Table 7-1). In fact, especially most of the internal solutions show much higher Rb concentrations than expected from the remaining brine at any stage of seawater concentration (Table 7-2). Therefore, the Rb contents of these internal solutions cannot solely originate from the primary solution that was syngedimentary enclosed in the salt.

To increase the Rb concentration of the internal solution after their enclosure requires other processes that control the Rb concentration in the solutions. Processes that can cause Rb enrichment in a saline solution are

- recrystallization of salts with low Rb distribution coefficients,
- dissolution of salts with high Rb concentrations.

In highly evaporated seawater solutions, the recrystallization of especially sylvite, langbeinite and kainite can enrich the Rb content in the host solution by contributing Rb from the primary precipitates that are being recrystallized (KÜHN 1963). Their low to very low distribution coefficients of Rb (Table 5-3) cause less incorporation of Rb into the secondary mineral than the primary mineral supplied. The excess in Rb from the primary mineral, mostly carnallite, remains in the solution.

Dissolution of carnallite would also increase the Rb content in the solution, in addition to its high  $^{87}\text{Sr}/^{86}\text{Sr}$  values as described above. Rb is highly compatible in carnallite, which even causes the Rb concentration in carnallite to be dependent on its position in the precipitation series. Within one carnallite sequence, the Rb contents of the salt decrease upwards since the highly compatible Rb is incorporated in the first carnallite precipitates. The subsequent carnallite precipitates experience much smaller Rb concentrations in the solution and therefore have lower Rb concentrations (HOLSER 1979). In consequence, dissolution of the lower part of the sequence would lead to higher Rb content in the solution than dissolution of the upper part. In any case, the

Rb content of the solution will increase and the decay of the share of  $^{87}\text{Rb}$  will lead to higher  $^{87}\text{Sr}/^{86}\text{Sr}$  ratios in the solution.

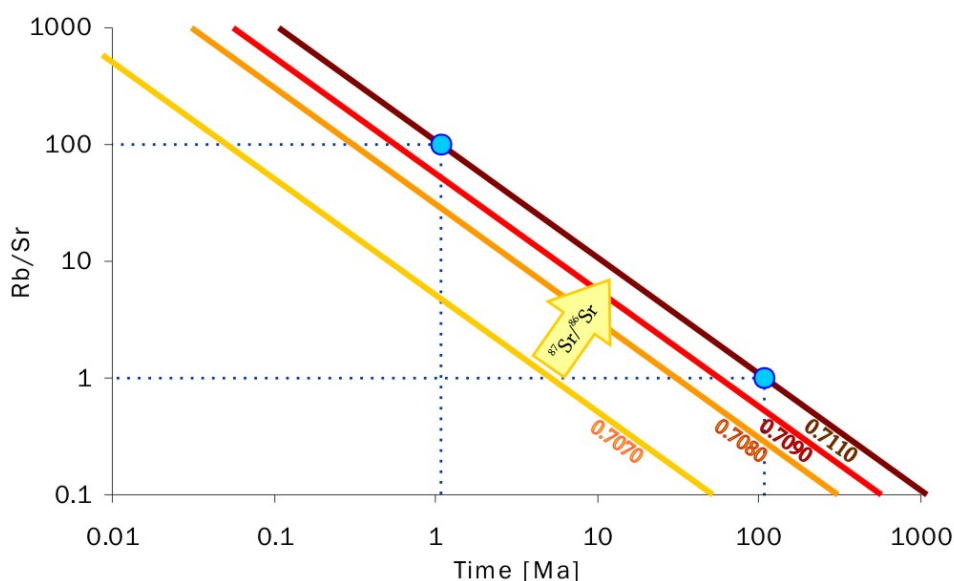


**Figure 7-5:** Increase of the  $^{87}\text{Sr}/^{86}\text{Sr}$  ratio with time and Rb/Sr ratio; calculations are based on an initial  $^{87}\text{Sr}/^{86}\text{Sr}$  ratio of 0.7068 (lowest seawater ratio during Zechstein ages); timing of increase of the  $^{87}\text{Sr}/^{86}\text{Sr}$  ratio depends on the Rb/Sr ratio; at high Rb/Sr, less time is needed for the same increase as at low Rb/Sr (blue lines).

The recrystallization of carnallite from a saline solution goes along with incorporation of large amounts of Rb into the secondary carnallite. This recrystallization would deplete the solution in Rb since the K/Rb ratio in the precipitate decreases with repeated recrystallization from 405 to 40 under incorporation of more and more Rb (FEIT & KUBIERSCHKY 1892, KÜHN 1963, PETROVA 1973). To a certain extent, this process also occurs during the recrystallization of sylvite (KÜHN 1972b). However, if sylvite is the recrystallization product of carnallite, the net Rb budget in the solution is positive due to the difference in Rb in the solved carnallite (more) and formed sylvite (less). More Rb is released from carnallite than is withdrawn from the solution by sylvite precipitation (BAADSGAARD 1987, SCHREIBER & EL TABAKH 2000).

Another process that causes a shift to higher Rb/Sr ratios is the precipitation of Sr-rich Ca-minerals that occurs if Mg is present in the solution, since Ca and Mg cannot coexist in such solutions as described in Chapter 5.7. The precipitation of Ca-minerals goes

along with incorporation of Sr into the crystal lattice due to similar chemical behavior of Ca and Sr (see Chapter 6.4.2). This loss of Sr from the solution can have great influence on the whole Rb-Sr budget and certainly supports the increase of the  $^{87}\text{Sr}/^{86}\text{Sr}$  ratio of the solution. The more Sr is co-precipitated from the solution, the faster the  $^{87}\text{Sr}/^{86}\text{Sr}$  ratio can increase due to an increase of the Rb/Sr ratio. The extent of  $^{87}\text{Sr}$  ingrowth from  $^{87}\text{Rb}$  and therefore the elevation of the  $^{87}\text{Sr}/^{86}\text{Sr}$  ratio depends on the Rb/Sr ratio as well as the time of ingrowth. For large Rb/Sr ratios the  $^{87}\text{Sr}/^{86}\text{Sr}$  ratio can be significantly elevated over a short time scale of thousands of years despite the long half life of  $^{87}\text{Rb}$  ( $\tau = 48.8$  billion yrs; FAURE 1986). For very small Rb/Sr ratios billions of years are necessary to increase the  $^{87}\text{Sr}/^{86}\text{Sr}$  ratio (Figure 7-5).

The ingrowth of  $^{87}\text{Sr}$  with time due to decay of  $^{87}\text{Rb}$  can be calculated using the general decay equation

$$N = N_0 \times e^{-\lambda t} \quad (\text{Equation 7-5})$$

where N is the number of radioactive parent atoms,  $N_0$  the initial number of atoms at time t equal 0, and  $\lambda$  is the decay constant of  $^{87}\text{Rb}$ .

For the calculation of the ingrowth of  $^{87}\text{Sr}$ , the general decay equation will be solved for the fraction N of  $^{87}\text{Sr}$  that results from beta decay of  $^{87}\text{Rb}_0$  (FAURE 1986, eqn. 4.9):

$$^{87}\text{Sr} = ^{87}\text{Rb}_0 \times (1 - e^{-\lambda t}) \quad (\text{Equation 7-6})$$

The resulting  $^{87}\text{Sr}$  fraction must be added to the initial ratio  $^{87}\text{Sr}_i/^{86}\text{Sr}_i$  to obtain the final  $^{87}\text{Sr}_f/^{86}\text{Sr}_f$  ratio in the solutions:

$$\frac{^{87}\text{Sr}_f}{^{86}\text{Sr}_f} = \frac{^{87}\text{Sr} + ^{87}\text{Sr}_i}{^{86}\text{Sr}_i} \quad (\text{Equation 7-7})$$

The initial  $^{87}\text{Sr}/^{86}\text{Sr}$  ratio is calculated from the natural abundances of the different Sr isotopes of 7.04% for  $^{87}\text{Sr}$  and 9.87% for  $^{86}\text{Sr}$  (see Chapter 5.2.1; FAURE 1986). As an example, if a solution yields an initial  $^{87}\text{Sr}/^{86}\text{Sr}$  ratio of 0.7068 and has a Rb/Sr ratio of 1, the increase of the  $^{87}\text{Sr}/^{86}\text{Sr}$  ratio to e.g. 0.7110 would happen within 108 My. For a solution with a Rb/Sr ratio of 100, the same increase in  $^{87}\text{Sr}/^{86}\text{Sr}$  would take only 1.08 My (Figure 7-5).

While the variations in Rb/Sr ratio over time can be back-calculated from the concentrations today, the time span for which the Sr isotope system in the solution has



been closed is unknown. The saline solution may have been closed in terms of Sr isotope systematics since its deposition, which is 258 My (onset of the Zechstein age) or it may have closed any point in time after that. Therefore, the onset of percolation through the salt deposits could have happened at any point in time after the onset of the Zechstein age 258 My ago.

All the described processes of dissolution of high Rb and high  $^{87}\text{Sr}/^{86}\text{Sr}$  ratio salts, respectively, recrystallization of low Rb salts from high Rb salts, and leaching of Sr from clays can alter the  $^{87}\text{Sr}/^{86}\text{Sr}$  ratio in a solution. The usefulness of the  $^{87}\text{Sr}/^{86}\text{Sr}$  ratio for the determination of the origin of a solution depends on a precise quantification of the Sr and Rb budget. Due to many uncertainties, an age determination of saline solutions using the Rb-Sr dating method is not advisable, as shown by KLINGENBERG (1998). Nevertheless, the Sr isotope composition can still give information about the relative importance of salt-water interaction during the life time of the saline solution.

The correlation of the Sr isotope composition of salt minerals with the corresponding seawater curve (see Chapter 5.5.1) may be useful to test whether the salts yield the isotope values of the open sea during Zechstein ages (e.g. KRAMM & WEDEPOHL 1991). For this study, a correlation of the solution data with the Sr seawater curve is unlikely to produce meaningful trends since all the named processes alter the Sr isotope composition in external and internal solutions.

#### ***Processes in internal and external solutions***

The concepts that have been developed in the previous section will now be applied to the internal and external solutions of the northern German mines. The patterns of the  $^{87}\text{Sr}/^{86}\text{Sr}$  ratio and the Rb contents (Figure 7-6) indicate two different processes that influence the  $^{87}\text{Sr}/^{86}\text{Sr}$  ratio of external and internal solutions. While the external solutions stagnate within a certain range of Rb contents (up to 6.2 ppm Rb) with the exception of LS 5 L499 900 m, the internal solutions show a trend of increasing  $^{87}\text{Sr}/^{86}\text{Sr}$  ratios with increasing Rb

contents up to 177 ppm. TH 2 Qu 30/31 yields very low Rb values similar to the regional groundwater values (Figure 7-6).

For the external samples from Hesse and Thuringia (lower yellow field in Figure 7-6), the studied corresponding aquifers *su*, *Ca3* and *pr* show  $^{87}\text{Sr}/^{86}\text{Sr}$  ratios in a very narrow range (blue field in Figure 7-6), making a clear distinction between aquifers challenging. However, most external solution samples from this region are in a similar range as the groundwater samples. This similarity between groundwater and external solutions gives rise to the possible usefulness of Sr isotopes for the source determination of external solutions. Unfortunately, in this region the  $^{87}\text{Sr}/^{86}\text{Sr}$  ratios of the the *su* and the *Ca3* aquifers are too similar for an exact determination.

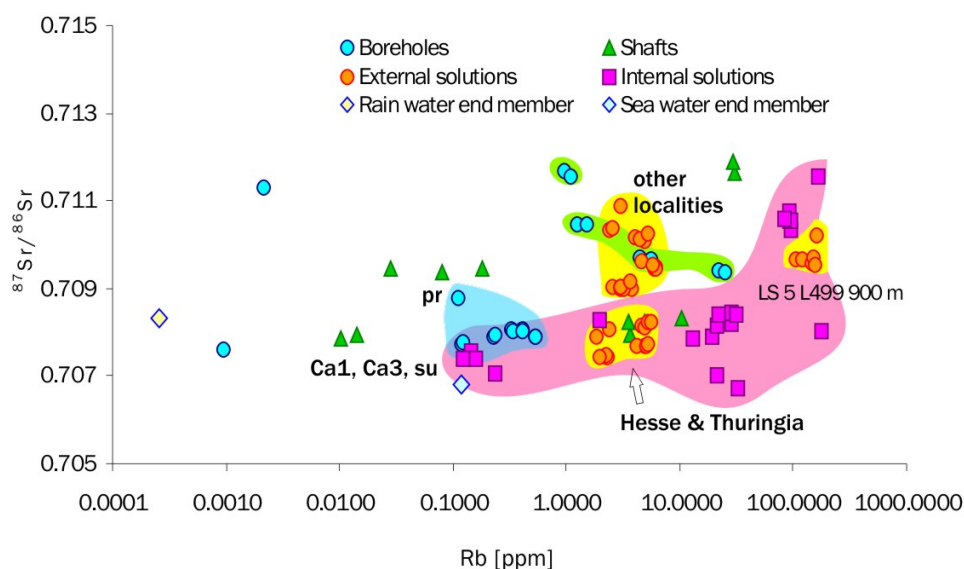


**Figure 7-6:**  $^{87}\text{Sr}/^{86}\text{Sr}$  vs. Rb (log) distribution within the boreholes, the shaft waters, and the external and internal solutions; the pink field indicates an interdependency in behavior for the internal solutions with increasing Sr isotopic compositions and concentrations.

The samples with higher  $^{87}\text{Sr}/^{86}\text{Sr}$  ratios than those in Hesse and Thuringia are either from other regions or were in contact to basalts that intruded into the salts after deposition (TH 3 4. s. Abt.; see Chapter 3.3.2). Such water-rock interaction can alter the  $^{87}\text{Sr}/^{86}\text{Sr}$  ratio since the basalt may contain a very different Sr isotope composition.

The positive linear trend between Rb and the  $^{87}\text{Sr}/^{86}\text{Sr}$  ratio in the internal solutions (Figures 7-7) is primarily formed by those samples yielding Rb excess (more Rb than the corresponding brine during seawater concentration; see Chapter 6.4.2) most likely caused by dissolution of carnallite (or recrystallization of sylvite). All solutions with excess Rb, as described in Chapter 6.4.2, show  $^{87}\text{Sr}/^{86}\text{Sr}$  ratios higher than 0.7103 (HE 1 N81, TH 1 Ort 90 n. N HZ 158). The positive trend between the  $^{87}\text{Sr}/^{86}\text{Sr}$  ratios and the Rb contents is also supported by those solutions with less elevated Rb concentrations (cluster of internal solutions in Figure 7-6).

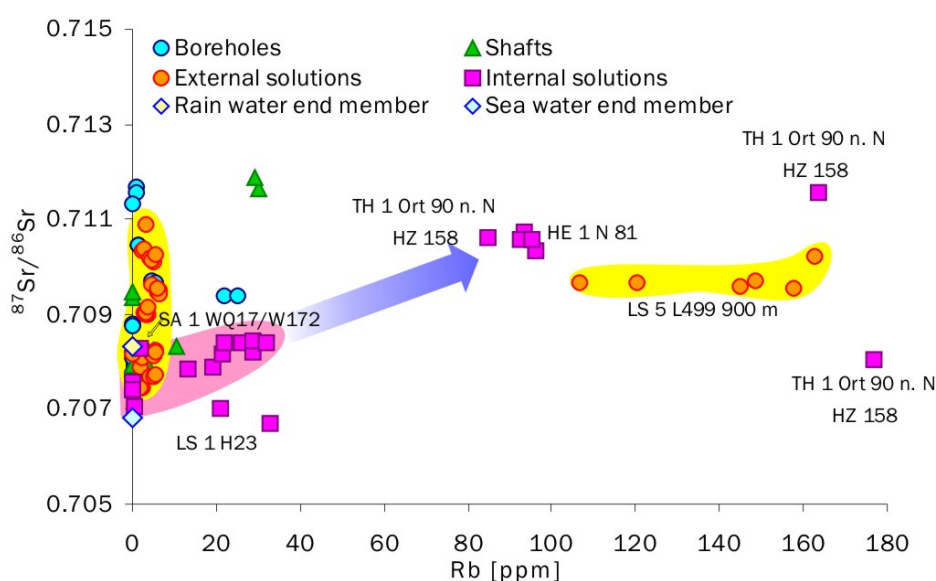


**Figure 7-7:**  $^{87}\text{Sr}/^{86}\text{Sr}$  vs. Rb distribution within the boreholes, the shaft waters, and the external and internal solutions; the internal data show a trend of increasing  $^{87}\text{Sr}/^{86}\text{Sr}$  ratios with increasing Rb contents. The external solutions show no correlation.

The elevated  $^{87}\text{Sr}/^{86}\text{Sr}$  ratios of the internal solutions can be qualitatively assessed in light of the Rb addition, the  $^{87}\text{Sr}$  ingrowth through time and the possible precipitation of Sr by formation of Ca-minerals. In a possible scenario, an evaporating brine with 100 ppm Rb and 0.1 ppm Sr would yield a  $^{87}\text{Sr}/^{86}\text{Sr}$  ratio equal to the Permian  $^{87}\text{Sr}/^{86}\text{Sr}$  seawater ratio of around 0.7068 (= initial  $^{87}\text{Sr}/^{86}\text{Sr}$  ratio at the deep mark of the Zechstein Sr seawater curve) when enclosed into the salt deposits. Under such conditions, it would take the  $^{87}\text{Sr}/^{86}\text{Sr}$  ratio about 80,000 y to increase from 0.7068 up to

0.7100. For a Rb content of 10 ppm, it would still take less than 1 My. The Sr concentration in solution would increase by only 0.0005 ppm during this process. Therefore, the Sr concentration would not be affected in significant amounts to influence the Rb/Sr ratio. This calculation shows that the increase in Rb may have happened in the near past, if only considering the Rb/Sr budget found in the solutions. In Figure 7-8 the  $^{87}\text{Sr}/^{86}\text{Sr}$  isolines are plotted to visualize the possible increase of the  $^{87}\text{Sr}/^{86}\text{Sr}$  ratio depending on the Rb/Sr ratio and time. The internal solution data plotted in this diagram visualize the general increase in needed time with lower Rb/Sr ratios in the solution to adjust the  $^{87}\text{Sr}/^{86}\text{Sr}$  ratios from initial to those measured in the solutions.

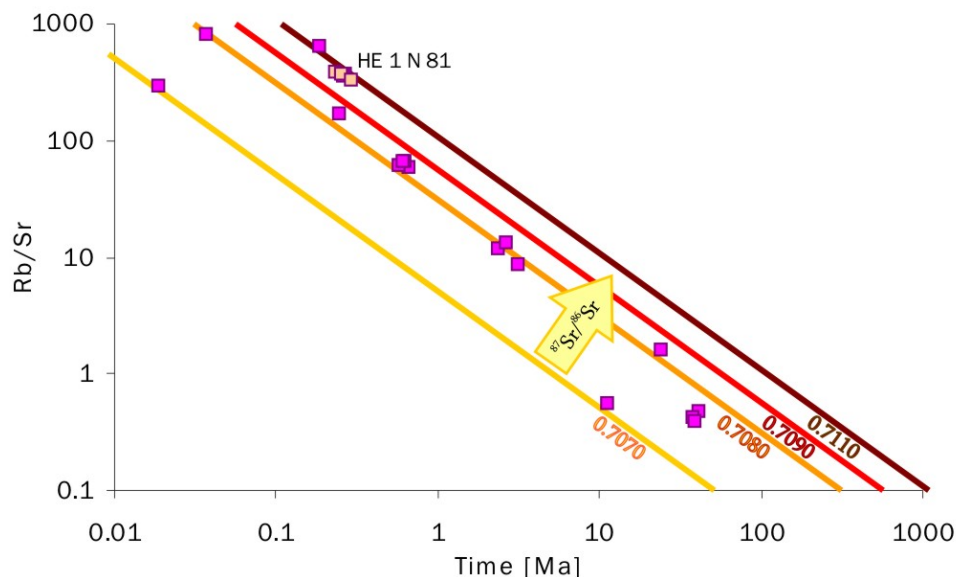


**Figure 7-8:** Increase of the  $^{87}\text{Sr}/^{86}\text{Sr}$  ratio with time and Rb/Sr ratio; calculations are based on an initial  $^{87}\text{Sr}/^{86}\text{Sr}$  ratio of 0.7068 (lowest seawater ratio during Zechstein ages).

As shown by the calculations in the last paragraph, the timing of carnallite dissolution adds a second variable parameter in interpreting the Sr isotope composition of the internal solutions. The dissolution of carnallite or its recrystallization to sylvite that leads to the elevated Rb concentrations in the internal solutions may have happened contemporaneously close to the deposition or in the near past. In case of dissolution during or shortly after deposition, the  $^{87}\text{Sr}/^{86}\text{Sr}$  ratio should be high due to extensive decay of  $^{87}\text{Rb}$  over the time span of 258 My when syngenetic solutions were

incorporated into the Zechstein deposits. In contrast, if the dissolution happened in the near past, the  $^{87}\text{Sr}/^{86}\text{Sr}$  ratios should be much lower since less  $^{87}\text{Rb}$  could decay.

Another possibility to explain the short time needed for an increase in Sr isotope composition is the epigenetic enclosure of external solutions in the course of the past 258 Ma. As one example for epigenetic incorporation, the sample group HE 1 N81 with an excess Rb of about 75 ppm could be only about 300,000 yrs old if the increase of the  $^{87}\text{Sr}/^{86}\text{Sr}$  ratio from 0.7068 to 0.7103 started with its inclusion (Figure 7-8). A possible scenario for the adjustment of the Rb/Sr budget in internal solutions will be shown later in this chapter.

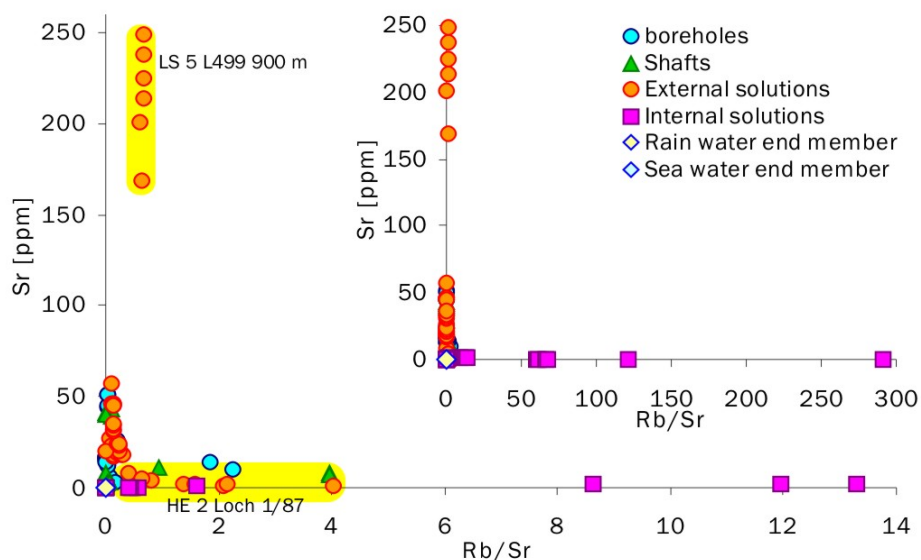


**Figure 7-9:** Rb/Sr ratios in the external and internal solutions; the high ratios of the internal solutions indicate the degree of incorporation of excess Rb.

The external solutions are less affected by Rb ingrowth than the internal solutions because of their low Rb/Sr ratios (Figure 7-9). In general, the external solutions show a range in  $^{87}\text{Sr}/^{86}\text{Sr}$  ratios between 0.7074 and 0.7109 that is similar to that of the internal solutions. However, the Rb concentrations are much lower, not exceeding 6.2 ppm. In contrast, the Sr concentrations are much higher than in the internal solutions, ranging from 17 ppm up to 248 ppm (excluding the outlier HE 1 Loch 1/87 with about 3 ppm). Here, the decay of Rb cannot be the reason for elevated  $^{87}\text{Sr}/^{86}\text{Sr}$  ratios since the needed portion of  $^{87}\text{Sr}$  could not be produced by decay of such few ppm of  $^{87}\text{Rb}$  over realistic

time scales. For example, the external solution of site LS 1 CN 8/9 yields about 2.3 ppm Rb, 18.8 ppm Sr, and an  $^{87}\text{Sr}/^{86}\text{Sr}$  ratio of 0.7074. To increase this value to 0.7084, it would take about 215 My, which is far more than it takes the solution from the aquifer to the seepage site (days-months).

In contrast to the internal solutions, the original Sr isotope composition in the external solutions is not largely overprinted by dissolution of evaporitic minerals. The  $^{87}\text{Sr}/^{86}\text{Sr}$  ratios at most sites are fairly constant for each site, as shown in Figure 7-10. If much dissolution of e.g. carnallite would occur, the  $^{87}\text{Sr}/^{86}\text{Sr}$  ratio would vary proportionally to the element composition, especially Rb, as observed in the internal solutions (Figure 7-6). However, some dissolution must occur since several elements show generally higher concentrations in the external solutions than in the uncontaminated groundwater equivalents, like Rb, K, and Mg (Figures 7-4c1 and c3).

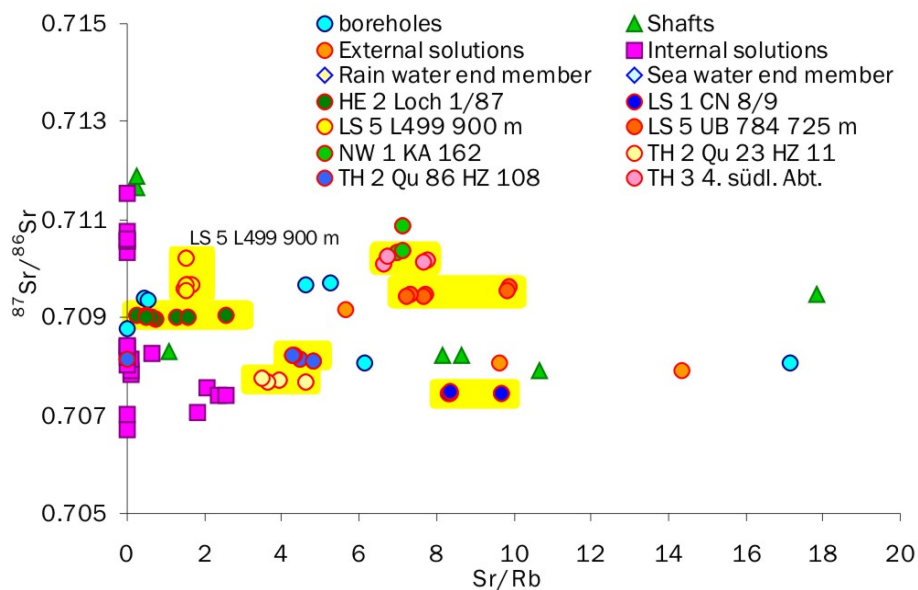


**Figure 7-10:** Variations of the Sr/Rb ratio with the  $^{87}\text{Sr}/^{86}\text{Sr}$  ratio. Most external solutions show higher variations in the Sr/Rb ratios than in the  $^{87}\text{Sr}/^{86}\text{Sr}$  ratio (yellow fields).

### ***Box Model to explain the Behavior of $^{87}\text{Sr}/^{86}\text{Sr}$ in the Solutions***

In the following, several simplified scenarios are discussed to describe the possible histories of the internal and external solutions. The different flow paths of the saline solutions can be summarized in one box model (Figure 7-11). The evaluation of the

compositional differences between the solutions after different flow paths can provide additional information for determining their origin.

For the assessment of the relationship between initial and final Sr isotope composition, three scenarios will be considered exemplarily: (1a) internal solution in a simple salt body (closed system), (1b) internal solution in a multi-layered salt body (open system), and (2a) transport of an external solution from aquifer through a salt body multi-layered with clay (Figure 7-11). The more complicated scenarios are not considered here due to their large number of unknowns. In such multi-component mixtures (flow paths 4), different salts, clays, and different solutions are influenced for both the Rb concentration and the  $^{87}\text{Sr}/^{86}\text{Sr}$  ratio. Such complex variations make a calculation of the mixing components speculative. Mixed solutions that are thought to have experienced a complex flow path and dissolution history may only be identified qualitatively by considering several tracers, as shown in Chapter 7.3.

#### ***Internal solutions in a closed system with $^{87}\text{Rb}$ decay and $^{87}\text{Sr}$ ingrowth***

The simplest case in the box model in Figure 7-11 is the case of an internal solution that has been incorporated in rock salt and solely percolates through this rock salt deposit until it reaches the seepage site (flow path 1a in Figure 7-11). In this case, a closed system without input of Rb is presented. A possible loss of Sr caused by precipitation of Ca-minerals will be neglected for this simplest scenario.

In the following, the  $^{87}\text{Sr}/^{86}\text{Sr}$  ratio of the internal saline solutions will be back-calculated on the  $^{87}\text{Sr}/^{86}\text{Sr}$  ratio at the deep mark of the global Sr seawater curve in the late Permian (see Chapter 5.5.1). This  $^{87}\text{Sr}/^{86}\text{Sr}$  ratio of 0.7068 will serve as initial value to be applied to equation 7-6. For evaporitic minerals with low Rb concentrations, like rock salt, the initial  $^{87}\text{Sr}/^{86}\text{Sr}$  ratio should be retained since deposition. The initial was adapted from the Permian Sr seawater curve of DENISON et al. (1994).

Using equation 7-6 and the Rb and Sr concentrations measured in the solutions allows the estimation of the time needed for the  $^{87}\text{Sr}/^{86}\text{Sr}$  ratio to increase to the measured value. Table 7-2 shows the time scales that would be needed for such increase of the  $^{87}\text{Sr}/^{86}\text{Sr}$  ratio from the initial to the recent ratio via decay of  $^{87}\text{Rb}$ . For the internal

solutions, those time scales needed to change the  $^{87}\text{Sr}/^{86}\text{Sr}$  ratio are short with less than 40 My. These short time scales would suggest a late postsedimentary incorporation of aquifer water into the salt deposits.

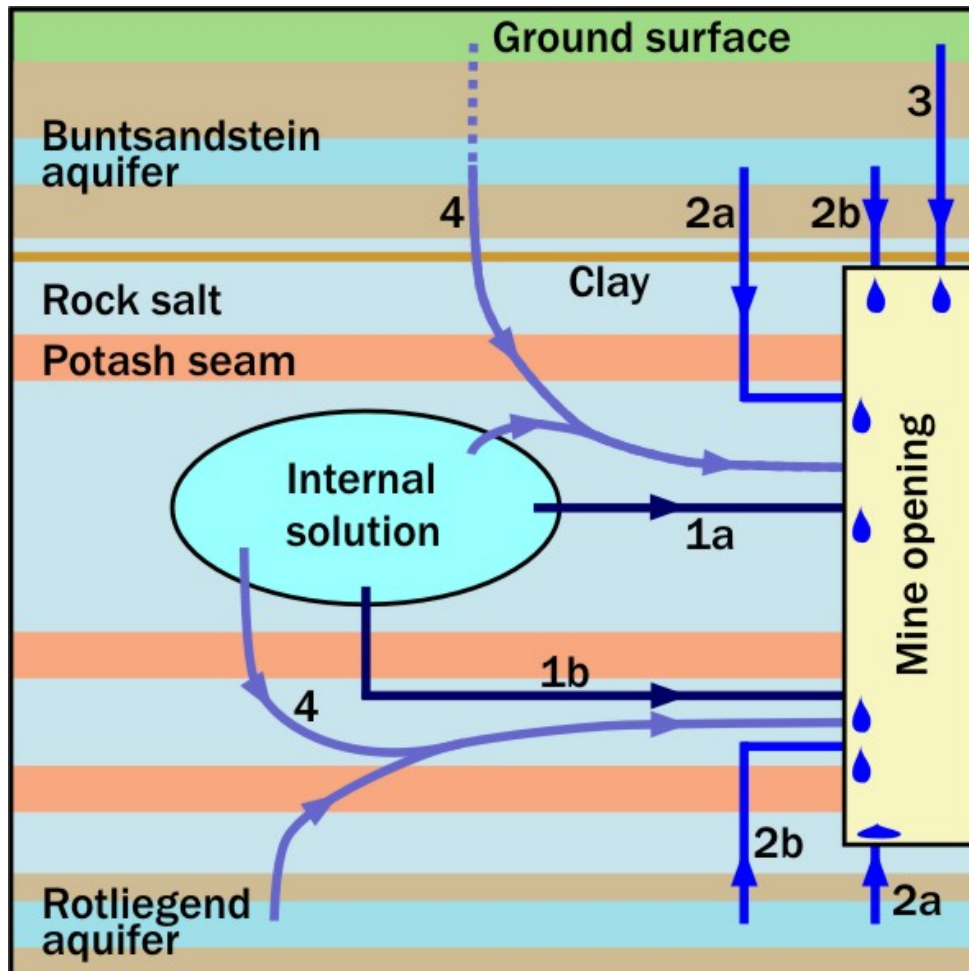


**Figure 7-11:** Box model showing the different possible flow paths of internal and external solutions; 1a,b = Internal solutions; 2a,b = External solutions (aquifer); 3 = External solutions (meteoric); 4 = Mix of internal and external.

One possible explanation of the calculated short time scales may be the low Sr concentration of the internal solutions. The Sr concentration should have increased during concentration of the original seawater up to the inclusion of the liquids in the salt deposits. This increase results from the low distribution coefficients of Sr of  $< 1$  in all evaporites that form later than gypsum precipitation (Table 5-3). The low Sr



concentrations in the internal solutions of this study can be attributed to ongoing precipitation of Ca-minerals and dolomitization in the presence of both Ca and Mg in solution (see Chapter 5.7). At carnallite saturation, the Sr concentration in solution should be 3.6 ppm following ZHEREBTSOVA & VOLKOVA (1966; Table 7-1). However, the internal solutions show Sr concentrations not exceeding 1.6 ppm. Thus, complete closed systems without input or loss of either Sr or Rb is not existent in the mines of this study. Instead, a system with continuous loss of Sr and late addition of a third end member, like carnallite, may be a more likely scenario.

***Internal solutions in a system with Sr precipitation and late carnallite assimilation***

The calculations in the preceding section have shown that an open system with loss of Sr from internal solutions by precipitation and the addition of Rb caused mainly by dissolution of carnallite is very likely for the internal solutions. Therefore, the calculations must be adjusted accordingly with respect to the Rb and Sr concentrations. Following USDOWSKI (1973; Table 5-3), the distribution coefficient of Sr in marine Ca-minerals range between 50 and 1240 (25°C). At halite saturation, an evaporating seawater solution yields about 29 ppm Sr (Table 7-1). At such concentrations, small amounts of celestite may precipitate under incorporation of some of the Sr. Since later precipitates do not incorporate Sr, the Sr concentration in the evaporating brine should increase up to bischofite-saturation. Actually, ongoing postdepositional precipitation of Ca-minerals caused by the presence of high Mg concentrations in the enclosed solution (see Chapter 5.7) results in a Sr concentration of only 0.29 ppm Sr at bischofite-saturation (Table 7-1). Since most of the internal solution samples are enriched beyond carnallite saturation (points Q and R in the quinary seawater phase system; e.g. Figure 6-11), the initial Sr concentration should not exceed the 3.6 ppm Sr that are present in solution at carnallite saturation (Table 7-1).

Parallel to the loss of Sr from the solutions, the Rb concentration increases up to the point of a Q (or R) solution (onset of carnallite precipitation) to 5.36 ppm (ZHEREBTSOVA & VOLKOVA 1966). From there on, it decreases during primary carnallite crystallization down to 0.08 ppm in a Z solution (FONTES & MATRAY 1993).

In many internal solutions, the Rb content is highly elevated above 5.36 ppm Rb most likely due to dissolution and recrystallization of carnallite and sylvite. Dissolution of both would lead to higher Rb concentrations in the solution. Recrystallization of secondary sylvite from carnallite releases Rb into the solution because sylvite incorporates less Rb than carnallite (see also beginning of this chapter). In addition to the increase in Rb, the  $^{87}\text{Sr}/^{86}\text{Sr}$  ratio may be directly affected by carnallite dissolution since carnallitic sequences in general yield higher  $^{87}\text{Sr}/^{86}\text{Sr}$  ratios due to ongoing decay of  $^{87}\text{Rb}$  within the mineral.

The range of time needed to dissolve significant amounts of carnallite can be evaluated with the aid of the external solutions. In contrast to the internal solutions, the external solutions do not show elevated Rb concentrations (max. 6.2 ppm Rb; except LS 5 L499 900 m with max. 163 ppm Rb). In fact, the external solutions need only days to flow through the salt deposit, as proven by the corresponding sites LS 5 UB 784 725 m and LS 5 L499 900 m (see Chapter 3.3.3). These short time scales and low Rb concentrations imply that the process of dissolution of significant amounts of carnallite (or recrystallization of sylvite) takes more than days. Even those external solutions that seep from a potash seam (e.g. TH 2 Qu 23 HZ 11) show elevated K contents, but similar Rb contents to those solutions from rock salt beds (e.g. TH 2 Qu 86 HZ 108). However, the very low Rb concentrations in the aquifer water samples of  $< 1$  ppm are in the regular range of regular groundwater (WEDEPOHL 1978, and references therein). Since the Rb concentrations of the external solutions are higher than those of the corresponding groundwater, at least some incorporation of Rb must occur on their way through the salt deposits.

By using the Rb/Sr conditions in the residual brine at carnallite saturation (5.36 ppm Rb, 3.6 ppm Sr), the required time to adjust the  $^{87}\text{Sr}/^{86}\text{Sr}$  ratio in the internal solutions to the modern values (0.1-81 My; Table 7-2) becomes more realistic when compared with the simple closed system (0.001-40 My). This calculation shows that at least for some time span more Sr and less Rb must have been present in the internal solutions to reach the present  $^{87}\text{Sr}/^{86}\text{Sr}$  ratio. Otherwise they could only have been incorporated postsedimentary.

**Table 7-2:** Calculated time for ingrowth of  $^{87}\text{Sr}$  in internal solutions to increase the  $^{87}\text{Sr}/^{86}\text{Sr}$  ratio from initial (contemporaneous seawater of original strata) to the final ratio measured in the internal solutions. Different initial  $^{87}\text{Sr}/^{86}\text{Sr}$  ratios correspond to the stratigraphic position of each solution.

| #    | Site                    | Rb<br>[ppm] | Sr<br>[ppm] | $^{87}\text{Sr}/^{86}\text{Sr}$<br>final | $^{87}\text{Sr}/^{86}\text{Sr}$<br>initial | $^{87}\text{Sr}$ [ppm]<br>needed<br>ingrowth | needed<br>time [My]<br>for<br>ingrowth** | needed<br>time [My]<br>for<br>ingrowth*** |
|------|-------------------------|-------------|-------------|--|--|--|--|---|
| 24   | HE 1 N81                | 93.53       | 0.25        | 0.71075                                  | 0.70684                                    | 0.000002                                     | 0.01                                     | 67.5                                      |
| 23   | HE 1 N81                | 96.37       | 0.25        | 0.71032                                  | 0.70684                                    | 0.000085                                     | 0.2                                      | 60.3                                      |
| 47   | HE 1 N81                | 92.53       | 0.25        | 0.71056                                  | 0.70684                                    | 0.000092                                     | 0.3                                      | 64.3                                      |
| 69   | HE 1 N81                | 95.38       | 0.25        | 0.71056                                  | 0.70684                                    | 0.000093                                     | 0.3                                      | 64.5                                      |
| 3    | LS 1 H23 470 m          | 0.14        | 0.30        | 0.70756                                  | 0.70680                                    | 0.000022                                     | 40                                       | 13.2                                      |
| 48.1 | LS 1 H23 470 m          | 32.60       | 0.27        | 0.70671                                  | 0.70670                                    | 0.000000                                     | 0.001                                    | 0.1                                       |
| 4    | LS 1 H23 500 m          | 0.23        | 0.42        | 0.70704                                  | 0.70680                                    | 0.000010                                     | 12                                       | 4.2                                       |
| 5    | LS 1 H23 500 m          | 21.05       | 0.07        | 0.70701                                  | 0.70680                                    | 0.000001                                     | 0.02                                     | 3.6                                       |
| 49   | LS 1 H23 500 m 16 6/2   | 0.16        | 0.37        | 0.70741                                  | 0.70680                                    | 0.000023                                     | 37                                       | 10.6                                      |
| 58   | LS 1 H23 500 m 16 6/2   | 0.12        | 0.31        | 0.70739                                  | 0.70680                                    | 0.000018                                     | 40                                       | 10.2                                      |
| 7    | LS 3 353 m S R.         | 13.10       | 1.52        | 0.70786                                  | 0.70680                                    | 0.000159                                     | 3.0                                      | 18.4                                      |
| 56   | LS 3 353 m S R.         | 18.99       | 1.59        | 0.70790                                  | 0.70680                                    | 0.000172                                     | 2.4                                      | 19.0                                      |
| 79   | LS 3 353 m S R.         | 21.21       | 1.60        | 0.70815                                  | 0.70680                                    | 0.000213                                     | 2.6                                      | 23.4                                      |
| 108  | SA 1 WQ17/W172          | 1.98        | 1.23        | 0.70828                                  | 0.70680                                    | 0.000180                                     | 24                                       | 25.6                                      |
| 19   | TH 1 Ort 90 n. N HZ 158 | 176.91      | 0.21        | 0.70803                                  | 0.70684                                    | 0.000025                                     | 0.04                                     | 20.5                                      |
| 26   | TH 1 Ort 90 n. N HZ 158 | 163.66      | 0.25        | 0.71155                                  | 0.70684                                    | 0.000002                                     | 0.004                                    | 81.4                                      |
| 39   | TH 1 Ort 90 n. N HZ 158 | 84.59       | 0.25        | 0.71061                                  | 0.70684                                    | 0.000095                                     | 0.3                                      | 65.0                                      |
| 18   | TH 2 Qu 30/31           | 26.14       | 0.43        | 0.70840                                  | 0.70684                                    | 0.000066                                     | 0.7                                      | 26.9                                      |
| 29   | TH 2 Qu 30/31           | 28.57       | 0.47        | 0.70819                                  | 0.70684                                    | 0.000062                                     | 0.6                                      | 23.3                                      |
| 41   | TH 2 Qu 30/31           | 22.04       | *0.13       | 0.70840                                  | 0.70684                                    | 0.000021                                     | 0.2                                      | 1.0                                       |
| 65   | TH 2 Qu 30/31           | 28.84       | 0.44        | 0.70843                                  | 0.70684                                    | 0.000069                                     | 0.6                                      | 27.4                                      |
| 82   | TH 2 Qu 30/31           | 31.83       | 0.47        | 0.70841                                  | 0.70684                                    | 0.000073                                     | 0.6                                      | 27.0                                      |

\*data from ICP-analysis; \*\* ingrowth was calculated by using the original Rb and Sr concentrations of the samples; \*\*\* ingrowth was calculated for all samples with 5.36 ppm Rb and 3.6 ppm Sr (contents of an evaporating seawater at carnallite saturation)

### ***External solutions in an open system under influence of clays***

The influence of clays on the Rb and Sr budget and  $^{87}\text{Sr}/^{86}\text{Sr}$  ratios of an external solution will be shown exemplarily on the seepage site LS 5 L499 900 m due to the complexity of this process.

Different effects can be observed at the external site LS 5 L499 900 m. Here, the  $^{87}\text{Sr}/^{86}\text{Sr}$  ratio is relatively high (mean = 0.70973; 216 ppm Sr) and changes irregularly with time (Figure 7-12). Major and trace elements vary gradually with time. While K

and Na decrease, Rb, Mg, Ca, and Sr increase. The corresponding drilling LS 5 UB 784 725 m is a cased underground borehole drilled into the T5/T6 clays and shows no significant changes in major or trace elements. Its  $^{87}\text{Sr}/^{86}\text{Sr}$  ratio and Sr concentrations are lower than that of the corresponding seepage site LS 5 L499 900 m, but show a similar pattern of fluctuations (Figure 7-12).

**Table 7-3:** Clays in the flow path of LS 5 L499 900 m used for the calculations in the mixing model.

| Abbrev. | Clay                                | $^{87}\text{Sr}/^{86}\text{Sr}$ | Sr [ppm] |
|---------|-------------------------------------|---------------------------------|----------|
| T5      | Randlicher Tonstein (Friesland-Ton) | 0.71481                         | 178      |
| T4      | Roter Salzton (Aller-Ton)           | 0.70941                         | 913      |
| Na3tm   | Tonmittelsalz, Steinsalz tonig      | 0.70881                         | 1934     |
| Na3tm   | Tonmittelsalz, Tonmittel            | 0.70924                         | 1158     |

In the following calculations, borehole LS 5 UB 784 725 m will be used as the groundwater end member (mean  $^{87}\text{Sr}/^{86}\text{Sr} = 0.70951$ ; 47 ppm Sr) for a mixture of groundwater and different clays that may be in the flow path between LS 5 UB 784 725 m and LS 5 L499 900 m.

Since the groundwater gets in contact with several clays on its flow path through the salt, the four most extensive clays will be included in the simplified mixing calculation (Table 7-3; for calculations see Appendix VI). The mixing calculations are done in four steps, one for each clay layer.

Figure 7-13 shows the modeled amounts in which the groundwater takes up Sr from the four salt clays up to its final  $^{87}\text{Sr}/^{86}\text{Sr}$  ratio and Sr concentration when seeping at site LS 5 L499 900 m. The first outermost clay of *T5* takes the highest influence on the final data since it yields the highest  $^{87}\text{Sr}/^{86}\text{Sr}$  ratios. The three salt internal clay beds from the *Roter Salzton* (*T4*) and the *Tonmittelsalz* (*Na3tm*, two segments) have lower  $^{87}\text{Sr}/^{86}\text{Sr}$  ratios than the final, but are needed to decrease the  $^{87}\text{Sr}/^{86}\text{Sr}$  ratio after percolation through the *T5* (Figure 7-13). If only one of these clays would be leached, the final Sr budget in the solution of LS 5 L499 900 m could not be reached. Either the  $^{87}\text{Sr}/^{86}\text{Sr}$  ratio or the Sr concentration would not be adjustable.

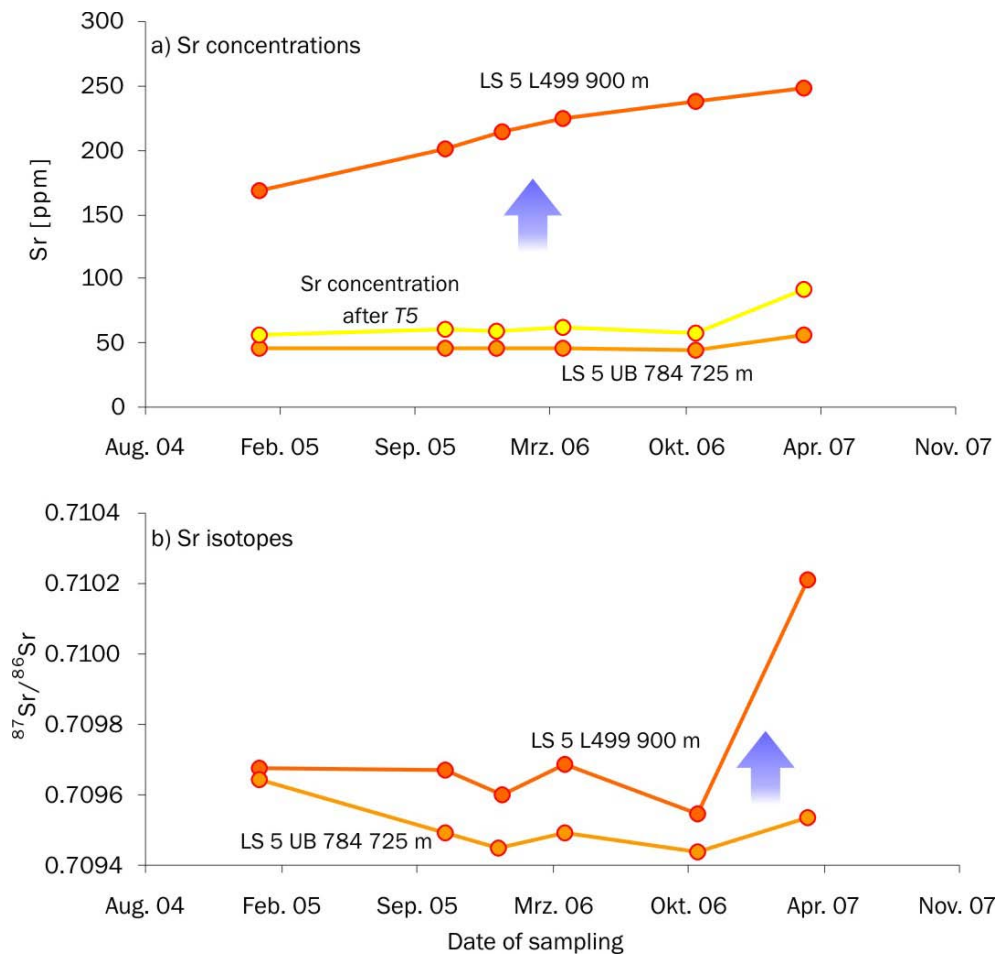


**Figure 7-12:** Variations of Sr concentration (Sr) and isotope composition (Iso) with time of sampling for the corresponding sites LS 4 L499 900 m and LS 5 UB 784 725 m; yellow circles indicate the needed Sr concentration after passage through the T5 to model the final values via addition of other salt clays.

Figure 7-12 shows the needed Sr concentrations of each sample ( $n=6$ ) after the groundwater passed the T5. In contrast to the final Sr concentrations of LS 5 L499 900 m the 'T5-solutions' do not increase gradually but fluctuate in a similar pattern as the initial Sr concentrations of LS 5 UB 784 725 m. In this model, each of the six samples takes up the same amounts from each of the three following clays. Hence, the final Sr budget is mainly controlled by the T5. If more Sr is taken from the T5 by the fluid of LS 5 UB 784 725 m, the final solution LS 5 L499 900 m shows higher  $^{87}\text{Sr}/^{86}\text{Sr}$  ratios (Figure 7-12a). The results from this calculations are not unique, but they show the diverse

processes that may happen during the percolation of an external solution through the salt body. Additional solution samples from intermediate sites between T5 and Na3tm would help to further characterize the water-rock interaction.

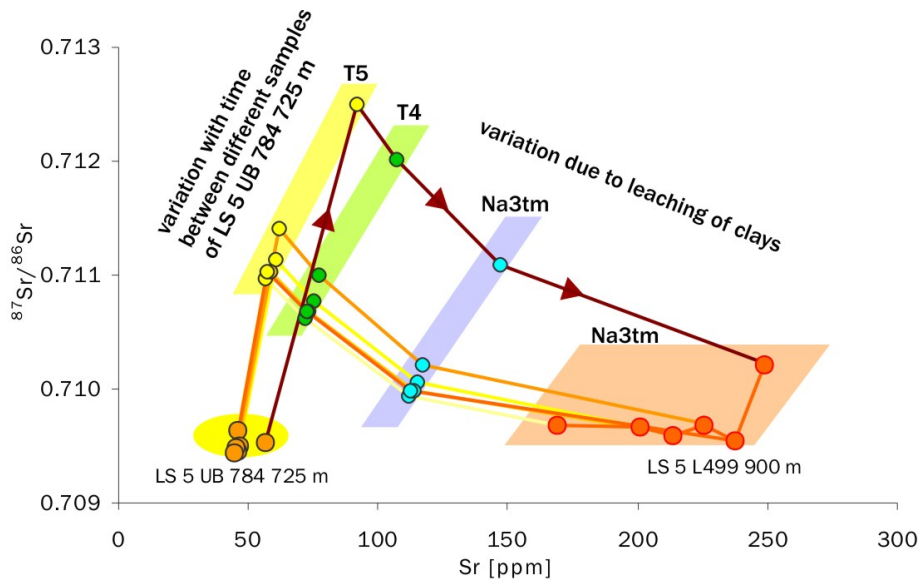


**Figure 7-13:** Shifts in Sr concentration and isotope composition caused by salt clays upon percolation of solution LS 5 UB 784 725 m through the salt down to site LS 5 L499 900 m (percolation path from lower left through the clays over to lower right).

### 7.2.2 The Ca/Sr Ratio

The Ca/Sr ratio is at this point a good parameter to decide between the external or internal origin of a saline solution, respectively. As shown in Chapter 6.4.2 (Figures 6-12 and 6-13) all external samples yield a Ca/Sr ratio of around 38, even those of HE 2 Loch 1/87 where both elements are present in only small concentrations. The internal solutions show more variable Ca/Sr ratios, but overall a median of 245 is maintained. This difference may be attributed to the ratio in which especially gypsum takes up Ca and Sr upon precipitation from the internal solution if Mg is present. However, such precipitation seems to occur at the external site HE 2 Loch 1/87 (see Chapter 7.3). If the Ca/Sr ratio would be influenced by that precipitation, the samples of HE 2 Loch 1/87 should show the internal ratios. Since even HE 2 Loch 1/87 shows the external median, the difference between the ratios of external and internal solutions cannot be

attributed to the ratio in which both are incorporated into precipitating gypsum, and therefore may be maintained since incorporation of the internal solutions within the salt deposits.

This theory can be tested on the initial Ca/Sr ratio of residual brines. According to FONTES & MATRAY (1993) an evaporating brine would yield about 44 ppm Ca and 0.3 ppm Sr at onset of bischofite precipitation, which would make a Ca/Sr ratio of 153. This ratio is in fairly good agreement with the ratio of 245 in the internal solutions. Therefore, it is likely that the Ca/Sr of the residual brine is only affected minimally after incorporation into the salt deposits and even after precipitation of Ca-minerals, like gypsum, from the internal solution. To support this theory, the Ca/Sr ratio of 38 in the external samples is on the same order of magnitude as that of the groundwater samples of 68.

Overall, the Ca/Sr ratio is a good first indicator for the origin of a seeping solution besides the Ca/Mg ratio, which is smaller in internal solutions due to depletion in Ca through precipitation of Ca-minerals.

### **7.3 Evaluation of the Seepage Sites with Ambiguous Geochemical Patterns**

#### ***HE 2 103 n. N***

The single sample of site HE 2 103 n. N shows distinct lower evolved cation concentrations (Figure 7-4 c4) than most other samples with internal origin (except TH 2 Qu 30/31, see below). The stable isotope concentrations for HE 2 103 n.N that are located close to the intersection of the concentration hook with the GMWL (Figure 6-1a) are most consistent with an epigenetic enclosure of this solution under retention of the stable isotope pattern of the original groundwater. Strontium isotopes were not determinable due to very low Sr concentrations.

#### ***HE 2 Loch 1/87***

The cation pattern of this sample group shows characteristics similar to most of the external solutions (Figure 7-4 c3). However, the Ca and the Sr concentrations are highly depleted and therefore resemble the low values of the internal solutions. Since the Ca and Sr contents of internal

solutions are mainly controlled by precipitation of Ca-minerals, a similar process could explain the low Ca and Sr concentrations in HE 2 Loch 1/87. At this site, the sulfate components of the Portland cement that was used for filling unused boreholes may give rise to increased precipitation of gypsum under incorporation of Sr. The highly reactive solution might leach the Portland cement in uncertain amounts, thereby altering the composition of the liquid, especially the Ca and Sr concentrations.

Regarding the Sr isotope composition of these samples, the  $^{87}\text{Sr}/^{86}\text{Sr}$  ratio is elevated to 0.70902 (n=8) if compared to the rest of the Hessian and Thuringian samples with 0.70797 (n=14; Figure 6-5 a and b) and the corresponding Buntsandstein and Platy dolomite aquifers with 0.70794 (n=8). Sr isotope composition of sample HE 2 Loch 1/87 resembles much closer the Rotliegend aquifer sampled at site HE b11 431 (n=2) with 0.70877. Thus, HE 2 Loch 1/87 may originate from the Rotliegend aquifer. The difference in  $^{87}\text{Sr}/^{86}\text{Sr}$  ratio between the aquifer water and the solution may be caused by fast ingrowth of  $^{87}\text{Sr}$  through decay of  $^{87}\text{Rb}$  since the Rb/Sr ratio is with 1.63 about one order of magnitude higher than in the other external solutions (0.24, n=35; Figure 7-9). According to the calculations in Chapter 7.2.1, the increase in  $^{87}\text{Sr}/^{86}\text{Sr}$  ratio by decay of  $^{87}\text{Rb}$  would still take about 4 million years. However, this increase of the  $^{87}\text{Sr}/^{86}\text{Sr}$  ratio could also be caused by the ongoing assimilation of the borehole cement, although this process is only speculative because the  $^{87}\text{Sr}/^{86}\text{Sr}$  ratio of this end member is unknown and therefore a mixture is not quantifiable.

#### ***TH 1 Ort 90 n. N HZ 158***

The five samples of site TH 1 Ort 90 n. N HZ 158 show highly varying  $^{87}\text{Sr}/^{86}\text{Sr}$  ratios (Figure 6-5b), and less pronounced variations in the element concentrations, while having the second highest Rb concentrations in this study (Figure 7-14). The stable isotope contents show only minor variations (Figure 6-2). At this site, the solution flows out of the level ground and is collected in a 'brine pool'. Such ascending brines are generally considered to be of external origin (pers. comm. Dr. W. Beer, K+S Group, 2008). However, the cation concentrations as well as the stable isotope contents are similar to that of the main cluster of internal solutions. This pattern would support an internal origin, whether



syngenetic or epigenetic is impossible to determine based on such scattered  $^{87}\text{Sr}/^{86}\text{Sr}$  ratios.

### *TH 2 Qu 30/31*

Solution TH 2 Qu 30/31 is the least evolved sample group of the internal solutions, as Figure 6-9 shows. In addition, it has with 789 (n=5) one of the highest Ca/Sr ratios in this study (Figure 6-13). Especially this high Ca/Sr ratio would define it as internal, since the internal solutions show generally much higher Ca/Sr ratios than the external solutions. However, the Mg and Rb concentrations are lower than in the other internal solutions, whereas Na shows higher values (Figure 7-4 c4), which would argue for an external origin. The stable isotopes cannot be related unequivocally to the other external or internal solutions since the solutions of TH 2 Qu 30/31 plot close to the intersection of the GMWL and the concentration hook (Figure 6-1b).

One reasonable explanation for the trends in element contents and stable isotope composition would be late epigenetic incorporation of this solution into the salt. This explanation is supported by the  $^{87}\text{Sr}/^{86}\text{Sr}$  ratios of the samples from TH 2 Qu 30/31 which are similar to that of the surrounding aquifers in that region.

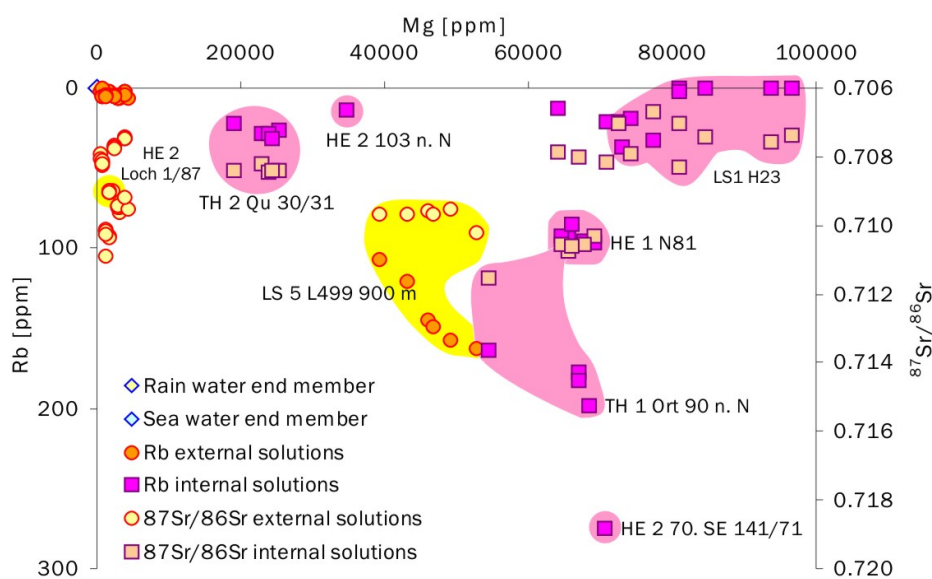


**Figure 7-14:**  $^{87}\text{Sr}/^{86}\text{Sr}$  and Rb vs. Mg distribution within sites under question (two y-axes only for comparison purposes).

***LS 1 H23***

The two interconnected internal sites LS 1 H 23 470 m and LS 1 H 23 500 m show ambiguous element concentrations (Figure 7-4) and stable and Sr isotope compositions (Figures 6-1c and 6-5c) irrespective of the sampling site. Those variations are not in relation to the date of sampling or seasonal variations. Since the samples were taken from boreholes that were under pressure, a certain variation in the stable isotope compositions could be explained by exchange with air that is drawn into the boreholes after every sampling (pers. comm. Dr. S. Zeibig, K+S Group 2008). In that case, the flow time of the boreholes should be adjusted accordingly to ensure that only 'fresh' solution is sampled. However, the  $^{87}\text{Sr}/^{86}\text{Sr}$  ratio should not be affected by such air contamination. Evidence for epigenetic origin of this solution is given by the similarity of the  $^{87}\text{Sr}/^{86}\text{Sr}$  ratios of LS 1 H23 with those of the external solution LS 1 CN 8/9. Both solutions drain the Hauptanhydrit *A3*, and therefore LS 1 H23 may be a relict of external solutions that percolated through the *A3*.

***LS 5 L499 900 m***

The cation contents of the external solutions in general resemble that of the cluster of the aquifer waters (Figures 7-4 c1 and c3). The samples of LS 5 L499 900 m are the only external group that shows a completely different pattern than the cluster of external samples. While the pattern of K, Rb, Na, and Mg resembles that of most of the internal solutions, the Ca and Sr contents are the highest in this study. Due to such high Sr and Ca concentrations, the solutions cannot have an internal origin since all internal samples show Sr concentrations below 1.6 ppm.

Figure 7-14 shows an increase in Rb and Mg contents while the  $^{87}\text{Sr}/^{86}\text{Sr}$  ratio remains constant. Additionally, the Sr contents increase proportionally to Rb (Figure 7-9). Dissolution of large amounts of high-Sr evaporitic minerals, like celestite or tachhydrite, cannot be the only reason for the increasing element concentrations due to fairly constant  $^{87}\text{Sr}/^{86}\text{Sr}$  ratios. In this case the  $^{87}\text{Sr}/^{86}\text{Sr}$  ratios would decrease to the ratio of the dissolved material (about 0.7068). In addition, the proportional high increase of Sr and Rb cannot be caused by one evaporitic mineral since they all yield

completely different amounts of Sr and Rb, one being high and one low. Therefore, the only contributors can be the salt clays that are intercalated within the flow path of the solution. This hypothesis is supported by the stable isotope composition of these samples. As shown in Chapter 7.1.1, the stable isotopes in saline solutions can be fractionated by membrane filtration away from the GMWL in direction of the hook. Such fractionation might occur for LS 5 L 499 900 m because the stable isotope concentrations of its source solution, LS 5 UB 784 725 m, would follow a trend in direction of LS 25 L499 900 m (Figure 7-3).

## 8. CONCLUSIONS

The preceding evaluation of different geochemical techniques to trace the origin of saline solutions that seep into German rock salt or potash mines showed the usefulness of several tracing tools that incorporate the element concentrations, stable isotopes and strontium isotopes.

The history of seepage solutions can be evaluated most effectively by considering the cation contents in saline solutions normalized to seawater and compared on a logarithmic scale. With this method, both the differences in Na and Mg as well as Ca and Sr concentrations can be shown in one diagram, which are the most indicative elements for internal (Mg high) and external (Na, Ca, Sr high) solutions. In addition, using this data representation is effective in showing the deviation from seawater for the data known to be of internal origin with respect to the evaporation stage of each sample.

The stable isotope contents of the saline solutions can particularly highlight the origin of a saline solution. While external solutions are in the range of both the GMWL and the rainwater, the internal solutions deviate from the GMWL in direction of higher  $\delta^{18}\text{O}$ . For evaluation of this shift, the concentration hook method shows many advantages if compared to the method of SCHMIEDL et al. (1982) that has been conventionally applied in seepage tracing so far. For the hook, the decrease in activity of both  $\delta^2\text{H}$  and  $\delta^{18}\text{O}$  during seawater concentration is taken into account, which is disregarded in the other method. In addition, the concentration stage of internal solutions can be determined and compared to the cation pattern by using this hook. However, since the humidity may greatly influence the shape of the hook, a future experimental determination of the course of the hook via seawater evaporation with varying humidity would increase the usefulness of this tool for seepage tracing.

For seepage tracing, Sr isotope systematics are a good complement to the element concentrations and the stable isotopes. In general, the  $^{87}\text{Sr}/^{86}\text{Sr}$  ratios of the external solutions are in good agreement with those of the aquifers from which they originate. Furthermore, in combination with the Sr concentration they can give evidence for

natural as well as anthropogenic contamination of the solutions. For epigenetic internal solutions, the  $^{87}\text{Sr}/^{86}\text{Sr}$  ratios can be used to back-calculate the timing of enclosure if the Rb concentration and the concentration stage are known. However, syngenetic internal solutions are not easily identified since even small contaminations with Rb after enclosure can alter the original seawater ratio, which otherwise should be preserved in the solution. For both epigenetic and syngenetic solutions, the loss of Sr by precipitation of gypsum from the solutions must be taken into account, since otherwise the Sr budget will be misinterpreted.

*A cautionary remark needs to be made in terms of sampling protocols for seepage sites in salt mines. All of the applied tracers are only useful and accurate if the sampling is always performed under the same conditions and undisturbed by anthropogenic influences. Several locations in this study have shown contamination by air or anthropogenic influences around the seepage site. Therefore, special attention should be paid on a strict but simple sampling protocol to be adjusted on the special local circumstances at each seepage site.*

### ***External Solutions***

Overall, the element composition of the external solutions is very distinct with higher Na, Ca, and Sr concentrations and lower Mg, K, and Rb concentrations than the internal solutions. Only one sampling series from LS 5 L499 900 m shows an element pattern that almost equals a Q-solution derived from seawater or massive dissolution of evaporitic minerals. However, the Ca and Sr concentrations are much higher than in the internal solutions and even highly increase with time, which indicates the external origin and disequilibrium with the Ca-rich phases on the flow path.

The stable isotope compositions of the external solutions are in the range of the GMWL for most samples. The samples from Hesse and Thuringia have similar  $\delta^2\text{H}$  and  $\delta^{18}\text{O}$  as the aquifers from which they can originate in those regions. The external samples from Lower Saxony and North-Rhine Westphalia show both higher  $\delta^2\text{H}$  and  $\delta^{18}\text{O}$  than the samples from Hesse and Thuringia. Unfortunately, no aquifer samples were available

for Lower Saxony and North-Rhine Westphalia. Again, the sample series of LS 5 L499 900 m shows an atypical pattern of stable isotopes, with highly increased  $\delta^{18}\text{O}$  and less pronounced increase of  $\delta^2\text{H}$ . This pattern may be attributed to membrane filtration through salt clays, which can cause such fractionation of the stable isotopes.

The Sr isotopic composition of the samples known to be of external origin can potentially be used as tracer for the source aquifer of external seepages. This applies in particular to regions with aquifers that show large differences in Sr isotope compositions. However, the presented aquifer data do not show such large variations. In Hesse and Thuringia, the most important aquifers of the Lower Buntsandstein and the Plattendolomit show similar  $^{87}\text{Sr}/^{86}\text{Sr}$  ratios. Many of the external seepage samples yield the same Sr isotopic composition and thus cannot be unambiguously assigned to a specific aquifer. However, this pattern implies that overall the  $^{87}\text{Sr}/^{86}\text{Sr}$  ratio of an external solution resembles that of the corresponding aquifer. Therefore, this tracer seems to be one option to classify the origin of the external seepages, but in this special case, the similarity of the  $^{87}\text{Sr}/^{86}\text{Sr}$  ratios of the aquifers precludes detailed classification. For the other external solutions from Lower Saxony and North Rhine-Westphalia, no aquifer samples were available. However, most of the seepage samples from these federal states show higher  $^{87}\text{Sr}/^{86}\text{Sr}$  ratios than those of the aquifers in Hesse and Thuringia. Consequently, the  $^{87}\text{Sr}/^{86}\text{Sr}$  ratios of the aquifers of each groundwater basin surrounding one or several mines must be evaluated separately to point out possible differences between the aquifers. If such differences are present, a determination of the seepage origin may be possible. *In the future, this hypothesis should be tested on the aquifers surrounding the mines under question in Lower Saxony and North-Rhine Westphalia. In all cases, the Sr concentrations in the seepage samples must be determined additionally since highly elevated Sr concentrations may indicate an influence of clay minerals, as shown by the samples of LS 5 L499 900 m.*

### ***Internal Solutions***

The internal solutions show larger variations than in external solutions in their element compositions. This can be attributed to different concentration stages, dependent on

either the stage of seawater concentration (syngenetic solutions) or the degree and extent of dissolution of evaporitic minerals (epigenetic solutions). For most of the internal solutions, the cation concentrations indicate a concentration stage where the solution is in equilibrium with carnallite (Q-solutions).

The stable isotope contents of the internal solutions follow a concentration hook to the right side of the GMWL. This concentration hook is caused by changing activities of the stable isotopes during seawater evaporation. However, epigenetic solutions never were subject to such evaporation after they reached their concentration stage. For these samples, the dissolution of hydrated minerals, like gypsum or carnallite, may cause a similar shift in the stable isotope composition in direction to the hook because the water of hydration of such phases is fractionated in this direction upon crystallization. *In the future, this fractionation of the stable isotopes during crystallization and dissolution should be tested experimentally to improve the understanding for the extent of this effect.*

For both external and internal samples that have stable isotope compositions in the range of the GMWL where the hook reaches it, the comparison with the concentration hook is not useful stand alone. Here, other tracers like e.g. the Sr concentration need to be consulted to distinguish between external and internal origin.

The Sr isotope systematics of epigenetic internal solutions can be used to back-calculate the timing of enclosure of the solution within the salt. For such calculations, the Rb/Sr budget of the solution needs to be evaluated carefully to minimize misinterpretation. If no Rb excess occurred after enclosure, even syngenetic internal solutions can be identified since they should have retained the  $^{87}\text{Sr}/^{86}\text{Sr}$  ratio of Late Permian seawater (about 0.7068).

## 9. REFERENCES

- AGGARWAL, PK, GAT, JR & FROEHLICH, KFO (Eds) (2005) *Isotopes in the Water Cycle- Past, Present and Future of a Developing Science*. IAEA Springer Dortrecht: 381pp
- ALBARÈDE, F, MICHARD, A, MINSTER, JF & MICHARD, G (1981)  $^{87}\text{Sr}/^{86}\text{Sr}$  ratios in hydrothermal waters and deposits from the East Pacific Rise at  $21^\circ$  N. *Earth Planet Sci Lett* 55: 229-236
- ALSHARHAN, AS & KENDALL, CGSTC (2003) Holocene coastal carbonates and evaporites of the southern Arabian Gulf and their ancient analogues. *Earth Sci Rev* 61: 191-243
- BAADSGAARD, H (1987) Rb-Sr and K-Ca isotope systematics in minerals from potassium horizons in the Prairie evaporite formation, Saskatchewan, Canada. *Chem Geol* 66: 1-15
- BANNER, JL & HANSON, GN (1990) Calculation of simultaneous isotopic and trace element variations during water-rock interactions with applications to carbonate diagenesis. *Geochim Cosmochim Acta* 54: 3123-3137
- BANNER, JL, MUSGROVE, ML & CAPO, RC (1994) Tracing ground-water evolution in a limestone aquifer using Sr isotopes; effects of multiple sources of dissolved ions and mineral-solution reactions. *Geology* 22(8): 687-690
- BEER, WW (1996) Kalilagerstätten in Deutschland. *Kali Steinsalz* 12: 18-30
- BERLITZ, HD, GROSCH, W & SCHIEBERLE, P (2007) *Lehrbuch der Lebensmittelchemie*. Springer Berlin: 1119 pp.
- BERNER, RA (1975) The role of magnesium in the crystal growth of calcite and aragonite from sea water. *Geochim Cosmochim Acta* 39: 489-505
- BLOCH, MR & SCHNERB, J (1953) On the Cl<sup>-</sup>/Br<sup>-</sup> -ratio and the distribution of Br<sup>-</sup> ions in liquids and solids during evaporation of bromide-containing chloride solutions. *Bull Res Counc Israel* 1: 151-158
- BORCHERT, H (1940) Die Salzlagerstätten des deutschen Zechsteins. *Archiv Lagerstättenforsch* 67: 196 pp.



- BORCHERT, H & MUIR, R O (1964) Salt deposits; the origin, metamorphism and deformation of evaporites. Van Nostrand-Reinhold Princeton: 338 pp.
- BOTTRELL, S H, LEOSON, M A & NEWTON, R J (1996) Origin of brine inflows at Boulby potash mine, Cleveland, England. *Trans. Inst. Mining Metall. B* 105: 159-164
- BRAITSCH, O & HERRMANN, AG (1963) Zur geochemie des Broms in salinaren Sedimenten; Teil 1: Experimentelle Bestimmung der Br-Verteilung in verschiedenen natürlichen Salzsystemen. *Geochim Cosmochim Acta* 27: 361-391
- BRAITSCH, O (1964) The temperature of evaporite formation. In: NAIRN, A E M (Ed.) *Problems in Paleoclimatology*. Wiley Interscience New York: 479-490
- BRAITSCH, O (1966) Bromine and rubidium as indicators of environment during sylvite and carnallite deposition of the upper Rhine-Valley evaporites; in RAU, JL (Ed.) (1966) *Second Symposium on Salt*. Northern Ohio Geol Soc 1: 293-301
- BRAITSCH, O (1971) Salt deposits, their origin and composition. Springer Berlin: 297 pp.
- BRASS, GW & TUREKIAN, KK (1974) Strontium distribution in Geosecs oceanic profiles. *Earth Pla Sci Lett* 23: 141-14
- BROWN, J & BEARMAN, G (Ed.) (1997) *Seawater: its composition, properties, and behavior*. Open University Pergamon Press Oxford: 168 pp.
- BUNDESMINISTERIUM DER JUSTIZ (2001) *Trinkwasserverordnung 2001*.  
[http://bundesrecht.juris.de/trinkwv\\_2001/](http://bundesrecht.juris.de/trinkwv_2001/), retrieved in May 2008
- BURKE, WH, DENISON, RE, HETHERINGTON, EA, KOEPNICK, RB, NELSON, HF & OTTO, JB (1982) Variation of seawater  $^{87}\text{Sr}/^{86}\text{Sr}$  throughout Phanerozoic time. *Geology* 10: 516-519
- CARLSON, G (2005) Total dissolved solids from conductivity. Technical Note In Situ Inc. 14
- CHACKO, T, COLE, TR & HORITA, J (2001) Equilibrium oxygen, hydrogen and carbon isotope fractionation factors applicable to geological systems. In: VALLEY, JW & COLE, DR (Eds) *Stable Isotope Geochemistry*. *Rev Min Min Soc Am* 43: 1-81
- CHOU, IM & HAAS Jr, JL (1981) Strontium chloride solubility in complex brines. *Sci Basis Nucl Waste Manage* 3: 499-506

- CLARK, DN (1980) The diagenesis of Zechstein carbonates. *Contrib Sedimentol* 9: 167-203
- CLARK, ID & FRITZ, P (1997) *Environmental isotopes in hydrogeology*. CRC Press LLC Boca Raton 328 pp.
- CLAUER, N & CHAUDHURI, S (Eds) (1992) *Isotopic signatures and sedimentary records*. Springer Berlin 529 pp.
- COOPER, AH (2002) Halite karst geohazards (natural and man-made) in the United Kingdom. *Env Geol* 42: 505-512
- COPLEN, TB & HANSHAW, BB (1973) Ultrafiltration by a compacted clay membrane-I. Oxygen and hydrogen isotopic fractionation. *Geochim Cosmochim Acta* 37: 2295-2310
- COPLEN, TB (1994) Reporting of stable hydrogen, carbon and oxygen isotopic abundances. *Pure Appl Chem* 66: 273-276
- CRAIG, H (1961a) Standard for Reporting Concentrations of Deuterium and Oxygen-18 in Natural Waters. *Science* 133: 1833-1834
- CRAIG, H (1961b) Isotopic Variations in Meteoric Waters. *Science* 133: 1702-1703
- CROCK, JG, LICHTER, FE & WILDEMAN, TR (1984) The group separation of the rare-earth elements and yttrium from geologic materials by cation-exchange chromatography. *Chem Geol* 45: 149-163
- D'ANS, J (1933) *Die Lösungsgleichgewichte der Systeme der ozeanischen Salzablagerungen*. Verlagsges Ackerbau Berlin: 254 pp.
- D'ANS, J (1947) Über die Bildung und Umbildung der Kalilagerstätten. *Naturwiss* 34(10): 295-301
- D'ANS, J (1961) Über die Bildungsmöglichkeiten des Tachhydrits in Kalisalzlagerstätten. *Kali Steinsalz* 3(4): 119-125
- DENISON, RE, KOEPNICK, RB, BURKE, WH, HETHERINGTON, EA & FLETCHER, A (1994) Construction of the Mississippian, Pennsylvanian and Permian seawater  $^{87}\text{Sr}/^{86}\text{Sr}$  curve. *Chem Geol* 112: 145-167
- DE VILLIERS, S (1999) Seawater strontium and Sr/Ca variability in the Atlantic and Pacific oceans. *Earth Pla Sci Lett* 171: 623-634

- DICKIN, AP (2005) Radiogenic isotope geology. Cambridge University Press: 492 pp.
- EASTOE, C J, LONG, A & KNAUTH, L P (1999) Stable chlorine isotopes in the Palo Duro Basin, Texas: Evidence for preservation of Permian evaporite brines. *Geochim Cosmochim Acta* 63(9): 1375-1382
- ECKE, HH & LÖFFLER, T (1985) Palynostratigraphic data from evaporite-solution breccia at the eastern margin of the Leinetal Graben near Northeim (Southern Lower Saxony, F. R.). *Neues Jahrb Paläont Abh* 170(2): 167-182
- EGGENKAMP, H G M, KREULEN, R & KOSTER VAN GROOS, A F (1995) Chlorine stable isotope fractionation in evaporites. *Geochim Cosmochim Acta* 59(24): 5169-5175
- EHGARTNER, B, NEIL J & HINKEBEIN, T (1998) Gas Releases from Salt. SMRI Spr Mtg 68: 37 pp.
- ELBRACHT, J, MEYER, R & REUTTER, E (2007) Hydrogeologische Räume und Teilräume in Niedersachsen. *GeoBer* 3: 3-106
- ELDERFIELD, H & GREAVES, MJ (1981) Strontium isotope geochemistry of Icelandic geothermal systems and implications for seawater chemistry. *Geochim Cosmochim Acta* 45(11): 2201-2212
- ELDERFIELD, H & SCHULTZ, A (1996) Mid-ocean ridge hydrothermal fluxes and the chemical composition of the ocean. *Annu Rev Earth Planet Sci* 24: 191-224
- FAURE, G (1986) Principles of isotope geology. John Wiley & Sons New York: 589 pp.
- FEIT, W & KUBIERSCHKY, K (1892) Die Gewinnung von Rubidium- und Caesiumverbindungen aus Carnallit. *Chemiker Zeitung* 16: 335-340
- FISCHER, AG (1984) The two Phanerozoic supercycles. In: Berggren, WA & Van Couvering, JA (Eds.) *Catastrophes and earth history*. Princeton University Press: 464 pp.
- FLECKER, R, DE VILLIERS, S & ELLAM, RM (2002) Modelling the effect of evaporation on the salinity- $^{87}\text{Sr}/^{86}\text{Sr}$  relationship in modern and ancient marginal-marine systems: the Mediterranean Messinian Salinity Crisis. *Earth Planet Sci Lett* 203(1): 221-233

- FONTES, JCH (1966) Interêt en géologie d'une étude isotopique de l'évaporation cas de l'eau de mer. C R Hebd Séances Acad Sci Paris 263(25): 1950-1953
- FONTES, JCH & GONFIANTINI, R (1967b) Comportement isotopique au cours de l'évaporation de deux bassins sahariens. Earth Planet Sci Lett 3(3): 258-266
- FONTES, JCH & GONFIANTINI, R (1967a) Fractionnement isotopique de l'hydrogène dans l'eau de cristallisation du gypse. C R Hebd Séances Acad Sci Paris 265: 4-63
- FONTES, JCH & MATRAY, JM (1993) Geochemistry and origin of formation brines from the Paris Basin, France: 1. Brines associated with Triassic salts. Chem Geol 109: 149-175
- FOURRÉ, E, JEAN-BAPTIST, B, DAPOIGNY, A, BAUMIER, D, PETIT, J-R & JOUZEL, J (2006) Past and recent tritium levels in Arctic and Antarctic polar caps. Earth Planet Sci Lett 245(1-2): 56-64
- FRAPE, SK & FRITZ, P (1984) Water-rock interaction and chemistry of groundwaters from the Canadian shield. Geochim Cosmochim Acta 48: 1617-1627
- FRITSCH, HG, HEMFLER, M, KÄMMERER, D, LEßMANN, B, MITTELBACH, G, PETERS, A, POSCHL, W, RUMOHR, S & SCHLÖSSER-KLUGER, S (2003) Beschreibung der hydrogeologischen Teilräume von Hessen gemäß EU-Wasserrahmenrichtlinie (EU-WRRL). Geol Jb Hessen 130: 5-19
- FULDA, E (1935) Zechstein. Handb vergl Strat Deutschland, Bornträger Berlin: 409 pp.
- GAT, JR (1996) Oxygen and hydrogen isotopes in the hydrologic cycle. Annu Rev Earth Pla Sci 24: 225-262
- GELLERMANN, R, Hebert, D, Radke, S & Remus, W (1991) Isotopenhydrogeologische Untersuchungen am Endlager für radioactive Abfälle Morsleben. Isotopenpraxis 27(4): 178-184
- GENDZWILL, D & MARTIN, N (1996) Flooding and loss of Patience Lake potash mine. CIM Bulletin 89(1000): 62-73
- GERMAN STRATIGRAPHIC COMMISSION (Ed.) (2002) Stratigraphic Table of Germany 2002.
- GEYH, MA & RAMBOW, D (1997) Isotopenhydrologische Untersuchungen an Grundwässern aus dem Buntsandstein Nordhessens. Geol Jb Hessen 125: 43-62

- GLENNIE, KW (1986) Development of N.W. Europe's southern Permian gas basin. *Geol Soc London Spec Pub* 23: 3-22
- GOERGEY, R (1912) Zur Kenntnis der Kalisalzlager von Wittelsheim im Oberelsass. *Tschermak's Mineral Petrogr Mitt* 31: 339-468
- GOLDBERG, ED (1965) Minor elements in sea water. *Chem Oceanography* 1: 163-196
- GONFIANTINI, R (1965, in Italian) Isotopic effects in the evaporation of seawater. *Atti Soc Toscana Sci Nat Series A*: 72
- GONFIANTINI, R (1986) Environmental isotopes in lake studies. In: FRITZ, P & FONTES, JCH (Eds.) *Handbook of environmental isotope geochemistry II: The terrestrial environment*. Elsevier Amsterdam: 113-168
- GONFIANTINI, R & FONTES, J CH (1963) Oxygen isotopic fractionation in the water of crystallisation of gypsum. *Nature* 200(4907): 644-646
- GRABCZAK, J & ZUBER, A (1986) A combined isotope and chemical approach to determining the origin of brines in salt mines. *Freib. Forschungsh. C* 417: 105-115
- GROAT, CG (1981) Rig lost; lake fills salt mine. *Geotimes* 26(3): 14
- GRUSZCZYŃSKI, M, HAŁAS, S, HOFFMAN, A & MAŁKOWSKI, K (1989) A brachiopod calcite record of oceanic carbon and oxygen isotope shifts at the Permian/Triassic transition. *Nature* 337: 64-68
- GRUSZCZYŃSKI, M, HOFFMAN, A, MAŁKOWSKI, K & VEIZER, J. (1992) Seawater strontium isotopic perturbation at the Permian-Triassic boundary, West Spitzbergen, and its implications for the interpretation of strontium isotopic data. *Geology* 20: 779-782
- HABFAST, K (1998) Fractionation correction and multiple collectors in thermal ionization isotope ratio mass spectrometry. *Int Jour Mass Spec* 176: 133-148
- HALLAM, A (1984) Pre-Quaternary sea-level changes. *Ann Rev Earth Pla Sci* 12: 205-243
- HARDIE, LA (1996) Secular variation in seawater chemistry: An explanation for the coupled secular variation in the mineralogies of marine limestones and potash evaporites over the past 600 m.y.. *Geology* 24(3): 279-283

- HARDIE, LA (2003) Secular variations in Precambrian seawater chemistry and the timing of Precambrian aragonite seas and calcite seas. *Geology* 31(9): 785-788
- HEINZINGER, K (1980) Oxygen isotope fractionation in saline aqueous solutions. In: NISSENBAUM, A (Edt) *Hypersaline brines and evaporitic environments. Develop Sedimentol* 28: 278 pp.
- HEBERT, D, FRÖHLICH, K & SCHMIEDL, HD (1983) Methodische Beiträge zur Tritiumanalyse an salinaren Wässern. *Freib Forsch C* 388: 159-169
- HERRMANN, AG (1961) Über das Vorkommen einiger Spurenelemente in Salzlösungen aus dem deutschen Zechstein. *Kali Steinsalz* 3(7): 209-220
- HERRMANN, AG (1972) Bromine distribution coefficients for halite precipitated from modern sea water under natural conditions. *Contr Min Pet* 37: 249-252
- HERRMANN, AG (1981) Grundkenntnisse über die Entstehung mariner Salzlagerstätten. *Aufschluss* 32: 45-72
- HERRMANN, A G, SIEBRASSE, G & KÖNNECKE, K (1978) Computerprogramme zur Berechnung von Mineral- und Gesteinsumbildungen bei der Einwirkung von Lösungen auf Kali- und Steinsalzlagerstätten (Lösungsmetamorphose). *Kali Steinsalz* 12: 115-124
- HERRMANN, AG (1997) Fluid inclusions: Neue Erkenntnisse über den Stoffbestand NaCl-gesättigter Meerwasserlösungen im Zechstein 3. *Kali Steinsalz* 12(4): 115-124
- HERRMANN, A G, SIEWERS, U, HAZARIM, B, LODZIAK, J, WECK, H D & STRABURG, S (2000) Die Herkunft von Haupt-, Neben- und Spurenelementen in Salzlösungen der Zechsteinevaporite Mittel- und Norddeutschlands. *Kali Steinsalz* 13(14): 771-783
- HERRMANN, A G, SIEWERS, U, HARAZIM, B & USDOWSKI, E (2003) Kriterien zur Beurteilung von Salzlösungen in Zechsteinevaporiten Mittel- und Norddeutschlands. *Kali Steinsalz* 3/2003: 24-35
- HILDEN, H D (1988) *Geologie am Niederrhein*. Geol Landesamt NRW Krefeld: 142 pp.
- HOLSER, W T (1979) Trace elements and isotopes in evaporites. In: BURNS, R G (Ed.) *Marine minerals*. *Rev Mineral, Amer Soc Mineral* 6: 295-346

- HOLSER, WT, in RIBBE, PH (Ed.) (1979) Marine Minerals. *Rev Min* 6: 211-346
- HORITA, J (1989) Analytical aspects of stable isotopes in brines. *Chem Geol* 79: 107-112
- HORITA, J, FRIEDMAN, TJ, LAZAR, B & HOLLAND, HD (1991) The composition of Permian seawater. *Geochim Cosmochim Acta* 55(2): 417-432
- HORITA, J, WESOLOWSKI, DJ & COLE, DR (1993a) The activity-composition relationship of oxygen and hydrogen isotopes in aqueous salt solutions: I. Vapor-liquid water equilibration of single salt solutions from 50 to 100°C. *Geochim Cosmochim Acta* 57: 2797-2817
- HORITA, J, COLE, DR & WESOLOWSKI, DJ (1993b) The activity-composition relationship of oxygen and hydrogen isotopes in aqueous salt solutions: II. Vapor-liquid water equilibration of single salt solutions from 50 to 100°C and geochemical implications. *Geochim Cosmochim Acta* 57: 4703-4711
- HORITA, J (2005) Saline Waters. In: AGGARWAL, PK, GAT, JR & FROELICH, KFO (Eds) *Isotopes in the Water Cycle-Past, Present and Future of a Developing Science*. IAEA Springer Dordrecht: 381pp
- HORITA, J, ZIMMERMANN, H & HOLLAND, HD (2002) Chemical evolution of seawater during the Phanerozoic: Implications from the record of marine evaporites. *Geochim Cosmochim Acta* 66(21): 3733-3756
- HUTTON, J (1795) *Theory of the Earth*. Wheldon & Wesley (reprint 1959) 1: 620 pp.
- JÄNECKE, E (1906) Über eine neue Darstellungform der wässrigen Lösungen zweier und dreier gleichioniger Salze, reziproker Salzpaare und der van't Hoff'schen Untersuchungen über ozeanische Salzablagerungen. *Zeit anorg Chemie* 51(1): 132-157
- JÄNECKE, E (1923) *Die Entstehung der deutschen Kalisalzlager*. Vieweg Braunschweig: 111 pp.
- JAFFRÉS, JBD, SHIELDS, GA & WALLMANN, K (2007) The oxygen isotope evolution of seawater: A critical review of a long-standing controversy and an improved geologic water cycle model for the past 3.4 billion years. *Earth-Sci Rev* 83: 83-122

- JENSEN, GKS, ROSTRON, BJ, DUKE, MJM & HOLMDEN, C (2006) Bromine and stable isotopic profiles of formation waters from potash mine shafts, Saskatchewan, Canada. *Jour Geochem Explor* 89(1-3): 170-173
- JEREMIC, ML (1994) *Rock Mechanics in Salt Mining*. Taylor & Francis Group: 532 pp.
- JOHNSON, TM & DEPAULO, DJ (1994) Interpretation of isotopic data in groundwater-rock systems: Model development and application to Sr isotope data from Yucca mountain. *Water Res research* 30(5): 1571-1587
- K+S GRUPPE (2006) *Wachstum erleben - Die Geschichte der K+S Gruppe*. K+S Aktiengesellschaft Kassel: 352 pp.
- KÄDING, K-C (1978) Stratigraphische Gliederung des Zechsteins im Werra-Fulda-Becken. *Geol Jahrb Hessen* 106: 123-130
- KÄDING, K-C & SESSLER, W (1994) Befahrung des Kalibergwerkes NeuhoF-Ellers der Kali und Salz AG bei Fulda (Excursion G am 8. April 1994). *Jber Mitt oberrhein geol Ver N F* 76: 191-197
- KAMO, SL, CZAMANSKE, GK, AMELIN, Y, FEDORENKO, VA, DAVIS, DW & TROFIMOV, VR (2003) Rapid eruption of Siberian flood-volcanic rocks and evidence for coincidence with the Permian-Triassic boundary and mass extinction at 251 Ma. *Earth Pla Sci Lett* 214: 75-91
- KINSMAN, DJJ (1970) Trace cations in aragonite. *Geol Soc Amer Abstr Progr* 2: 596-597
- KLAUS, JS, HANSEN, BT & BUAPENG, S (2007)  $^{87}\text{Sr}/^{86}\text{Sr}$  ratio: a natural tracer to monitor groundwater flow paths during artificial recharge in the Bangkok area, Thailand. *Hydrogeol Jour* 15: 745-758
- KLINGENBERG, I (1998) Die Verteilung der Isotope des Strontiums, Schwefels und Lithiums in salinaren Lösungen des Salzstocks Gorleben und der Salzstruktur des Allertalgrabens. *Papierflieger* 1998: 82 pp.
- KNAUSS, KG, WOLERY, TJ & JACKSON, KJ (1990) A new approach to measure pH in brines and other concentrated electrolytes. *Geochim Cosmochim Acta* 54: 1519-1523



- KNAUTH, LP & BEEUNAS, MA (1986) Isotope geochemistry of fluid inclusions in Permian halite with implications for the isotopic history of ocean water and the origin of saline formation waters. *Geochim Cosmochim Acta* 50(3): 419-433
- KNIPPING, B (1987) Basalt intrusions in evaporites. *Lecture Notes Earth Sci* 24: 131 pp.
- KORTE, C, KOZUR, HW, BRUCKSCHEN, P & VEIZER, J (2003) Strontium isotope evolution of Late Permian and Triassic seawater. *Geochim Cosmochim Acta* 67(1): 47-62
- KORTE, C, KOZUR, HW, JOACHIMSKI, MM, STRAUSS, H, VEIZER, J & SCHWARK, L (2004) Carbon, sulfur, oxygen and strontium isotope records, organic geochemistry and biostratigraphy across the Permian/Triassic boundary in Abadeh, Iran. *Int J Earth Sci* 93: 565-581
- KORTE, C, JASPER, T, KOZUR, HW & VEIZER, J (2006)  $^{87}\text{Sr}/^{86}\text{Sr}$  record of Permian seawater. *Palaeo* 240: 89-107
- KOVALEVYCH, VM, PERYT, TM, CARMONA, V, SYDOR, DV, VOVNYUK, SV & HAŁAS, S (2002a) Evolution of Permian seawater: evidence from fluid inclusions in halite. *N Jb Min Abh* 178: 27-62
- KOVALEVYCH, VM, PERYT, TM, BEER, W, GELUK, M & HAŁAS, S (2002b) Geochemistry of Early Triassic seawater as indicated by study of the Röt halite in the Netherlands, Germany and Poland. *Chem Geol* 182: 549-563
- KRAMM, U & WEDEPOHL KH (1991) The isotopic composition of strontium and sulfur in seawater of Late Permian (Zechstein) age. *Chem Geol* 90: 253-262
- KRULL, O (1917) Beiträge zur Geologie der Kalisalzlager. *Kali (Halle)* 11(14): 227-231
- KÜHN, R (1955) Mineralogische Fragen der in den Kalisalzlagerstätten vorkommenden Salze. *Kalisymp Berlin 1955*: 51-105
- KÜHN, R (1963) Rubidium als geochemisches Leitelement bei der lagerstättenkundlichen Charakterisierung von Carnalliten und natürlichen Salzlösungen. *Neues Jahrb Mineral Monatsh* 5: 107-115
- KÜHN, R (1968) Geochemistry of the German potash deposits. *Min Soc Amer Mem* 88: 427-504
- KÜHN, R (1972a) in Richter-Bernburg, G: *Geology of Saline Deposits*. UNESCO Earth Sci Ser 7: 77-89

- KÜHN, R (1972b) Zur Kenntnis der Rubidiumgehalte von Kalisalzen ozeanischer Salzlagerstätten nebst einiger lagerstättenkundlichen Ausdeutungen. *Geol Jahrb* 90: 127-220
- LAUBSCHER, H (1988) Material balance in Alpine orogeny. *Geol Soc Am Bull* 100 (9): 1313-1328
- LEHMANN, H-W (1974) Geochemie und Genesis der Tiefenwässer der Norddeutschen Senke. *Zeitschr angew Geologie* 20(11): 502-557
- LLOYD, RM (1965) Oxygen isotope enrichment of sea water by evaporation. *Geochim Cosmochim Acta* 30: 801-814
- LLOYD, JW & HEATHCOTE, JA (1985) Natural inorganic hydrochemistry in relation to groundwater: an introduction. Oxford University Press New York: 296 pp.
- LÖWENGART, S (1928) Das Tote Meer, seine Entstehung und die Möglichkeit seiner Ausbeutung. *Zeit prakt Geol* 36: 86-89
- LOWENSTEIN, TK, TIMOFEEFF, MN, KOVALEVYCH, VM & HORITA, J (2005) The major-ion composition of Permian seawater. *Geochim Cosmochim Acta* 69: 1701-1719
- LYONS, WB, TYLER, SW, GAUDETTE, HE & LONG, DT (1995) The use of strontium isotopes in determining groundwater mixing and brine fingering in a playa spring zone, Lake Tyrrell, Australia. *Jour Hydrol* 167(1-4): 225-239
- MALIKOVA, IM (1967, in Russian) Distribution of Rubidium, Thallium and Bromine in Potassium Salt Deposits. Akad Sci USSR Sibir Otd Inst Geol Geofiz Novosibirsk: 149pp
- MARTIN, EE & MACDOUGALL, JD (1995) Sr and Nd isotopes at the Permian/Triassic boundary: A record of climate change. *Chem Geol* 125: 73-99
- MAY, I, SCHNEPF, M & NAESER, C R (1961) Interaction of anhydrite with solutions of strontium and cesium. *US Geol Surv Prof Paper* 424D: 336-338
- MCINTIRE, WL (1968) Effect of temperature on the partition of rubidium between sylvite crystals and aqueous solutions. *Geol Soc Amer Spec Pap* 88: 505-524
- MCNUTT, RH, FRAPE, SK & FRITZ, P (1984) Strontium isotopic composition of some brines from the Precambrian shield of Canada. *Isotope Geosci* 2: 205-215

- MCNUTT, RH, FRAPE, SK, FRITZ, P, JONES, MG & MACDONALD, IM (1990) The  $^{87}\text{Sr}/^{86}\text{Sr}$  values of Canadian Shield brines and fracture minerals with application to groundwater mixing, fracture history, and geochronology. *Geochim Cosmochim Acta* 54: 205-215
- MERLIVAT, & JOUZEL, (1979) Global climatic interpretation of the deuterium-oxygen 18 relationship for precipitation. *Jour Geophys Res* 84(C8): 5029
- MII, HS, GROSSMAN, EL & YANCEY, TE (1997) Stable carbon and oxygen isotope shifts in Permian seas of West Spitzbergen - Global change or diagenetic artifact? *Geology* 25: 227-230
- MÖLLER, P, GEYER, S, SALAMEH, E & DULSKI, P (2006) Sources of mineralization of thermal groundwater of Jordan. *Acta Hydrochim Hydrobiol* 34: 86-100
- MÖLLER, P, WEISE, SM, TESMER, M, DULSKI, P, PEKDEGER, A, BAYER, U & MAGRI, F (2007) Salinization of groundwater in the Northern German Basin: results from conjoint investigations of major, trace element and multi-isotope distribution. *Int J Earth Sci (Geol Rundsch)* online first
- MOOK, WG (Ed.) (2000) *Environmental Isotopes in the Hydrological Cycle: Principles and Applications*. IAEA 1: 280 pp.
- MOORE, LJ, MOODY, JR, BARNES, IL, GRAMICH, JW, MURPHY, TJ, PAULSEN, PJ & SHIELDS, WR (1973) Trace determination of rubidium and strontium in silicate glass standard reference materials. *Anal Chem* 45: 2384-2387
- MOSER & RAUERT (1980) *Isotopenmethoden in der Hydrogeologie*. Bornträger Berlin: 400 pp.
- MÜLLER, G (1962) Zur Geochemie des Strontiums in ozeanischen Evaporiten unter besonderer Berücksichtigung der sedimentären Cölestinlagerstätte von Hemmelte-West (Süd-Oldenburg). *Geologie Beih* 11: 1-90
- MÜLLER, E P & PAPENDIECK, G (1975) Zur Verteilung, Genese und Dynamik von Tiefenwässern unter besondere Berücksichtigung des Zechsteins. *Z. geol Wiss Berlin* 3: 167-196
- MUMINDZHANOVA, MA & OSICHKINA, RG (1982) Experimental determination of coefficients of rubidium and cesium distribution between sylvite crystals and a

- solution in potassium chloride-water and sodium chloride-potassium chloride-water system (in Russian). *Uzb Khim Zh* 1: 11-15
- NIELSEN, H & RAMBOW, D (1969) S-Isotopenuntersuchungen an Sulfaten hessischer Mineralwässer. *Notizbl Hess L-Amt Bodenforsch* 97: 352-366
- OCHSENIUS (1876) Über die Salzbildung der Egelnschen Mulde. *Z. Dtsch. Geol. Ges.* 28(4): 654-667
- OCHSENIUS (1877) Die Bildung der Steinsalzlager und ihrer Mutterlaugensalze unter spezieller Berücksichtigung der Flöze von Douglashall in der Egelnschen Mulde. CEM Pfeffer Halle/Saale: 172 pp.
- OHRDORF, R (1968) Ein Beitrag zur Geochemie des Lithiums in Sedimentgesteinen. *Geochim Cosmochim Acta* 32: 191-208
- OSICHKINA, RG (2006) Regularities of trace element distribution in water-salt systems as indicator for the genesis of potassium salt rocks: an example from the Upper Jurassic Halogen formation of Central Asia. *Geochem Int* 44(2): 164-174
- PAUL, J (1986) Environmental analysis of basin and schwellen facies in the lower Zechstein of Germany. *Geol Soc London Spec Pub* 22: 143-147
- PERROW, C (1984) *Normal Accidents: Living with High Risk Technologies*. Basic Books New York: 451 pp.
- PETROVA, NS (1973) Partition of Rb between carnallite and solution in the NaCl-MgCl<sub>2</sub>-H<sub>2</sub>O system at 25°C. *Geochem Int* 10(3): 709-714
- PHILLIPS, FM & BENTLEY, HW (1987) Isotopic fractionation during ion filtration: I. Theory. *Geochim Cosmochim Acta* 51: 683-693
- PIERRET, MC, CLAUER, N, BOSCH, D, BLANC, G & FRANCE-LANORD, C (2001) Chemical and isotopic (<sup>87</sup>Sr/<sup>86</sup>Sr, δ<sup>18</sup>O, δD) constraints to the formation processes of Red-Sea brines. *Geochim Cosmochim Acta* 65(8): 1259-1275
- PILOT, J & VOGEL, J (1972) Isotopengeochemische Untersuchungen an Wässern. *Ber deutsch Ges geol Wiss A* 17(2): 233-247
- PUCHELT, H, LUTZ, F & SCHOCK, HH (1972) Verteilung von Bromid zwischen Lösungen und chloridischen Salzmineralen. *Naturwiss* 59: 34-35

- RADZINSKI, K H (1996) Tätigkeitsbericht 2003-2005. Geol Landesamt Sachsen-Anhalt: 11-18
- REICHERT, J (1966) Verteilung anorganischer Fremdionen bei der Kristallisation von Alkalichloriden. *Contr Min Pet* 13: 134-160
- RENNE, PR & BASU, AR (1991) Rapid eruption of the Siberian Traps flood basalts at the Permo-Triassic boundary. *Science* 253(5016): 179-179
- RICHTER-BERNBURG, G (1953a) Über saline Sedimentation. *Zeit Deut Geol Ges* 105: 593-645
- RICHTER-BERNBURG, G (1953b) Stratigraphische Gliederung des Deutschen Zechsteins. *Z Deut Geol Ges* 105: 843-854
- ROBINSON, RA & STOKES, R H (2002) *Electrolyte solutions*. Butterworths London: 590 pp.
- ROEDDER, E (1984) The fluids in salt. *Amer Mineral* 69: 413-439
- SACHSE, D, RADKE, J, GAUPP, R, SCHWARK, L, LÜNIGER, G & GLEIXNER, G (2004) Reconstruction of palaeohydrological conditions in a lagoon during the 2nd Zechstein cycle through simultaneous use of dD values of individual n-alkanes and d18O and d13C values of carbonates. *Int J Earth Sci* 93: 554-564
- SANDBERG, PA (1975) New interpretations of Great Salt Lake ooids and of ancient non-skeletal carbonate mineralogy. *Sedimentology* 22: 497-537
- SCHECK, M & BAYER, U (1999) Evolution of the Northeast German Basin-inferences from a 3D structural model and subsidence analysis. *Tectonophysics* 313: 145-169
- SCHMIEDL, H D, RUNGE, A, JORDAN, H, KOCH, K, PILOT, J & ELERT, K H (1982) Die Deuterium- und Sauerstoff-18-Isotopenanalyse - ein modernes Verfahren zur Bewertung untertägiger Salzlösungsvorkommen in Kali- und Steinsalzgruben. *Z. geol. Wiss. Berlin* 10: 73-85
- SCHMIEDL, H D, JORDAN, H, PILOT, J, STIEHL, G, KUNAT, A, KOCH, K & ELERT, K (1983) Der Einsatz der D- und 18-O-Analyse im Kali- und Steinsalzbergbau der DDR zur bergmännischen Bewertung von untertägigen Salzlösungsvorkommen und Tiefenwässern. *Freib Forschungsh C* 388: 138-148

- SCHMIEDL, H D, SCHWANDT, A, SPILKER, M, BÖTTGER, T, PILOT, J, STIEHL, G & JORDAN, H (1986) Möglichkeiten und Grenzen der D- und  $^{18}\text{O}$ -Analyse zur Erkennung offener und geschlossener Systeme beim Abbau von Zechsteinlagerstätten. *Freib Forschungsh* 417: 127-136
- SCHMITZ, B, INGRAM, SL, DOCKERY III, DT & ÅBERG, G (1997) Testing  $^{87}\text{Sr}/^{86}\text{Sr}$  as a paleosalinity indicator on mixed marine, brackish-water and terrestrial vertebrate skeletal apatite in late Paleocene-early Eocene near-coastal sediments, Mississippi. *Chem Geol* 140(3-4): 275-287
- SCHOCK, HH & PUCHELT, H (1971) Rubidium and cesium distribution in salt minerals I: Experimental investigations. *Geochim Cosmochim Acta* 35(3): 307-317
- SCHOLLE, PA, PERYT, TM & ULMER-SCHOLLE, DS (Ed.) (1995a) *The Permian of Northern Pangea, Vol 1*. Springer Berlin Heidelberg: 261 pp.
- SCHOLLE, PA, PERYT, TM & ULMER-SCHOLLE, DS (Ed.) (1995b) *The Permian of Northern Pangea, Vol 2*. Springer Berlin Heidelberg: 312 pp.
- SCHREIBER, BC & EL TABAKH, M (2000) Deposition and early alteration of evaporites. *Sedimentology* 47(1) 215-238
- SINCERO, AP (2003) *Physical-chemical treatment of waste and wastewater*. IWA Publishing London: 856 pp.
- SKOWRONEK, F, FRITSCHKE, J-G, ARAGON, U & RAMBOW, D (1999) Die Versenkung und Ausbreitung von Salzabwasser im Untergrund des Werra-Kaligebietes. *Geol Abh Hessen* 105: 83 pp.
- SOFER, Z (1978) Isotopic composition of hydration water in gypsum. *Geochim Cosmochim Acta* 42: 1141-1149
- SOFER, Z & GAT, JR (1972) Activities and concentrations of oxygen-18 in concentrated aqueous salt solutions: analytical and geophysical implications. *Earth Pla Sci Lett* 15: 232-238
- SOFER, Z & GAT, JR (1975) The isotope composition of evaporating brines: effect of the isotope activity ratio in saline solutions. *Earth Pla Sci Lett* 26: 179-186
- SONNENFELD, P (1984) *Brines and evaporites*. Academic Press Inc Orlando: 613 pp.

- STAMPFLI, GM & BOREL, GD (2002) A plate tectonic model for the Paleozoic and Mesozoic constrained by dynamic plate boundaries and restored synthetic oceanic isochrons. *Earth Planet Sci Lett* 196: 17-33
- STEWART, FH (1963) Marine evaporites. *US Geol Surv Prof Paper* 440-Y: 53 pp.
- STOSCH, H-G (2002) Einführung in die Isotopengeochemie. <http://petrol.natur.cuni.cz/~janousek/izokurz/PDF/Stosch%20Isotopengeochemie.pdf>, retrieved in August 2008: 246 pp.
- STROHMENGER, C, VOIGT, E & ZIMDARS, J (1996) Sequence stratigraphy and cyclic development of Basal Zechstein carbonate-evaporite deposits with emphasis on Zechstein 2 off-platform carbonates (Upper Permian, Northeast Germany). *Sed Geol* 102: 33-54
- TAUBE, H (1954) Use of oxygen isotope effects in the study of hydration of ions. *J Phys Chem* 58: 523-528
- UREY, HC (1946) The thermodynamic properties of isotopic substances. *Jour Chem Soc*: 562-581
- USDOWSKI, E (1973) Das geochemische Verhalten des Strontiums bei der Genese und Diagenese von Ca-Karbonat- und Ca-Sulfat-Mineralen. *Contr Mineral Petrol* 38: 177-195
- USDOWSKI, E & DIETZEL, M (1997) Atlas and data of solid-solution equilibria of marine evaporites. Springer Berlin Heidelberg: 316 pp.
- VALIASHKO, MG & MANDRYKINA, TV (1952, in Russian) Bromine in salt deposits as a genetic and prospecting indicator. *Trudy Vses Nauchno-Isled Inst Galurgii* 23: 54-92
- VAN'T HOFF, JH (1905) Zur Bildung der ozeanischen Salzablagerungen I. Vieweg & Sohn Braunschweig: 85 pp.
- VAN'T HOFF, JH (1909) Zur Bildung der ozeanischen Salzablagerungen II. Vieweg & Sohn Braunschweig: 90 pp.
- VAN'T HOFF, JH (1912) Untersuchungen über die Bildungsverhältnisse der ozeanischen Salzablagerungen, insbesondere des Stassfurter Salzlagers. Akad Verlagsges Leipzig: 359 pp.

- VEIZER, J, ALA, D, AZMY, K, BRUCKSCHEN, P, BUHL, D, BRUHN, F, CARDEN, GAF, DIENER, A, EBNETH, S, GODDERIS, Y, JASPER, T, KORTE, C, PAWELLEK, F, PODLAHA, OG & STRAUSS, H (1999)  $^{87}\text{Sr}/^{86}\text{Sr}$ ,  $\delta^{13}\text{C}$  and  $\delta^{18}\text{O}$  evolution of Phanerozoic seawater. *Chem Geol* 161: 59-88
- VIERHUFF, H, WAGNER, W & AUST, H (1981) Die Grundwasservorkommen in der Bundesrepublik Deutschland. *Geol Jahrbuch* 30(C): 110 pp.
- WADLEIGH, MA, VEIZER, J & BROOKS, C (1985) Strontium and its isotopes in Canadian rivers: Fluxes and global implications. *Geochim Cosmochim Acta* 49(8): 1727-1736
- WALTER, L M, STUEBER, A M & HUSTON, T J (1990) Br-Cl-Na systematics in Illinois basin fluids: Constraints on fluid origin and evolution. *Geology* 18: 315-318
- WEAST, R C (1986) *CRC Handbook of Chemistry and Physics*. CRC Press Inc. Boca Raton: 2424 pp.
- WEDEPOHL, KH (1978) *Handbook of geochemistry II*. Springer Berlin
- WERNER, AG (1787) Zur Klassifikation und Beschreibung der verschiedenen Gebirgsarten. *Hochschulveröff Bergakademie Freiberg*: 28 pp.
- WIEGAND, B, DIETZEL, M, BIELERT, U, GROTH, P & HANSEN, BT (2001)  $^{87}\text{Sr}/^{86}\text{Sr}$ -Verhältnisse als tracer für geochemische Prozesse in einem Lockergesteinsaquifer (Liebenau, NW-Deutschland. *Acta hydrochim hydrobiol* 29(2-3): 139-152
- ZHARKOV, M A (1981) *History of Paleozoic Salt Accumulation*. Springer Berlin Heidelberg: 308 pp.
- ZHARKOV, M A (1984) *Paleozoic Salt Bearing Formations of the World*. Springer Berlin Heidelberg: 427 pp.
- ZHEREBTSOVA, IK & VOLKOVA, NN (1966) Experimental study of the behavior of microelements in process of natural solar evaporation of Black Sea water and brine of Lake Sasyk-Sivash (in Russian). *Geokhimiya* 7: 832-844
- ZIEGLER, PA (1990) *Geological atlas of Western and Central Europe*. Elsevier Scientific Publishing Co.: 130 pp.



ZUBER, A, GRABCAK, J & GARLICKI, A (2000) Catastrophic and dangerous inflows to salt mines in Poland as related to the origin of water determined by isotope methods. *Envir Geol* 39(3-4): 299-311

## APPENDIX

|              |  |
|--------------|--|
| Appendix I   | Table of major evaporitic minerals and their composition (after BRAITSCH 1971)   |
| Appendix IIa | Table of sampling sites, stratigraphy at the emersion/abstraction, formation and sampling conditions   |
| Appendix IIb | Table of strontium and stable isotope compositions and intensive parameters  |
| Appendix IIc | Table of cation concentrations (Be, Sc, Ti, V, Ga, Y, Zr, Nb, Mo, Cd, Sn, Sb, La, Ce, Pr, Nd, Sm, Eu, Gd, Tb, Dy, Ho, Er, Tm, Yb, Lu, Hf, Ta, W, Tl, Bi, Th, U below detection limit due to analysis after dilution) |
| Appendix III | Table of amounts of Ag <sub>2</sub> O [mg] used for neutralization prior to stable isotope analyses  |
| Appendix IV  | Procedure for columnar elution of Sr in saline solutions, and regular procedure for Rb, Sr and REE   |
| Appendix V   | Precipitating phases of the invariant points of the quinary seawater phase system in Figure 5-7 (after BORCHERT 1940); seawater at each point saturated with halite plus the named phases                            |
| Appendix VI  | Calculations for two-component mixture of <sup>87</sup> Sr/ <sup>86</sup> Sr following Equation 7-4  |

**Appendix I:** Table of major evaporitic minerals and their composition  
(after BRAITSCH 1971)

| <b>SULFATES</b>  | <b>Abbr.</b> | <b>Empirical Formula</b>  |
|------------------|--------------|---|
| Anhydrite        | a            | $\text{CaSO}_4$   |
| Gypsum           | g            | $\text{CaSO}_4 \times 2\text{H}_2\text{O}$                                |
| Syngenite        | sg           | $\text{K}_2\text{Ca}(\text{SO}_4)_2 \times \text{H}_2\text{O}$            |
| Görgeyite        | gö           | $\text{K}_2\text{Ca}_5(\text{SO}_4)_6 \times \text{H}_2\text{O}$          |
| Leonite          | le           | $\text{K}_2\text{Mg}(\text{SO}_4)_2 \times 4\text{H}_2\text{O}$           |
| Schönite         | sh           | $\text{K}_2\text{Mg}(\text{SO}_4)_2 \times 6\text{H}_2\text{O}$           |
| Langbeinite      | lg           | $\text{K}_2\text{Mg}_2(\text{SO}_4)_3$                                    |
| Polyhalite       | p            | $\text{K}_2\text{MgCa}_2(\text{SO}_4)_4 \times 2\text{H}_2\text{O}$       |
| Glaserite        | gs           | $\text{K}_3\text{Na}(\text{SO}_4)_2$                                      |
| Kainite          | k            | $\text{KMgClSO}_4 \times 2,75\text{H}_2\text{O}$                          |
| Leonhardtite     | lh           | $\text{MgSO}_4 \times 4\text{H}_2\text{O}$                                |
| Pentahydrate     | 5h           | $\text{MgSO}_4 \times 5\text{H}_2\text{O}$                                |
| Hexahydrate      | hx           | $\text{MgSO}_4 \times 6\text{H}_2\text{O}$                                |
| Epsomite         | e            | $\text{MgSO}_4 \times 7\text{H}_2\text{O}$                                |
| Kieserite        | ks           | $\text{MgSO}_4 \times \text{H}_2\text{O}$                                 |
| Glauberite       | gb           | $\text{Na}_2\text{Ca}(\text{SO}_4)_2$                                     |
| Vanthoffite      | vh           | $\text{Na}_6\text{Mg}(\text{SO}_4)_4$                                     |
| Blödite          | bl           | $\text{Na}_2\text{Mg}(\text{SO}_4)_2 \times 4\text{H}_2\text{O}$          |
| Löweite          | lö           | $\text{Na}_{12}\text{Mg}_7(\text{SO}_4)_{13} \times 15\text{H}_2\text{O}$ |
| D'Ansite         | da           | $\text{Na}_{21}\text{MgCl}_3(\text{SO}_4)_{10}$                           |
| Thenardite       | t            | $\text{Na}_2\text{SO}_4$  |
| Mirabilite       | m            | $\text{Na}_2\text{SO}_4 \times 10\text{H}_2\text{O}$                      |
| <b>CHLORIDES</b> |              |   |
| Tachhydrite      | ta           | $\text{CaMg}_2\text{Cl}_6 \times 12\text{H}_2\text{O}$                    |
| Rokühnite        | rk           | $\text{FeCl}_2 \times 2\text{H}_2\text{O}$                                |
| Erythrosiderite  | er           | $\text{K}_2\text{FeCl}_5 \times \text{H}_2\text{O}$                       |
| Rinneite         | ri           | $\text{K}_3\text{NaFeCl}_6$   |
| Chlorocalcite    | cc           | $\text{KCaCl}_3$  |
| Sylvite          | sy           | $\text{KCl}$  |
| Carnallite       | c            | $\text{KMgCl}_3 \times 6\text{H}_2\text{O}$                               |
| Bischofite       | bi           | $\text{MgCl}_2 \times 6\text{H}_2\text{O}$                                |
| Halite           | h            | $\text{NaCl}$   |

Appendix IIa: Table of sampling sites, stratigraphy at the emersion/abstraction, formation and sampling conditions

| FEDERAL STATE | Ct. #  | Region                | NAME                  | DATE                 | LOCATION                       | STRATIGRAPHY at emersion/abstraction     | FORMATION / Folge | SAMPLER                         | APPEARANCE   | SAMPLING   |
|---------------|--------|-----------------------|-----------------------|----------------------|--------------------------------|--|-------------------|---------------------------------|--|--|
|               | 109    | RW 1                  | RW 1 G6               | 10.09.2007           | Uni Göttingen Nord             | -  | -                 | Klaus                           |  | sampled on roof of geology building  |
|               | 76     | RW 2                  | RW 2 Ulster           | 15.06.2006           | River Ulster water at Räsa     | -  | -                 |                                 | colorless, algae infestation   | river  |
|               | 75     | RW 3                  | RW 3 Werra            | 15.06.2006           | River Werra water at Unterrohn | -  | -                 |                                 | colorless, algae infestation   | river  |
| BOREHOLES     | 32     | TH b1                 | TH b1 130             | 12.10.2005           | Sampling depth 95 m            | Ca3                                      | Leine             | Küchenmeister/Thorreiter        | colorless, orange precipitation  | well   |
|               | 96     | TH b1                 | TH b1 130             | 11.10.2006           | Sampling depth 95 m            | Ca3                                      | Leine             | "                               | colorless, orange precipitation  | "  |
|               | 63     | TH b2                 | TH b2 111             | 15.05.2006           | Sampling depth 70 m            | su, subrosion water from pr              | Buntsandstein     | "                               | colorless  | well   |
|               | 104    | TH b2                 | TH b2 111             | 14.05.2007           | Sampling depth 70 m            | su, subrosion water from pr              | Buntsandstein     | "                               | colorless  | "  |
|               | 31     | TH b3                 | TH b3 3               | 11.10.2005           | Sampling depth 175 m           | su (lowermost)                           | Buntsandstein     | "                               | colorless, orange precipitation  | well   |
|               | 90     | TH b3                 | TH b3 3               | ??..10.2006          | Sampling depth 175 m           | su (lowermost)                           | Buntsandstein     | "                               | colorless, orange precipitation  | "  |
|               | 34     | HE b4                 | HE b4 389             | 29.09.2005           | Sampling depth 135 m           | su                                       | Buntsandstein     | "                               | colorless, gray precipitation  | tap  |
|               | 95     | HE b4                 | HE b4 389             | ??..10.2006          | Sampling depth 135 m           | su                                       | Buntsandstein     | "                               | colorless, gray precipitation  | "  |
|               | 60     | TH b5                 | TH b5 45              | 15.05.2006           | Sampling depth 90 m            | Ca3                                      | Leine             | "                               | colorless  | well   |
|               | 105    | TH b5                 | TH b5 45              | 16.05.2007           | Sampling depth 90 m            | Ca3                                      | Leine             | "                               | colorless  | "  |
|               | 61     | TH b6                 | TH b6 114             | 15.05.2006           | Sampling depth 210 m           | Ca1                                      | Werra             | "                               | colorless  | well   |
|               | 106    | TH b6                 | TH b6 114             | 14.05.2007           | Sampling depth 210 m           | Ca1                                      | Werra             | "                               | colorless  | "  |
|               | 62     | TH b7                 | TH b7 115             | 15.05.2006           | Sampling depth 235 m           | Ca3                                      | Leine             | "                               | colorless  | well   |
|               | 107    | TH b7                 | TH b7 115             | 14.05.2007           | Sampling depth 235 m           | Ca3                                      | Leine             | "                               | colorless  | "  |
|               | 14     | TH b8                 | TH b8 346             | 20.07.2005           | Sampling depth 80 m            | su (influenced by waste water disposal)  | Buntsandstein     | "                               | light orange   | well   |
|               | 94     | TH b8                 | TH b8 346             | ??..10.2006          | Sampling depth 80 m            | su (influenced by waste water disposal)  | Buntsandstein     | "                               | light orange   | "  |
|               | 35     | HE b9                 | HE b9 430             | 07.10.2005           | Sampling depth 870 m           | Ca3 (influenced by waste water disposal) | Leine             | "                               | colorless, gray-orange precipitation   | well   |
|               | 92     | HE b9                 | HE b9 430             | 05.10.2006           | Sampling depth 870 m           | Ca3 (influenced by waste water disposal) | Leine             | "                               | colorless, gray-orange precipitation   | "  |
|               | 10     | HE b10                | HE b10 528            | 03.06.2005           | Sampling depth 100 m           | su (influenced by waste water disposal)  | Buntsandstein     | "                               | light yellow   | packer in well   |
|               | 93     | HE b10                | HE b10 528            | ??..10.2006          | Sampling depth 100 m           | su (influenced by waste water disposal)  | Buntsandstein     | "                               | light yellow   | "  |
| 33            | HE b11 | HE b11 431            | 30.09.2005            | Sampling depth 518 m | pr                             | Rotliegend                               | "                 | colorless, orange precipitation | well   |  |
| 91            | HE b11 | HE b11 431            | ??..10.2006           | Sampling depth 518 m | pr                             | Rotliegend                               | "                 | colorless, orange precipitation | "  |  |
| HESSE         | 24     | HE 1                  | HE 1 N81              | 07.06.2005           | N 81, Rev 8, 160. Durchhieb    | K1H / Na1y                               | Werra             |                                 | colorless  | soda straws from ridge   |
|               | 23     | HE 1                  | HE 1 N81              | 07.11.2005           | N 81, Rev 8, 160. Durchhieb    | K1H / Na1y                               | Werra             |                                 | colorless  | "  |
|               | 47     | HE 1                  | HE 1 N81              | 02.02.2006           | N 81, Rev 8, 160. Durchhieb    | K1H / Na1y                               | Werra             | Klaus, U. Fischer               | colorless  | "  |
|               | 69     | HE 1                  | HE 1 N81              | 08.05.2006           | N 81, Rev 8, 160. Durchhieb    | K1H / Na1y                               | Werra             |                                 | colorless  | "  |
|               | 20     | HE 1                  | HE 1 Shaft H 546 m    | 01.06.2005           | Shaft at 546 m                 | Ca3                                      | Leine             | Nitschke                        | colorless, dark suspended matter   | gutter at inleakage from tubing  |
|               | 22     | HE 1                  | HE 1 Shaft R 555 m    | 01.06.2005           | Shaft at 555 m, 1. Level       | Ca3                                      | Leine             | Nitschke                        | colorless, dark suspended matter   | gutter at inleakage (555 m) from tubing, container at 1. Level                     |
|               | 55     | HE 1                  | HE 1 Shaft R 555 m    | 28.02.2006           | Shaft at 555 m, 1. Level       | Ca3                                      | Leine             | Klaus/Nitschke/Girenz           | colorless  | directly from gutter at 555 m  |
|               | 70     | HE 2                  | HE 2 103 n. N         | 02.05.2006           | 103 n. N                       |  | Werra             | GBAL Stehling                   | colorless, orange precipitation  |  |
|               | 16     | HE 2                  | HE 2 70.SE 141/71     | 15.06.2005           | Betriebspunkt 70.SE, 141/71    |  | Werra             |                                 | yellow, gel-like precipitation   |  |
|               | 38     | HE 2                  | HE 2 Loch 1/87        | 01.10.2005           | Loch 1/87, 4. EW               | pr                                       | Rotliegend        | GBAL Stehling                   | colorless, orange precipitation  | sampling from borehole   |
|               | 44     | HE 2                  | HE 2 Loch 1/87        | 21.12.2005           | Loch 1/87, 4. EW               | pr                                       | Rotliegend        | "                               | colorless, orange precipitation  | "  |
|               | 71     | HE 2                  | HE 2 Loch 1/87        | 21.03.2006           | Loch 1/87, 4. EW               | pr                                       | Rotliegend        | "                               | colorless, orange precipitation  | "  |
|               | 87     | HE 2                  | HE 2 Loch 1/87        | 24.07.2006           | Loch 1/87, 4. EW               | pr                                       | Rotliegend        | "                               | colorless, orange precipitation  | "  |
|               | 86     | HE 2                  | HE 2 Loch 1/87        | 29.09.2006           | Loch 1/87, 4. EW               | pr                                       | Rotliegend        | "                               | colorless, orange precipitation  | "  |
| 99            | HE 2   | HE 2 Loch 1/87        | 03.01.2007            | Loch 1/87, 4. EW     | pr                             | Rotliegend                               | "                 | colorless, orange precipitation | "  |  |
| 100           | HE 2   | HE 2 Loch 1/87        | 06.03.2007            | Loch 1/87, 4. EW     | pr                             | Rotliegend                               | "                 | colorless, orange precipitation | "  |  |
| 101           | HE 2   | HE 2 Loch 1/87        | 29.03.2007            | Loch 1/87, 4. EW     | pr                             | Rotliegend                               | "                 | colorless, orange precipitation | "  |  |
| 11            | HE 2   | HE 2 Shaft E          | 09.06.2005            | Shaft                | su                             | Buntsandstein                            | Kimm              | colorless                       | shaft  |  |
| LOWER SAXONY  | 15     | LS 1                  | LS 1 CN 8/9           | 20.07.2005           | CN 8/9                         | T3/A3                                    | Leine             | Beer                            | colorless  | leakage from ridge, collection by funnel   |
|               | 50     | LS 1                  | LS 1 CN 8/9           | 08.02.2006           | CN 8/9                         | T3/A3                                    | Leine             | Klaus, Argut                    | colorless  | "  |
|               | 57     | LS 1                  | LS 1 CN 8/9           | 26.04.2006           | CN 8/9                         | T3/A3                                    | Leine             | "                               | colorless  | "  |
|               | 80.1   | LS 1                  | LS 1 CN 8/9           | 27.07.2006           | CN 8/9                         | T3/A3                                    | Leine             | "                               | colorless  | "  |
|               | 80.2   | LS 1                  | LS 1 CN 8/9           | 27.07.2006           | CN 8/9                         | T3/A3                                    | Leine             | "                               | colorless  | "  |
|               | 3      | LS 1                  | LS 1 H23 470 m        | 24.01.2005           | 470 m level                    | A3                                       | Leine             | Klaus,Zeibig                    | gray, suspended matter, later on orange                                      | on scaffold from several boreholes, pressure before 10-40 bar and afterwards 0 bar |
|               | 48.1   | LS 1                  | LS 1 H23 470 m        | 08.02.2006           | 470 m level                    | A3                                       | Leine             | Klaus, Argut                    | gray, suspended matter, later on orange                                      | "  |
|               | 48.2   | LS 1                  | LS 1 H23 470 m        | 08.02.2006           | 470 m level                    | A3                                       | Leine             | "                               | gray, suspended matter, later on orange                                      | "  |
|               | 48.3   | LS 1                  | LS 1 H23 470 m        | 08.02.2006           | 470 m level                    | A3                                       | Leine             | "                               | gray, suspended matter, later on orange                                      | "  |
|               | 48.4   | LS 1                  | LS 1 H23 470 m        | 08.02.2006           | 470 m level                    | A3                                       | Leine             | "                               | gray, suspended matter, later on orange                                      | "  |
|               | 59.2   | LS 1                  | LS 1 H23 470 m        | 26.04.2006           | 470 m level                    | A3                                       | Leine             | "                               | gray, suspended matter, later on orange                                      | "  |
|               | 59.1   | LS 1                  | LS 1 H23 470 m 19 1/1 | 26.04.2006           | 470 m level                    | A3                                       | Leine             | "                               | red-brown, black precipitation   | on scaffold from several boreholes, pressure before 32 bar and afterwards 0 bar    |
|               | 59.3   | LS 1                  | LS 1 H23 470 m 21 1/0 | 26.04.2006           | 470 m level                    | A3                                       | Leine             | "                               | red-brown, black precipitation   | on scaffold from several boreholes, pressure before 10-40 bar and afterwards 0 bar |
|               | 59.4   | LS 1                  | LS 1 H23 470 m 21 3/3 | 26.04.2006           | 470 m level                    | A3                                       | Leine             | "                               | red-brown, black precipitation   | on scaffold from several boreholes, pressure before 46 bar and afterwards 0 bar    |
|               | 4      | LS 1                  | LS 1 H23 500 m        | 24.01.2005           | 500 m level                    | A3                                       | Leine             | Klaus,Zeibig                    | colorless, later on orange   | sampling from borehole with standing brine, pressure 4 bar, after 1 min flow       |
|               | 5      | LS 1                  | LS 1 H23 500 m        | 24.01.2005           | 500 m level                    | A3                                       | Leine             | "                               | yellow   | sampling from borehole with standing brine, pressure 4 bar, after 5 min flow       |
|               | 49     | LS 1                  | LS 1 H23 500 m 16 6/2 | 08.02.2006           | 500 m level                    | A3                                       | Leine             | Klaus, Argut                    | colorless, later on orange   | sampling from borehole with standing brine after 1 min flow                        |
| 58            | LS 1   | LS 1 H23 500 m 16 6/2 | 26.04.2006            | 500 m level          | A3                             | Leine                                    | "                 | red-brown                       | sampling from borehole with standing brine, pressure 8 bar, after 5 min flow |  |

Appendix IIa (continued): Table of sampling sites, stratigraphy at the emersion/abstraction, formation and sampling conditions

| FEDERAL STATE            | Ct. # | Region             | NAME                    | DATE                         | LOCATION                                  | STRATIGRAPHY at emersion/abstraction     | FORMATION / Folge      | SAMPLER                         | APPEARANCE  | SAMPLING   |
|--------------------------|-------|--------------------|-------------------------|------------------------------|---|--|------------------------|---------------------------------|---|--|
| LOWER SAXONY (continued) | 8     | LS 2               | LS 2 BL Shaft 1 160.5 m | 19.05.2005                   | Shaft 1 at 160.5 m                        | ju (overlying rock), grauer/roter Mergel | Jura                   | Klaus,Gierenz                   | colorless   | leakage from shaft, collected via PE-tube at lower level in reservoir          |
|                          | 77    | LS 2               | LS 2 BL Shaft 1 160.5 m | 06.07.2006                   | Shaft 1 at 160.5 m                        | ju (overlying rock), grauer/roter Mergel | Jura                   | "                               | colorless   | "  |
|                          | 9     | LS 2               | LS 2 BL Shaft 2 104 m   | 19.05.2005                   | Shaft 2 at 104 m                          | ju (overlying rock), Münder Mergel       | Jura                   | Klaus,Gierenz                   | colorless   | gutter at inleakage from tubing  |
|                          | 78    | LS 2               | LS 2 BL Shaft 2 104 m   | 06.07.2006                   | Shaft 2 at 104 m                          | ju (overlying rock), Münder Mergel       | Jura                   | "                               | colorless   | "  |
|                          | 7     | LS 3               | LS 3 353 m S R.         | 12.05.2005                   | 353 mS Riedel                             | A3                                       | Leine                  | Argut, IW                       | light yellow  | leakage from ridge, collection by funnel on scaffold                           |
|                          | 56    | LS 3               | LS 3 353 m S R.         | 26.04.2006                   | 353 mS Riedel                             | A3                                       | Leine                  | Klaus, Argut                    | colorless   | "  |
|                          | 79    | LS 3               | LS 3 353 m S R.         | 27.07.2006                   | 353 mS Riedel                             | A3                                       | Leine                  | "                               | colorless   | "  |
|                          | 6     | LS 4               | LS 4 Shaft 2 140 m      | 19.01.2005                   | Shaft 2 at 140 m                          | Salt surface/gypsum                      |                        | Klaus,Zeibig                    | colorless   | sampling from tap, collected behind tubing                                     |
|                          | 1     | LS 5               | LS 5 L499 900 m         | 17.01.2005                   | 900 m level                               | Na3η                                     | Leine                  | Klaus,Holländer                 | yellow, later on orange-brown                           | sampling by tarp (5x5 m) with drain in the middle                              |
|                          | 36    | LS 5               | LS 5 L499 900 m         | 18.10.2005                   | 900 m level                               | Na3η                                     | Leine                  | Holländer                       | colorless, orange precipitation                         | "  |
|                          | 52    | LS 5               | LS 5 L499 900 m         | 10.01.2006                   | 900 m level                               | Na3η                                     | Leine                  | "                               | yellow, orange precipitation                            | "  |
|                          | 74    | LS 5               | LS 5 L499 900 m         | 10.04.2006                   | 900 m level                               | Na3η                                     | Leine                  | "                               | yellow, orange precipitation                            | "  |
|                          | 97    | LS 5               | LS 5 L499 900 m         | 24.10.2006                   | 900 m level                               | Na3η                                     | Leine                  | "                               | yellow, orange precipitation                            | "  |
|                          | 103   | LS 5               | LS 5 L499 900 m         | 03.04.2007                   | 900 m level                               | Na3η                                     | Leine                  | "                               | yellow, orange precipitation                            | "  |
|                          | 2     | LS 5               | LS 5 UB 784 725 m       | 17.01.2005                   | 725 m level                               | T5r-T6                                   | Ohre-Friesland         | Klaus,Holländer                 | colorless, later on yellow                              | sampling from cased borehole   |
|                          | 37    | LS 5               | LS 5 UB 784 725 m       | 18.10.2005                   | 725 m level                               | T5r-T6                                   | Ohre-Friesland         | Holländer                       | colorless, orange precipitation                         | "  |
|                          | 45    | LS 5               | LS 5 UB 784 725 m       | 02.01.2006                   | 725 m level                               | T5r-T6                                   | Ohre-Friesland         | "                               | colorless, orange precipitation                         | "  |
|                          | 73    | LS 5               | LS 5 UB 784 725 m       | 10.04.2006                   | 725 m level                               | T5r-T6                                   | Ohre-Friesland         | "                               | colorless, orange precipitation                         | "  |
|                          | 98    | LS 5               | LS 5 UB 784 725 m       | 24.10.2006                   | 725 m level                               | T5r-T6                                   | Ohre-Friesland         | "                               | colorless, orange precipitation                         | "  |
|                          | 102   | LS 5               | LS 5 UB 784 725 m       | 03.04.2007                   | 725 m level                               | T5r-T6                                   | Ohre-Friesland         | "                               | colorless, orange precipitation                         | "  |
| 46                       | LS 5  | LS 5 UB 810        | 15.12.2005              | Borehole UB 810              | inflow from adjoining Röt                 | Buntsandstein                            | Holländer              | colorless, orange precipitation | "   |  |
| THURINGIA                | 19    | TH 1               | TH 1 Ort 90 n. N HZ 158 | 27.05.2005                   | 2. Level, NE-Feld, 6. E-Abf., Ort 90 n. N | Na1α/b/K1Th                              | Werra                  | Pippig                          | colorless, orange precipitation                         | scooped from brine pool oozing out of level ground                             |
|                          | 26    | TH 1               | TH 1 Ort 90 n. N HZ 158 | 09.09.2005                   | 2. Level, NE-Feld, 6. E-Abf., Ort 90 n. N | Na1α/b/K1Th                              | Werra                  | "                               | colorless, orange precipitation                         | "  |
|                          | 39    | TH 1               | TH 1 Ort 90 n. N HZ 158 | 20.12.2005                   | 2. Level, NE-Feld, 6. E-Abf., Ort 90 n. N | Na1α/b/K1Th                              | Werra                  | "                               | colorless, orange precipitation                         | "  |
|                          | 67    | TH 1               | TH 1 Ort 90 n. N HZ 158 | 04.04.2006                   | 2. Level, NE-Feld, 6. E-Abf., Ort 90 n. N | Na1α/b/K1Th                              | Werra                  | "                               | colorless, orange precipitation                         | "  |
|                          | 84    | TH 1               | TH 1 Ort 90 n. N HZ 158 | 28.07.2006                   | 2. Level, NE-Feld, 6. E-Abf., Ort 90 n. N | Na1α/b/K1Th                              | Werra                  | Klaus, Pippig                   | colorless, orange precipitation                         | since march 2005; abstracted at Ort 87 n. N from HZ 158                        |
|                          | 40    | TH 2               | TH 2 Qu 23 HZ 207 E     | 20.12.2005                   | Qu 23 n.W, 1. level                       | Na1α, welling up from pr                 | Werra/Rotliegend       | Pippig                          | colorless   | "  |
|                          | 28    | TH 2               | TH 2 Qu 23 HZ 11        | 09.09.2005                   | Qu 23 n.W, 1. level                       | Na1α, welling up from pr                 | Werra/Rotliegend       | Pippig                          | colorless, orange precipitation                         | tap at the feed pipe from sub-saliniferous                                     |
|                          | 42    | TH 2               | TH 2 Qu 23 HZ 11        | 20.12.2005                   | Qu 23 n.W, 1. level                       | Na1α, welling up from pr                 | Werra/Rotliegend       | "                               | colorless, orange precipitation                         | "  |
|                          | 64    | TH 2               | TH 2 Qu 23 HZ 11        | 04.04.2006                   | Qu 23 n.W, 1. level                       | Na1α, welling up from pr                 | Werra/Rotliegend       | "                               | colorless, orange precipitation                         | "  |
|                          | 81    | TH 2               | TH 2 Qu 23 HZ 11        | 28.07.2006                   | Qu 23 n.W, 1. level                       | Na1α, welling up from pr                 | Werra/Rotliegend       | Klaus, Pippig                   | colorless, orange precipitation                         | since 1969; from cavern within seam Thüringen, abstracted from Qu 58 via HZ 11 |
|                          | 18    | TH 2               | TH 2 Qu 30/31           | 20.05.2005                   | Qu 30/31, 2. level                        | K1H                                      | Werra                  | Pippig                          | colorless   | leakage from ridge, sampled from bucket below soda straws                      |
|                          | 29    | TH 2               | TH 2 Qu 30/31           | 09.09.2005                   | Qu 30/31, 2. level                        | K1H                                      | Werra                  | "                               | colorless   | "  |
|                          | 41    | TH 2               | TH 2 Qu 30/31           | 20.12.2005                   | Qu 30/31, 2. level                        | K1H                                      | Werra                  | "                               | colorless   | "  |
|                          | 65    | TH 2               | TH 2 Qu 30/31           | 04.04.2006                   | Qu 30/31, 2. level                        | K1H                                      | Werra                  | "                               | colorless   | "  |
|                          | 82    | TH 2               | TH 2 Qu 30/31           | 28.07.2006                   | Qu 30/31, 2. level                        | K1H                                      | Werra                  | Klaus, Pippig                   | colorless   | "  |
|                          | 30    | TH 2               | TH 2 Qu 86 HZ 119       | 09.09.2005                   | Qu 86 n.S, 2. Level, Ort 18 n. S          | Na1α, from gneiss below pr               | Rotliegend             | Heidenreich                     | colorless, orange precipitation                         | Borehole chamber for SLV Qu 86, overfall weir from borehole                    |
|                          | 17    | TH 2               | TH 2 Qu 86 HZ 108       | 20.05.2005                   | Qu 86, 2. level                           | Na1α                                     | Rotliegend             | Pippig                          | colorless, orange precipitation                         | inflow from sub-saliniferous at Ort 19, collected by borehole 108              |
|                          | 27    | TH 2               | TH 2 Qu 86 HZ 108       | 09.09.2005                   | Qu 86, 2. level                           | Na1α                                     | Werra                  | "                               | colorless, orange precipitation                         | "  |
|                          | 43    | TH 2               | TH 2 Qu 86 HZ 108       | 20.12.2005                   | Qu 86, 2. level                           | Na1α                                     | Werra                  | "                               | colorless, orange precipitation                         | "  |
|                          | 66    | TH 2               | TH 2 Qu 86 HZ 108       | 04.04.2006                   | Qu 86, 2. level                           | Na1α                                     | Werra                  | "                               | colorless, orange precipitation                         | "  |
| 83                       | TH 2  | TH 2 Qu 86 HZ 108  | 28.07.2006              | Qu 86, 2. level              | Na1α                                      | Werra                                    | Klaus, Pippig          | colorless, orange precipitation | abstracted at Qu 85 via Ort 14/15 from HZ 108           |  |
| 25                       | TH 3  | TH 3 4. südl. Abt. | 07.10.2005              | 2. Sohle, 4. südl. Abt. n. E | Na1α/K1Th, welling up through basalt      | Werra                                    | Fliege                 | colorless, orange precipitation | upwelling through basalt dike from Rotliegend           |  |
| 51                       | TH 3  | TH 3 4. südl. Abt. | 20.12.2005              | 2. Sohle, 4. südl. Abt. n. E | Na1α/K1Th, welling up through basalt      | Werra                                    | "                      | colorless, orange precipitation | "   |  |
| 68                       | TH 3  | TH 3 4. südl. Abt. | 06.04.2006              | 2. Sohle, 4. südl. Abt. n. E | Na1α/K1Th, welling up through basalt      | Werra                                    | "                      | colorless, orange precipitation | "   |  |
| 85                       | TH 3  | TH 3 4. südl. Abt. | 28.07.2006              | 2. Sohle, 4. südl. Abt. n. E | Na1α/K1Th, welling up through basalt      | Werra                                    | "                      | colorless, orange precipitation | "   |  |
| 54                       | TH 3  | TH 3 Shaft 1 543 m | 28.02.2006              | Shaft 1 at 543 m bg          | Ca3                                       | Leine                                    | Klaus/Nitschke/Gierenz | colorless, orange precipitation | pipeline through tubing segment 14-2/3, pressure 55 bar |  |
| 89                       | TH 3  | TH 3 Shaft 1 543 m | 07.08.2006              | Shaft 1 at 543 m bg          | Ca3                                       | Leine                                    | Nitschke               | colorless, orange precipitation | pipeline through tubing segment 14-2/3, pressure 60 bar |  |
| NORTH RHINE-WESTPHALIA   | 53    | NW 1               | NW 1 KA 162             | 22.12.2005                   | Kammer 162                                | Na1α                                     | Werra                  | Becker                          | colorless   | scooped from brine pool  |
|                          | 72    | NW 1               | NW 1 KA 162             | 08.03.2006                   | Kammer 162                                | Na1α                                     | Werra                  | "                               | colorless   | "  |
|                          | 88    | NW 1               | NW 1 KA 162             | 23.08.2006                   | Kammer 162                                | Na1α                                     | Werra                  | "                               | colorless   | "  |
| SAXONY-ANHALT            | 21    | SA 1               | SA 1 WQ17/W172          | 19.01.2006                   | WQ17/W172                                 | A3                                       | Leine                  | Klaus, Wendzel                  | colorless, later on orange                              | sampling from open fissure via PE tube   |
|                          | 108   | SA 1               | SA 1 WQ17/W172          | 29.03.2007                   | WQ17/W172                                 | A3                                       | Leine                  | Wendzel                         | colorless, later on orange                              | "  |

Appendix IIb: Table of strontium and stable isotope compositions and intensive parameters

| FEDERAL STATE | Ct. #  | Region                | NAME                  | DATE                 | LOCATION                       | $^{87}\text{Sr}/^{86}\text{Sr}$<br><i>unspiked</i> | $\pm 2\sigma$ | Sr [ppm] | $\delta^{18}\text{O}(\text{H}_2\text{O})$<br>V-SMOW | $\delta^2\text{H}(\text{H}_2\text{O})$<br>V-SMOW | $\delta_2\text{H Exz.}$<br>calculated | $^3\text{H}$<br>[TU] | $\pm 2\sigma$ | T [°C] | $\rho$ [g/cm <sup>3</sup> ] | pH   | Influx [l/min] | EC [mS/cm] |   |
|---------------|--------|-----------------------|-----------------------|----------------------|--------------------------------|--|---------------|----------|---|--|---------------------------------------|----------------------|---------------|--------|-----------------------------|------|----------------|------------|---|
|               | 109    | RW 1                  | RW 1 G6               | 10.09.2007           | Uni Göttingen Nord             | 0.708323   | 0.000036      | 0.02     | -5.3  | -32.6  | 10.1                                  |                      |               |        |                             |      |                |            |   |
|               | 76     | RW 2                  | RW 2 Ulster           | 15.06.2006           | River Ulster water at Rása     | 0.708069   | 0.000007      | 0.36     |   |  |                                       |                      |               | 16     |                             | 8    |                | 0.6        |   |
|               | 75     | RW 3                  | RW 3 Werra            | 15.06.2006           | River Werra water at Unterrohn | 0.708183   | 0.000012      | 0.68     |   |  |                                       |                      |               | 17     |                             | 7.9  |                | 0.7        |   |
| BOREHOLES     | 32     | TH b1                 | TH b1 130             | 12.10.2005           | Sampling depth 95 m            | 0.708069   | 0.000011      | 5.56     | -9.00   | -62.2  | 9.9                                   | 0.4                  | 0.4           | 11.8   |                             | 6.5  |                | 75         |   |
|               | 96     | TH b1                 | TH b1 130             | 11.10.2006           | Sampling depth 95 m            | 0.708066   | 0.000009      | 2.55     | -8.98   | -62.1  | 9.7                                   |                      |               |        |                             |      |                |            |   |
|               | 63     | TH b2                 | TH b2 111             | 15.05.2006           | Sampling depth 70 m            | 0.711677   | 0.000021      | 44.30    | -10.53  | -70.1  | 14.1                                  |                      |               | 11.1   | 1.047                       | 7.3  |                | 91         |   |
|               | 104    | TH b2                 | TH b2 111             | 14.05.2007           | Sampling depth 70 m            | 0.711553   | 0.000024      | 45.09    | -10.12  | -70.2  | 10.8                                  |                      |               |        |                             |      |                |            |   |
|               | 31     | TH b3                 | TH b3 3               | 11.10.2005           | Sampling depth 175 m           | 0.708027   | 0.000005      | 17.46    | -10.10  | -66.2  | 14.6                                  | <0.5                 | -             | 13.2   |                             | 6.7  |                | 160        |   |
|               | 90     | TH b3                 | TH b3 3               | ??..10.2006          | Sampling depth 175 m           | 0.708022   | 0.000011      | 16.57    | -9.80   | -65.4  | 13.0                                  |                      |               |        |                             |      |                |            |   |
|               | 34     | HE b4                 | HE b4 389             | 29.09.2005           | Sampling depth 135 m           | 0.707591   | 0.000030      | 0.08     | -9.10   | -60.8  | 12.0                                  | <0.5                 | -             | 11.9   |                             | 6.7  |                | 347        |   |
|               | 95     | HE b4                 | HE b4 389             | ??..10.2006          | Sampling depth 135 m           | 0.711306   | 0.000010      | 0.08     | -8.81   | -60.3  | 10.1                                  |                      |               |        |                             |      |                |            |   |
|               | 60     | TH b5                 | TH b5 45              | 15.05.2006           | Sampling depth 90 m            | 0.707884   | 0.000013      | 13.02    | -8.96   | -60.2  | 11.5                                  |                      |               | 11.3   | 1.025                       | 10   |                | 51         |   |
|               | 105    | TH b5                 | TH b5 45              | 16.05.2007           | Sampling depth 90 m            | 0.707910   | 0.000018      | 12.47    | -9.08   | -61.9  | 10.7                                  |                      |               |        |                             |      |                |            |   |
|               | 61     | TH b6                 | TH b6 114             | 15.05.2006           | Sampling depth 210 m           | 0.707879   | 0.000015      | 17.43    | -9.42   | -61.6  | 13.7                                  |                      |               | 13.2   | 1.034                       | 6.8  |                | 64         |   |
|               | 106    | TH b6                 | TH b6 114             | 14.05.2007           | Sampling depth 210 m           | 0.707935   | 0.000019      | 17.45    | -9.20   | -63.2  | 10.4                                  |                      |               |        |                             |      |                |            |   |
|               | 62     | TH b7                 | TH b7 115             | 15.05.2006           | Sampling depth 235 m           | 0.707738   | 0.000017      | 16.08    | -9.28   | -61.2  | 13.0                                  |                      |               | 12.7   | 1.021                       | 7    |                | 41         |   |
|               | 107    | TH b7                 | TH b7 115             | 14.05.2007           | Sampling depth 235 m           | 0.707761   | 0.000012      | 16.15    | -9.31   | -61.6  | 12.9                                  |                      |               |        |                             |      |                |            |   |
|               | 14     | TH b8                 | TH b8 346             | 20.07.2005           | Sampling depth 80 m            | 0.710452   | 0.000014      | 51.32    | -7.20   | -39.4  | 18.2                                  | <0.5                 | -             | 11     | 1.094                       | 6    |                | 159        |   |
|               | 94     | TH b8                 | TH b8 346             | ??..10.2006          | Sampling depth 80 m            | 0.710449   | 0.000009      | 50.89    | -6.52   | -38.1  | 14.1                                  |                      |               |        |                             |      |                |            |   |
|               | 35     | HE b9                 | HE b9 430             | 07.10.2005           | Sampling depth 870 m           | 0.709396   | 0.000014      | 9.67     | -9.40   | -63.8  | 11.4                                  | 4.4                  | 0.6           | 12.2   |                             | 6.4  |                | 176        |   |
|               | 92     | HE b9                 | HE b9 430             | 05.10.2006           | Sampling depth 870 m           | 0.709376   | 0.000016      | 13.63    | -9.16   | -62.3  | 10.9                                  |                      |               |        |                             |      |                |            |   |
| 10            | HE b10 | HE b10 528            | 03.06.2005            | Sampling depth 100 m | 0.709697                       | 0.000005   | 23.39         | -10.90   | -66.2   | 21.0   | 9.3                                   | 0.9                  | 13.4          | 1.133  | 5.9                         |      | 189            |            |   |
| 93            | HE b10 | HE b10 528            | ??..10.2006           | Sampling depth 100 m | 0.709676                       | 0.000006   | 25.71         | -8.92    | -62.8   | 8.6  |                                       |                      |               |        |                             |      |                |            |   |
| 33            | HE b11 | HE b11 431            | 30.09.2005            | Sampling depth 518 m | 0.708778                       | 0.000046   | 14.98         | -10.20   | -67.7   | 13.9   | <0.5                                  | -                    | 11.5          |        | 6.4                         | 8    | 29000          |            |   |
| 91            | HE b11 | HE b11 431            | ??..10.2006           | Sampling depth 518 m | 0.708764                       | 0.000012   | 14.06         | -10.14   | -68.7   | 12.3   |                                       |                      |               |        |                             |      |                |            |   |
| HESSE         | 24     | HE 1                  | HE 1 N81              | 07.06.2005           | N 81, Rev 8, 160. Durchhieb    | 0.710749   | 0.000045      |          | -4.50   | -50.7  | -14.7                                 |                      |               | 25     | 1.284                       |      |                | -          |   |
|               | 23     | HE 1                  | HE 1 N81              | 07.11.2005           | N 81, Rev 8, 160. Durchhieb    | 0.710323   | 0.000535      | 0.25     | -4.80   | -51.9  | -13.5                                 |                      |               | 25     | 1.285                       |      |                | -          |   |
|               | 47     | HE 1                  | HE 1 N81              | 02.02.2006           | N 81, Rev 8, 160. Durchhieb    | 0.710557   | 0.000028      | 0.25     | -7.40   | -61.3  | -2.1                                  | <0.5                 | -             | 24     | 1.284                       |      | 0.3            | -          |   |
|               | 69     | HE 1                  | HE 1 N81              | 08.05.2006           | N 81, Rev 8, 160. Durchhieb    | 0.710560   | 0.000022      | 0.25     | -4.63   | -50.8  | -13.8                                 |                      |               | 25     | 1.284                       |      |                | -          |   |
|               | 20     | HE 1                  | HE 1 Shaft H 546 m    | 01.06.2005           | Shaft at 546 m                 | 0.707930   | 0.000004      | 39.31    |   |  |                                       |                      |               | -      |                             |      |                | -          |   |
|               | 22     | HE 1                  | HE 1 Shaft R 555 m    | 01.06.2005           | Shaft at 555 m, 1. Level       | 0.708230   | 0.000016      | 28.85    | -3.50   | -34.4  | -6.4                                  | 5.8                  | 0.7           | -      |                             | 6.82 | 1.5            | -          |   |
|               | 55     | HE 1                  | HE 1 Shaft R 555 m    | 28.02.2006           | Shaft at 555 m, 1. Level       | 0.708236   | 0.000018      | 42.80    | 0.35  | -19.9  | -22.6                                 |                      |               | 11     | 1.173                       | 8    |                | -          |   |
|               | 70     | HE 2                  | HE 2 103 n. N         | 02.05.2006           | 103 n. N                       |  |               |          | -10.36  | -71.4  | 11.5                                  |                      |               | 20     | 1.290                       |      |                | -          |   |
|               | 16     | HE 2                  | HE 2 70.SE 141/71     | 15.06.2005           | Betriebspunkt 70.SE, 141/71    |  |               |          | -10.60  | -63.0  | 21.8                                  |                      |               | -      |                             |      |                | -          |   |
|               | 38     | HE 2                  | HE 2 Loch 1/87        | 01.10.2005           | Loch 1/87, 4. EW               | 0.709049   | 0.000012      | 0.64     | -10.30  | -65.2  | 17.2                                  |                      |               | 22.8   | 1.210                       | 6.2  |                | -          |   |
|               | 44     | HE 2                  | HE 2 Loch 1/87        | 21.12.2005           | Loch 1/87, 4. EW               | 0.708984   | 0.000006      | 2.16     | -10.60  | -66.9  | 17.9                                  |                      |               | 22.8   | 1.210                       |      |                | -          |   |
|               | 71     | HE 2                  | HE 2 Loch 1/87        | 21.03.2006           | Loch 1/87, 4. EW               | 0.709038   | 0.000012      | 1.44     | -10.04  | -64.0  | 16.3                                  |                      |               | 22.2   | 1.210                       |      |                | -          |   |
|               | 87     | HE 2                  | HE 2 Loch 1/87        | 24.07.2006           | Loch 1/87, 4. EW               | 0.709015   | 0.000018      | 2.15     | -9.24   | -63.4  | 10.5                                  |                      |               | 22     | 1.208                       |      |                | -          |   |
|               | 86     | HE 2                  | HE 2 Loch 1/87        | 29.09.2006           | Loch 1/87, 4. EW               | 0.709049   | 0.000016      | 8.22     | -9.90   | -65.4  | 13.8                                  |                      |               | 22     | 1.208                       |      |                | -          |   |
| 99            | HE 2   | HE 2 Loch 1/87        | 03.01.2007            | Loch 1/87, 4. EW     | 0.708996                       | 0.000009   | 1.77          | -10.59   | -66.0   | 18.7   |                                       |                      | 22            | 1.208  |                             |      | -              |            |   |
| 100           | HE 2   | HE 2 Loch 1/87        | 06.03.2007            | Loch 1/87, 4. EW     | 0.708998                       | 0.000014   | 4.09          | -10.65   | -66.0   | 19.2   |                                       |                      | 22.2          | 1.208  |                             |      | -              |            |   |
| 101           | HE 2   | HE 2 Loch 1/87        | 29.03.2007            | Loch 1/87, 4. EW     | 0.709018                       | 0.000020   | 4.75          | -10.15   | -65.0   | 16.2   |                                       |                      | 22.2          | 1.208  |                             |      | -              |            |   |
| 11            | HE 2   | HE 2 Shaft E          | 09.06.2005            | Shaft                | 0.709450                       | 0.000005   | 8.15          |          |   |  |                                       |                      | 23.2          | 1.001  |                             |      | 2.82           |            |   |
| LOWER SAXONY  | 15     | LS 1                  | LS 1 CN 8/9           | 20.07.2005           | CN 8/9                         | 0.707444   | 0.000006      | 18.81    | -9.50   | -62.5  | 13.5                                  |                      |               | 27     | 1.212                       |      | 1.08           | -          |   |
|               | 50     | LS 1                  | LS 1 CN 8/9           | 08.02.2006           | CN 8/9                         | 0.707453   | 0.000007      | 19.06    | -9.40   | -63.9  | 11.3                                  |                      |               |        |                             |      |                | -          |   |
|               | 57     | LS 1                  | LS 1 CN 8/9           | 26.04.2006           | CN 8/9                         | 0.707478   | 0.000015      | 18.71    | -9.42   | -63.8  | 11.5                                  |                      |               | 27.8   | 1.21                        | 6.5  |                | -          |   |
|               | 80.1   | LS 1                  | LS 1 CN 8/9           | 27.07.2006           | CN 8/9                         | 0.707448   | 0.000026      | 18.74    | -9.40   | -65.7  | 9.5                                   |                      |               | 26.6   | 1.212                       |      |                | -          |   |
|               | 80.2   | LS 1                  | LS 1 CN 8/9           | 27.07.2006           | CN 8/9                         | 0.707496   | 0.000015      | 19.19    | -9.05   | -62.9  | 9.5                                   |                      |               | -      |                             |      |                | -          |   |
|               | 3      | LS 1                  | LS 1 H23 470 m        | 24.01.2005           | 470 m level                    | 0.707561   | 0.000015      | 0.30     | -3.91   | -39.2  | -7.9                                  | <0.6                 | -             | -      |                             |      |                | -          |   |
|               | 48.1   | LS 1                  | LS 1 H23 470 m        | 08.02.2006           | 470 m level                    | 0.706705   | 0.000083      | 0.27     | -6.30   | -48.3  | 2.1                                   |                      |               |        |                             |      |                | -          |   |
|               | 48.2   | LS 1                  | LS 1 H23 470 m        | 08.02.2006           | 470 m level                    |  |               | 0.00     |   |  |                                       |                      |               |        |                             |      |                |            | - |
|               | 48.3   | LS 1                  | LS 1 H23 470 m        | 08.02.2006           | 470 m level                    | 0.706442   | 0.000200      | 0.14     |   |  |                                       |                      |               |        |                             |      |                | -          |   |
|               | 48.4   | LS 1                  | LS 1 H23 470 m        | 08.02.2006           | 470 m level                    | 0.705425   | 0.003722      | 0.15     |   |  |                                       |                      |               |        |                             |      |                | -          |   |
|               | 59.2   | LS 1                  | LS 1 H23 470 m        | 26.04.2006           | 470 m level                    |  |               |          | -6.06   | -44.8  | 3.7                                   |                      |               |        |                             |      |                | -          |   |
|               | 59.1   | LS 1                  | LS 1 H23 470 m 19 1/1 | 26.04.2006           | 470 m level                    |  |               |          | -6.38   | -45.1  | 6.0                                   |                      |               | 31.9   | 1.312                       | 6    |                | -          |   |
|               | 59.3   | LS 1                  | LS 1 H23 470 m 21 1/0 | 26.04.2006           | 470 m level                    |  |               |          | -5.17   | -39.0  | 2.3                                   |                      |               | 31.9   | 1.34                        | 5    |                | -          |   |
|               | 59.4   | LS 1                  | LS 1 H23 470 m 21 3/3 | 26.04.2006           | 470 m level                    |  |               |          | -7.07   | -47.8  | 8.8                                   |                      |               | 31.7   | 1.335                       | 5.5  |                | -          |   |
|               | 4      | LS 1                  | LS 1 H23 500 m        | 24.01.2005           | 500 m level                    | 0.707043   | 0.000160      | 0.42     | -4.26   | -39.5  | -5.4                                  | <0.5                 | -             | -      |                             |      |                | -          |   |
|               | 5      | LS 1                  | LS 1 H23 500 m        | 24.01.2005           | 500 m level                    | 0.707010   | 0.000297      | 0.07     | -5.83   | -45.7  | 0.9                                   | 1.1                  | 0.5           | -      |                             |      |                | -          |   |
| 49            | LS 1   | LS 1 H23 500 m 16 6/2 | 08.02.2006            | 500 m level          | 0.707414                       | 0.000018   | 0.37          | -4.20    | -37.9   | -4.3   |                                       |                      |               |        |                             |      | -              |            |   |
| 58            | LS 1   | LS 1 H23 500 m 16 6/2 | 26.04.2006            | 500 m level          | 0.707393                       | 0.000014   | 0.31          | -3.97    | -36.8   | -5.0   |                                       |                      | 32            | 1.35   | 6                           |      | -              |            |   |

Appendix IIb (continued): Table of strontium and stable isotope compositions and intensive parameters

| FEDERAL STATE               | Ct. # | Region             | NAME                    | DATE                         | LOCATION                                  | $^{87}\text{Sr}/^{86}\text{Sr}$ | $\pm 2\sigma$ | Sr [ppm] | $\delta^{18}\text{O}(\text{H}_2\text{O})$ V-SMOW | $\delta^2\text{H}(\text{H}_2\text{O})$ V-SMOW | $\delta_2\text{H}$ Exz. calculated | $^3\text{H}$ [TU] | $\pm 2\sigma$ | T [°C] | $\rho$ [g/cm <sup>3</sup> ] | pH   | Influx [l/min] | EC [mS/cm] |   |
|-----------------------------|-------|--------------------|-------------------------|------------------------------|---|---------------------------------|---------------|----------|--|---|------------------------------------|-------------------|---------------|--------|-----------------------------|------|----------------|------------|---|
| LOWER SAXONY<br>(continued) | 8     | LS 2               | LS 2 BL Shaft 1 160.5 m | 19.05.2005                   | Shaft 1 at 160.5 m                        | 0.709364                        | 0.000005      | 3.45     | -7.91  | -54.7   | 8.6                                | <0.7              | -             | 20     | >1.09                       |      |                |            |   |
|                             | 77    | LS 2               | LS 2 BL Shaft 1 160.5 m | 06.07.2006                   | Shaft 1 at 160.5 m                        | 0.709466                        | 0.000018      | 3.29     | -8.58  | -57.0   | 11.6                               |                   |               | 20.5   | 1.007                       |      |                |            |   |
|                             | 9     | LS 2               | LS 2 BL Shaft 2 104 m   | 19.05.2005                   | Shaft 2 at 104 m                          | 0.707852                        | 0.000005      | 41.64    | -7.46  | -52.8   | 6.9                                | 1.3               | 0.5           | 16     | >1.09                       |      |                |            |   |
|                             | 78    | LS 2               | LS 2 BL Shaft 2 104 m   | 06.07.2006                   | Shaft 2 at 104 m                          | 0.707928                        | 0.000017      | 40.35    | -8.25  | -57.4   | 8.6                                |                   |               | 18     | 1.01                        |      |                |            |   |
|                             | 7     | LS 3               | LS 3 353 m S R.         | 12.05.2005                   | 353 mS Riedel                             | 0.707859                        | 0.000016      | 1.52     | 3.25   | -16.0   | -42.0                              | 0.8               | 0.5           | 24     |                             |      |                | -          |   |
|                             | 56    | LS 3               | LS 3 353 m S R.         | 26.04.2006                   | 353 mS Riedel                             | 0.707899                        | 0.000013      | 1.59     | 3.33   | -14.9   | -41.5                              |                   |               | 24     |                             | 5    | 0.035          |            |   |
|                             | 79    | LS 3               | LS 3 353 m S R.         | 27.07.2006                   | 353 mS Riedel                             | 0.708155                        | 0.000046      | 1.60     | 2.61   | -14.8   | -35.7                              |                   |               | 24     |                             |      |                | -          |   |
|                             | 6     | LS 4               | LS 4 Shaft 2 140 m      | 19.01.2005                   | Shaft 2 at 140 m                          | 0.708320                        | 0.000010      | 10.99    | -9.57  | -64.2   | 12.4                               | <0.5              | -             | -      |                             |      |                |            | - |
|                             | 1     | LS 5               | LS 5 L499 900 m         | 17.01.2005                   | 900 m level                               | 0.709675                        | 0.000003      | 169.00   | -1.80  | -37.0   | -22.6                              | <0.8              | -             | 36     | 1.257                       |      |                |            |   |
|                             | 36    | LS 5               | LS 5 L499 900 m         | 18.10.2005                   | 900 m level                               | 0.709668                        | 0.000045      | 200.81   | -1.70  | -34.2   | -20.6                              |                   |               | 36     | 1.259                       | 1.59 |                |            |   |
|                             | 52    | LS 5               | LS 5 L499 900 m         | 10.01.2006                   | 900 m level                               | 0.709598                        | 0.000020      | 213.57   | -2.00  | -34.6   | -18.6                              |                   |               | 36     | 1.262                       |      |                |            |   |
|                             | 74    | LS 5               | LS 5 L499 900 m         | 10.04.2006                   | 900 m level                               | 0.709688                        | 0.000029      | 225.19   | -0.53  | -30.4   | -26.1                              |                   |               | 35.5   | 1.270                       |      |                |            |   |
|                             | 97    | LS 5               | LS 5 L499 900 m         | 24.10.2006                   | 900 m level                               | 0.709548                        | 0.000012      | 237.56   | -0.57  | -30.4   | -25.9                              |                   |               | 40     | 1.266                       |      |                |            |   |
|                             | 103   | LS 5               | LS 5 L499 900 m         | 03.04.2007                   | 900 m level                               | 0.710212                        | 0.000006      | 248.56   | -0.35  | -31.5   | -28.7                              |                   |               | 35     | 1.272                       |      |                |            |   |
| 2                           | LS 5  | LS 5 UB 784 725 m  | 17.01.2005              | 725 m level                  | 0.709641                                  | 0.000003                        | 45.81         | -6.20    | -48.7  | 0.9   | <0.5                               | -                 | 40            | 1.196  |                             |      |                |            |   |
| 37                          | LS 5  | LS 5 UB 784 725 m  | 18.10.2005              | 725 m level                  | 0.709494                                  | 0.000011                        | 46.46         | -7.60    | -48.3  | 12.5  |                                    |                   | 42            | 1.200  | 4.87                        |      |                |            |   |
| 45                          | LS 5  | LS 5 UB 784 725 m  | 02.01.2006              | 725 m level                  | 0.709450                                  | 0.000030                        | 45.70         | -7.20    | -47.5  | 10.1  |                                    |                   | 40            | 1.198  |                             |      |                |            |   |
| 73                          | LS 5  | LS 5 UB 784 725 m  | 10.04.2006              | 725 m level                  | 0.709490                                  | 0.000015                        | 45.40         | -6.75    | -45.1  | 8.9   |                                    |                   | 40            | 1.198  |                             |      |                |            |   |
| 98                          | LS 5  | LS 5 UB 784 725 m  | 24.10.2006              | 725 m level                  | 0.709440                                  | 0.000011                        | 44.70         | -6.75    | -46.8  | 7.2   |                                    |                   | 36            | 1.200  |                             |      |                |            |   |
| 102                         | LS 5  | LS 5 UB 784 725 m  | 03.04.2007              | 725 m level                  | 0.709533                                  | 0.000010                        | 56.83         | -6.92    | -43.2  | 12.2  |                                    |                   | 40.3          | 1.2    |                             |      |                |            |   |
| 46                          | LS 5  | LS 5 UB 810        | 15.12.2005              | Borehole UB 810              | 0.709166                                  | 0.000007                        | 20.87         | -8.50    | -48.8  | 19.2  |                                    |                   | 31            | 1.200  |                             |      |                |            |   |
| THURINGIA                   | 19    | TH 1               | TH 1 Ort 90 n. N HZ 158 | 27.05.2005                   | 2. Level, NE-Feld, 6. E-Abf., Ort 90 n. N | 0.708027                        | 0.000015      | 0.21     | -5.10  | -50.0   | -9.2                               |                   |               | 18     |                             |      |                | 3          |   |
|                             | 26    | TH 1               | TH 1 Ort 90 n. N HZ 158 | 09.09.2005                   | 2. Level, NE-Feld, 6. E-Abf., Ort 90 n. N | 0.711552                        | 0.000066      |          | -6.00  | -52.2   | -4.2                               |                   |               | 19     |                             | 5.4  |                | 4.5        |   |
|                             | 39    | TH 1               | TH 1 Ort 90 n. N HZ 158 | 20.12.2005                   | 2. Level, NE-Feld, 6. E-Abf., Ort 90 n. N | 0.710606                        | 0.000040      | 0.25     | -5.90  | -53.3   | -6.1                               |                   |               | 17.3   | 1.29                        | 5.21 |                | 4.5        |   |
|                             | 67    | TH 1               | TH 1 Ort 90 n. N HZ 158 | 04.04.2006                   | 2. Level, NE-Feld, 6. E-Abf., Ort 90 n. N |                                 |               |          | -6.14  | -51.5   | -2.4                               |                   |               | 19     |                             |      |                | 3          |   |
|                             | 84    | TH 1               | TH 1 Ort 90 n. N HZ 158 | 28.07.2006                   | 2. Level, NE-Feld, 6. E-Abf., Ort 90 n. N |                                 |               |          | -5.80  | -51.1   | -4.7                               |                   |               | 19.5   |                             |      |                |            |   |
|                             | 40    | TH 2               | TH 2 Qu 23 HZ 207 E     | 20.12.2005                   | Qu 23 n.W, 1. level                       | 0.707899                        | 0.000012      | 26.79    | -10.20   | -68.7   | 12.9                               |                   |               | 20.5   | 1.2                         |      |                | 145        |   |
|                             | 28    | TH 2               | TH 2 Qu 23 HZ 11        | 09.09.2005                   | Qu 23 n.W, 1. level                       | 0.707707                        | 0.000005      | 19.08    | -10.10   | -68.5   | 12.3                               |                   |               | 20.5   |                             | 6.94 |                | 200        |   |
|                             | 42    | TH 2               | TH 2 Qu 23 HZ 11        | 20.12.2005                   | Qu 23 n.W, 1. level                       | 0.707680                        | 0.000022      | 18.88    | -10.40   | -68.3   | 14.9                               |                   |               | 20.5   | 1.21                        |      |                | -          |   |
|                             | 64    | TH 2               | TH 2 Qu 23 HZ 11        | 04.04.2006                   | Qu 23 n.W, 1. level                       | 0.707696                        | 0.000015      | 18.40    | -10.14   | -68.2   | 13.0                               |                   |               | 21     |                             |      |                | 180        |   |
|                             | 81    | TH 2               | TH 2 Qu 23 HZ 11        | 28.07.2006                   | Qu 23 n.W, 1. level                       | 0.707745                        | 0.000013      | 18.49    | -9.98  | -68.7   | 11.1                               |                   |               | 22     |                             |      |                | 180        |   |
|                             | 18    | TH 2               | TH 2 Qu 30/31           | 20.05.2005                   | Qu 30/31, 2. level                        | 0.708398                        | 0.000012      | 0.43     | -10.80   | -71.0   | 15.4                               |                   |               | 17.7   |                             |      |                | -          |   |
|                             | 29    | TH 2               | TH 2 Qu 30/31           | 09.09.2005                   | Qu 30/31, 2. level                        | 0.708188                        | 0.000024      | 0.47     | -11.20   | -71.8   | 17.8                               |                   |               | 16.5   |                             | 6.64 |                | 0.7        |   |
|                             | 41    | TH 2               | TH 2 Qu 30/31           | 20.12.2005                   | Qu 30/31, 2. level                        | 0.708396                        | 0.000010      |          | -11.00   | -72.7   | 15.3                               |                   |               | 16.5   | 1.23                        |      |                | 0.0001     |   |
|                             | 65    | TH 2               | TH 2 Qu 30/31           | 04.04.2006                   | Qu 30/31, 2. level                        | 0.708427                        | 0.000009      | 0.44     | -10.74   | -72.0   | 14.0                               |                   |               | 17     |                             |      |                | 0.5        |   |
|                             | 82    | TH 2               | TH 2 Qu 30/31           | 28.07.2006                   | Qu 30/31, 2. level                        | 0.708406                        | 0.000009      | 0.47     | -9.03  | -67.1   | 5.1                                |                   |               | 18     |                             |      |                | 0.5        |   |
|                             | 30    | TH 2               | TH 2 Qu 86 HZ 119       | 09.09.2005                   | Qu 86 n.S, 2. Level, Ort 18 n. S          | 0.708073                        | 0.000013      | 23.01    | -10.00   | -65.79  | 14.2                               |                   |               | 19     |                             | 6.55 |                | 60         |   |
|                             | 17    | TH 2               | TH 2 Qu 86 HZ 108       | 20.05.2005                   | Qu 86, 2. level                           | 0.708155                        | 0.000007      | 20.36    | -10.10   | -65.31  | 15.5                               |                   |               | 18.7   |                             |      |                | 13         |   |
|                             | 27    | TH 2               | TH 2 Qu 86 HZ 108       | 09.09.2005                   | Qu 86, 2. level                           | 0.708165                        | 0.000006      | 20.48    | -9.90  | -66.7   | 12.5                               |                   |               | 18     |                             | 6.54 |                | 13         |   |
|                             | 43    | TH 2               | TH 2 Qu 86 HZ 108       | 20.12.2005                   | Qu 86, 2. level                           | 0.708123                        | 0.000023      | 23.71    | -10.60   | -68.1   | 16.8                               |                   |               | 18     | 1.2                         |      |                | -          |   |
| 66                          | TH 2  | TH 2 Qu 86 HZ 108  | 04.04.2006              | Qu 86, 2. level              | 0.708249                                  | 0.000025                        | 22.83         | -9.95    | -67.2  | 12.3  |                                    |                   | 18.5          |        |                             |      | 13             |            |   |
| 83                          | TH 2  | TH 2 Qu 86 HZ 108  | 28.07.2006              | Qu 86, 2. level              | 0.708217                                  | 0.000014                        | 23.70         | -9.82    | -66.1  | 12.4  |                                    |                   | 19            |        |                             |      | 12             |            |   |
| 25                          | TH 3  | TH 3 4. südl. Abt. | 07.10.2005              | 2. Sohle, 4. südl. Abt. n. E | 0.710181                                  | 0.000007                        | 31.02         | -9.50    | -61.4  | 14.6  |                                    |                   | 27.5          |        | 6.37                        |      | 2.4            |            |   |
| 51                          | TH 3  | TH 3 4. südl. Abt. | 20.12.2005              | 2. Sohle, 4. südl. Abt. n. E | 0.710102                                  | 0.000021                        | 32.11         | -11.30   | -66.6  | 23.8  |                                    |                   | 27            |        |                             |      | -              |            |   |
| 68                          | TH 3  | TH 3 4. südl. Abt. | 06.04.2006              | 2. Sohle, 4. südl. Abt. n. E | 0.710138                                  | 0.000037                        | 34.14         | -10.27   | -63.5  | 18.7  |                                    |                   | 27            |        |                             |      | 2.5            |            |   |
| 85                          | TH 3  | TH 3 4. südl. Abt. | 28.07.2006              | 2. Sohle, 4. südl. Abt. n. E | 0.710249                                  | 0.000032                        | 35.64         | -10.10   | -63.1  | 17.7  |                                    |                   | 28.5          |        |                             |      | 2.5            |            |   |
| 54                          | TH 3  | TH 3 Shaft 1 543 m | 28.02.2006              | Shaft 1 at 543 m bg          | 0.711655                                  | 0.000007                        | 7.59          | -8.38    | -60.7  | 6.4   |                                    |                   | 27            | 1.182  | 6                           |      | 2              |            |   |
| 89                          | TH 3  | TH 3 Shaft 1 543 m | 07.08.2006              | Shaft 1 at 543 m bg          | 0.711880                                  | 0.000020                        | 7.36          | -8.14    | -59.4  | 5.7   |                                    |                   | 29            | 1.181  |                             |      |                |            |   |
| NORTH RHINE-<br>WESTPHALIA  | 53    | NW 1               | NW 1 KA 162             | 22.12.2005                   | Kammer 162                                | 0.710326                        | 0.000009      | 16.87    | -3.20  | -22.8   | 2.8                                |                   |               | -      |                             |      |                | -          |   |
|                             | 72    | NW 1               | NW 1 KA 162             | 08.03.2006                   | Kammer 162                                | 0.710367                        | 0.000008      | 18.15    | -2.72  | -20.3   | 1.4                                |                   |               | -      |                             |      |                | -          |   |
|                             | 88    | NW 1               | NW 1 KA 162             | 23.08.2006                   | Kammer 162                                | 0.710895                        | 0.000015      | 21.44    | -2.84  | -19.1   | 3.6                                |                   |               | -      |                             |      |                | -          |   |
| SAXONY-ANHALT               | 21    | SA 1               | SA 1 WQ17/W172          | 19.01.2006                   | WQ17/W172                                 | 0.708445                        | 0.000016      | 1.17     | 2.60   | -14.0   | -34.8                              |                   |               | -      | 1.3105                      |      |                | 0.5        |   |
|                             | 108   | SA 1               | SA 1 WQ17/W172          | 29.03.2007                   | WQ17/W172                                 | 0.708281                        | 0.000017      | 1.23     | 3.18   | -13.5   | -38.9                              |                   |               | -      |                             |      |                |            |   |

Appendix IIc: Table of cation concentrations (Be, Sc, Ti, V, Ga, Y, Zr, Nb, Mo, Cd, Su, Sb, La, Ce, Pr, Nd, Sm, Eu, Gd, Tb, Dy, Ho, Er, Tm, Yb, Lu, Hf, Ta, W, Tl, Bi, Th, U below detection limit due to analysis after dilution)

| FEDERAL STATE | Ct. #  | Region         | NAME               | DATE                 | LOCATION                       | Na        | K        | Ca      | Mg       | Fe    | Cr   | Al   | Si   | Li    | V    | Mn   | Co   | Ni   | Cu   | Zn   | Rb     | Sr    | Cs   | Ba   | Pb   |
|---------------|--------|----------------|--------------------|----------------------|--------------------------------|-----------|----------|---------|----------|-------|------|------|------|-------|------|------|------|------|------|------|--------|-------|------|------|------|
| METEORIC      | 109    | RW 1           | RW 1 G6            | 10.09.2007           | Uni Göttingen Nord             | 2.17      | 1.09     | 0.78    | 0.12     | 0.00  | 0.00 | 0.00 | 0.00 | 0.00  | 0.00 | 0.00 | 0.00 | 0.01 | 0.01 | 0.12 | 0.00   | 0.00  | 0.00 | 0.00 | 0.00 |
|               | 76     | RW 2           | RW 2 Ulster        | 15.06.2006           | River Ulster water at Räsa     | 9.65      | 2.32     | 54.49   | 15.22    | 0.00  | 0.00 | 0.02 | 1.54 | 0.00  | 0.00 | 0.00 | 0.00 | 0.00 | 0.00 | 0.02 | 0.00   | 0.69  | 0.00 | 0.11 | 0.00 |
|               | 75     | RW 3           | RW 3 Werra         | 15.06.2006           | River Werra water at Unterrohn | 36.80     | 3.86     | 37.67   | 10.74    | 0.00  | 0.00 | 0.01 | 0.89 | 0.01  | 0.00 | 0.00 | 0.00 | 0.00 | 0.00 | 0.00 | 0.01   | 0.57  | 0.00 | 0.14 | 0.00 |
| BOREHOLES     | 32     | TH b1          | TH b1 130          | 12.10.2005           | Sampling depth 95 m            | 18061.44  | 134.84   | 285.67  | 265.52   | 0.00  | 0.00 | 0.00 | 0.00 | 0.84  | 0.17 | 1.58 | 0.00 | 0.12 | 0.20 | 0.00 | 0.32   | 5.63  | 0.01 | 0.13 | 0.03 |
|               | 96     | TH b1          | TH b1 130          | 11.10.2006           | Sampling depth 95 m            | 18571.12  | 138.81   | 141.99  | 269.15   | 0.00  | 0.08 | 0.00 | 0.00 | 1.26  | 0.32 | 0.11 | 0.00 | 0.08 | 0.24 | 0.00 | 0.42   | 5.03  | 0.01 | 0.11 | 0.03 |
|               | 63     | TH b2          | TH b2 111          | 15.05.2006           | Sampling depth 70 m            | 23660.76  | 239.39   | 1607.34 | 372.03   | 0.00  | 0.05 | 0.48 | 0.00 | 5.80  | 0.21 | 5.80 | 0.00 | 0.12 | 0.28 | 0.00 | 0.96   | 56.24 | 0.17 | 0.01 | 0.04 |
|               | 104    | TH b2          | TH b2 111          | 14.05.2007           | Sampling depth 70 m            | 21547.49  | 209.73   | 1447.85 | 333.31   | 0.05  | 0.03 | 0.32 | 0.00 | 6.63  | 0.18 | 6.68 | 0.00 | 0.10 | 0.38 | 0.00 | 1.09   | 61.60 | 0.19 | 0.01 | 0.05 |
|               | 31     | TH b3          | TH b3 3            | 11.10.2005           | Sampling depth 175 m           | 43808.79  | 342.17   | 1193.37 | 289.23   | 0.16  | 0.00 | 0.18 | 0.00 | 0.83  | 0.41 | 3.74 | 0.00 | 0.18 | 0.48 | 0.00 | 0.34   | 20.49 | 0.01 | 0.00 | 0.15 |
|               | 90     | TH b3          | TH b3 3            | ?.10.2006            | Sampling depth 175 m           | 44159.02  | 363.35   | 1136.56 | 310.94   | 11.99 | 0.00 | 0.07 | 0.00 | 1.06  | 0.46 | 5.12 | 0.00 | 0.14 | 0.64 | 0.00 | 0.41   | 23.24 | 0.01 | 0.00 | 0.09 |
|               | 34     | HE b4          | HE b4 389          | 29.09.2005           | Sampling depth 135 m           | 19.92     | 1.94     | 35.62   | 18.65    | 0.00  | 0.00 | 0.01 | 5.03 | 0.03  | 0.00 | 0.01 | 0.00 | 0.00 | 0.00 | 0.04 | 0.00   | 0.11  | 0.00 | 0.31 | 0.00 |
|               | 95     | HE b4          | HE b4 389          | ?.10.2006            | Sampling depth 135 m           | 17.55     | 2.58     | 30.49   | 18.52    | 0.00  | 0.00 | 0.01 | 5.77 | 0.04  | 0.00 | 0.01 | 0.00 | 0.00 | 0.00 | 0.00 | 0.00   | 0.14  | 0.00 | 0.22 | 0.00 |
|               | 60     | TH b5          | TH b5 45           | 15.05.2006           | Sampling depth 90 m            | 12511.78  | 182.72   | 1088.43 | 137.34   | 0.04  | 0.02 | 0.39 | 0.00 | 0.48  | 0.16 | 0.01 | 0.00 | 0.03 | 0.14 | 0.00 | 0.54   | 17.34 | 0.01 | 0.01 | 0.02 |
|               | 105    | TH b5          | TH b5 45           | 16.05.2007           | Sampling depth 90 m            | 12078.59  | 182.67   | 1078.13 | 134.49   | 0.00  | 0.05 | 0.37 | 0.00 | 0.46  | 0.09 | 0.01 | 0.00 | 0.03 | 0.26 | 0.00 | 0.54   | 16.54 | 0.08 | 0.01 | 0.02 |
|               | 61     | TH b6          | TH b6 114          | 15.05.2006           | Sampling depth 210 m           | 16097.25  | 147.22   | 1534.19 | 163.45   | 13.83 | 0.09 | 0.35 | 0.00 | 0.52  | 0.17 | 3.09 | 0.00 | 0.13 | 0.18 | 0.00 | 0.23   | 22.57 | 0.03 | 0.00 | 0.03 |
|               | 106    | TH b6          | TH b6 114          | 14.05.2007           | Sampling depth 210 m           | 16508.17  | 153.84   | 1533.18 | 168.73   | 0.03  | 0.00 | 0.34 | 0.00 | 0.54  | 0.14 | 3.23 | 0.00 | 0.25 | 0.40 | 0.00 | 0.24   | 23.26 | 0.03 | 0.01 | 0.04 |
|               | 62     | TH b7          | TH b7 115          | 15.05.2006           | Sampling depth 235 m           | 9802.27   | 86.59    | 1370.35 | 149.15   | 0.20  | 0.00 | 0.58 | 0.00 | 0.28  | 0.10 | 0.14 | 0.00 | 0.15 | 0.11 | 0.00 | 0.12   | 20.69 | 0.01 | 0.01 | 0.02 |
|               | 107    | TH b7          | TH b7 115          | 14.05.2007           | Sampling depth 235 m           | 9712.34   | 88.94    | 1347.81 | 146.62   | 0.00  | 0.00 | 0.44 | 0.00 | 0.28  | 0.09 | 0.17 | 0.00 | 0.11 | 0.25 | 0.00 | 0.12   | 21.18 | 0.01 | 0.01 | 0.02 |
|               | 14     | TH b8          | TH b8 346          | 20.07.2005           | Sampling depth 80 m            | 45126.30  | 816.04   | 2387.25 | 1721.03  | 0.00  | 0.05 | 0.55 | 0.00 | 11.06 | 0.30 | 3.88 | 0.00 | 0.07 | 0.34 | 0.00 | 1.23   | 53.95 | 0.01 | 0.03 | 0.05 |
|               | 94     | TH b8          | TH b8 346          | ?.10.2006            | Sampling depth 80 m            | 44817.28  | 750.49   | 2328.43 | 1692.16  | 0.06  | 0.00 | 0.78 | 0.00 | 15.04 | 0.40 | 5.31 | 0.00 | 0.11 | 0.61 | 0.00 | 1.53   | 67.56 | 0.02 | 0.00 | 0.06 |
|               | 35     | HE b9          | HE b9 430          | 07.10.2005           | Sampling depth 870 m           | 46950.42  | 6062.84  | 786.19  | 8412.31  | 0.00  | 0.00 | 0.00 | 0.00 | 4.24  | 0.55 | 2.76 | 0.00 | 1.37 | 0.48 | 0.00 | 21.87  | 15.33 | 0.38 | 0.00 | 0.08 |
|               | 92     | HE b9          | HE b9 430          | 05.10.2006           | Sampling depth 870 m           | 43535.57  | 5708.87  | 735.63  | 8142.15  | 0.42  | 0.18 | 0.28 | 0.00 | 5.09  | 0.62 | 3.59 | 0.00 | 0.16 | 0.70 | 0.00 | 25.29  | 18.44 | 0.42 | 0.00 | 0.10 |
|               | 10     | HE b10         | HE b10 528         | 03.06.2005           | Sampling depth 100 m           | 55789.13  | 2852.18  | 1262.83 | 6689.83  | 0.00  | 0.00 | 0.00 | 0.00 | 0.65  | 0.58 | 1.41 | 0.00 | 0.18 | 0.56 | 0.00 | 4.46   | 24.86 | 0.03 | 0.00 | 0.09 |
| 93            | HE b10 | HE b10 528     | ?.10.2006          | Sampling depth 100 m | 52161.55                       | 2589.58   | 1172.27  | 6089.62 | 4.47     | 0.00  | 0.00 | 0.00 | 0.97 | 0.60  | 1.57 | 0.00 | 0.17 | 0.76 | 0.00 | 5.59 | 31.67  | 0.04  | 0.00 | 0.16 |      |
| 33            | HE b11 | HE b11 431     | 30.09.2005         | Sampling depth 518 m | 5972.88                        | 68.19     | 743.35   | 202.92  | 0.00     | 0.00  | 0.31 | 0.00 | 0.40 | 0.05  | 2.66 | 0.00 | 0.15 | 0.10 | 0.20 | 0.11 | 17.89  | 0.00  | 0.03 | 0.02 |      |
| 91            | HE b11 | HE b11 431     | ?.10.2006          | Sampling depth 518 m | 5860.63                        | 66.43     | 742.06   | 200.43  | 0.00     | 0.00  | 0.27 | 0.00 | 0.00 | 0.00  | 0.00 | 0.00 | 0.00 | 0.00 | 0.00 | 0.00 | 0.00   | 0.00  | 0.00 | 0.00 |      |
| HESSE         | 24     | HE 1           | HE 1 N81           | 07.06.2005           | N 81, Rev 8, 160. Durchhieb    | 9345.94   | 17279.53 | 18.50   | 65560.48 | 0.00  | 0.24 | 0.36 | 0.00 | 1.84  | 2.86 | 2.07 | 0.01 | 0.01 | 0.12 | 0.00 | 93.53  | 0.00  | 0.88 | 0.00 | 0.07 |
|               | 23     | HE 1           | HE 1 N81           | 07.11.2005           | N 81, Rev 8, 160. Durchhieb    | 9953.43   | 18180.74 | 24.70   | 69191.09 | 0.00  | 0.27 | 0.00 | 0.00 | 1.80  | 2.78 | 2.26 | 0.01 | 0.01 | 0.15 | 0.00 | 96.37  | 0.00  | 0.91 | 0.00 | 0.07 |
|               | 47     | HE 1           | HE 1 N81           | 02.02.2006           | N 81, Rev 8, 160. Durchhieb    | 9394.55   | 17346.23 | 21.74   | 64539.43 | 0.00  | 0.00 | 1.04 | 0.00 | 1.77  | 2.41 | 2.10 | 0.01 | 0.02 | 0.10 | 0.00 | 92.53  | 0.00  | 0.83 | 0.00 | 0.06 |
|               | 69     | HE 1           | HE 1 N81           | 08.05.2006           | N 81, Rev 8, 160. Durchhieb    | 9797.58   | 17619.15 | 21.63   | 67714.26 | 0.00  | 0.33 | 0.06 | 0.00 | 1.84  | 2.47 | 2.02 | 0.01 | 0.01 | 0.14 | 0.00 | 95.38  | 0.00  | 0.82 | 0.00 | 0.08 |
|               | 20     | HE 1           | HE 1 Shaft H 546 m | 01.06.2005           | Shaft at 546 m                 | 70246.75  | 1643.39  | 1177.90 | 2849.63  | 0.00  | 0.00 | 0.53 | 0.00 | 18.86 | 0.78 | 0.51 | 0.00 | 0.07 | 0.70 | 0.00 | 3.69   | 46.03 | 0.10 | 0.00 | 0.13 |
|               | 22     | HE 1           | HE 1 Shaft R 555 m | 01.06.2005           | Shaft at 555 m, 1. Level       | 48907.62  | 1750.60  | 1276.61 | 2346.32  | 0.00  | 0.00 | 0.69 | 0.00 | 8.40  | 0.46 | 0.28 | 0.00 | 0.04 | 0.64 | 1.69 | 3.54   | 32.89 | 0.10 | 0.00 | 0.11 |
|               | 55     | HE 1           | HE 1 Shaft R 555 m | 28.02.2006           | Shaft at 555 m, 1. Level       | 81022.26  | 2161.01  | 917.87  | 3084.46  | 0.20  | 0.00 | 0.00 | 0.00 | 18.81 | 0.84 | 0.40 | 0.00 | 0.04 | 1.18 | 0.00 | 4.94   | 48.29 | 0.13 | 0.00 | 0.15 |
|               | 70     | HE 2           | HE 2 103 n. N      | 02.05.2006           | 103 n. N                       | 49699.82  | 26526.75 | 12.88   | 34766.53 | 0.00  | 0.00 | 0.00 | 0.00 | 2.35  | 1.88 | 3.61 | 0.01 | 0.01 | 0.60 | 0.00 | 13.97  | 0.00  | 0.29 | 0.00 | 0.08 |
|               | 16     | HE 2           | HE 2 70.SE 141/71  | 15.06.2005           | Betriebspunkt 70.SE, 141/71    | 8300.84   | 13738.62 | 17.10   | 70583.24 | 0.00  | 0.00 | 0.00 | 0.00 | 1.33  | 2.52 | 1.35 | 0.01 | 0.01 | 0.11 | 0.00 | 275.13 | 0.00  | 1.07 | 0.00 | 0.08 |
|               | 38     | HE 2           | HE 2 Loch 1/87     | 01.10.2005           | Loch 1/87, 4. EW               | 95850.20  | 2727.85  | 18.38   | 1630.60  | 0.66  | 0.00 | 0.00 | 0.00 | 4.35  | 0.65 | 0.03 | 0.00 | 0.02 | 1.09 | 0.00 | 2.59   | 0.09  | 0.13 | 0.00 | 0.11 |
|               | 44     | HE 2           | HE 2 Loch 1/87     | 21.12.2005           | Loch 1/87, 4. EW               | 95532.60  | 2668.76  | 8.19    | 1693.64  | 0.00  | 0.15 | 0.00 | 0.00 | 5.52  | 0.99 | 0.00 | 0.00 | 0.01 | 1.36 | 0.00 | 2.97   | 0.00  | 0.14 | 0.00 | 0.13 |
|               | 71     | HE 2           | HE 2 Loch 1/87     | 21.03.2006           | Loch 1/87, 4. EW               | 98346.61  | 2732.19  | 24.08   | 1770.25  | 0.00  | 0.14 | 0.14 | 0.00 | 6.47  | 1.73 | 0.02 | 0.00 | 0.00 | 1.08 | 0.00 | 3.00   | 0.62  | 0.14 | 0.00 | 0.58 |
|               | 87     | HE 2           | HE 2 Loch 1/87     | 24.07.2006           | Loch 1/87, 4. EW               | 101695.69 | 2717.14  | 12.62   | 1865.73  | 0.00  | 0.00 | 0.37 | 0.00 | 6.87  | 1.16 | 0.13 | 0.00 | 0.02 | 1.39 | 0.00 | 3.38   | 0.02  | 0.16 | 0.00 | 0.11 |
|               | 86     | HE 2           | HE 2 Loch 1/87     | 29.09.2006           | Loch 1/87, 4. EW               | 96072.30  | 2503.76  | 10.83   | 1747.26  | 0.00  | 0.00 | 0.00 | 0.00 | 6.51  | 1.10 | 0.12 | 0.00 | 0.01 | 1.25 | 0.00 | 3.24   | 0.00  | 0.15 | 0.00 | 0.21 |
| 99            | HE 2   | HE 2 Loch 1/87 | 03.01.2007         | Loch 1/87, 4. EW     | 116759.39                      | 3170.66   | 22.39    | 2122.33 | 0.06     | 0.03  | 0.12 | 0.00 | 6.93 | 0.94  | 1.77 | 0.00 | 0.03 | 2.12 | 0.00 | 3.78 | 0.68   | 0.18  | 0.00 | 0.14 |      |
| 100           | HE 2   | HE 2 Loch 1/87 | 06.03.2007         | Loch 1/87, 4. EW     | 99442.35                       | 2701.97   | 25.29    | 1789.80 | 0.00     | 0.12  | 0.00 | 0.00 | 6.15 | 0.84  | 1.59 | 0.00 | 0.03 | 1.98 | 3.19 | 3.24 | 0.84   | 0.15  | 0.00 | 0.12 |      |
| 101           | HE 2   | HE 2 Loch 1/87 | 29.03.2007         | Loch 1/87, 4. EW     | 97287.33                       | 2560.77   | 20.94    | 1734.22 | 0.00     | 0.00  | 0.00 | 0.00 | 5.65 | 0.83  | 1.32 | 0.00 | 0.03 | 1.94 | 0.10 | 2.98 | 0.24   | 0.14  | 0.00 | 0.11 |      |
| 11            | HE 2   | HE 2 Shaft E   | 09.06.2005         | Shaft                | 29.54                          | 19.72     | 621.49   | 120.58  | 0.00     | 0.00  | 0.06 | 4.87 | 0.14 | 0.00  | 0.00 | 0.00 | 0.01 | 0.00 | 0.09 | 0.03 | 9.14   | 0     |      |      |      |



**Appendix IIc (continued):** Table of cation concentrations (Be, Sc, Ti, V, Ga, Y, Zr, Nb, Mo, Cd, Su, Sb, La, Ce, Pr, Nd, Sm, Eu, Gd, Tb, Dy, Ho, Er, Tm, Yb, Lu, Hf, Ta, W, Tl, Bi, Th, U below detection limit due to analysis after dilution)

| FEDERAL STATE               | Ct. # | Region            | NAME                    | DATE            | LOCATION                                  | Na        | K        | Ca      | Mg       | Fe      | Cr   | Al   | Si    | Li     | V    | Mn      | Co   | Ni   | Cu     | Zn     | Rb     | Sr     | Cs   | Ba   | Pb    |
|-----------------------------|-------|-------------------|-------------------------|-----------------|---|-----------|----------|---------|----------|---------|------|------|-------|--------|------|---------|------|------|--------|--------|--------|--------|------|------|-------|
| LOWER SAXONY<br>(continued) | 8     | LS 2              | LS 2 BL Shaft 1 160.5 m | 19.05.2005      | Shaft 1 at 160.5 m                        | 4824.23   | 69.90    | 112.96  | 43.76    | 0.00    | 0.00 | 0.03 | 1.77  | 0.69   | 0.08 | 0.00    | 0.00 | 0.00 | 0.05   | 0.00   | 0.08   | 3.84   | 0.00 | 0.01 | 0.01  |
|                             | 77    | LS 2              | LS 2 BL Shaft 1 160.5 m | 06.07.2006      | Shaft 1 at 160.5 m                        | 8276.97   | 119.63   | 149.35  | 74.32    | 0.00    | 0.03 | 0.05 | 3.80  | 1.68   | 0.10 | 0.00    | 0.00 | 0.01 | 0.11   | 0.00   | 0.18   | 8.27   | 0.00 | 0.17 | 0.01  |
|                             | 9     | LS 2              | LS 2 BL Shaft 2 104 m   | 19.05.2005      | Shaft 2 at 104 m                          | 829.67    | 24.49    | 865.69  | 210.70   | 0.39    | 0.01 | 0.63 | 2.56  | 0.18   | 0.03 | 0.00    | 0.00 | 0.02 | 0.01   | 0.10   | 0.01   | 22.51  | 0.00 | 0.01 | 0.01  |
|                             | 78    | LS 2              | LS 2 BL Shaft 2 104 m   | 06.07.2006      | Shaft 2 at 104 m                          | 850.55    | 25.36    | 874.65  | 214.40   | 0.00    | 0.01 | 0.20 | 0.56  | 0.23   | 0.02 | 0.00    | 0.00 | 0.02 | 0.01   | 0.00   | 0.01   | 26.80  | 0.00 | 0.01 | 0.01  |
|                             | 7     | LS 3              | LS 3 353 m S R.         | 12.05.2005      | 353 mS Riedel                             | 6821.49   | 14151.88 | 158.53  | 64058.69 | 0.37    | 0.15 | 0.00 | 0.00  | 73.07  | 2.39 | 1090.63 | 0.01 | 0.01 | 0.06   | 299.60 | 13.10  | 1.05   | 4.29 | 0.00 | 16.83 |
|                             | 56    | LS 3              | LS 3 353 m S R.         | 26.04.2006      | 353 mS Riedel                             | 7215.54   | 13830.15 | 173.68  | 74237.14 | 1.37    | 0.07 | 0.00 | 0.00  | 129.85 | 2.63 | 1654.24 | 0.01 | 0.02 | 0.14   | 428.88 | 18.99  | 2.17   | 5.69 | 0.00 | 24.31 |
|                             | 79    | LS 3              | LS 3 353 m S R.         | 27.07.2006      | 353 mS Riedel                             | 8300.22   | 15401.17 | 181.76  | 70777.24 | 2.13    | 0.03 | 0.00 | 0.00  | 118.45 | 2.70 | 1574.72 | 0.01 | 0.02 | 0.13   | 402.18 | 21.21  | 2.18   | 6.20 | 0.00 | 23.01 |
|                             | 6     | LS 4              | LS 4 Shaft 2 140 m      | 19.01.2005      | Shaft 2 at 140 m                          | 87733.38  | 36522.35 | 1072.56 | 3344.32  | 0.00    | 0.00 | 0.64 | 0.00  | 0.62   | 1.21 | 3.69    | 0.00 | 0.03 | 0.81   | 0.43   | 10.40  | 13.71  | 0.18 | 0.02 | 0.08  |
|                             | 1     | LS 5              | LS 5 L499 900 m         | 17.01.2005      | 900 m level                               | 28122.62  | 34107.61 | 5316.31 | 39240.50 | 4182.63 | 0.00 | 5.10 | 21.77 | 19.57  | 0.46 | 265.98  | 0.13 | 0.09 | 3.51   | 34.13  | 106.73 | 189.03 | 6.02 | 4.50 | 0.50  |
|                             | 36    | LS 5              | LS 5 L499 900 m         | 18.10.2005      | 900 m level                               | 22288.53  | 27428.86 | 5623.10 | 43223.33 | 2946.47 | 0.08 | 4.39 | 0.00  | 24.17  | 0.51 | 318.72  | 0.14 | 0.10 | 3.95   | 40.11  | 120.41 | 220.45 | 7.10 | 4.64 | 0.37  |
|                             | 52    | LS 5              | LS 5 L499 900 m         | 10.01.2006      | 900 m level                               | 21315.04  | 26399.35 | 6236.86 | 45945.70 | 3385.76 | 0.09 | 6.54 | 0.00  | 30.64  | 0.77 | 383.96  | 0.17 | 0.15 | 5.01   | 51.53  | 145.03 | 278.52 | 8.48 | 5.65 | 0.33  |
|                             | 74    | LS 5              | LS 5 L499 900 m         | 10.04.2006      | 900 m level                               | 18187.56  | 24105.47 | 6384.61 | 46728.48 | 3496.75 | 0.87 | 5.99 | 0.00  | 31.83  | 0.79 | 394.22  | 0.21 | 3.26 | 5.11   | 52.56  | 148.66 | 291.56 | 8.64 | 5.38 | 0.32  |
|                             | 97    | LS 5              | LS 5 L499 900 m         | 24.10.2006      | 900 m level                               | 16146.25  | 21117.51 | 6714.11 | 49046.46 | 3550.96 | 0.20 | 7.81 | 0.00  | 34.86  | 0.86 | 406.97  | 0.18 | 0.43 | 5.16   | 55.96  | 157.51 | 322.18 | 9.31 | 5.78 | 0.21  |
|                             | 103   | LS 5              | LS 5 L499 900 m         | 03.04.2007      | 900 m level                               | 16443.30  | 22188.23 | 7502.54 | 52675.19 | 4592.03 | 0.21 | 7.34 | 0.00  | 37.51  | 0.77 | 414.60  | 0.18 | 0.40 | 5.37   | 60.11  | 162.77 | 355.37 | 9.78 | 5.94 | 0.26  |
| 2                           | LS 5  | LS 5 UB 784 725 m | 17.01.2005              | 725 m level     | 91161.90                                  | 1998.76   | 1897.11  | 3129.20 | 2.73     | 0.13    | 1.32 | 0.00 | 2.13  | 0.46   | 2.75 | 0.00    | 0.04 | 1.06 | 0.00   | 4.63   | 40.16  | 0.16   | 0.08 | 0.07 |       |
| 37                          | LS 5  | LS 5 UB 784 725 m | 18.10.2005              | 725 m level     | 94745.84                                  | 1877.94   | 1961.77  | 3021.00 | 0.42     | 0.44    | 0.82 | 0.00 | 3.62  | 0.73   | 3.89 | 0.00    | 0.06 | 1.10 | 0.00   | 6.03   | 57.14  | 0.20   | 0.05 | 0.11 |       |
| 45                          | LS 5  | LS 5 UB 784 725 m | 02.01.2006              | 725 m level     | 93494.11                                  | 1855.40   | 1961.23  | 2922.61 | 1.73     | 0.00    | 2.45 | 0.00 | 4.00  | 0.69   | 3.82 | 0.00    | 0.07 | 1.42 | 0.00   | 5.96   | 57.81  | 0.20   | 0.05 | 0.09 |       |
| 73                          | LS 5  | LS 5 UB 784 725 m | 10.04.2006              | 725 m level     | 99525.15                                  | 1941.31   | 2037.36  | 2983.88 | 0.00     | 0.00    | 0.00 | 0.00 | 4.47  | 0.89   | 3.68 | 0.00    | 0.07 | 1.31 | 0.00   | 6.19   | 62.25  | 0.21   | 0.10 | 0.18 |       |
| 98                          | LS 5  | LS 5 UB 784 725 m | 24.10.2006              | 725 m level     | 89609.24                                  | 1732.00   | 1923.35  | 2771.43 | 0.37     | 0.06    | 0.19 | 0.00 | 4.04  | 0.77   | 3.81 | 0.00    | 0.07 | 1.56 | 0.00   | 6.20   | 61.99  | 0.20   | 0.06 | 0.10 |       |
| 102                         | LS 5  | LS 5 UB 784 725 m | 03.04.2007              | 725 m level     | 95114.96                                  | 2088.80   | 2374.56  | 4453.61 | 2.06     | 0.14    | 1.07 | 0.00 | 5.68  | 0.70   | 4.86 | 0.00    | 0.07 | 1.48 | 0.00   | 5.80   | 68.79  | 0.18   | 0.09 | 0.10 |       |
| 46                          | LS 5  | LS 5 UB 810       | 15.12.2005              | Borehole UB 810 | 95123.97                                  | 1840.69   | 847.48   | 3795.26 | 0.00     | 0.00    | 0.00 | 0.00 | 5.91  | 0.74   | 8.88 | 0.00    | 0.06 | 1.43 | 142.15 | 3.69   | 26.14  | 0.08   | 0.00 | 0.19 |       |
| THURINGIA                   | 19    | TH 1              | TH 1 Ort 90 n. N HZ 158 | 27.05.2005      | 2. Level, NE-Feld, 6. E-Abf., Ort 90 n. N | 10145.68  | 18461.88 | 29.87   | 66942.51 | 0.04    | 0.20 | 0.00 | 0.00  | 6.69   | 2.77 | 3.09    | 0.01 | 0.01 | 0.14   | 0.00   | 176.91 | 0.00   | 1.68 | 0.00 | 0.08  |
|                             | 26    | TH 1              | TH 1 Ort 90 n. N HZ 158 | 09.09.2005      | 2. Level, NE-Feld, 6. E-Abf., Ort 90 n. N | 8412.29   | 15833.48 | 25.00   | 54354.04 | 0.16    | 0.00 | 0.46 | 0.00  | 6.20   | 2.24 | 2.40    | 0.00 | 0.00 | 0.12   | 0.00   | 163.66 | 0.00   | 1.53 | 0.00 | 0.08  |
|                             | 39    | TH 1              | TH 1 Ort 90 n. N HZ 158 | 20.12.2005      | 2. Level, NE-Feld, 6. E-Abf., Ort 90 n. N | 9627.77   | 17314.36 | 21.47   | 66004.52 | 0.00    | 0.34 | 0.55 | 0.00  | 1.43   | 2.29 | 1.85    | 0.01 | 0.01 | 0.15   | 0.00   | 84.59  | 0.00   | 0.79 | 0.00 | 0.06  |
|                             | 67    | TH 1              | TH 1 Ort 90 n. N HZ 158 | 04.04.2006      | 2. Level, NE-Feld, 6. E-Abf., Ort 90 n. N | 10647.96  | 18391.63 | 15.51   | 66930.83 | 0.00    | 0.28 | 0.00 | 0.00  | 7.61   | 2.98 | 3.51    | 0.01 | 0.02 | 0.21   | 2.09   | 182.48 | 0.00   | 1.72 | 0.00 | 0.09  |
|                             | 84    | TH 1              | TH 1 Ort 90 n. N HZ 158 | 28.07.2006      | 2. Level, NE-Feld, 6. E-Abf., Ort 90 n. N | 9868.07   | 17055.54 | 11.01   | 68510.89 | 0.63    | 0.07 | 0.00 | 0.00  | 7.96   | 3.17 | 2.80    | 0.01 | 0.01 | 0.20   | 11.55  | 198.28 | 0.00   | 1.86 | 0.00 | 0.09  |
|                             | 40    | TH 2              | TH 2 Qu 23 HZ 207 E     | 20.12.2005      | Qu 23 n.W, 1. level                       | 95713.47  | 731.61   | 1162.93 | 423.51   | 0.00    | 0.00 | 0.00 | 0.00  | 1.75   | 0.76 | 1.48    | 0.00 | 0.04 | 0.97   | 0.00   | 1.87   | 25.77  | 0.66 | 0.00 | 0.11  |
|                             | 28    | TH 2              | TH 2 Qu 23 HZ 11        | 09.09.2005      | Qu 23 n.W, 1. level                       | 93642.86  | 7824.71  | 307.30  | 2458.47  | 0.79    | 0.28 | 0.00 | 0.00  | 2.16   | 1.18 | 2.34    | 0.00 | 0.02 | 1.00   | 0.49   | 4.83   | 20.26  | 0.80 | 0.00 | 0.11  |
|                             | 42    | TH 2              | TH 2 Qu 23 HZ 11        | 20.12.2005      | Qu 23 n.W, 1. level                       | 95860.32  | 7872.20  | 325.99  | 2423.64  | 0.00    | 0.13 | 0.00 | 0.00  | 1.87   | 1.02 | 2.06    | 0.00 | 0.02 | 1.04   | 0.00   | 4.10   | 18.60  | 0.68 | 0.00 | 0.09  |
|                             | 64    | TH 2              | TH 2 Qu 23 HZ 11        | 04.04.2006      | Qu 23 n.W, 1. level                       | 95513.21  | 7846.30  | 339.62  | 2463.59  | 0.14    | 0.37 | 0.00 | 0.00  | 2.30   | 0.83 | 2.60    | 0.00 | 0.03 | 1.48   | 0.00   | 5.03   | 24.73  | 0.83 | 0.00 | 0.11  |
|                             | 81    | TH 2              | TH 2 Qu 23 HZ 11        | 28.07.2006      | Qu 23 n.W, 1. level                       | 99031.42  | 8056.87  | 381.48  | 2500.34  | 0.00    | 0.10 | 0.08 | 0.00  | 2.65   | 1.00 | 2.39    | 0.00 | 0.02 | 1.56   | 0.00   | 5.31   | 25.53  | 0.89 | 0.00 | 0.13  |
|                             | 18    | TH 2              | TH 2 Qu 30/31           | 20.05.2005      | Qu 30/31, 2. level                        | 70628.24  | 8563.20  | 190.29  | 25311.97 | 0.00    | 0.23 | 0.04 | 0.00  | 6.50   | 1.71 | 0.54    | 0.00 | 0.00 | 0.76   | 0.00   | 26.14  | 0.00   | 1.02 | 0.00 | 0.12  |
|                             | 29    | TH 2              | TH 2 Qu 30/31           | 09.09.2005      | Qu 30/31, 2. level                        | 62938.65  | 7812.19  | 173.33  | 22826.21 | 0.00    | 0.00 | 0.00 | 0.00  | 7.10   | 1.82 | 0.61    | 0.00 | 0.00 | 0.72   | 0.00   | 28.57  | 0.00   | 1.10 | 0.00 | 0.23  |
|                             | 41    | TH 2              | TH 2 Qu 30/31           | 20.12.2005      | Qu 30/31, 2. level                        | 61265.09  | 7365.60  | 141.31  | 19086.37 | 0.00    | 0.00 | 0.00 | 0.00  | 5.21   | 1.41 | 0.53    | 0.00 | 0.00 | 0.64   | 0.00   | 22.04  | 0.00   | 0.85 | 0.00 | 0.08  |
|                             | 65    | TH 2              | TH 2 Qu 30/31           | 04.04.2006      | Qu 30/31, 2. level                        | 64032.97  | 8005.61  | 179.83  | 23854.02 | 0.00    | 0.05 | 0.00 | 0.00  | 7.61   | 1.72 | 0.80    | 0.00 | 0.01 | 0.90   | 0.00   | 28.84  | 0.00   | 1.08 | 0.00 | 0.08  |
|                             | 82    | TH 2              | TH 2 Qu 30/31           | 28.07.2006      | Qu 30/31, 2. level                        | 65100.30  | 8175.31  | 181.92  | 24371.42 | 0.62    | 0.12 | 0.00 | 0.00  | 8.75   | 1.73 | 0.72    | 0.00 | 0.01 | 1.20   | 0.00   | 31.83  | 0.00   | 1.16 | 0.00 | 0.09  |
|                             | 30    | TH 2              | TH 2 Qu 86 HZ 119       | 09.09.2005      | Qu 86 n.S, 2. Level, Ort 18 n. S          | 91966.44  | 606.94   | 1078.18 | 436.93   | 0.00    | 0.32 | 0.50 | 0.00  | 1.95   | 0.79 | 2.39    | 0.02 | 0.07 | 1.11   | 0.00   | 2.39   | 27.97  | 0.74 | 0.00 | 0.14  |
|                             | 17    | TH 2              | TH 2 Qu 86 HZ 108       | 20.05.2005      | Qu 86, 2. level                           | 96779.63  | 792.43   | 964.71  | 734.13   | 0.00    | 0.27 | 0.06 | 0.00  | 2.35   | 0.98 | 3.21    | 0.00 | 0.03 | 0.95   | 0.00   | 4.53   | 21.09  | 0.83 | 0.00 | 0.12  |
|                             | 27    | TH 2              | TH 2 Qu 86 HZ 108       | 09.09.2005      | Qu 86, 2. level                           | 90735.86  | 768.91   | 891.75  | 668.29   | 0.00    | 0.02 | 0.59 | 0.00  | 0.00   | 0.00 | 0.00    | 0.00 | 0.00 | 0.00   | 0.00   | 0.00   | 0.00   | 0.00 | 0.00 | 0.00  |
|                             | 43    | TH 2              | TH 2 Qu 86 HZ 108       | 20.12.2005      | Qu 86, 2. level                           | 99212.14  | 849.08   | 1018.71 | 758.32   | 0.00    | 0.05 | 0.44 | 0.00  | 2.85   | 0.95 | 3.05    | 0.00 | 0.05 | 1.34   | 0.00   | 4.95   | 26.14  | 0.93 | 0.00 | 0.11  |
|                             | 66    | TH 2              | TH 2 Qu 86 HZ 108       | 04.04.2006      | Qu 86, 2. level                           | 101484.78 | 785.65   | 1060.23 | 790.22   | 0.03    | 0.14 | 0.47 | 0.00  | 3.25   | 0.98 | 4.06    | 0.00 | 0.06 | 1.38   | 0.00   | 5.29   | 27.75  | 0.97 | 0.00 | 0.14  |
| 83                          | TH 2  | TH 2 Qu 86 HZ 108 | 28.07.2006              | Qu 86, 2. level | 101290.62                                 |           |          |         |          |         |      |      |       |        |      |         |      |      |        |        |        |        |      |      |       |

**Appendix III:** Table of amounts of Ag<sub>2</sub>O [mg] used for neutralization prior to stable isotope analyses

| Sample # | Ag <sub>2</sub> O | Sample # | Ag <sub>2</sub> O | Sample # | Ag <sub>2</sub> O |
|----------|-------------------|----------|-------------------|----------|-------------------|
| 10       | 500               | 47       | 700               | 80.1     | 100               |
| 12       | 500               | 48       | 1000              | 80.2     | 100               |
| 14       | 500               | 49       | 1200              | 81       | 100               |
| 15       | 500               | 50       | 500               | 82       | 300               |
| 16       | 600               | 51       | 600               | 83       | 500               |
| 17       | 500               | 52       | 500               | 84       | 1000              |
| 18       | 500               | 53       | 500               | 85       | 500               |
| 19       | 800               | 54       | 300               | 86       | 100               |
| 21       | 1000              | 55       | 400               | 87       | 100               |
| 22       | 500               | 56       | 1200              | 88       | 200               |
| 23       | 1000              | 57       | 500               | 89       | 200               |
| 24       | 1000              | 58       | 1400              | 90       | 500               |
| 25       | 500               | 59.1     | 1000              | 91       | 500               |
| 26       | 1000              | 59.2     | 1000              | 92       | 500               |
| 27       | 500               | 59.3     | 1100              | 93       | 200               |
| 28       | 500               | 59.4     | 1000              | 94       | 100               |
| 29       | 600               | 60       | 100               | 95       | 100               |
| 30       | 500               | 61       | 100               | 96       | 200               |
| 31       | 500               | 62       | 200               | 97       | 1000              |
| 32       | 500               | 63       | 200               | 98       | 500               |
| 33       | 500               | 64       | 200               | 99       | 200               |
| 34       | 500               | 65       | 600               | 100      | 500               |
| 35       | 500               | 66       | 500               | 101      | 500               |
| 36       | 600               | 67       | 1000              | 102      | 400               |
| 37       | 500               | 68       | 200               | 103      | 700               |
| 38       | 500               | 69       | 1000              | 104      | 200               |
| 39       | 900               | 70       | 1000              | 105      | 200               |
| 40       | 500               | 71       | 100               | 106      | 200               |
| 41       | 500               | 72       | 500               | 107      | 200               |
| 42       | 500               | 73       | 500               | 108      | 1100              |
| 43       | 500               | 74       | 1000              | 109      | 0                 |
| 44       | 500               | 77       | 100               |          |                   |
| 45       | 500               | 78       | 100               |          |                   |
| 46       | 500               | 79       | 1100              |          |                   |

**Appendix IV:** Procedure for columnar elution of Sr in saline solutions,  
and regular procedure for Rb, Sr and REE

| <b>Procedure for Sr in saline solutions</b> | <b>Acid</b>          | <b>Amount</b> |
|---|----------------------|---------------|
| Conditioning                                | 2.5N HCl             | 15 ml         |
| Load sample                                 | 2.5N HCl             | 1,5 ml        |
| Wash sample                                 | 2.5N HCl             | 1,5 ml        |
| Wash sample                                 | 2.5N HCl             | 17 ml         |
| <i>Wash columns and place beaker</i>        |                      |               |
| Trap Sr                                     | 2.5N HCl             | 5 ml          |
| Wash  | 6N HCl               | -             |
| <i>Wash columns and place beaker</i>        |                      | -             |
| Cleaning                                    | 6N HCl               | 1 Reservoir   |
| Cleaning                                    | 6N HCl               | 1 Reservoir   |
| Backwash                                    | H <sub>2</sub> O**** | 1 Reservoir   |

| <b>Regular procedure for Rb, Sr and REE</b> | <b>Acid</b>          | <b>Amount</b> |
|---|----------------------|---------------|
| Conditioning                                | 2.5N HCl             | 15 ml         |
| Load sample                                 | 2.5N HCl             | 1,5 ml        |
| Wash sample                                 | 2.5N HCl             | 1 ml          |
| Wash sample                                 | 2.5N HCl             | 6,5 ml        |
| <i>Wash columns and place beaker</i>        |                      |               |
| Trap Rb                                     | 2.5N HCl             | 3 ml          |
| Wash  | 2.5N HCl             | 6 ml          |
| <i>Wash columns and place beaker</i>        |                      |               |
| Trap Sr                                     | 2.5N HCl             | 7 ml          |
| Wash  | 6N HCl               | 3 ml          |
| <i>Wash columns and place beaker</i>        |                      |               |
| Trap REE                                    | 6N HCl               | 7 ml          |
| Cleaning                                    | 6N HCl               | 1 Reservoir   |
| Cleaning                                    | 6N HCl               | 1 Reservoir   |
| Backwash                                    | H <sub>2</sub> O**** | 1 Reservoir   |

**Appendix V:** Precipitating phases of the invariant points of the quinary seawater phase system in Figure 5-7 (after BORCHERT 1940); seawater at each point saturated with halite plus the named phases

| <b>Point</b> | <b>Phases</b> |             |            |
|--------------|---------------|-------------|------------|
| M            | Sylvite       | Glaserite   | Schönite   |
| N            | Sylvite       | Leonite     | Schönite   |
| P            | Sylvite       | Leonite     | Kainite    |
| Q            | Sylvite       | Carnallite  | Kainite    |
| S            | Thenardite    | Glaserite   | Blödite    |
| T            | Schönite      | Glaserite   | Blödite    |
| U            | Schönite      | Leonite     | Blödite    |
| V            | Epsomite      | Leonite     | Blödite    |
| W            | Epsomite      | Leonite     | Kainite    |
| X            | Epsomite      | Hexahydrate | Kainite    |
| Y            | Kieserite     | Hexahydrate | Kainite    |
| R            | Kieserite     | Carnallite  | Kainite    |
| Z            | Kieserite     | Carnallite  | Bischofite |
| H            | Thenardite    | Blödite     |            |
| I            | Epsomite      | Blödite     |            |
| J            | Epsomite      | Hexahydrate |            |
| K            | Kieserite     | Hexahydrate |            |
| L            | Kieserite     | Bischofite  |            |
| D            | Carnallite    | Bischofite  |            |
| E            | Carnallite    | Sylvite     |            |
| F            | Glaserite     | Sylvite     |            |
| G            | Glaserite     | Thenardite  |            |

**Appendix VI:** Calculations for two-component mixture of  $^{87}\text{Sr}/^{86}\text{Sr}$  following Equation 7-4

$$\left(\frac{^{87}\text{Sr}}{^{86}\text{Sr}}\right)_M = \frac{1}{\text{Sr}_M} \times \frac{\text{Sr}_A \text{Sr}_B \left[ \left(\frac{^{87}\text{Sr}}{^{86}\text{Sr}}\right)_B - \left(\frac{^{87}\text{Sr}}{^{86}\text{Sr}}\right)_A \right]}{(\text{Sr}_A - \text{Sr}_B)} + \frac{\text{Sr}_A \left(\frac{^{87}\text{Sr}}{^{86}\text{Sr}}\right)_A - \text{Sr}_B \left(\frac{^{87}\text{Sr}}{^{86}\text{Sr}}\right)_B}{\text{Sr}_A - \text{Sr}_B}$$

| End members | $^{87}\text{Sr}/^{86}\text{Sr}$ | Sr [ppm] | Phase             |
|-------------|---------------------------------|----------|-------------------|
| A           | 0.709641                        | 45.81    | LS 5 UB 784 725 m |
| B           | 0.71481                         | 178      |                   |
| M           | 0.71097                         | 56.6     |                   |
| A           | 0.71097                         | 56.6     | T4                |
| B           | 0.70941                         | 913      |                   |
| M           | 0.71062                         | 71.6     |                   |
| A           | 0.71062                         | 71.6     | Na3tm             |
| B           | 0.70881                         | 1934     |                   |
| M           | 0.70995                         | 111.6    |                   |
| A           | 0.70995                         | 111.6    | Na3tm             |
| B           | 0.70924                         | 1158     |                   |
| M           | 0.70968                         | 169.00   |                   |

## RESUME

### **Janina Simone Klaus**

Geboren am 21.03.1978 in München

Staatsangehörigkeit deutsch

- » Allgemeine Hochschulreife erlangt am 20.06.1997 an der Freien Waldorfschule in Kassel
- » Aufnahme des Studiums der Geowissenschaften am GZG Göttingen zum Wintersemester 1997/1998
- » Bachelor of Sciences der Geowissenschaften erlangt am 14.02.2001
- » Arbeit als Wissenschaftliche Hilfskraft in der Abteilung Isotopengeologie des GZG 2001-2005
- » Diplom mit Vertiefungsrichtung Umweltgeologie erlangt am 02.12.2003
- » Aushilfe in der Geologie der K+S AG in 2004
- » Beginn der Doktorarbeit zum Sommersemester 2005

## PUBLIKATIONSLISTE

- Heller, C, **Klaus, J**, Müller, K, Schimmelpfennig, I, Deicke, M, Ruppert, H & Schneider, J (2001) Veränderungen von pH-Werten und Schwermetallgehalten in ausgewählten Gewässern des Westharzes - Ergebnisse aus Bachelorarbeiten; Terra Nostra Vol 5/01, p 32-34 (Abstract).
- Hansen, B T, Wemmer, K, Pawlig, S, **Klaus, J**, Assavapatchara, S, Nontaso, M, Chairangsee, C & Putthapiban, P (2002) Isotopic Evidence for a Late Cretaceous Age of the Potash and Rock Salt Deposits at Bamnet Narong, NE Thailand; Proceed Sympos Geol Thailand 2002 (Abstract).
- Klaus, J S**, Hansen, B T, Beer, W W (2005) Strontium Isotopes as a Geochemical Tracer for the Evolution of Brines in Permian Evaporite Deposits of the Central European Basin, Germany; EOS Trans AGU 86 (52) Fall Meet Suppl, Abstract H23F-1485.
- Klaus, J S**, Hansen, B T, Beer, W W (2006)  $^{87}\text{Sr}/^{86}\text{Sr}$ ,  $^{10}\text{O}$ ,  $^2\text{H}$  and  $^3\text{H}$  as Geochemical Tracers for the Evolution of Brines in Evaporitic Deposits of the German Zechstein Basin; Schriftenr Deutsche Ges Geow, Vol 45, p 102 (Abstract).
- Klaus, J S**, Hansen, B T, Buapeng, S (2007)  $^{87}\text{Sr}/^{86}\text{Sr}$  Ratios: A Natural Tracer to Monitor Groundwater Flow Paths During Freshwater Reinjection in the Bangkok Area, Thailand; Hydrogeol Jour 15: 745-758.
- Klaus, J S**, Beer, W W, Hansen, B T (2007) Detecting the origin of saline solutions in salt deposits of the German Zechstein basin. Geochim. Cosmochim. Acta 71(15) Suppl. 1: A488 (Abstract)